Summer 8-14-2015

Transcriptional and Post-transcriptional Regulation of Hepcidin and Iron Metabolism by Lipid Signaling in the Liver

Sizhao Lu
University of Nebraska Medical Center

Transcriptional and Post-transcriptional Regulation of Hepcidin and Iron Metabolism by Lipid Signaling in the Liver

By

Sizhao Lu

A DISSERTATION

Presented to the Faculty of
the University of Nebraska Graduate College
in partial Fulfillment of the Requirements
for the Degree of Doctor of Philosophy

Biochemistry and Molecular Biology Graduate Program

Under the Supervision of Professor Duygu Dee Harrison-Findik

University of Nebraska Medical Center
Omaha, Nebraska
August, 2015

Supervisory Committee:
Justin L. Mott, M.D., Ph.D.
Kusum Kharbanda, Ph.D.
Robert G. Bennett, Ph.D.

Transcriptional and Post-transcriptional Regulation of Hepcidin and Iron Metabolism by Lipid Signaling in the Liver

Sizhao Lu, Ph.D.

University of Nebraska Medical Center, 2015

Advisor: Duygu Dee Harrison-Findik, Ph.D.

Although iron is required for essential biological processes, excess iron is detrimental due to oxidative damage induced by iron-mediated Fenton reactions, which promote tissue injury. Cellular iron uptake, transport and storage must therefore be tightly regulated. This task is accomplished mainly through hepcidin, the key iron-regulatory hormone. Hepcidin is synthesized primarily in hepatocytes as a circulatory antimicrobial peptide. It controls iron metabolism by inhibiting iron absorption from the duodenum and iron release from reticuloendothelial macrophages. Besides synthesizing hepcidin, the liver plays an important role in maintaining iron homeostasis by serving as the main storage organ for excess iron. Patients with liver diseases frequently display disturbances of iron metabolism but the underlying mechanisms are unclear. Due to obesity epidemic worldwide, the incidence of nonalcoholic fatty liver disease (NAFLD) is on the rise. This study therefore focuses on the regulation of hepcidin in NAFLD. NAFLD is the hepatic manifestation of metabolic syndrome, which is characterized by visceral adiposity, dyslipidemia and insulin resistance. Both the level and distribution of iron in the livers of NAFLD patients have been shown to correlate with disease severity. NAFLD patients have also been reported to display changes in hepcidin expression. The significance and relevance of these alterations regarding NAFLD pathogenesis are unclear. Although impaired fatty acid metabolism and

lipid accumulation in the liver are major contributors to the pathogenesis of NAFLD, the role of lipids or lipid derivatives in hepcidin regulation have not been investigated. The studies presented in this dissertation identified new and unique mechanisms of hepcidin gene regulation by saturated fatty acids and the biologically active lipid derivative, ceramide in human hepatoma cells. The post-transcriptional regulation of hepcidin expression by palmitic acid was mediated through AU-rich element binding protein, Human Antigen R (HuR) and novel class of protein kinase C isoforms. Ceramide, on the other hand, induced hepcidin transcription via inflammatory JAK/STAT3 signaling. Furthermore, by using high fat-fed hepcidin knockout mice as an *in vivo* model, I have implicated a role for hepcidin in the regulation of hepatic lipid metabolism, and characterized these mice as a potential experimental model to study liver injury in NAFLD.

GENERAL HYPOTHESIS AND OBJECTIVES

Obesity and metabolic syndrome are increasing worldwide in epidemic proportions affecting both adult and adolescent populations. Nonalcoholic fatty liver disease (NAFLD) is the hepatic manifestation of metabolic syndrome. The more severe form, nonalcoholic steatohepatitis (NASH) is characterized by inflammation, apoptosis, hepatocyte ballooning, fibrosis and cirrhosis. NAFLD/NASH patients also exhibit elevated serum and hepatic iron content. Iron acts as a secondary risk factor in liver diseases but the molecular mechanisms by which iron contributes to NAFLD/NASH pathogenesis are unclear.

Hepcidin is the key iron regulatory hormone, which is primarily synthesized in the liver. Hepcidin inhibits iron transport in the duodenum and iron release from macrophages by blocking the transport function of the iron exporter, ferroportin. Various factors such as, iron, inflammation and endoplasmic reticulum (ER) stress have been reported to activate the transcription of hepcidin gene, *HAMP*. Some studies, but not all, have also shown elevated levels of hepcidin in the liver and sera of obese and/or NAFLD patients. The potential mechanisms underlying this increase are unclear but a role for elevated inflammatory cytokines or liver iron content in NAFLD patients have been proposed.

Lipid accumulation in the liver (steatosis) is one of the initial pathological changes observed in NAFLD. Fat accumulates in the liver when the lipid uptake and lipogenesis outweigh the rate of lipid oxidation and secretion. Besides serving as energy storage molecules and structural components, lipids and lipid intermediates (e.g. ceramide) also act as intracellular signaling molecules. Lipid-induced signaling participates in the pathogenesis of NAFLD but its role in the regulation of hepcidin and iron metabolism has not been investigated.

We hypothesized that fatty acids and ceramide regulate hepatic *HAMP* mRNA levels through distinct cell signaling mechanisms. Both fatty acids and ceramide are potent inducers of apoptosis in hepatocytes. However, the direct effect of apoptosis on human and mouse hepcidin gene expression is unknown. We therefore addressed this question by using both *in vitro* and *in vivo* models of apoptosis induced by Fas signaling (*see Chapter III*). The role of fatty acid- (*Chapter IV*) or ceramide- (*Chapter V*) induced cellular signaling pathways in *HAMP* regulation was investigated in HepG2 human hepatoma cells. We further hypothesized that hepcidin (i.e. iron)-mediated changes in liver lipid metabolism contributes to NAFLD/NASH pathogenesis. To test this hypothesis, we employed hepcidin knockout mice with iron overload phenotype that were fed either a high-fat and high-sucrose or regular (control) diets. We also characterized these mice as potential experimental models to study the mechanisms of liver injury in NASH.

The following specific aims have been proposed.

AIM 1. To identify the post-transcriptional mechanisms by which saturated fatty acids stabilize hepcidin mRNA in human hepatoma cells.

AIM 2. To investigate the regulation of hepatic hepcidin transcription by ceramide-mediated cell signaling in hepatoma cells.

AIM 3. To characterize hepcidin knockout mice with high-fat and high-sucrose intake as a novel experimental model to study liver injury and to confirm the role of hepcidin-induced iron overload in NAFLD/NASH pathology.

TABLE OF CONTENT

LIST OF FIGURES

LIST OF TABLES

Chapter II

LIST OF ABBREVIATIONS

ACC	Acetyl-CoA Carboxylase
AMPK	AMP-Activated Protein Kinase
APAF-1	Apoptotic Peptidase Activating Factor 1
apoB	apolipoprotein B
ARE	AU-rich Element
ATGL	Adipose Triglyceride Lipase
BMP	Bone Morphogenic Protein
BMP	Bone Morphogenetic Protein
ChIP	Chromatin Immunoprecipitation
ChREBP	Carbohydrate Response Element Binding Protein
Cide	Cell-death-inducing DFFA-like effector
CPT	Carnitine-Palmitoyl-Transferase
CREBH	Cyclic AMP Response Element–Binding protein H
DAG	Diacylglycerol
DEPC	Diethylpyrocarbonate
DISC	Death-Inducing Signaling Complex
DMT1	Divalent Metal Transporter 1
DNL	De Novo Lipogenesis
ER	Endoplasmic Reticulum
ERK1/2	Extracellular Signal-Regulated Protein Kinases 1 and 2
FADD	Fas-Associated Protein with Death Domain
FAS	Fatty Acid Synthase
FAT	Fatty Acid Translocase
FATP	Fatty Acid Transport Proteins
FFA	Free Fatty Acid
FLIPL	Flice-Inhibitory Protein Long Form
FSP27	Fat-Specific Protein 27
G6PC	Glucose-6-Phosphatase
GAPDH	Glyceraldehyde Dehydogenase
H & E	Hematoxylin and Eosin
HCP1	Heme Carrier Protein 1
HFE	Hemochromatosis
HJV	Hemojuvelin
HNF	Hepatic Nuclear Factor
HO-1	Heme Oxygenase-1
HSL	Hormone-Sensitive Lipase
HuR	Human Antigen R
IRE1	Inositol-Requiring Enzyme 1
IRP	Iron-Regulatory RNA-Binding Proteins
JAK	Janus Kinase
JNK	c-Jun N-terminal Kinase
LPL	Lipoprotein Lipases
LXR	Liver X Receptors

MAPK	Mtogen-Activated Protein Kinase
MCD	Methionine-and Choline-Deficient
miRNA	microRNA
mTORC1	Mammalian Target of Rapamycin Complex 1
MTP	Microsomal Triglyceride Transfer Protein
NAFLD	Nonalcoholic Fatty Liver Disease
NASH	Nonalcoholic Steatohepatitis
ncRNA	non-coding RNA
OA	Oleic Acid
PA	Palmitic Acid
PBS	Phosphate-Buffered Saline
PCK1	Phosphoenolpyruvate Carboxykinase 1
PI3K	Phosphoinositide 3-Kinase
PKA	Protein Kinase A
PKC	Protein Kinase C
PP2A	Protein Phosphatase 2A
PPAR	Peroxisome Proliferator-Activated Receptors
PPRE	PPAR Response Elements
PVDF	Polyvinylidene Fluoride
qPCR	Real-time PCR
RISC	RNA-Iduced Silencing Complex
RNP-IP	Ribonucleoprotein Immunoprecipitation
RXR	Retinoid X Receptor
SA	Stearic Acid
SCD-1	Stearoyl-CoA Desaturase-1
SDS-PAGE	SDS-Polyacrylamide Gel Electrophoresis
SMase	Sphingomyelinase
SPT	Serine Palmitoyltransferase
SRE	Sterol Regulatory Element
SREBP-1c	Sterol Regulatory Element Binding Protein-1c
STAT3	Signal Transducer and Activator of Transcription 3
TAG	Triacylglycerol
TBS	Tris-Buffered Saline
TFR	Transferrin Receptor
TLR	Toll-Like Receptors
TNF	Tumor Necrosis Factor
TNFR1	TNF Receptor 1
TRAIL-R2	TRAIL Receptor 2
UPR	Unfolded Protein Response
VLDL	Very Low Density Lipoproteins
X5P	Xylulose 5-Phosphate
XBP1	X-box Binding Protein 1
αSMA	α Smooth Muscle Actin

ACKNOWLEDGEMENTS

First and foremost, I would like to thank my supervisor, Dr. Duygu Dee Harrison-Findik, for her mentorship through my graduate training. Despite my lack of experience, she took me in her laboratory and taught me from the very basics of scientific research and critical thinking. I am constantly inspired and encouraged by her strong enthusiasm in research and knowledge. I am thankful that she allowed me the freedom and resources to pursue my ideas, and, at the same time, helped me focus on the questions of great importance. To me, she is not only a mentor but a friend with great wisdom and experience of life. I owe every bit of my accomplishments to her mentorship.

I feel fortunate to have an especially supportive, knowledgeable and experienced supervisory committee. I thank the supervisory committee members for all their insightful suggestions during committee meetings and daily research. Especially, I thank Dr. Kusum Kharbanda for her help in the study of apoptosis and steatosis, Dr. Justin Mott for his advices during the investigation of post-transcriptional regulation, and Dr. Robert Bennett for his expertise on molecular biology and fibrosis.

I would like to thank the past and present members of the laboratory, Lisa Gerjevic, Jonathan Chaky and Emily Zmijewski for their support and company.

None of the achievements would be possible without the support from my loving family. I am thankful for the encouragement and support of my parents during all these years. I am especially grateful for the love and sacrifices of my wife, Xi Li, who had faith in me and our marriage even during the toughest time of my life.

Last but not least, I would also like to acknowledge the funding support from Graduate Studies Research Assistantships & Fellowships.

Chapter I

Introduction

Review of Nonalcoholic Fatty Liver Disease, Iron Metabolism and Hepcidin

1 GENERAL SUMMARY

Due to changes both in dietary and life style habits, the global rate of obesity has been increasing dramatically in the past two decades (1). According to the studies conducted in 2010, over one billion of the world's population, including developing countries, has been estimated to be overweight, with 475 million out of these classified as obese (1). In U.S.A., the prevalence of obesity in both men and women has been estimated to be above 35% (approximately 73.3million in total number) in the year of 2010 (2). These numbers are expected to increase further in the near future (3). Most dramatically, the rate of obesity in the adolescent population is increasing at an alarming rate (1).

Once considered as an advantage in ancient times when food resources were limited (4), obesity in our modern era is unfortunately recognized as a morbid state. Besides imposing a direct negative impact on the quality of life, obesity is also closely associated with metabolic syndrome (5). Metabolic syndrome is defined as a series of health conditions including excess body fat (in particular visceral adiposity), dyslipidemia and abnormal cholesterol levels, high blood sugar, insulin resistance, and hypertension, which acting in concert increase the risk for type 2 diabetes mellitus and cardiovascular disease.

Insulin resistance, a key feature of metabolic syndrome, is associated with changes in the secretion and signaling of the hormone, insulin (6). The β cells of pancreas are the major site of insulin production. Under normal physiological conditions, the increases in the level of blood sugar (often post-prandial) stimulate the secretion of insulin. Insulin released into the circulation modulates glucose and lipid metabolism in a wide range of metabolic tissues to maintain blood glucose at a normal level. The action of insulin is accomplished through its binding to insulin receptors, which are members of the receptor tyrosine kinase family and expressed on the plasma membrane of target cells. The formation of the insulin and insulin receptor dimer complex induces the auto-phosphorylation of tyrosine residues on the cytoplasmic receptor domains. This subsequently

results in phosphorylation of the insulin receptor substrates (IRS), IRS1 and IRS2, on tyrosine residues (7). IRS, in association with the activated lipid kinase, phosphoinositide 3-kinase (PI3K), further induces the phosphorylation and activation of the downstream protein kinase, PKB (a.k.a Akt). Insulin regulates glucose metabolism by inducing the translocation of insulin signaling-sensitive glucose transporters, such as GLUT4 in muscle and adipose tissue from the storage sites to the plasma membrane, and thereby stimulating the uptake and utilization of glucose by these metabolic tissues (8). In order to control and limit glucose output by the liver, insulin simultaneously stimulates the synthesis of glycogen and suppresses gluconeogenesis (9). In addition to glucose metabolism, insulin regulates lipid metabolism in the liver by inducing the expression of enzymes involved in de novo lipogenesis through the transcription factor, sterol regulatory element-binding protein-1c (SREBP-1c). On the other hand, insulin regulates lipid metabolism in the adipose tissue by both decreasing lipolysis via the inhibition of the hormone sensitive lipase (HSL) and stimulating lipogenesis (10). Taken together, these actions of insulin exert a total effect of maintaining a normal postprandial level of blood glucose in healthy individuals. However, in the condition of insulin resistance, as observed with obesity and metabolic syndrome, the effect of insulin is blunted. As a result, glucose uptake by the muscle and glycogen storage, but not gluconeogenesis, in the liver are inhibited. This in turn leads to a significant elevation of blood glucose levels and thereby contributes to hyperglycemia. Similarly, in an insulin-resistant state, the inhibition of HSL and lipolysis, and the increase in lipogenesis by insulin are compromised. These changes then trigger the increased breakdown of triglycerides and release of fatty acids into the circulation.

Liver is one of the first organs assaulted by the metabolic changes induced by insulin resistance and metabolic syndrome. The excess fat in the circulation due to insulin resistance, are taken up the by the liver resulting in fat accumulation (i.e. **steatosis**). The changes in liver insulin signaling also contribute to the elevated levels of de novo lipid synthesis in the liver.

The diagnosis of nonalcoholic fatty liver disease (NAFLD) is established when the level of steatosis exceeds 5% of the liver tissue (11) in patients with little or no alcohol consumption (12). NAFLD is therefore the hepatic manifestation of metabolic syndrome (13, 14). Analytical studies with NAFLD patients have shown that the major source of fat in the liver is the uptake of surplus fat from the circulation, due to adipose tissue lysis or excess dietary fat, accompanied by the increase in de novo lipogenesis (15). Liver disposes of its excess lipid content in the form of VLDL secretion (16) and fatty acid oxidation (17). Fatty acid oxidation also fulfills the energy requirements of this metabolically active organ. The imbalance between lipid input and output in the liver plays an important role in steatosis. The detailed molecular mechanisms of hepatic lipid accumulation in NAFLD are discussed in later sections (*see sections 2.6 of this chapter*).

NAFLD encompasses a spectrum of pathological conditions including steatosis, steatohepatitis, fibrosis, cirrhosis and hepatocellular carcinoma (12, 14, 18). Majority of NAFLD patients exhibit simple steatosis, which is currently considered to be a benign condition. However, if untreated, some of these patients can develop severe forms of nonalcoholic steatohepatitis (NASH), which is characterized by inflammation (steatohepatitis) and fibrotic changes due to the activation of stellate cells (12). A small percentage of NASH patients also present advanced stages of fibrosis and cirrhosis, which may ultimately lead to hepatocellular carcinoma and death (19).

The mechanisms of NAFLD/NASH disease progression has been under intense investigation in recent decades. The so-called “two-hit hypothesis” was quickly adopted from the pathogenesis of alcoholic liver disease (ALD) as a popular theory to explain NAFLD/NASH pathogenesis (20). As the name suggests, it describes the process in two consecutive steps. Namely, the “first-hit”, which is widely accepted to be insulin resistance (21), promotes the development of simple steatosis. In the absence of a second-hit, steatosis remains to be benign and does not progress to severe forms of disease. However, the presence of a further hit (i.e. second-hit), such as abnormalities in

mitochondrial function, oxidative stress, lipid peroxidation, or inflammatory cytokines and adipokines, then exacerbates hepatocellular injury and triggers NASH pathology (20–22).

In recent years, the "two-hit hypothesis" model of NAFLD/NASH pathogenesis has been challenged. First, it has been recognized that steatosis is the consequence of the interplay between multiple factors (i.e. insulin resistance, adipose tissue inflammation, and altered adipokine secretion) rather than a simple phenomenon which was previously defined as the "first hit" (23). As a result, a "multiple parallel-hits hypothesis" has been coined proposing that many progressive hits collectively contribute to the pathogenesis of NAFLD/NASH (24). Secondly, clinical observations have indicated that NASH is not always preceded by steatosis (23, 25). They questioned the initial notion that steatosis and NASH represent the early and advanced stages of NAFLD, respectively (23). It is feasible that the absence of typical NAFLD/NASH pathological features, especially in patients with advanced cirrhosis, might be due to the portosystemic shunting (26). Nevertheless, there is not enough direct evidence to support the sequential progression of NASH from simple steatosis (27).

Although the mechanisms of NASH has not been clearly understood, iron has been proposed to contribute to NASH pathogenesis. Being a transition metal, iron participates in the Fenton reaction resulting in the production of highly toxic hydroxyl radicals (*see section 3 of this chapter below for detailed overview*) (28). NAFLD patients frequently display elevated iron levels (29, 30), which have been shown to correlate with the severity of disease and fibrosis (31–33). Despite these observations, the regulation of iron homeostasis and how it contributes to the NAFLD/NASH pathogenesis are not well understood.

2 REGULATION OF LIPID METABOLISM IN HEALTH AND NAFLD

Lipids are a class of hydrophobic molecules with both structural and bioenergetics functions. Free fatty acids (FFA) are molecules consisting of a carbon chain with hydrogen atoms along the length, and a carboxyl group and a hydrogen atom at either ends of the chain (**Figure 1.1A**). Based on the

presence of single or double bonds in the carbon backbone, they can be classified as saturated (e.g. palmitic, stearic acid) or unsaturated (e.g. oleic acid) (**Figure 1.1A**). Triacylglycerols (TAG), which are present both in plant oils and animal fats in our diet, are comprised of three fatty acids joined by a glycerol molecule (**Figure 1.1A**).

Fatty acids serve as major energy storage molecules. Namely, the oxidation of fatty acid yields more ATP than any other biological substrate. Furthermore, fatty acids are important substrates for the production of other lipid intermediates such as sphingolipids, which are essential for membrane biogenesis and for the mediation of important intracellular signaling pathways.

As an endocrine organ, liver is important for the regulation of fatty acid metabolism. Under normal conditions, healthy humans store fatty acids mainly in the adipose tissue in the form of non-toxic triglycerides. In pathological conditions, liver takes over the burden of eliminating excess fatty acids from the circulation. Unesterified free fatty acids in turn induces apoptosis and lipotoxicity further activating certain cell signaling pathways, which lead to liver injury, as observed with NAFLD patients. Here we provide a brief review of hepatic lipid metabolism and signaling focusing on both physiological and NAFLD conditions.

2.1 Extrahepatic sources of fatty acids in the liver

Dietary fatty acids are one of the sources of fatty acids contributing to steatosis in the livers of NAFLD patients (15). In the postprandial state, TAG obtained as dietary fats are hydrolyzed by various lipases, which are present in the lumen of the intestine, to release free fatty acids (FFA). FFAs are taken up by the absorptive enterocytes (34) to be re-synthesized into TAG in the endoplasmic reticulum (ER) and packaged into chylomicrons (**Figure 1.1B**). Chylomicrons are subsequently secreted into the blood stream through the lymphatic circulation. Lipoprotein lipases (LPL) present in the peripheral vascular beds can lyse TAG within the chylomicrons to release fatty acids to both the local tissues and blood (35). After losing part of their TAG content, chylomicrons

are converted to remnant particles, which are smaller in size. These remnants are then readily taken up by the liver (36) (**Figure 1.1B**).

The specific mechanisms of fatty acid uptake into hepatocytes are not well understood. Passive diffusion (37), and fatty acid transporters such as fatty acid transport proteins (FATPs) and fatty acid translocase (FAT/CD36) (38, 39), are believed to play a role in this process. Under physiological conditions, hepatocytes also store limited amount of triglycerides in the form of small lipid droplets for immediate energy requirements (40). Lipid droplets are decorated with families of lipid-droplet surface proteins on the phospholipid monolayer, including perilipin and cell-death-inducing DFFA-like effector (Cide). It is believed, that the presence of perilipins restrict lipolysis under basal conditions whereas their phosphorylation by protein kinase A stimulates lipolysis (41, 42). Among the three isoforms of Cide proteins (Cidea, Cideb and Cidec), Cidec, also known as FSP27, is highly expressed in the white adipose tissue (43). The important role of DICEC/FSP27 in lipid storage was underlined by the observations that overexpression of FSP27 resulted in triglyceride accumulation whereas FSP27 knockdown decreased the size of lipid droplets (44).

In cases of energy deprivation, such as fasting, the lipolysis activity of the adipose tissue is elevated to supply fatty acids as an energy source for relevant tissues (41). The enzyme, adipose triglyceride lipase (ATGL) specifically catalyzes the hydrolysis of TAG to produce diacylglycerol (DAG) and fatty acids. The enzyme, hormone-sensitive lipase (HSL) can then release additional fatty acids from DAG (**Figure 1.1B**). Releasing of the first fatty acid is the rate-limiting step in this reaction, and free fatty acids released into the circulation are bound by albumin for the uptake into hepatocytes.

2.2 Hepatic lipogenesis

In NAFLD patients, de novo lipogenesis (i.e. freshly synthesized lipids within the liver) also contributes to steatosis (15, 45). Under non-pathological conditions, such as dietary carbohydrate supply exceeding the capacity of the liver for glycogen storage, substrates are diverted to pathways

of free fatty acid synthesis within the liver (**Figure 1.1B**) (46). The de novo lipogenesis (DNL) pathway has been extensively studied (36, 47) and will be described here briefly . The catabolism of glucose through the tricarboxylic acid cycle yields citrate, which is subsequently transported to the cytosol and converted to acetyl-CoA. The enzymes, acetyl-CoA carboxylase (ACC) catalyze the conversion of acetyl-CoA to malonyl-CoA. Malonyl-CoA, which serves as a two-carbon donor, is added to the acetyl-CoA primer by the enzyme, fatty acid synthase (FAS). Palmitic acid (PA) is the primary product of FAS. Palmitic acid precursor can be elongated by two carbon atoms to produce the saturated FA, stearic acid. The desaturation of saturated FA, which is catalyzed by stearoyl-CoA desaturase-1(SCD-1), yields unsaturated FA, such as oleic acid. (48).

Insulin regulates mRNA expression of lipogenic genes through the activation of the transcription factor, sterol regulatory element binding protein-1c (SREBP-1c). SREBPs are considered to be the master transcriptional regulators of genes involved in lipid metabolism (49). This family consists of three members, SREBP-1a, SREBP-1c and SREBP-2. SREBP-1c is the predominant isoform responsible for the regulation of lipogenic genes in the liver (49). Insulin signaling regulates SREBP-1c both at the transcriptional and post-translational levels. The newly synthesized SREBP precursor is anchored at ER membrane (50) in association with both the SREBP cleavage activating protein, SCAP and the ER-retention protein, Insig (51). The activation of SREBP requires its dissociation from Insig and subsequent translocation to the Golgi apparatus. In Golgi, SREBP-1c protein is cleaved and its active N-terminal fraction released to be imported into the nucleus (52). The suppression of Insig-2a (53) and SREBP-1c phosphorylation by Akt are important steps in insulin-signaling-mediated processing of SREBP-1c. Furthermore, insulin up-regulates the nuclear translocation of SREBP-1c through the activation of mammalian target of rapamycin complex 1 (mTORC1), a nutrient- and growth factor-responsive kinase (54). Activation of transcription factors, such as liver X receptors (LXRs) (55) and SREBP-1c itself (56) are also believed to be mechanisms by which insulin can up-regulate SREBP-1c at the transcriptional level. Most of

SREBP-1c targets genes, such as acetyl-CoA carboxylase (ACC) and fatty acid synthase (FAS), participate in de novo fatty acid synthesis pathway and harbor sterol regulatory element (SRE) DNA-binding sequences in their promoters (49).

Glucose modulates the expression of genes involved in lipogenesis through the activation of the transcription factor, carbohydrate response element binding protein (ChREBP). The phosphorylation of ChREBP and its physical interaction with other molecules allows it to sense the level of intracellular glucose (49). Under basal conditions, when intracellular glucose levels are normal, ChREBP is phosphorylated by both by the cAMP-dependent protein kinase (a.k.a. protein kinase A, PKA) and the AMP-activated protein kinase (AMPK) (57, 58). When glucose levels are elevated, this leads to the stimulation of the pentose phosphate pathway and thereby the production of xylulose 5-phosphate (X5P). X5P subsequently activates protein phosphatase 2A (PP2A). Following dephosphorylation by PP2A, ChREBP is activated and translocates to the nucleus (59). Besides the post-translational modifications, the activity of ChREBP as a glucose sensor is mediated by intramolecular interaction between the low glucose inhibitory domain (LID) and a glucose response activation conserved element (GRACE) of ChREBP. When the glucose level is low, the interaction between LID and GRACE inhibits the DNA-binding activity of ChREBP. However, with high levels of glucose , this inhibition is eliminated resulting in ChREBP activation (58, 60). Activated ChREBP then binds to the promoters of genes, which are involved in glycolysis and lipogenesis, and activates their transcription (49).

2.3 Hepatic fatty acid secretion

Very low density lipoproteins (VLDL) are a class of lipoproteins important for lipid transport in the liver. Triglycerides accumulated in the liver are primarily exported via VLDL secretion to prevent steatosis (**Figure 1.1B**). Similar to chylomicrons in the intestine (*see section 2.1 above*), the assembly of VLDL requires apolipoprotein B (apoB) as the scaffold protein. Following its synthesis, the liver-specific form of apolipoprotein B, apoB-100, is translocated across the ER

membrane into the lumen and subsequently lipidated by microsomal triglyceride transfer protein (MTP) to form the primordial VLDL particles (61). Through the physical interaction, MTP stabilizes the newly synthesized apoB-100 (62, 63). Accordingly, in the absence of MTP, apoB-100 is not optimally lipidated and becomes prone to proteasomal degradation (64). Furthermore, liver-specific deletion of MTP in mice has been reported to cause a significant decrease in VLDL synthesis accompanied by an increase in cytosolic fat droplets (65). The primordial VLDL particles subsequently fuse with the triglyceride-rich particles to form the mature VLDL particles (61).

The expression of MTP is directly associated with VLDL secretion and is therefore frequently employed as marker for the study of hepatic lipid secretion (66). The promoter of MTP gene harbors multiple DNA-binding sites including hepatic nuclear factor-1 and 4 (HNF-1 and 4) response element, direct repeat (DR) 1, forkhead box (FOX), and sterol and insulin response elements (SRE/IRE). The binding of transcription factors, HNF-1α and 4α are important for the basal transcriptional expression of MTP (67–69). The agonists of PPARα are believed to stimulate MTP expression through the DR1 sequence in its promoter (70). Both the FOX and SRE/IRE response element sites have been suggested to mediate the inhibitory effect of insulin on MTP transcription (71, 72), It should however be noted that it is unclear whether insulin plays a significant role in the regulation of MTP expression and VLDL secretion because various experimental models of hyperinsulinemia display strong MTP promoter activity (73–75). Furthermore, excess dietary sucrose, fructose or fat supply induce MTP expression through yet unidentified mechanisms (75, 76).

2.4 Hepatic fatty acid oxidation

Besides the synthesis or transport, oxidation of fatty acids is also an important component of hepatic lipid metabolism (**Figure 1.1B**). Liver is the central organ for fatty acids oxidation, which is the major pathway for fatty acid disposal and energy production. Of the three organelles, namely mitochondria, peroxisomes and ER, which participate in the oxidation of fatty acids, mitochondrial

β-oxidation pathway plays the most prominent role (36). When lipolysis is stimulated under non-pathological (e.g. fasting) or pathological (e.g. insulin resistance) conditions, fatty acids are activated to acyl-CoA esters and shuttled into the mitochondrial matrix. The carnitine-palmitoyl-transferase (CPT) system facilitates the transport of acyl-CoA into mitochondria in a two-step reaction (36). The enzyme, CPT1, which is located at the outer membrane of mitochondria, converts acyl-CoA to acylcarnitines. CPT1 catalyzes the rate-limiting step of β-oxidation (77) and its activity is inhibited by malonyl-CoA, a metabolic intermediate in the lipogenesis pathway (*see section 2.2 above*). Acylcarnitines are then transported across the mitochondrial inner membrane via the enzyme, carnitine acylcarnitine translocase. The enzyme, CPT2, which is localized in the mitochondrial inner membrane, then catalyzes the reverse reaction to restore CoA group to acylcarnitines. The released carnitines are subsequently used for the next round of shuttling reactions. Once inside the mitochondrial matrix, acyl-CoA carbon chain is shortened by 2 carbons at a time through a four-step β-oxidation reaction to produce acetyl-CoA.

Peroxisome proliferator-activated receptor α (PPARα) is the major transcription factor participating in the regulation of genes related to fatty acid uptake and oxidation. Peroxisome proliferator-activated receptors (PPARs) are a group of nuclear receptors and transcription factors belonging to the steroid receptor superfamily (78). PPAR family contains three isoforms, PPARα, PPARβ/δ, and PPARγ. The liver and other organs with high FA oxidation capacity mainly express the isoforms, PPARα and PPARβ/δ (79). PPARα is activated by lipid intermediates, which arise from the lipogenesis and lipolysis pathways, and fatty acid catabolism pathways (80). Upon activation, PPARα forms heterodimers with another nuclear receptor, retinoid X receptor (RXR) (80). Together with other co-activators (80), the PPARα/RXR heterodimer complex activates the transcription of the target genes involved in the regulation of FA transport and β-oxidation by binding to PPAR response element (PPRE) in their promoters (81). PPARα promotes fatty acid uptake by up-regulating the expression of FA transporters, such as FATP1 and FAT/CD36 (82, 83).

Moreover, PPARα activates mitochondrial β-oxidation by controlling the transcription of rate-limiting enzymes, CPT1 and CPT2 (84, 85). In addition, PPARα regulates the transcription of SREBP-1c , thereby controlling lipogenesis (86). Although PPARβ/δ are not highly expressed in the liver, their levels have been suggested to be elevated in steatotic livers (87). They might act in concert with PPARα in the transcriptional regulation of genes responsible for hepatic lipid metabolism (87). In addition, PPARγ is highly expressed in fat tissues and plays a major role in the maintenance of lipid homeostasis by controlling lipogenesis in the white adipose tissue (88). The participation of PPARβ/δ and PPARγ in the pathogenesis of steatosis is currently being investigated.

2.5 Lipid derivatives in the liver

Besides fatty acids, fat accumulation in the liver gives rise to other lipid derivatives such as lysophosphatidic acid and ceramide (**Figure 1.1B**). However, the involvement of these intermediates in NAFLD pathogenesis is not well understood. We were particularly interested in ceramide because of its connection to saturated fatty acids. Ceramide belongs to the sphingolipid family of lipids. This family is unique in that besides their traditional role as structural molecules for membrane biogenesis, they have recently been recognized as intracellular second messengers. One of the pathways for ceramide (and other sphingolipid) synthesis, is so-called “de novo synthesis pathway”, which utilizes saturated fatty acid, especially palmitic acid, as the starting substrate (**Figure 1.2**). Ceramide is synthesized through a four-step reaction catalyzed by enzymes localized in the ER (89). Serine palmitoyltransferase (SPT), which transfers a serine residue to palmitoyl-CoA to produce 3-keto-sphinganine is the rate-limiting enzyme of de novo ceramide synthesis pathway. Ceramide can further be modified to produce other species of the sphingolipid family (**Figure 1.2**). In addition to the de novo pathway, two other alternative pathways exist for ceramide biosynthesis. One of them is the “sphingomyelinase (SMase) pathway”, which hydrolyses sphingomyelin located in the cell membrane for the rapid production of ceramide. The other

pathway known as the “salvage pathway” recycles ceramide from the catabolism of sphingolipids (**Figure 1.2**) (90).

The rate of de novo ceramide synthesis is correlated with the availability of its substrate. The activity of SPT, which catalyzes the rate-limiting first step of the de novo ceramide synthesis pathway, is stimulated by serine and palmitoyl-CoA (91). Both endotoxin (i.e. lipopolysaccharide, LPS) and inflammation have been shown to be involved in the pathogenesis of NAFLD. The family of toll-like receptors (TLR) are important for the regulation of innate immune responses and each member is activated by different ligands (92). TLR4 is activated by the binding of LPS but besides LPS, saturated fatty acids also serve as natural ligands for TLR4 (93). Moreover, the activation of TLR4 by saturated fatty acids and LPS up-regulates the expression SPT, the enzyme required for de novo ceramide synthesis (94). This up-regulation is dependent on the activation of pro-inflammatory kinase, IKKβ, which is part of the TLR-specific signaling cascade (94). Inflammatory cytokines, in particular TNF-α, have been shown to stimulate the activity of sphingomyelinase (SMase) for the rapid production of ceramide (95, 96). Ceramide production in NAFLD and diabetes patients is elevated, and the increase in ceramide production has been shown to contribute to the pathogenesis of metabolic diseases. Patients with type 2 diabetes exhibit elevated ceramide content in the serum (97, 98) and skeletal muscle (99) . Hepatic steatosis correlates with over-production of ceramide in the adipose tissue (100). High-fat diet-intake has been shown to increase hepatic ceramide content in animal models (101, 102). Weight loss in NASH patients has also been reported to lead to the suppression of genes, which are related to ceramide production (103).

2.6 Mechanisms of hepatic lipid accumulation in NAFLD

Steatosis, as observed in the livers of NAFLD patients, develops as a result of both hepatic and systemic dysregulation of lipid metabolism, which cannot be compensated by the lipid oxidation and export capacity of the liver (12). Although obesity and insulin resistance cause changes in lipid

metabolism, there are other factors, which make the liver conducive to excessive accumulation of hepatic triglycerides. Here, we briefly review the changes which contribute to hepatic steatosis by focusing on major players relevant to this process.

In obese individuals, the adipose tissue is significantly expanded by increases in both adipocyte mass and synthesis. Visceral adiposity induces an inflammatory state and macrophages are infiltrated into the adipose tissue. This results in an increase in both the local and systemic expression of inflammatory cytokines and adipokines (104). Inflammatory cytokines inhibit insulin signaling and are therefore considered to be one of the major contributors of insulin resistance in obesity (105). Insulin resistance in adipose tissue impairs the inhibitory effect of insulin on the enzyme activity of hormone-sensitive lipase (HSL) (10). As a result of this, the rate of lipolysis is elevated despite the presence of high levels of insulin in the circulation (**Figure 1.3**). In agreement, NAFLD patients have been shown to exhibit an increase in the lipolysis activity of their subcutaneous adipose tissues (106). By using stable-isotope labeling method, Donnelly et al. have analytically demonstrated that in NAFLD patients, about 60% of hepatic triglyceride content originates from the uptake of fatty acids originating from the adipose tissue. This study further emphasizes the importance of adipocyte lipolysis in the development of hepatic steatosis (107).

Dietary fat is another prominent source of hepatic triglycerides (**Figure 1.3**). Based on the species and structure, the dietary fats are usually categorized as polyunsaturated, monounsaturated, and saturated fatty acids, and trans-fats (12). In animal models fed with different compositions of high-fat diets, it has been demonstrated that saturated and monounsaturated, but not polyunsaturated fatty acids, are capable of inducing hepatic steatosis (108). The effect of saturated fats was further confirmed by a number of other studies using both animal models and tissue culture cells (109, 110). In a retrospective study comparing the dietary composition of NASH patients with age and BMI-matched controls, NASH patients consumed significantly higher amounts of saturated fats

from their diet (111). Trans-fats, which commonly exist in modern diets, have also been shown to cause NASH in rodent models (112).

Both adipose tissue lipolysis and dietary fat absorption elevate the level of circulating fatty acids, which are taken up by the liver. The differential expression of the fatty acid transporter, FAT/CD36, in the livers (i.e. elevated) and adipose tissues (i.e. decreased) of NAFLD patients, compared to controls (113, 114), strongly points out a role for hepatocyte transporters in elevated fatty acid uptake.

The increased rate of freshly synthesized lipids within the liver (i.e. de novo lipogenesis) also adds to the burden of hepatic triglyceride accumulation (**Figure 1.3**). Isotope studies with NAFLD patients pointed out that 26% of the liver triglycerides derive from de novo lipogenesis, compared to 5% in normal control individuals (15, 115). De novo lipogenesis is regulated by both blood glucose and insulin levels through the transcription factors, ChREBP and SREBP-1c, respectively (*see section 2.2 above*). Peripheral insulin resistance hampers the uptake and utilization of glucose in metabolic tissues (e.g. muscle), and consequently causes hyperglycemia. In addition, the hepatic insulin-resistance further increases the levels of blood glucose by both activating gluconeogenesis and suppressing glycogenesis (9). Increased glucose levels activate ChREBP, which subsequently actives the expression of the enzymes participating in lipogenesis. Accordingly, the deletion of ChREBP in mice significantly decreased the expression of a variety of genes involved in lipogenesis (116). Overexpression of ChREBP, on the other hand, stimulated the expression of lipogenic genes resulting in steatosis (117). Furthermore, steatosis level in NASH patients has been shown to correlate with elevated hepatic ChREBP expression (117). Taken together, these studies highlight the significance of ChREBP in lipogenesis and thereby steatosis, as observed in NAFLD patient livers. In addition to glucose, insulin stimulates lipogenesis by activating the transcription factor, SREBP-1c. However, the studies with both the experimental rodent models and NAFLD patients have shown, that despite the presence of insulin resistance, hepatic up-regulation of

SREBP-1c was not affected (118, 119). In a mouse model of steatosis, the absence of SREBP-1c ameliorated fatty liver phenotype (120) further supporting the importance of SREBP1-c in steatosis.

Oxidation of fatty acids is essential to satisfy the energy requirements for metabolic functions and to maintain lipid homeostasis in the liver (121). In agreement, mice with disrupted expression of β-oxidation genes developed hepatic steatosis (122, 123). As mentioned earlier, PPARα is a central player in the regulation of β-oxidation. In a genetic rat model of NAFLD, agonists of PPARα significantly alleviated steatosis (124). This improvement was associated with the up-regulation of a spectrum of genes involved in β-oxidation. In NAFLD patients, CPT1, the rate-limiting enzyme of mitochondrial β-oxidation, was down-regulated (113). In addition, the livers of NAFLD patients displayed abnormalities in mitochondrial structure and function, suggesting disturbances in the mitochondrial β-oxidation pathway in these livers (125–128).

VLDL secretion is responsible for the export of extra triglycerides from the liver. Inhibition of MTP, the key enzyme of VLDL assembly and secretion, results in hepatic lipid accumulation (129). As supported by multiple studies, the level of VLDL secretion is elevated in NAFLD patients compared to control individuals (121, 130, 131). It should however be noted, that the initial linear increase in VLDL secretion in correlation with hepatic lipid content has been shown to reach a plateau without further increase in VLDL secretion despite elevated hepatic triglyceride loading (121). This saturation phenomenon might be due to the limited capability of the liver to secrete large VLDL particles (121).

In summary, the development of hepatic steatosis occurs as a net result of the overwhelmed capacity of the liver for lipid oxidation and secretion in concert with an increase in the overall rate of hepatic lipid uptake and de novo synthesis (**Figure 1.3**).

2.7 Lipid-mediated signaling pathways in NAFLD

Hepatic steatosis compromises the metabolic processes in the liver and sensitizes hepatocytes to secondary insults, such as mitochondrial dysfunction, oxidative stress, ER stress, apoptosis and inflammation (12). The accumulation of triglycerides in the form of lipid droplets is not detrimental per se but rather considered to be both a protective response and a measure of the lipid burden in hepatocytes (132). Indeed, the inhibition of triglyceride production alleviates steatosis but exacerbates the level of fibrosis and injury in the liver (133). Free fatty acids and other lipid intermediates are considered to be the most harmful lipid species in hepatocytes (132, 134). In this section, a brief summary of the signaling events induced by fatty acids and the lipid derivative, ceramide will be discussed.

2.7.1 Fatty acid-induced signaling

i- Fatty acid-induced apoptosis

The word apoptosis, derived from a Greek word meaning “leaves falling from a tree” (135), describes a specific type of programmed cell death process characterized by membrane blebbing, shrinkage of the cell, chromatin condensation, nuclear fragmentation and the formation apoptotic bodies (136). Apoptosis can be induced either through the binding of a death ligand to a specific cell surface receptor (i.e. extrinsic pathway) or the leakage of cytochrome *c* through the mitochondrial outer membrane (i.e. intrinsic pathway) (137). Death receptors, including tumor necrosis factor (TNF)-α receptor, TNF-related apoptosis-inducing ligand (TRAIL), and Fas are highly expressed at a basal level in healthy hepatocytes (137). Binding of the corresponding ligand to the receptor stimulates the cleavage and activation of cysteine-aspartic proteases called initiator caspases, which include caspase 8 and 10. These caspases then activate the downstream caspases, caspases 3, 7 and 6 for the execution of the apoptotic process (136). The intrinsic apoptotic pathway, which is initiated when the pro-apoptotic Bcl-2 family proteins, such as Bax and Bak, permeabilize the mitochondrial outer membrane and release cytochrome *c*. Cytochrome *c* subsequently activates

caspase-9, which then activates the executioner caspases (i.e. caspase 3, 7 and 6). The activation of apoptosis in hepatocytes requires the cross-talks between the extrinsic and the intrinsic pathways through the cleavage of BH-3 only protein, Bid, which facilitates the leakage of cytochrome *c* (136).

Fatty acids, in particular saturated fatty acids, induce apoptosis (i.e. lipoapoptosis) in various cell types including hepatocytes (138, 139). The differences between the efficacy of saturated and unsaturated fatty acids to induce apoptosis might be due to their innate properties. Namely, unsaturated fatty acids are more readily esterified to form triglycerides, which decreases their toxicity (140). In fact, unsaturated fatty acids rescue apoptosis induced by the saturated fatty acid, palmitate by enhancing the conversion of palmitate to triglyceride (134). In hepatoma cells, fatty acid-induced apoptosis is dependent on the phosphorylation of c-Jun N-terminal kinase (JNK), which directly activates the proapoptotic Bcl-2 family of proteins (139). Moreover, JNK mediates saturated fatty acid-induced up-regulation of death receptor expression in hepatoma cells, and thus sensitizes the cells to further insult via the death (141). In addition, saturated fatty acids also induce ER stress, which plays an essential role in the induction of lipoapoptosis, as shown in hepatoma cells (142, 143). In NAFLD patients with severe form of disease, lipoapoptosis in hepatocytes of the liver is accompanied by an increase in the expression of cell surface death receptors (144, 145). Furthermore, the presence of plasma markers specific for hepatic apoptosis in NAFLD patients have been proposed to be strong and independent predictors of NASH (146).

ii- Fatty acid-induced protein kinase C activation

A role for lipid-mediated activation of protein kinase C (PKC) signaling has been proposed in metabolic syndrome and NAFLD (147). Based on the requirement for diacylglycerol (DAG) and/or calcium (Ca^{2+}) for enzymatic activity, PKC isoforms are categorized into three groups; classical (PKCα, β, and γ), novel (PKC ε, η and θ) and atypical (PKC ζ and λ) kinases (148). The activation of classical PKC isoforms requires both Ca^{2+} and DAG, while the novel PKC isoforms require only DAG. Atypical PKC isoforms do not require DAG or Ca^{2+} for enzymatic activity (149). G protein-

coupled receptors and receptor tyrosine kinases, which are the classical PKC activators, induce the hydrolysis of phosphatidylinositol 4, 5-bisphosphate via phospholipase C for the production of DAG. DAG then activates specific PKC isoforms, as mentioned above (150). However, in cases of insulin resistance and metabolic syndrome, DAG levels are increased due to elevated de novo lipogenesis and fatty acid production (151, 152). Feeding of rodents with high-fat diets has been shown to result in increased hepatic DAG levels and the activation of PKC was associated with the development of insulin resistance (153). In a mouse model where NASH was induced by the administration of a methionine-and choline-deficient (MCD) diet, the levels of PKC activation were elevated in the liver (154). Similarly, in hepatoma cells, saturated, but not unsaturated, fatty acids induced production of DAG, which was accompanied by the activation of PKC (155, 156). The molecular mechanisms of PKC activation and its contribution to NAFLD pathogenesis are not completely understood. Nevertheless, a role for PKC, in particular novel class PKC isoforms (e.g. PKC ε), in insulin resistance has been proposed (147). A study conducted with liver biopsies from patients undergoing bariatric surgery has shown that hepatic DAG and PKCε content are the strongest predictors of insulin resistance (157). Furthermore, a rat model of PKCε knockdown was protected against high-fat-feeding-induced hepatic insulin resistance (158). PKCε has also been reported to inhibit insulin signaling through its integration with the insulin receptor and impairing its kinase activity (158).

2.7.2 Ceramide-induced signaling

In connection with lipid accumulation and inflammatory signaling, the production of lipid derivative, ceramide is stimulated in NAFLD livers (*see section 2.5 of this chapter*). Patients with type II diabetes have also been reported to exhibit elevated levels of ceramide in the blood stream (97, 98). There are only limited number of studies showing ceramide production in the livers of NAFLD patients (159). The liver however has been suggested to be a key organ for ceramide synthesis (90). Similarly, studies with high-fat diet-fed mice have also reported elevated hepatic

ceramide content (101, 102). The precise role of ceramide in the pathogenesis of NAFLD and metabolic syndrome are not well understood. Some studies have shown that ceramide, by antagonizing Akt (i.e. insulin) signaling, can participate in the development of insulin resistance in skeletal muscle and fat tissues (160, 161). Other studies have reported the involvement of ceramide in different signaling pathways related to inflammation. In an *in vitro* model of human fibroblasts, JAK/STAT3 signaling pathway has been shown to be activated by elevated ceramide levels, which was dependent on JAK2 kinase isoform (162). Similarly, the DNA-binding activity of NF-κB has been shown to be stimulated by ceramide treatment of various cancer cell lines (163, 164). Furthermore, ceramide and its derivatives have been shown to activate NF-κB in HepG2 human hepatoma cells (165). Studies using tissue culture cells have reported a role for stress-activated kinase, JNK in mediating the effects of ceramide analogs (166–168). The signaling pathways activated by ceramide in hepatocytes will be further discussed in later chapters (*see chapter V*).

3 REGULATION OF IRON METABOLISM AND ITS RELATIONSHIP TO NAFLD

This section will provide a brief review of iron physiology and the proteins involved in the regulation of iron homeostasis with an emphasis on the role of central iron regulator, hepcidin. The relationship of iron to NAFLD pathogenesis will also be discussed.

3.1 Physiology of Iron

Iron is an essential element for all living organisms from bacteria to humans (169). An adult human body contains an average of 3 to 4 g of iron per kg of body weight distributed in different parts of the body (170). Most of it is integrated into hemoglobin for red blood cell synthesis in bone marrow. As red blood cells are essential for the tissue delivery of oxygen, iron is connected with cellular respiration. Similarly, iron is also utilized for the synthesis of muscle oxygen-binding protein, myoglobin. Oxygen is required for aerobic respiration in mitochondria to generate ATP. Enzymes in the electron transport chain of aerobic respiration harbor conserved iron sulfur (Fe-S) clusters, which are important for their biological function. Iron is also associated with DNA replication,

DNA repair, cell cycle and growth. Ribonucleotide reductase is a pivotal enzyme for DNA synthesis and needs iron as a cofactor for optimal activity. In mammalian cells, iron deprivation has been shown to attenuate ribonucleotide reductase activity and arrest cell growth (171).

Iron however can act like a double-edged sword. Despite being indispensable for fundamental biological functions, as mentioned above, excess free iron can also be deleterious. As a transition metal, iron shuttles between ferric (Fe^{3+}) and ferrous (Fe^{2+}) forms by accepting and donating electrons, and takes part in Fenton reaction. The interaction of iron with H_2O_2 results in the production of a highly reactive oxygen species called hydroxyl radical (•OH) (28). •OH can attack DNA backbone and other macromolecules including proteins and lipids thereby causing lipid peroxidation, DNA damage and injury to cellular membranes (172). The levels of iron in the human body must therefore be tightly regulated.

The regulation of iron homeostasis is achieved at multiple sites in the body (173). Dietary iron is absorbed by the enterocytes in the duodenum. On the other hand, macrophages of the reticuloendothelial system are responsible for recycling iron from hemoglobin by phagocytosing senescent erythrocytes. The transport of iron in the circulation is carried out by the transferrin protein (174). One molecule of transferrin has the capacity to bind two atoms of Fe^{3+}. This facilitates safe transport of iron to distant organs via transferrin binding to transferrin receptors 1 and 2. Transferrin receptor 1 is ubiquitously expressed whereas transferrin receptor 2 is primarily expressed in the liver. Transferrin receptor 2 displays less affinity for transferrin compared to transferrin receptor 1 (175).

The liver is an important organ for iron metabolism for various reasons some of which will be discussed later. Most importantly, the liver carries the major burden of iron overload by serving as the prominent storage organ for excess iron, and thereby protecting the body from its harmful effects (176). Tissue iron is stored in the iron-storage protein, ferritin. Each ferritin molecule has the capacity to store up to 4,500 atoms of Fe^{3+} in its spherical structure, which is available for

recycling (177). Both transferrin and ferritin proteins are also frequently used in the clinic as diagnostic markers to assess the iron status of patients. In the last two decades, novel proteins such as multi-transmembrane iron transporter proteins and soluble regulators have been discovered, which revolutionized our understanding of iron metabolism. These proteins will be discussed below.

3.2 Iron import and export pathways

Iron from the diet is absorbed mostly in the form of inorganic ferric iron or heme on the apical site of enterocytes in the duodenum (173). The intestinal uptake of dietary heme is not well understood. A role of heme carrier protein 1 (HCP1) has been suggested (178) but the specificity of HCP1 for heme uptake is controversial. The iron is subsequently released from the heme molecule via heme oxygenase-1 (HO-1) (179). On the other hand, the mechanisms of inorganic iron uptake are well defined. Prior to uptake, ferric iron is reduced to soluble ferrous iron by a ferric reductase on the apical surface of enterocytes (180). The apical divalent metal transporter 1 (DMT1) is then responsible for the transport of ferrous iron into the enterocyte (181). DMT1 is a Fe^{2+}/H^{+} co-transporter (182), and its transport of Fe^{2+} is dependent on a proton gradient. Once within the enterocyte, iron is either incorporated into ferritin (*see above*) for intracellular storage or exported via the basolateral site into to the circulation. Basolateral iron export is accomplished by the only known mammalian iron exporter protein, ferroportin. DMT1 and ferroportin have similar structures, both being multi-transmembrane proteins (173).

Unlike enterocytes, macrophages of the reticuloendothelial system take up iron via phagocytosis, and digestion of senescent erythrocytes (*see above*). Iron released from heme molecules via HO-1 is subsequently exported by ferroportin. Due to its overlapping role in different organs, ferroportin is a major determinant of circulating iron levels. The regulation of this iron exporter was better understood after the discovery of the central iron-regulatory hormone, hepcidin. The interaction between ferroportin and hepcidin resembles the interaction of a circulatory hormone (i.e. hepcidin) with its receptor (ferroportin), which will be discussed further below.

3.3 Hepcidin, the key iron regulatory hormone

Since iron homeostasis is regulated at multiple distant sites, the presence of soluble factors, which play a key role in controlling the cross-talk between these sites, was long suspected. This hypothesis was confirmed by the discovery of hepcidin. The fact that hepcidin is mainly synthesized in hepatocytes also gave the liver center stage in the regulation of iron metabolism (**Figure 1.4**).

Hepcidin was discovered independently by different laboratories (183–185). Krause et al. and Hunter et al. have identified hepcidin as a small peptide with weak antimicrobial activity in the human blood ultrafiltrate (183) and urine (184), respectively. The involvement of hepcidin in iron metabolism was indicated by Pigeon et al., who have shown the induction of hepcidin mRNA in a mouse model with iron loading (185). Interestingly, the coincidental disruption of surrounding chromosomal regions in a USF2 knockout mouse model (186) has been reported to result in iron overload. This observation then led to the discovery that, hepcidin gene (*HAMP*), which was co-deleted due to its proximity to USF2 gene (185), is responsible for the regulation of iron homeostasis. A direct role of USF2 in iron regulation was however excluded because a USF2 knockout mouse model from another laboratory, which does not have disruption of *HAMP* gene, does not display an iron overload phenotype (187). The important role of *HAMP* in iron metabolism was also supported by human studies with primary genetic iron overload disorders. Mutations in *HAMP* gene was identified in patients with juvenile hemochromatosis, a severe early-onset form of genetic iron overload disorder associated with hemojuvelin (HJV) gene (188). Similarly attenuated *HAMP* expression, which was unresponsive to oral iron administration, was observed in genetic hemochromatosis (GH) patients harboring mutations in GH gene, Hfe (189). The regulation of hepcidin by iron and its effect on iron homeostasis has been depicted in **Figure 1.5**.

Although humans express a single hepcidin gene, *HAMP*, mice expresses two hepcidin genes, *Hamp* and *Hamp2*. Various studies, including the one from our laboratory (190), indicate, that *Hamp* mouse gene is the equivalent of human *HAMP* gene regarding the regulation of iron

metabolism (187, 191). Overexpression of *Hamp*, but not *Hamp2*, resulted in severe iron deficiency and anemia (187, 191). Studies with different *Hamp* and *Hamp2* knockout mouse lines generated in our laboratory have also shown, that further ablation of *Hamp2* gene in *Hamp* knockout mice did not exacerbate the iron-overload phenotype observed with *Hamp* deletion (190).

Hepcidin is synthesized as an 84 amino acid pre-prohepcidin protein with an N-terminal 24-amino acid signal sequence, which is cleaved to yield prohepcidin protein (173). The prohepcidin precursor protein is subsequently cleaved by proteases, such as furin-like prohormone convertases (171), at the C-terminus to form the 25-amino acid mature, hepcidin peptide. This soluble form is released into the circulation to function as a biologically active protein (**Figure 1.6**). Furthermore, shorter (truncated at the N-terminal) forms of 20- and 22-amino acid hepcidin peptides have been detected in human serum and urine (184, 192).

Hepatocytes are the major site of hepcidin synthesis (193). Other cell types such as adipocytes in obesity (194) and macrophages (195) have been reported to exhibit very low levels of hepcidin mRNA expression. In accordance with the importance of hepatocytes as the major site of synthesis, liver-specific hepcidin knockout mice have been shown to display similar levels of systemic iron-overload as the global hepcidin knockout mice, which lacked hepcidin expression in all of the organs (190, 196).

Biologically active hepcidin peptide harbors intramolecular disulfide bridges. It adopts a simple hairpin structure with 4 disulfide bonds forming between the 8 cysteine residues (197). The five N-terminal amino acids are critical for the biological function of hepcidin (198). By contrast, the disruption of the C-terminal amino acids and the mutation of any of the cysteine residues have been reported to exert negligible effects on the function of hepcidin (198).

The mechanistic insight into the function of hepcidin in iron metabolism was first described by Nemeth et al. (199). Using a stable cell line expressing GFP-tagged ferroportin, they have shown

that hepcidin induced the internalization and lysosomal degradation of ferroportin on the plasma membrane through a direct and specific interaction, which resembled the binding of a ligand to its receptor. Further reports have shown that hepcidin-induced internalization of ferroportin is dependent on tyrosine phosphorylation, while the degradation process involved ubiquitination (200). By inducing the degradation of ferroportin, hepcidin interferes with cellular iron transport, and ultimately decreases serum iron levels. Vice versa, a decrease in hepcidin expression will cause an increase in cellular iron transport resulting in elevated levels of serum iron (**Figure 1.5**).

After a pivotal role has been established for hepcidin as the master switch of iron metabolism, intensive investigations were performed to understand the regulation of its expression. The evidence for the circulatory hepcidin protein to be regulated at the level of secretion is not strong (201). The growing consensus however was that hepcidin is regulated at the mRNA level (202–204). Accordingly, several studies have shown that hepcidin is transcriptionally regulated by iron loading, inflammatory signals, erythroid activity, endoplasmic reticulum (ER) stress and growth factor signaling (205–208). A brief overview of the pathways relevant to this dissertation has been presented below.

Besides being an iron-regulatory protein itself, the expression of hepcidin is strictly regulated by iron (**Figures 1.5**). Bone morphogenic protein (BMP) receptor and SMAD signaling pathways play a central role in the feedback regulation of hepcidin in response to iron loading. Hepcidin has been shown to be stimulated by various BMP ligands (209, 210). BMP6 knockout mice exhibited severe iron overload with very low hepcidin expression levels, which highlighted the specificity of BMP6 ligand in iron homeostasis (211). Liver-specific SMAD4 knockout mice also exhibited a dramatic decrease in hepcidin expression levels accompanied by iron overload (207). Furthermore, the ablation of SMAD4 in these mice abrogated the response of hepcidin transcription to iron loading (207). Overexpression of SMAD4 stimulated the transcription of hepcidin gene through the BMP-response elements in the promoter (207, 212). As mentioned above, hemochromatosis patients with

mutations in hemochromatosis gene, HFE, transferrin receptor 2 (TRF2) or hemojuvelin (HJV) genes display decreased hepcidin expression (202). These studies suggest that the hepatocyte cell surface proteins encoded by these genes are upstream regulators of hepcidin in response to iron loading. The exact mechanisms underlying cellular iron sensing are still unclear but the modulation of BMP/SMAD signaling pathway by TRF2, HFE or HJV might be one of the potential mechanisms (202, 204).

Besides being an iron-regulatory protein, hepcidin also serves as an acute phase protein, and is associated with innate immunity and infection. As an antimicrobial peptide, the regulation of hepcidin by inflammatory cytokines has already been established (213, 214). Mediators of inflammation, such as LPS, turpentine, and interleukins, IL-1 and IL-6 have been shown as potent stimulators of hepcidin mRNA expression (213–215). IL-6 is one of the best studied mediators of hepcidin up-regulation in response to inflammatory stimuli. IL-6 knockout mice have been reported to exhibit decreased responsiveness to turpentine (213). IL-6 activates *HAMP* promoter through JAK/STAT3 signaling pathway and the subsequent binding of STAT3 to the cis-element in the promoter (205, 216). Inflammation-induced hepcidin up-regulation has been accepted as the major contributor in the development of anemia of chronic disease (217).

Oxidative and endoplasmic reticulum stress play a role in the pathogenesis of liver diseases (218). Endoplasmic reticulum (ER) stress, also called unfolded protein response (UPR), is the response of the cell to the accumulation of unfolded or misfolded proteins in the ER (218). A chemical inducer of ER stress, tunicamycin, has been shown to up-regulate hepcidin expression at the transcriptional level in human hepatoma cells and mice livers (219). One of the underlying mechanisms has been shown to be the activation of cyclic AMP response element–binding protein H (CREBH) and its trans-activation of the hepcidin gene promoter (219). Oxidative stress, on the order hand, has previously been shown by us to induce the suppression of hepcidin transcription in the liver by alcohol exposure (220).

Although studies up-to-now concentrated on the transcriptional regulation of hepcidin, post-transcriptional mechanisms can also be involved. MicroRNAs have recently been shown to regulate hepcidin mRNA expression. The microRNA, miR-122 indirectly regulates the transcription of mouse hepcidin genes by targeting 3'UTR regions of HFE and Hjv mRNA, which are upstream regulators of hepcidin expression (*see above*) (221). By using an iron deficiency mouse model and human hepatoma cells, Zumbrennen-Bullough et al. have reported, that an increase in miR-130a levels exerts a negative effect on BMP-6-induced *HAMP* transcription by reducing the mRNA stability of ALK2 gene, which encodes for BMP type I receptor (222). Although these studies investigated post-transcriptional mechanisms, the primary focus was still the transcriptional regulation of hepcidin gene. Hence, the confirmation for molecular mechanisms, which directly target the 3'UTR of hepcidin mRNA is still lacking. We present evidence and discuss such mechanisms in this study (*see Chapter IV*)

3.4 The relationship between iron and NAFLD pathogenesis

Elevated iron levels are frequently observed in patients with NAFLD and metabolic syndrome (223). About one third of the NAFLD patient population exhibit elevated levels of serum iron markers, such as serum ferritin (29, 224). Multiple large-scale population studies in different regions of the world confirmed an association between hyperferritinemia and type 2 diabetes (225–227). An association between serum ferritin levels and the increase in the number of features, which are indicative of metabolic syndrome, has been reported, suggesting a link between serum iron marker elevation and the progression of metabolic disease (30).

As explained above, the liver plays an important role in iron metabolism and protects the body from harmful effects by serving as the central iron storage organ. Valenti et al. reported that in a European population of NAFLD patients, iron accumulation in hepatocytes was associated with more severe liver damage and fibrosis (31). Concurrently, Nelson et al. have shown that different patterns of iron overload in the liver (i.e. hepatocellular, reticuloendothelial or mixed phenotype)

were observed in 34.5% of patients in the "Nonalcoholic Steatohepatitis Clinical Research Network" (32). In contrast to previously published studies, Nelson et al. further reported that patients with reticuloendothelial iron deposition phenotype in the liver are more likely to display more advanced NASH pathology with elevated hepatic inflammation and injury, and higher levels of fibrosis (32). Despite the inconsistencies in iron deposition patterns, which might be due to the differences in patient groups, these studies established a strong association between hepatic iron content and NAFLD disease progression.

The mechanisms by which iron overload and hepatic iron deposition contribute to the development of metabolic syndrome and NAFLD are unclear. Iron overload-induced production of reactive oxygen species might serve as an important secondary risk factor, which exacerbates NAFLD pathogenesis. In support of this theory, oxidative stress levels are elevated in NAFLD patients with hepatic iron overload compared to those without (228). High-fat diet-feeding induced higher levels of oxidative stress, as well as severe fibrosis and NASH pathology in HFE knockout mice, as compared to wild-type counterparts (229). Furthermore, a role for iron in insulin signaling has been proposed (230). Accordingly, phlebotomy has been reported to improve insulin sensitivity in patients with NAFLD (231) and chelating iron restored insulin receptor signaling in tissue culture cells (232). In addition, iron has been suggested to modulate lipid metabolism and steatosis (233, 234), which is further discussed in Chapter VI of the dissertation**.**

3.5 Modulation of hepcidin expression in NAFLD

Although a clear connection has been established between iron and NAFLD progression, the regulation of hepcidin has not been widely investigated. By using severely obese patients undergoing bariatric surgery, Bekri et al. reported that the increase in hepcidin mRNA levels in adipose tissue is associated with elevated inflammation markers but not with obesity or NASH conditions (194). However, the conclusions drawn from this study are inconclusive due to the study design and the emphasis put on adipocytes, which express negligible levels of hepcidin compared

to hepatocytes (194). Weiss et al. examined hepcidin mRNA expression in liver biopsies of NAFLD patients and reported significantly increased levels of hepatic hepcidin expression (33). Similarly, in a large scale patient study, Martinelli et al. have reported a linear relationship between serum hepcidin levels, measured by mass spectrometry analysis and the increase in characteristic features of metabolic syndrome (30). Another independent study with NAFLD patients from Turkey established an association between an increase in serum hepcidin levels and lipid parameters (235). Hamza et al. reported similar findings, namely that hepcidin-25 levels in the serum of obese children are significantly up-regulated compared to age- and sex-matched controls (236). However, it should be noted that elevated hepcidin expression levels were not detected in all the studies performed with obese diabetic individuals. Serum concentrations of hepcidin was decreased in patients with type 2 diabetes in association with insulin resistance (237). Moreover, hepatic hepcidin expression was significantly suppressed in a high-fat diet mouse model (238). Despite all these studies, the mechanisms which regulate hepcidin expression in NAFLD are not well understood. Certain factors, such as inflammatory cytokines or iron loading, have been proposed as potential contributors (33, 194, 239). The direct roles of lipids and/or lipid intermediates in the regulation of hepcidin expression, have however not been investigated.

Nevertheless, it is important to point out that, since hepcidin is the master switch of iron metabolism, any changes in hepcidin expression (i.e. inhibition or induction), will result in altered iron accumulation and sequestration in the livers of NAFLD patients contributing to disease progression. Namely, induction of hepcidin will ultimately inhibit ferroportin and iron export thereby sequestering iron in Kupffer cells of the liver, triggering oxidative stress, inflammation and fibrogenic signaling. On the other hand, hepcidin inhibition will lead to elevated iron absorption, due to elevated ferroportin and iron export, and excess iron will ultimately cause hepatocyte injury and exacerbate NAFLD pathology.

4 REFERENCES

1. Turconi, G., and Cena, H. (2013) Epidemiology of Obesity Current Status. in *Obesity : Epidemiology, Pathophysiology, and Prevention*, pp. 3–32, CRC Press
2. Flegal, K. M., Carroll, M. D., Kit, B. K., and Ogden, C. L. (2012) Prevalence of obesity and trends in the distribution of body mass index among US adults, 1999-2010. *JAMA.* **307**, 491–497
3. Hossain, P., Kawar, B., and Nahas, M. El (2007) Obesity and Diabetes in the Developing World — A Growing Challenge. *N. Engl. J. Med.* **356**, 213–215
4. Flier, J. S. (2004) Obesity Wars: Molecular Progress Confronts an Expanding Epidemic. *Cell*. **116**, 337–350
5. Després, J.-P., and Lemieux, I. (2006) Abdominal obesity and metabolic syndrome. *Nature*. **444**, 881–887
6. Ruderman, N. B., Carling, D., Prentki, M., and Cacicedo, J. M. (2013) AMPK, insulin resistance, and the metabolic syndrome. *J. Clin. Invest.* **123**, 2764–2772
7. Saltiel, A. R., and Kahn, C. R. (2001) Insulin signalling and the regulation of glucose and lipid metabolism. *Nature*. **414**, 799–806
8. Jornayvaz, F. R., Samuel, V. T., and Shulman, G. I. (2010) The Role of Muscle Insulin Resistance in the Pathogenesis of Atherogenic Dyslipidemia and Nonalcoholic Fatty Liver Disease Associated with the Metabolic Syndrome. *Annu. Rev. Nutr.* **30**, 273–290
9. Raddatz, D., and Ramadori, G. (2010) Hepatic Carbohydrate Metabolism. in *Molecular Pathology of Liver Diseases*, pp. 109–124, Springer Science & Business Media
10. Lomonaco, R., Ortiz-Lopez, C., Orsak, B., Webb, A., Hardies, J., Darland, C., Finch, J., Gastaldelli, A., Harrison, S., Tio, F., and Cusi, K. (2012) Effect of adipose tissue insulin resistance on metabolic parameters and liver histology in obese patients with nonalcoholic fatty liver disease. *Hepatology*. **55**, 1389–1397
11. Leevy, C. M. (1962) Fatty liver: a study of 270 patients with biopsy proven fatty liver and review of the literature. *Medicine (Baltimore)*. **41**, 249–276
12. Tiniakos, D. G., Vos, M. B., and Brunt, E. M. (2010) Nonalcoholic Fatty Liver Disease: Pathology and Pathogenesis. *Annu. Rev. Pathol. Mech. Dis.* **5**, 145–171
13. Marchesini, G., Bugianesi, E., Forlani, G., Cerrelli, F., Lenzi, M., Manini, R., Natale, S., Vanni, E., Villanova, N., Melchionda, N., and Rizzetto, M. (2003) Nonalcoholic fatty liver, steatohepatitis, and the metabolic syndrome. *Hepatology*. **37**, 917–923
14. Anstee, Q. M., Targher, G., and Day, C. P. (2013) Progression of NAFLD to diabetes mellitus, cardiovascular disease or cirrhosis. *Nat. Rev. Gastroenterol. Hepatol.* **10**, 330–344
15. Donnelly, K. L., Smith, C. I., Schwarzenberg, S. J., Jessurun, J., Boldt, M. D., and Parks, E. J. (2005) Sources of fatty acids stored in liver and secreted via lipoproteins in patients with nonalcoholic fatty liver disease. *J. Clin. Invest.* **115**, 1343–1351
16. Choi, S. H., and Ginsberg, H. N. (2011) Increased very low density lipoprotein (VLDL) secretion, hepatic steatosis, and insulin resistance. *Trends Endocrinol. Metab.* **22**, 353–363
17. Bartlett, K., and Eaton, S. (2004) Mitochondrial β-oxidation. *Eur. J. Biochem.* **271**, 462–469
18. Farrell, G. C., and Larter, C. Z. (2006) Nonalcoholic fatty liver disease: From steatosis to cirrhosis. *Hepatology*. **43**, S99–S112
19. Baffy, G., Brunt, E. M., and Caldwell, S. H. (2012) Hepatocellular carcinoma in non-alcoholic fatty liver disease: An emerging menace. *J. Hepatol.* **56**, 1384–1391
20. Day, C. P., and James, O. F. W. (1998) Steatohepatitis: A tale of two "hits"? *Gastroenterology*. **114**, 842–845
21. Basaranoglu, M. (2013) From fatty liver to fibrosis: A tale of "second hit." *World J. Gastroenterol.* **19**, 1158

22. Day, C. P. (2006) From Fat to Inflammation. *Gastroenterology*. **130**, 207–210
23. Yilmaz, Y. (2012) Review article: is non-alcoholic fatty liver disease a spectrum, or are steatosis and non-alcoholic steatohepatitis distinct conditions? *Aliment. Pharmacol. Ther.* **36**, 815–823
24. Tilg, H., and Moschen, A. R. (2010) Evolution of inflammation in nonalcoholic fatty liver disease: The multiple parallel hits hypothesis. *Hepatology*. **52**, 1836–1846
25. McPherson, S., Hardy, T., Henderson, E., Burt, A. D., Day, C. P., and Anstee, Q. M. (2015) Evidence of NAFLD progression from steatosis to fibrosing-steatohepatitis using paired biopsies: Implications for prognosis and clinical management. *J. Hepatol.* **62**, 1148–1155
26. Hübscher, S. G. (2006) Histological assessment of non-alcoholic fatty liver disease. *Histopathology*. **49**, 450–465
27. Pais, R., Pascale, A., Fedchuck, L., Charlotte, F., Poynard, T., and Ratziu, V. (2011) Progression from isolated steatosis to steatohepatitis and fibrosis in nonalcoholic fatty liver disease. *Clin. Res. Hepatol. Gastroenterol.* **35**, 23–28
28. Sutton, H. C., and Winterbourn, C. C. (1989) On the participation of higher oxidation states of iron and copper in fenton reactions. *Free Radic. Biol. Med.* **6**, 53–60
29. Mendler, M.-H., Turlin, B., Moirand, R., Jouanolle, A.-M., Sapey, T., Guyader, D., le Gall, J.-Y., Brissot, P., David, V., and Deugnier, Y. (1999) Insulin resistance–associated hepatic iron overload. *Gastroenterology*. **117**, 1155–1163
30. Martinelli, N., Traglia, M., Campostrini, N., Biino, G., Corbella, M., Sala, C., Busti, F., Masciullo, C., Manna, D., Previtali, S., Castagna, A., Pistis, G., Olivieri, O., Toniolo, D., Camaschella, C., and Girelli, D. (2012) Increased Serum Hepcidin Levels in Subjects with the Metabolic Syndrome: A Population Study. *PLoS ONE*. **7**, e48250
31. Valenti, L., Fracanzani, A. L., Bugianesi, E., Dongiovanni, P., Galmozzi, E., Vanni, E., Canavesi, E., Lattuada, E., Roviaro, G., Marchesini, G., and Fargion, S. (2010) HFE Genotype, Parenchymal Iron Accumulation, and Liver Fibrosis in Patients With Nonalcoholic Fatty Liver Disease. *Gastroenterology*. **138**, 905–912
32. Nelson, J. E., Wilson, L., Brunt, E. M., Yeh, M. M., Kleiner, D. E., Unalp-Arida, A., and Kowdley, K. V. (2010) Relationship between the pattern of hepatic iron deposition and histological severity in nonalcoholic fatty liver disease. *Hepatology*. **53**, 448–457
33. Aigner, E., Theurl, I., Theurl, M., Lederer, D., Haufe, H., Dietze, O., Strasser, M., Datz, C., and Weiss, G. (2008) Pathways Underlying Iron Accumulation in Human Nonalcoholic Fatty Liver Disease. *Am. J. Clin. Nutr.* **87**, 1374–1383
34. Hussain, M. M. (2014) Intestinal lipid absorption and lipoprotein formation: *Curr. Opin. Lipidol.* **25**, 200–206
35. Wang, H., and Eckel, R. H. (2009) Lipoprotein lipase: from gene to obesity. *Am. J. Physiol. - Endocrinol. Metab.* **297**, E271–E288
36. Huang, J., Borensztajn, J., and Reddy, J. K. (2011) Hepatic Lipid Metabolism. in *Molecular Pathology of Liver Diseases* (Monga, S. P. S. ed), pp. 133–146, Molecular Pathology Library, Springer US, [online] http://link.springer.com/chapter/10.1007/978-1-4419-7107-4_10 (Accessed March 22, 2015)
37. Bradbury, M. W. (2006) Lipid Metabolism and Liver Inflammation. I. Hepatic fatty acid uptake: possible role in steatosis. *Am. J. Physiol. - Gastrointest. Liver Physiol.* **290**, G194–G198
38. Doege, H., Baillie, R. A., Ortegon, A. M., Tsang, B., Wu, Q., Punreddy, S., Hirsch, D., Watson, N., Gimeno, R. E., and Stahl, A. (2006) Targeted Deletion of FATP5 Reveals Multiple Functions in Liver Metabolism: Alterations in Hepatic Lipid Homeostasis. *Gastroenterology*. **130**, 1245–1258

39. Wu, Q., Ortegon, A. M., Tsang, B., Doege, H., Feingold, K. R., and Stahl, A. (2006) FATP1 Is an Insulin-Sensitive Fatty Acid Transporter Involved in Diet-Induced Obesity. *Mol. Cell. Biol.* **26**, 3455–3467
40. Murphy, S., Martin, S., and Parton, R. G. (2009) Lipid droplet-organelle interactions; sharing the fats. *Biochim. Biophys. Acta BBA - Mol. Cell Biol. Lipids*. **1791**, 441–447
41. Duncan, R. E., Ahmadian, M., Jaworski, K., Sarkadi-Nagy, E., and Sul, H. S. (2007) Regulation of Lipolysis in Adipocytes. *Annu. Rev. Nutr.* **27**, 79–101
42. Tansey, J., Sztalryd, C., Hlavin, E., Kimmel, A., and Londos, C. (2004) The Central Role of Perilipin A in Lipid Metabolism and Adipocyte Lipolysis. *IUBMB Life*. **56**, 379–385
43. Gong, J., Sun, Z., and Li, P. (2009) CIDE proteins and metabolic disorders. *Curr. Opin. Lipidol.* **20**, 121–126
44. Traini, M., and Jessup, W. (2009) Lipid droplets and adipose metabolism: a novel role for FSP27/CIDEC. *Curr. Opin. Lipidol.* **20**, 147–149
45. Postic, C., and Girard, J. (2008) Contribution of de novo fatty acid synthesis to hepatic steatosis and insulin resistance: lessons from genetically engineered mice. *J. Clin. Invest.* **118**, 829–838
46. Kahn, A. (1997) Transcriptional regulation by glucose in the liver. *Biochimie*. **79**, 113–118
47. Wakil, S. J., and Abu-Elheiga, L. A. (2009) Fatty acid metabolism: target for metabolic syndrome. *J. Lipid Res.* **50**, S138–S143
48. Gutierrez-Juarez, R. (2006) Critical role of stearoyl-CoA desaturase-1 (SCD1) in the onset of diet-induced hepatic insulin resistance. *J. Clin. Invest.* **116**, 1686–1695
49. Xu, X., So, J.-S., Park, J.-G., and Lee, A.-H. (2013) Transcriptional control of hepatic lipid metabolism by SREBP and ChREBP. *Semin. Liver Dis.* **33**, 301–311
50. Brown, M. S., and Goldstein, J. L. (1997) The SREBP Pathway: Regulation of Cholesterol Metabolism by Proteolysis of a Membrane-Bound Transcription Factor. *Cell*. **89**, 331–340
51. Goldstein, J. L., Rawson, R. B., and Brown, M. S. (2002) Mutant Mammalian Cells as Tools to Delineate the Sterol Regulatory Element-Binding Protein Pathway for Feedback Regulation of Lipid Synthesis. *Arch. Biochem. Biophys.* **397**, 139–148
52. Yellaturu, C. R., Deng, X., Cagen, L. M., Wilcox, H. G., Mansbach, C. M., Siddiqi, S. A., Park, E. A., Raghow, R., and Elam, M. B. (2009) Insulin Enhances Post-translational Processing of Nascent SREBP-1c by Promoting Its Phosphorylation and Association with COPII Vesicles. *J. Biol. Chem.* **284**, 7518–7532
53. Yecies, J. L., Zhang, H. H., Menon, S., Liu, S., Yecies, D., Lipovsky, A. I., Gorgun, C., Kwiatkowski, D. J., Hotamisligil, G. S., Lee, C.-H., and Manning, B. D. (2011) Akt Stimulates Hepatic SREBP1c and Lipogenesis through Parallel mTORC1-Dependent and Independent Pathways. *Cell Metab.* **14**, 21–32
54. Peterson, T. R., Sengupta, S. S., Harris, T. E., Carmack, A. E., Kang, S. A., Balderas, E., Guertin, D. A., Madden, K. L., Carpenter, A. E., Finck, B. N., and Sabatini, D. M. (2011) mTOR Complex 1 Regulates Lipin 1 Localization to Control the SREBP Pathway. *Cell*. **146**, 408–420
55. Chen, G., Liang, G., Ou, J., Goldstein, J. L., and Brown, M. S. (2004) Central role for liver X receptor in insulin-mediated activation of Srebp-1c transcription and stimulation of fatty acid synthesis in liver. *Proc. Natl. Acad. Sci. U. S. A.* **101**, 11245–11250
56. Amemiya-Kudo, M., Shimano, H., Yoshikawa, T., Yahagi, N., Hasty, A. H., Okazaki, H., Tamura, Y., Shionoiri, F., Iizuka, Y., Ohashi, K., Osuga, J., Harada, K., Gotoda, T., Sato, R., Kimura, S., Ishibashi, S., and Yamada, N. (2000) Promoter Analysis of the Mouse Sterol Regulatory Element-binding Protein-1c Gene. *J. Biol. Chem.* **275**, 31078–31085
57. Kawaguchi, T., Takenoshita, M., Kabashima, T., and Uyeda, K. (2001) Glucose and cAMP regulate the L-type pyruvate kinase gene by phosphorylation/dephosphorylation of the carbohydrate response element binding protein. *Proc. Natl. Acad. Sci.* **98**, 13710–13715

58. Kawaguchi, T., Osatomi, K., Yamashita, H., Kabashima, T., and Uyeda, K. (2002) Mechanism for Fatty Acid "Sparing" Effect on Glucose-induced Transcription REGULATION OF CARBOHYDRATE-RESPONSIVE ELEMENT-BINDING PROTEIN BY AMP-ACTIVATED PROTEIN KINASE. *J. Biol. Chem.* **277**, 3829–3835
59. Kabashima, T., Kawaguchi, T., Wadzinski, B. E., and Uyeda, K. (2003) Xylulose 5-phosphate mediates glucose-induced lipogenesis by xylulose 5-phosphate-activated protein phosphatase in rat liver. *Proc. Natl. Acad. Sci.* **100**, 5107–5112
60. Li, M. V., Chang, B., Imamura, M., Poungvarin, N., and Chan, L. (2006) Glucose-Dependent Transcriptional Regulation by an Evolutionarily Conserved Glucose-Sensing Module. *Diabetes*. **55**, 1179–1189
61. Tiwari, S., and Siddiqi, S. A. (2012) Intracellular Trafficking and Secretion of VLDL. *Arterioscler. Thromb. Vasc. Biol.* **32**, 1079–1086
62. Hussain, M. M., Bakillah, A., and Jamil, H. (1997) Apolipoprotein B Binding to Microsomal Triglyceride Transfer Protein Decreases with Increases in Length and Lipidation: Implications in Lipoprotein Biosynthesis. *Biochemistry (Mosc.)*. **36**, 13060–13067
63. Hussain, M. M., Bakillah, A., Nayak, N., and Shelness, G. S. (1998) Amino Acids 430–570 in Apolipoprotein B Are Critical for Its Binding to Microsomal Triglyceride Transfer Protein. *J. Biol. Chem.* **273**, 25612–25615
64. Davidson, N. O., and Shelness, G. S. (2000) APOLIPOPROTEIN B: mRNA Editing, Lipoprotein Assembly, and Presecretory Degradation. *Annu. Rev. Nutr*. **20**, 169–193
65. Raabe, M., Véniant, M. M., Sullivan, M. A., Zlot, C. H., Björkegren, J., Nielsen, L. B., Wong, J. S., Hamilton, R. L., and Young, S. G. (1999) Analysis of the role of microsomal triglyceride transfer protein in the liver of tissue-specific knockout mice. *J. Clin. Invest.* **103**, 1287–1298
66. Hussain, M. M., Nijstad, N., and Franceschini, L. (2011) Regulation of microsomal triglyceride transfer protein. *Clin. Lipidol.* **6**, 293–303
67. Dai, K., Khatun, I., and Hussain, M. M. (2010) NR2F1 and IRE1β Suppress Microsomal Triglyceride Transfer Protein Expression and Lipoprotein Assembly in Undifferentiated Intestinal Epithelial Cells. *Arterioscler. Thromb. Vasc. Biol.* **30**, 568–574
68. Sheena, V., Hertz, R., Nousbeck, J., Berman, I., Magenheim, J., and Bar-Tana, J. (2005) Transcriptional regulation of human microsomal triglyceride transfer protein by hepatocyte nuclear factor-4α. *J. Lipid Res.* **46**, 328–341
69. Hayhurst, G. P., Lee, Y.-H., Lambert, G., Ward, J. M., and Gonzalez, F. J. (2001) Hepatocyte Nuclear Factor 4α (Nuclear Receptor 2A1) Is Essential for Maintenance of Hepatic Gene Expression and Lipid Homeostasis. *Mol. Cell. Biol.* **21**, 1393–1403
70. Améen, C., Edvardsson, U., Ljungberg, A., Asp, L., Åkerblad, P., Tuneld, A., Olofsson, S.-O., Lindén, D., and Oscarsson, J. (2005) Activation of Peroxisome Proliferator-activated Receptor α Increases the Expression and Activity of Microsomal Triglyceride Transfer Protein in the Liver. *J. Biol. Chem.* **280**, 1224–1229
71. Wolfrum, C., and Stoffel, M. (2006) Coactivation of Foxa2 through Pgc-1β promotes liver fatty acid oxidation and triglyceride/VLDL secretion. *Cell Metab.* **3**, 99–110
72. Sato, R., Miyamoto, W., Inoue, J., Terada, T., Imanaka, T., and Maeda, M. (1999) Sterol Regulatory Element-binding Protein Negatively Regulates Microsomal Triglyceride Transfer Protein Gene Transcription. *J. Biol. Chem.* **274**, 24714–24720
73. Phillips, C., Owens, D., Collins, P., and Tomkin, G. H. (2002) Microsomal triglyceride transfer protein: does insulin resistance play a role in the regulation of chylomicron assembly? *Atherosclerosis*. **160**, 355–360
74. Bartels, E. D., Lauritsen, M., and Nielsen, L. B. (2002) Hepatic Expression of Microsomal Triglyceride Transfer Protein and In Vivo Secretion of Triglyceride-Rich Lipoproteins Are Increased in Obese Diabetic Mice. *Diabetes*. **51**, 1233–1239

75. Lin, M. C., Arbeeny, C., Bergquist, K., Kienzle, B., Gordon, D. A., and Wetterau, J. R. (1994) Cloning and regulation of hamster microsomal triglyceride transfer protein. The regulation is independent from that of other hepatic and intestinal proteins which participate in the transport of fatty acids and triglycerides. *J. Biol. Chem.* **269**, 29138–29145
76. Qiu, W., Taghibiglou, C., Avramoglu, R. K., Van Iderstine, S. C., Naples, M., Ashrafpour, H., Mhapsekar, S., Sato, R., and Adeli, K. (2005) Oleate-Mediated Stimulation of Microsomal Triglyceride Transfer Protein (MTP) Gene Promoter: Implications for Hepatic MTP Overexpression in Insulin Resistance†. *Biochemistry (Mosc.)*. **44**, 3041–3049
77. Foster, D. W. (2012) Malonyl-CoA: the regulator of fatty acid synthesis and oxidation. *J. Clin. Invest.* **122**, 1958–1959
78. Bensinger, S. J., and Tontonoz, P. (2008) Integration of metabolism and inflammation by lipid-activated nuclear receptors. *Nature*. **454**, 470–477
79. Youssef, J. A., and Badr, M. Z. (2013) Tissue Distribution and Versatile Functions of PPARs. in *Peroxisome Proliferator-Activated Receptors*, pp. 33–69, Humana Press
80. Pawlak, M., Lefebvre, P., and Staels, B. (2015) Molecular mechanism of PPARα action and its impact on lipid metabolism, inflammation and fibrosis in non-alcoholic fatty liver disease. *J. Hepatol.* **62**, 720–733
81. Berger, J., and Moller, D. E. (2002) The Mechanisms of Action of PPARs. *Annu. Rev. Med.* **53**, 409–435
82. Martin, G., Schoonjans, K., Lefebvre, A.-M., Staels, B., and Auwerx, J. (1997) Coordinate Regulation of the Expression of the Fatty Acid Transport Protein and Acyl-CoA Synthetase Genes by PPARα and PPARγ Activators. *J. Biol. Chem.* **272**, 28210–28217
83. Motojima, K., Passilly, P., Peters, J. M., Gonzalez, F. J., and Latruffe, N. (1998) Expression of Putative Fatty Acid Transporter Genes Are Regulated by Peroxisome Proliferator-activated Receptor α and γ Activators in a Tissue- and Inducer-specific Manner. *J. Biol. Chem.* **273**, 16710–16714
84. Barrero, M. J., Camarero, N., Marrero, P. F., and Haro, D. (2003) Control of human carnitine palmitoyltransferase II gene transcription by peroxisome proliferator-activated receptor through a partially conserved peroxisome proliferator-responsive element. *Biochem. J.* **369**, 721
85. Mascaró, C., Acosta, E., Ortiz, J. A., Marrero, P. F., Hegardt, F. G., and Haro, D. (1998) Control of Human Muscle-type Carnitine Palmitoyltransferase I Gene Transcription by Peroxisome Proliferator-activated Receptor. *J. Biol. Chem.* **273**, 8560–8563
86. Fernández-Alvarez, A., Alvarez, M. S., Gonzalez, R., Cucarella, C., Muntané, J., and Casado, M. (2011) Human SREBP1c Expression in Liver Is Directly Regulated by Peroxisome Proliferator-activated Receptor α (PPARα). *J. Biol. Chem.* **286**, 21466–21477
87. Grygiel-Górniak, B. (2014) Peroxisome proliferator-activated receptors and their ligands: nutritional and clinical implications – a review. *Nutr. J.* **13**, 17
88. Tontonoz, P., and Spiegelman, B. M. (2008) Fat and Beyond: The Diverse Biology of PPARγ. *Annu. Rev. Biochem.* **77**, 289–312
89. Gault, C., Obeid, L., and Hannun, Y. (2010) An overview of sphingolipid metabolism: from synthesis to breakdown. *Adv. Exp. Med. Biol.* **688**, 1–23
90. Pagadala, M., Kasumov, T., McCullough, A. J., Zein, N. N., and Kirwan, J. P. (2012) Role of ceramides in nonalcoholic fatty liver disease. *Trends Endocrinol. Metab.* **23**, 365–371
91. Merrill, A. H. (2002) De Novo Sphingolipid Biosynthesis: A Necessary, but Dangerous, Pathway. *J. Biol. Chem.* **277**, 25843–25846
92. Layoun, A., Huang, H., Calvé, A., and Santos, M. M. Toll-Like Receptor Signal Adaptor Protein MyD88 Is Required for Sustained Endotoxin-Induced Acute Hypoferremic Response in Mice. *Am. J. Pathol.* 10.1016/j.ajpath.2012.01.046

93. Shi, H., Kokoeva, M. V., Inouye, K., Tzameli, I., Yin, H., and Flier, J. S. (2006) TLR4 links innate immunity and fatty acid–induced insulin resistance. *J. Clin. Invest.* **116**, 3015–3025
94. Holland, W. L., Bikman, B. T., Wang, L.-P., Yuguang, G., Sargent, K. M., Bulchand, S., Knotts, T. A., Shui, G., Clegg, D. J., Wenk, M. R., Pagliassotti, M. J., Scherer, P. E., and Summers, S. A. (2011) Lipid-induced insulin resistance mediated by the proinflammatory receptor TLR4 requires saturated fatty acid–induced ceramide biosynthesis in mice. *J. Clin. Invest.* **121**, 1858–1870
95. Wiegmann, K., Schütze, S., Machleidt, T., Witte, D., and Krönke, M. (1994) Functional dichotomy of neutral and acidic sphingomyelinases in tumor necrosis factor signaling. *Cell*. **78**, 1005–1015
96. Dressler, K. A., Mathias, S., and Kolesnick, R. N. (1992) Tumor necrosis factor-alpha activates the sphingomyelin signal transduction pathway in a cell-free system. *Science*. **255**, 1715–1718
97. Górska, M., Dobrzyń, A., and Baranowski, M. (2005) Concentrations of sphingosine and sphinganine in plasma of patients with type 2 diabetes. *Med. Sci. Monit. Int. Med. J. Exp. Clin. Res.* **11**, CR35–38
98. Haus, J. M., Kashyap, S. R., Kasumov, T., Zhang, R., Kelly, K. R., DeFronzo, R. A., and Kirwan, J. P. (2009) Plasma Ceramides Are Elevated in Obese Subjects With Type 2 Diabetes and Correlate With the Severity of Insulin Resistance. *Diabetes*. **58**, 337–343
99. Adams, J. M., Pratipanawatr, T., Berria, R., Wang, E., DeFronzo, R. A., Sullards, M. C., and Mandarino, L. J. (2004) Ceramide Content Is Increased in Skeletal Muscle From Obese Insulin-Resistant Humans. *Diabetes*. **53**, 25–31
100. Kolak, M., Westerbacka, J., Velagapudi, V. R., Wågsäter, D., Yetukuri, L., Makkonen, J., Rissanen, A., Häkkinen, A.-M., Lindell, M., Bergholm, R., Hamsten, A., Eriksson, P., Fisher, R. M., Orešič, M., and Yki-Järvinen, H. (2007) Adipose Tissue Inflammation and Increased Ceramide Content Characterize Subjects With High Liver Fat Content Independent of Obesity. *Diabetes*. **56**, 1960–1968
101. Holland, W. L., Brozinick, J. T., Wang, L.-P., Hawkins, E. D., Sargent, K. M., Liu, Y., Narra, K., Hoehn, K. L., Knotts, T. A., Siesky, A., Nelson, D. H., Karathanasis, S. K., Fontenot, G. K., Birnbaum, M. J., and Summers, S. A. (2007) Inhibition of Ceramide Synthesis Ameliorates Glucocorticoid-, Saturated-Fat-, and Obesity-Induced Insulin Resistance. *Cell Metab.* **5**, 167–179
102. Kurek, K., Piotrowska, D. M., Wiesiołek-Kurek, P., Łukaszuk, B., Chabowski, A., Górski, J., and Żendzian-Piotrowska, M. (2014) Inhibition of ceramide de novo synthesis reduces liver lipid accumulation in rats with nonalcoholic fatty liver disease. *Liver Int.* **34**, 1074–1083
103. Promrat, K., Longato, L., Wands, J. R., and de la Monte, S. M. (2011) Weight loss amelioration of non-alcoholic steatohepatitis linked to shifts in hepatic ceramide expression and serum ceramide levels. *Hepatol. Res.* **41**, 754–762
104. Curat, C. A., Wegner, V., Sengenès, C., Miranville, A., Tonus, C., Busse, R., and Bouloumié, A. (2006) Macrophages in human visceral adipose tissue: increased accumulation in obesity and a source of resistin and visfatin. *Diabetologia*. **49**, 744–747
105. Gregor, M. F., and Hotamisligil, G. S. (2011) Inflammatory Mechanisms in Obesity. *Annu. Rev. Immunol.* **29**, 415–445
106. Armstrong, M. J., Hazlehurst, J. M., Hull, D., Guo, K., Borrows, S., Yu, J., Gough, S. C., Newsome, P. N., and Tomlinson, J. W. (2014) Abdominal subcutaneous adipose tissue insulin resistance and lipolysis in patients with non-alcoholic steatohepatitis. *Diabetes Obes. Metab.* **16**, 651–660

107. Zelber-Sagi, S., Ratziu, V., and Oren, R. (2011) Nutrition and physical activity in NAFLD: An overview of the epidemiological evidence. *World J. Gastroenterol. WJG*. **17**, 3377–3389
108. Buettner, R., Parhofer, K. G., Woenckhaus, M., Wrede, C. E., Kunz-Schughart, L. A., Schölmerich, J., and Bollheimer, L. C. (2006) Defining high-fat-diet rat models: metabolic and molecular effects of different fat types. *J. Mol. Endocrinol.* **36**, 485–501
109. Joshi-Barve, S., Barve, S. S., Amancherla, K., Gobejishvili, L., Hill, D., Cave, M., Hote, P., and McClain, C. J. (2007) Palmitic acid induces production of proinflammatory cytokine interleukin-8 from hepatocytes. *Hepatology*. **46**, 823–830
110. Charlton, M., Krishnan, A., Viker, K., Sanderson, S., Cazanave, S., McConico, A., Masuoko, H., and Gores, G. (2011) Fast food diet mouse: novel small animal model of NASH with ballooning, progressive fibrosis, and high physiological fidelity to the human condition. *Am. J. Physiol. - Gastrointest. Liver Physiol.* **301**, G825–G834
111. Musso, G., Gambino, R., De Michieli, F., Cassader, M., Rizzetto, M., Durazzo, M., Fagà, E., Silli, B., and Pagano, G. (2003) Dietary habits and their relations to insulin resistance and postprandial lipemia in nonalcoholic steatohepatitis. *Hepatology*. **37**, 909–916
112. Tetri, L. H., Basaranoglu, M., Brunt, E. M., Yerian, L. M., and Neuschwander-Tetri, B. A. (2008) Severe NAFLD with hepatic necroinflammatory changes in mice fed trans fats and a high-fructose corn syrup equivalent. *Am. J. Physiol. - Gastrointest. Liver Physiol.* **295**, G987–G995
113. Greco, D., Kotronen, A., Westerbacka, J., Puig, O., Arkkila, P., Kiviluoto, T., Laitinen, S., Kolak, M., Fisher, R. M., Hamsten, A., Auvinen, P., and Yki-Järvinen, H. (2008) Gene expression in human NAFLD. *Am. J. Physiol. - Gastrointest. Liver Physiol.* **294**, G1281–G1287
114. Fabbrini, E., Magkos, F., Mohammed, B. S., Pietka, T., Abumrad, N. A., Patterson, B. W., Okunade, A., and Klein, S. (2009) Intrahepatic fat, not visceral fat, is linked with metabolic complications of obesity. *Proc. Natl. Acad. Sci.* **106**, 15430–15435
115. Dowman, J. K., Tomlinson, J. W., and Newsome, P. N. (2010) Pathogenesis of non-alcoholic fatty liver disease. *QJM*. **103**, 71–83
116. Iizuka, K., Bruick, R. K., Liang, G., Horton, J. D., and Uyeda, K. (2004) Deficiency of carbohydrate response element-binding protein (ChREBP) reduces lipogenesis as well as glycolysis. *Proc. Natl. Acad. Sci. U. S. A.* **101**, 7281–7286
117. Benhamed, F., Denechaud, P.-D., Lemoine, M., Robichon, C., Moldes, M., Bertrand-Michel, J., Ratziu, V., Serfaty, L., Housset, C., Capeau, J., Girard, J., Guillou, H., and Postic, C. (2012) The lipogenic transcription factor ChREBP dissociates hepatic steatosis from insulin resistance in mice and humans. *J. Clin. Invest.* **122**, 2176–2194
118. Shimomura, I., Bashmakov, Y., and Horton, J. D. (1999) Increased Levels of Nuclear SREBP-1c Associated with Fatty Livers in Two Mouse Models of Diabetes Mellitus. *J. Biol. Chem.* **274**, 30028–30032
119. Kohjima, M., Higuchi, N., Kato, M., Kotoh, K., Yoshimoto, T., Fujino, T., Yada, M., Yada, R., Harada, N., Enjoji, M., Takayanagi, R., and Nakamuta, M. (2008) SREBP-1c, regulated by the insulin and AMPK signaling pathways, plays a role in nonalcoholic fatty liver disease. *Int. J. Mol. Med.* 10.3892/ijmm.21.4.507
120. Yahagi, N., Shimano, H., Hasty, A. H., Matsuzaka, T., Ide, T., Yoshikawa, T., Amemiya-Kudo, M., Tomita, S., Okazaki, H., Tamura, Y., Iizuka, Y., Ohashi, K., Osuga, J., Harada, K., Gotoda, T., Nagai, R., Ishibashi, S., and Yamada, N. (2002) Absence of Sterol Regulatory Element-binding Protein-1 (SREBP-1) Ameliorates Fatty Livers but Not Obesity or Insulin Resistance inLep ob /Lep ob Mice. *J. Biol. Chem.* **277**, 19353–19357
121. Fabbrini, E., Sullivan, S., and Klein, S. (2010) Obesity and nonalcoholic fatty liver disease: Biochemical, metabolic, and clinical implications. *Hepatology*. **51**, 679–689

122. Ibdah, J. A., Perlegas, P., Zhao, Y., Angdisen, J., Borgerink, H., Shadoan, M. K., Wagner, J. D., Matern, D., Rinaldo, P., and Cline, J. M. (2005) Mice Heterozygous for a Defect in Mitochondrial Trifunctional Protein Develop Hepatic Steatosis and Insulin Resistance. *Gastroenterology*. **128**, 1381–1390
123. Zhang, D., Liu, Z.-X., Choi, C. S., Tian, L., Kibbey, R., Dong, J., Cline, G. W., Wood, P. A., and Shulman, G. I. (2007) Mitochondrial dysfunction due to long-chain Acyl-CoA dehydrogenase deficiency causes hepatic steatosis and hepatic insulin resistance. *Proc. Natl. Acad. Sci.* **104**, 17075–17080
124. Seo, Y. S., Kim, J. H., Jo, N. Y., Choi, K. M., Baik, S. H., Park, J.-J., Kim, J. S., Byun, K. S., Bak, Y.-T., Lee, C. H., Kim, A., and Yeon, J. E. (2008) PPAR agonists treatment is effective in a nonalcoholic fatty liver disease animal model by modulating fatty-acid metabolic enzymes. *J. Gastroenterol. Hepatol.* **23**, 102–109
125. Sanyal, A. J., Campbell–Sargent, C., Mirshahi, F., Rizzo, W. B., Contos, M. J., Sterling, R. K., Luketic, V. A., Shiffman, M. L., and Clore, J. N. (2001) Nonalcoholic steatohepatitis: Association of insulin resistance and mitochondrial abnormalities. *Gastroenterology*. **120**, 1183–1192
126. Pérez-Carreras, M., Del Hoyo, P., Martín, M. A., Rubio, J. C., Martín, A., Castellano, G., Colina, F., Arenas, J., and Solis-Herruzo, J. A. (2003) Defective hepatic mitochondrial respiratory chain in patients with nonalcoholic steatohepatitis. *Hepatol. Baltim. Md*. **38**, 999–1007
127. Kohjima, M., Enjoji, M., Higuchi, N., Kato, M., Kotoh, K., Yoshimoto, T., Fujino, T., Yada, M., Yada, R., Harada, N., Takayanagi, R., and Nakamuta, M. (2007) Re-evaluation of fatty acid metabolism-related gene expression in nonalcoholic fatty liver disease. *Int. J. Mol. Med.* 10.3892/ijmm.20.3.351
128. Caldwell, S. H., Swerdlow, R. H., Khan, E. M., Iezzoni, J. C., Hespenheide, E. E., Parks, J. K., and Parker Jr, W. D. (1999) Mitochondrial abnormalities in non-alcoholic steatohepatitis. *J. Hepatol.* **31**, 430–434
129. Cuchel, M., Bloedon, L. T., Szapary, P. O., Kolansky, D. M., Wolfe, M. L., Sarkis, A., Millar, J. S., Ikewaki, K., Siegelman, E. S., Gregg, R. E., and Rader, D. J. (2007) Inhibition of Microsomal Triglyceride Transfer Protein in Familial Hypercholesterolemia. *N. Engl. J. Med.* **356**, 148–156
130. Adiels, M., Taskinen, M.-R., Packard, C., Caslake, M. J., Soro-Paavonen, A., Westerbacka, J., Vehkavaara, S., Häkkinen, A., Olofsson, S.-O., Yki-Järvinen, H., and Borén, J. (2006) Overproduction of large VLDL particles is driven by increased liver fat content in man. *Diabetologia*. **49**, 755–765
131. Fabbrini, E., Mohammed, B. S., Magkos, F., Korenblat, K. M., Patterson, B. W., and Klein, S. (2008) Alterations in Adipose Tissue and Hepatic Lipid Kinetics in Obese Men and Women With Nonalcoholic Fatty Liver Disease. *Gastroenterology*. **134**, 424–431
132. McClain, C. J., Barve, S., and Deaciuc, I. (2007) Good fat/bad fat. *Hepatology*. **45**, 1343–1346
133. Yamaguchi, K., Yang, L., McCall, S., Huang, J., Yu, X. X., Pandey, S. K., Bhanot, S., Monia, B. P., Li, Y.-X., and Diehl, A. M. (2007) Inhibiting triglyceride synthesis improves hepatic steatosis but exacerbates liver damage and fibrosis in obese mice with nonalcoholic steatohepatitis. *Hepatology*. **45**, 1366–1374
134. Listenberger, L. L., Han, X., Lewis, S. E., Cases, S., Farese, R. V., Ory, D. S., and Schaffer, J. E. (2003) Triglyceride Accumulation Protects Against Fatty Acid-Induced Lipotoxicity. *Proc. Natl. Acad. Sci.* **100**, 3077–3082
135. Kerr, J. F. R., Wyllie, A. H., and Currie, A. R. (1972) Apoptosis: A Basic Biological Phenomenon with Wide-ranging Implications in Tissue Kinetics. *Br. J. Cancer*. **26**, 239–257

136. MALHI, H., GUICCIARDI, M. E., and GORES, G. J. (2010) Hepatocyte Death: A Clear and Present Danger. *Physiol. Rev.* **90**, 1165–1194
137. Dufour, J. F., Clavien, P.-A., Trautwein, C., and Graf, R. (eds.) (2005) *Signaling Pathways in Liver Diseases*, 1st Ed., Springer
138. Eitel, K., Staiger, H., Rieger, J., Mischak, H., Brandhorst, H., Brendel, M. D., Bretzel, R. G., Häring, H.-U., and Kellerer, M. (2003) Protein Kinase C δ Activation and Translocation to the Nucleus Are Required for Fatty Acid-Induced Apoptosis of Insulin-Secreting Cells. *Diabetes*. **52**, 991–997
139. Malhi, H., Bronk, S. F., Werneburg, N. W., and Gores, G. J. (2006) Free Fatty Acids Induce JNK-dependent Hepatocyte Lipoapoptosis. *J. Biol. Chem.* **281**, 12093–12101
140. Li, Z. Z., Berk, M., McIntyre, T. M., and Feldstein, A. E. (2009) Hepatic Lipid Partitioning and Liver Damage in Nonalcoholic Fatty Liver Disease ROLE OF STEAROYL-CoA DESATURASE. *J. Biol. Chem.* **284**, 5637–5644
141. Malhi, H., Barreyro, F. J., Isomoto, H., Bronk, S. F., and Gores, G. J. (2007) Free fatty acids sensitise hepatocytes to TRAIL mediated cytotoxicity. *Gut*. **56**, 1124–1131
142. Wei, Y., Wang, D., Topczewski, F., and Pagliassotti, M. J. (2006) Saturated Fatty Acids Induce Endoplasmic Reticulum Stress and Apoptosis Independently of Ceramide in Liver Cells. *Am. J. Physiol. - Endocrinol. Metab.* **291**, E275–E281
143. Wei, Y., Wang, D., Gentile, C. L., and Pagliassotti, M. J. (2009) Reduced endoplasmic reticulum luminal calcium links saturated fatty acid-mediated endoplasmic reticulum stress and cell death in liver cells. *Mol. Cell. Biochem.* **331**, 31–40
144. Feldstein, A. E., Canbay, A., Angulo, P., Taniai, M., Burgart, L. J., Lindor, K. D., and Gores, G. J. (2003) Hepatocyte apoptosis and fas expression are prominent features of human nonalcoholic steatohepatitis. *Gastroenterology*. **125**, 437–443
145. Ribeiro, P. S., Cortez-Pinto, H., Solá, S., Castro, R. E., Ramalho, R. M., Baptista, A., Moura, M. C., Camilo, M. E., and Rodrigues, C. M. (2004) Hepatocyte Apoptosis, Expression of Death Receptors, and Activation of NF-κB in the Liver of Nonalcoholic and Alcoholic Steatohepatitis Patients. *Am. J. Gastroenterol.* **99**, 1708–1717
146. Wieckowska, A., Zein, N. N., Yerian, L. M., Lopez, A. R., McCullough, A. J., and Feldstein, A. E. (2006) In vivo assessment of liver cell apoptosis as a novel biomarker of disease severity in nonalcoholic fatty liver disease. *Hepatology*. **44**, 27–33
147. Perry, R. J., Samuel, V. T., Petersen, K. F., and Shulman, G. I. (2014) The role of hepatic lipids in hepatic insulin resistance and type 2 diabetes. *Nature*. **510**, 84–91
148. Webb, B. L. J., Hirst, S. J., and Giembycz, M. A. (2000) Protein kinase C isoenzymes: a review of their structure, regulation and role in regulating airways smooth muscle tone and mitogenesis. *Br. J. Pharmacol.* **130**, 1433–1452
149. Mellor, H., and Parker, P. J. (1998) The extended protein kinase C superfamily. *Biochem. J.* **332**, 281–292
150. Schmitz-Peiffer, C., and Biden, T. J. (2008) Protein Kinase C Function in Muscle, Liver, and β-Cells and Its Therapeutic Implications for Type 2 Diabetes. *Diabetes*. **57**, 1774–1783
151. Geraldes, P., and King, G. L. (2010) Activation of Protein Kinase C Isoforms and Its Impact on Diabetic Complications. *Circ. Res.* **106**, 1319–1331
152. Birkenfeld, A. L., and Shulman, G. I. (2014) Nonalcoholic fatty liver disease, hepatic insulin resistance, and type 2 Diabetes. *Hepatology*. **59**, 713–723
153. Samuel, V. T., Liu, Z.-X., Qu, X., Elder, B. D., Bilz, S., Befroy, D., Romanelli, A. J., and Shulman, G. I. (2004) Mechanism of Hepatic Insulin Resistance in Non-alcoholic Fatty Liver Disease. *J. Biol. Chem.* **279**, 32345–32353
154. Greene, M. W., Burrington, C. M., Ruhoff, M. S., Johnson, A. K., Chongkrairatanakul, T., and Kangwanpornsiri, A. (2010) PKCδ Is Activated in a Dietary Model of Steatohepatitis

and Regulates Endoplasmic Reticulum Stress and Cell Death. *J. Biol. Chem.* **285**, 42115–42129

155. Lee, J., Cho, H.-K., and Kwon, Y. H. (2010) Palmitate induces insulin resistance without significant intracellular triglyceride accumulation in HepG2 cells. *Metabolism.* **59**, 927–934
156. Tan, S. H., Shui, G., Zhou, J., Li, J. J., Bay, B.-H., Wenk, M. R., and Shen, H.-M. (2012) Induction of Autophagy by Palmitic Acid via Protein Kinase C-mediated Signaling Pathway Independent of mTOR (Mammalian Target of Rapamycin). *J. Biol. Chem.* **287**, 14364–14376
157. Kumashiro, N., Erion, D. M., Zhang, D., Kahn, M., Beddow, S. A., Chu, X., Still, C. D., Gerhard, G. S., Han, X., Dziura, J., Petersen, K. F., Samuel, V. T., and Shulman, G. I. (2011) Cellular mechanism of insulin resistance in nonalcoholic fatty liver disease. *Proc. Natl. Acad. Sci.* **108**, 16381–16385
158. Samuel, V. T., Liu, Z.-X., Wang, A., Beddow, S. A., Geisler, J. G., Kahn, M., Zhang, X., Monia, B. P., Bhanot, S., and Shulman, G. I. (2007) Inhibition of protein kinase Cε prevents hepatic insulin resistance in nonalcoholic fatty liver disease. *J. Clin. Invest.* **117**, 739–745
159. Kotronen, A., Seppänen-Laakso, T., Westerbacka, J., Kiviluoto, T., Arola, J., Ruskeepää, A.-L., Orešič, M., and Yki-Järvinen, H. (2009) Hepatic Stearoyl-CoA Desaturase (SCD)-1 Activity and Diacylglycerol but Not Ceramide Concentrations Are Increased in the Nonalcoholic Human Fatty Liver. *Diabetes*. **58**, 203–208
160. Summers, S. A., Garza, L. A., Zhou, H., and Birnbaum, M. J. (1998) Regulation of Insulin-Stimulated Glucose Transporter GLUT4 Translocation and Akt Kinase Activity by Ceramide. *Mol. Cell. Biol.* **18**, 5457–5464
161. Bikman, B. T., and Summers, S. A. (2011) Ceramides as modulators of cellular and whole-body metabolism. *J. Clin. Invest.* **121**, 4222–4230
162. Ceramide induces interleukin 6 gene expression in human fibroblasts (1995) *J. Exp. Med.* **182**, 599–604
163. Fillet, M., Bentires-Alj, M., Deregowski, V., Greimers, R., Gielen, J., Piette, J., Bours, V., and Merville, M.-P. (2003) Mechanisms involved in exogenous C2- and C6-ceramide-induced cancer cell toxicity. *Biochem. Pharmacol.* **65**, 1633–1642
164. Demarchi, F., Bertoli, C., Greer, P. A., and Schneider, C. (2005) Ceramide triggers an NF-κB-dependent survival pathway through calpain. *Cell Death Differ.* **12**, 512–522
165. Kreydiyyeh, S. I., and Dakroub, Z. (2014) Ceramide and its metabolites modulate time-dependently the activity of the Na+/K+ ATPase in HepG2 cells. *Int. J. Biochem. Cell Biol.* **53**, 102–107
166. Kurinna, S. M., Tsao, C. C., Nica, A. F., Jiffar, T., and Ruvolo, P. P. (2004) Ceramide Promotes Apoptosis in Lung Cancer-Derived A549 Cells by a Mechanism Involving c-Jun NH2-Terminal Kinase. *Cancer Res.* **64**, 7852–7856
167. Chen, C.-L., Lin, C.-F., Chang, W.-T., Huang, W.-C., Teng, C.-F., and Lin, Y.-S. (2008) Ceramide induces p38 MAPK and JNK activation through a mechanism involving a thioredoxin-interacting protein-mediated pathway. *Blood.* **111**, 4365–4374
168. Saslowsky, D. E., Tanaka, N., Reddy, K. P., and Lencer, W. I. (2009) Ceramide activates JNK to inhibit a cAMP-gated K+ conductance and Cl– secretion in intestinal epithelia. *FASEB J.* **23**, 259–270
169. Drygalski, A. von, and Adamson, J. W. (2012) Iron Metabolism in Man. *J. Parenter. Enter. Nutr.* 10.1177/0148607112459648
170. Andrews, N. C. (1999) Disorders of Iron Metabolism. *N. Engl. J. Med.* **341**, 1986–1995
171. Nyholm, S., Mann, G. J., Johansson, A. G., Bergeron, R. J., Gräslund, A., and Thelander, L. (1993) Role of ribonucleotide reductase in inhibition of mammalian cell growth by potent iron chelators. *J. Biol. Chem.* **268**, 26200–26205

172. Lipinski, B. (2011) Hydroxyl Radical and Its Scavengers in Health and Disease. *Oxid. Med. Cell. Longev.* **2011**, e809696
173. Ganz, T. (2013) Systemic Iron Homeostasis. *Physiol. Rev.* **93**, 1721–1741
174. Bartnikas, T. B. (2012) Known and potential roles of transferrin in iron biology. *Biometals Int. J. Role Met. Ions Biol. Biochem. Med.* **25**, 677–686
175. Worthen, C. A., and Enns, C. A. (2014) The role of hepatic transferrin receptor 2 in the regulation of iron homeostasis in the body. *Drug Metab. Transp.* **5**, 34
176. Anderson, E. R., and Shah, Y. M. (2013) Iron homeostasis in the liver. *Compr. Physiol.* **3**, 315–330
177. Dognin, J., and Crichton, R. R. (1975) Mobilisation of iron from ferritin fractions of defined iron content by biological reductants. *FEBS Lett.* **54**, 234–236
178. Shayeghi, M., Latunde-Dada, G. O., Oakhill, J. S., Laftah, A. H., Takeuchi, K., Halliday, N., Khan, Y., Warley, A., McCann, F. E., Hider, R. C., Frazer, D. M., Anderson, G. J., Vulpe, C. D., Simpson, R. J., and McKie, A. T. (2005) Identification of an Intestinal Heme Transporter. *Cell*. **122**, 789–801
179. West, A. R., and Oates, P. S. (2008) Mechanisms of heme iron absorption: Current questions and controversies. *World J. Gastroenterol. WJG*. **14**, 4101–4110
180. Sharp, P., and Srai, S.-K. (2007) Molecular mechanisms involved in intestinal iron absorption. *World J. Gastroenterol. WJG*. **13**, 4716–4724
181. Choi, J., Masaratana, P., Latunde-Dada, G. O., Arno, M., Simpson, R. J., and McKie, A. T. (2012) Duodenal Reductase Activity and Spleen Iron Stores Are Reduced and Erythropoiesis Is Abnormal in Dcytb Knockout Mice Exposed to Hypoxic Conditions. *J. Nutr.* **142**, 1929–1934
182. Gunshin, H., Mackenzie, B., Berger, U. V., Gunshin, Y., Romero, M. F., Boron, W. F., Nussberger, S., Gollan, J. L., and Hediger, M. A. (1997) Cloning and characterization of a mammalian proton-coupled metal-ion transporter. *Nature*. **388**, 482–488
183. Krause, A., Neitz, S., Mägert, H.-J., Schulz, A., Forssmann, W.-G., Schulz-Knappe, P., and Adermann, K. (2000) LEAP-1, a novel highly disulfide-bonded human peptide, exhibits antimicrobial activity1. *FEBS Lett.* **480**, 147–150
184. Park, C. H., Valore, E. V., Waring, A. J., and Ganz, T. (2001) Hepcidin, a Urinary Antimicrobial Peptide Synthesized in the Liver. *J. Biol. Chem.* **276**, 7806–7810
185. Pigeon, C., Ilyin, G., Courselaud, B., Leroyer, P., Turlin, B., Brissot, P., and Loréal, O. (2001) A New Mouse Liver-specific Gene, Encoding a Protein Homologous to Human Antimicrobial Peptide Hepcidin, Is Overexpressed during Iron Overload. *J. Biol. Chem.* **276**, 7811–7819
186. Nicolas, G., Bennoun, M., Devaux, I., Beaumont, C., Grandchamp, B., Kahn, A., and Vaulont, S. (2001) Lack of hepcidin gene expression and severe tissue iron overload in upstream stimulatory factor 2 (USF2) knockout mice. *Proc. Natl. Acad. Sci.* **98**, 8780–8785
187. Nicolas, G., Bennoun, M., Porteu, A., Mativet, S., Beaumont, C., Grandchamp, B., Sirito, M., Sawadogo, M., Kahn, A., and Vaulont, S. (2002) Severe iron deficiency anemia in transgenic mice expressing liver hepcidin. *Proc. Natl. Acad. Sci.* **99**, 4596–4601
188. Roetto, A., Papanikolaou, G., Politou, M., Alberti, F., Girelli, D., Christakis, J., Loukopoulos, D., and Camaschella, C. (2003) Mutant antimicrobial peptide hepcidin is associated with severe juvenile hemochromatosis. *Nat. Genet.* **33**, 21–22
189. Piperno, A., Girelli, D., Nemeth, E., Trombini, P., Bozzini, C., Poggiali, E., Phung, Y., Ganz, T., and Camaschella, C. (2007) Blunted hepcidin response to oral iron challenge in HFE-related hemochromatosis. *Blood*. **110**, 4096–4100
190. Lu, S., Seravalli, J., and Harrison-Findik, D. (2015) Inductively coupled mass spectrometry analysis of biometals in conditional Hamp1 and Hamp1 and Hamp2 transgenic mouse models. *Transgenic Res.* 10.1007/s11248-015-9879-3

191. Lou, D.-Q., Nicolas, G., Lesbordes, J.-C., Viatte, L., Grimber, G., Szajnert, M.-F., Kahn, A., and Vaulont, S. (2004) Functional differences between hepcidin 1 and 2 in transgenic mice. *Blood*. **103**, 2816–2821
192. Campostrini, N., Traglia, M., Martinelli, N., Corbella, M., Cocca, M., Manna, D., Castagna, A., Masciullo, C., Silvestri, L., Olivieri, O., Toniolo, D., Camaschella, C., and Girelli, D. (2012) Serum levels of the hepcidin-20 isoform in a large general population: The Val Borbera study. *J. Proteomics*. **76**, 28–35
193. Troadec, M.-B., Fautrel, A., Drénou, B., Leroyer, P., Camberlein, E., Turlin, B., Guillouzo, A., Brissot, P., and Loréal, O. (2008) Transcripts of ceruloplasmin but not hepcidin, both major iron metabolism genes, exhibit a decreasing pattern along the portocentral axis of mouse liver. *Biochim. Biophys. Acta BBA - Mol. Basis Dis.* **1782**, 239–249
194. Bekri, S., Gual, P., Anty, R., Luciani, N., Dahman, M., Ramesh, B., Iannelli, A., Staccini–Myx, A., Casanova, D., Ben Amor, I., Saint–Paul, M., Huet, P., Sadoul, J., Gugenheim, J., Srai, S. K. S., Tran, A., and Le Marchand–Brustel, Y. (2006) Increased Adipose Tissue Expression of Hepcidin in Severe Obesity Is Independent From Diabetes and NASH. *Gastroenterology*. **131**, 788–796
195. Zhang, A.-S., Xiong, S., Tsukamoto, H., and Enns, C. A. (2004) Localization of iron metabolism-related mRNAs in rat liver indicate that HFE is expressed predominantly in hepatocytes. *Blood*. **103**, 1509–1514
196. Zumerle, S., Mathieu, J. R. R., Delga, S., Heinis, M., Viatte, L., Vaulont, S., and Peyssonnaux, C. (2014) Targeted disruption of hepcidin in the liver recapitulates the hemochromatotic phenotype. *Blood*. **123**, 3646–3650
197. Palaneeswari M., S., Ganesh, M., Karthikeyan, T., Devi, A. J. M., and Mythili, S. V. (2013) Hepcidin-Minireview. *J. Clin. Diagn. Res. JCDR*. **7**, 1767–1771
198. Nemeth, E., Preza, G. C., Jung, C.-L., Kaplan, J., Waring, A. J., and Ganz, T. (2006) The N-terminus of hepcidin is essential for its interaction with ferroportin: structure-function study. *Blood*. **107**, 328–333
199. Nemeth, E., Tuttle, M. S., Powelson, J., Vaughn, M. B., Donovan, A., Ward, D. M., Ganz, T., and Kaplan, J. (2004) Hepcidin Regulates Cellular Iron Efflux by Binding to Ferroportin and Inducing Its Internalization. *Science*. **306**, 2090–2093
200. De Domenico, I., Ward, D. M., Langelier, C., Vaughn, M. B., Nemeth, E., Sundquist, W. I., Ganz, T., Musci, G., and Kaplan, J. (2007) The Molecular Mechanism of Hepcidin-Mediated Ferroportin Down-Regulation. *Mol. Biol. Cell*. **18**, 2569–2578
201. Valore, E. V., and Ganz, T. (2008) Posttranslational processing of hepcidin in human hepatocytes is mediated by the prohormone convertase furin. *Blood Cells. Mol. Dis.* **40**, 132–138
202. Ganz, T. (2011) Hepcidin and iron regulation, 10 years later. *Blood*. **117**, 4425 –4433
203. Nemeth, E., and Ganz, T. (2006) Regulation of Iron Metabolism by Hepcidin. *Annu. Rev. Nutr*. **26**, 323–342
204. Lee, P. L., and Beutler, E. (2009) Regulation of Hepcidin and Iron-Overload Disease. *Annu. Rev. Pathol. Mech. Dis.* **4**, 489–515
205. Wrighting, D. M., and Andrews, N. C. (2006) Interleukin-6 induces hepcidin expression through STAT3. *Blood*. **108**, 3204–3209
206. Falzacappa, V., Vittoria, M., Vujic Spasic, M., Kessler, R., Stolte, J., Hentze, M. W., and Muckenthaler, M. U. (2007) STAT3 Mediates Hepatic Hepcidin Expression and Its Inflammatory Stimulation. *Blood*. **109**, 353–358
207. Wang, R.-H., Li, C., Xu, X., Zheng, Y., Xiao, C., Zerfas, P., Cooperman, S., Eckhaus, M., Rouault, T., Mishra, L., and Deng, C.-X. (2005) A role of SMAD4 in iron metabolism through the positive regulation of hepcidin expression. *Cell Metab.* **2**, 399–409

208. Kautz, L., Jung, G., Valore, E. V., Rivella, S., Nemeth, E., and Ganz, T. (2014) Identification of erythroferrone as an erythroid regulator of iron metabolism. *Nat. Genet.* 10.1038/ng.2996
209. Babitt, J. L., Huang, F. W., Wrighting, D. M., Xia, Y., Sidis, Y., Samad, T. A., Campagna, J. A., Chung, R. T., Schneyer, A. L., Woolf, C. J., Andrews, N. C., and Lin, H. Y. (2006) Bone morphogenetic protein signaling by hemojuvelin regulates hepcidin expression. *Nat. Genet.* **38**, 531–539
210. Babitt, J. L., Huang, F. W., Xia, Y., Sidis, Y., Andrews, N. C., and Lin, H. Y. (2007) Modulation of bone morphogenetic protein signaling in vivo regulates systemic iron balance. *J. Clin. Invest.* **117**, 1933–1939
211. Meynard, D., Kautz, L., Darnaud, V., Canonne-Hergaux, F., Coppin, H., and Roth, M.-P. (2009) Lack of the bone morphogenetic protein BMP6 induces massive iron overload. *Nat. Genet.* **41**, 478–481
212. Truksa, J., Lee, P., and Beutler, E. (2009) Two BMP responsive elements, STAT, and bZIP/HNF4/COUP motifs of the hepcidin promoter are critical for BMP, SMAD1, and HJV responsiveness. *Blood*. **113**, 688–695
213. Nemeth, E., Rivera, S., Gabayan, V., Keller, C., Taudorf, S., Pedersen, B. K., and Ganz, T. (2004) IL-6 mediates hypoferremia of inflammation by inducing the synthesis of the iron regulatory hormone hepcidin. *J. Clin. Invest.* **113**, 1271–1276
214. Lee, P., Peng, H., Gelbart, T., Wang, L., and Beutler, E. (2005) Regulation of hepcidin transcription by interleukin-1 and interleukin-6. *Proc. Natl. Acad. Sci. U. S. A.* **102**, 1906–1910
215. Smith, C. L., Arvedson, T. L., Cooke, K. S., Dickmann, L. J., Forte, C., Li, H., Merriam, K. L., Perry, V. K., Tran, L., Rottman, J. B., and Maxwell, J. R. (2013) IL-22 Regulates Iron Availability In Vivo through the Induction of Hepcidin. *J. Immunol.* 10.4049/jimmunol.1202716
216. Pietrangelo, A., Dierssen, U., Valli, L., Garuti, C., Rump, A., Corradini, E., Ernst, M., Klein, C., and Trautwein, C. (2007) STAT3 Is Required for IL-6-gp130–Dependent Activation of Hepcidin In Vivo. *Gastroenterology*. **132**, 294–300
217. Poggiali, E., Migone De Amicis, M., and Motta, I. Anemia of chronic disease: A unique defect of iron recycling for many different chronic diseases. *Eur. J. Intern. Med.* 10.1016/j.ejim.2013.07.011
218. Malhi, H., and Kaufman, R. J. (2011) Endoplasmic reticulum stress in liver disease. *J. Hepatol.* **54**, 795–809
219. Vecchi, C., Montosi, G., Zhang, K., Lamberti, I., Duncan, S. A., Kaufman, R. J., and Pietrangelo, A. (2009) ER Stress Controls Iron Metabolism Through Induction of Hepcidin. *Science*. **325**, 877–880
220. Harrison-Findik, D. D., Schafer, D., Klein, E., Timchenko, N. A., Kulaksiz, H., Clemens, D., Fein, E., Andriopoulos, B., Pantopoulos, K., and Gollan, J. (2006) Alcohol Metabolism-mediated Oxidative Stress Down-regulates Hepcidin Transcription and Leads to Increased Duodenal Iron Transporter Expression. *J. Biol. Chem.* **281**, 22974 –22982
221. Castoldi, M., Vujic Spasic, M., Altamura, S., Elmén, J., Lindow, M., Kiss, J., Stolte, J., Sparla, R., D'Alessandro, L. A., Klingmüller, U., Fleming, R. E., Longerich, T., Gröne, H. J., Benes, V., Kauppinen, S., Hentze, M. W., and Muckenthaler, M. U. (2011) The liver-specific microRNA miR-122 controls systemic iron homeostasis in mice. *J. Clin. Invest.* **121**, 1386–1396
222. Zumbrennen-Bullough, K. B., Wu, Q., Core, A. B., Canali, S., Chen, W., Theurl, I., Meynard, D., and Babitt, J. L. (2014) MicroRNA-130a Is Up-regulated in Mouse Liver by Iron Deficiency and Targets the Bone Morphogenetic Protein (BMP) Receptor ALK2 to Attenuate BMP Signaling and Hepcidin Transcription. *J. Biol. Chem.* **289**, 23796–23808

223. Dongiovanni, P., Fracanzani, A. L., Fargion, S., and Valenti, L. (2011) Iron in fatty liver and in the metabolic syndrome: A promising therapeutic target. *J. Hepatol.* **55**, 920–932
224. Aigner, E. (2014) Dysregulation of iron and copper homeostasis in nonalcoholic fatty liver. *World J. Hepatol.* **7**, 177
225. Ford, E. S., and Cogswell, M. E. (1999) Diabetes and serum ferritin concentration among U.S. adults. *Diabetes Care*. **22**, 1978–1983
226. Jiang, R., Manson, J. E., Meigs, J. B., Ma, J., Rifai, N., and Hu, F. B. (2004) Body iron stores in relation to risk of type 2 diabetes in apparently healthy women. *JAMA*. **291**, 711–717
227. Forouhi, N. G., Harding, A. H., Allison, M., Sandhu, M. S., Welch, A., Luben, R., Bingham, S., Khaw, K. T., and Wareham, N. J. (2007) Elevated serum ferritin levels predict new-onset type 2 diabetes: results from the EPIC-Norfolk prospective study. *Diabetologia*. **50**, 949–956
228. Maliken, B. D., Nelson, J. E., Klintworth, H. M., Beauchamp, M., Yeh, M. M., and Kowdley, K. V. (2013) Hepatic reticuloendothelial system cell iron deposition is associated with increased apoptosis in nonalcoholic fatty liver disease. *Hepatology*. **57**, 1806–1813
229. Tan, T. C. H., Crawford, D. H. G., Jaskowski, L. A., Subramaniam, V. N., Clouston, A. D., Crane, D. I., Bridle, K. R., Anderson, G. J., and Fletcher, L. M. (2013) Excess iron modulates endoplasmic reticulum stress-associated pathways in a mouse model of alcohol and high-fat diet-induced liver injury. *Lab. Invest.* **93**, 1295–1312
230. Fernández-Real, J. M., López-Bermejo, A., and Ricart, W. (2002) Cross-Talk Between Iron Metabolism and Diabetes. *Diabetes*. **51**, 2348–2354
231. Valenti, L., Fracanzani, A. L., Dongiovanni, P., Bugianesi, E., Marchesini, G., Manzini, P., Vanni, E., and Fargion, S. (2007) Iron Depletion by Phlebotomy Improves Insulin Resistance in Patients With Nonalcoholic Fatty Liver Disease and Hyperferritinemia: Evidence from a Case-Control Study. *Am. J. Gastroenterol.* **102**, 1251–1258
232. Dongiovanni, P., Valenti, L., Ludovica Fracanzani, A., Gatti, S., Cairo, G., and Fargion, S. (2008) Iron Depletion by Deferoxamine Up-Regulates Glucose Uptake and Insulin Signaling in Hepatoma Cells and in Rat Liver. *Am. J. Pathol.* **172**, 738–747
233. Cunnane, S. C., and McAdoo, K. R. (1987) Iron Intake Influences Essential Fatty Acid and Lipid Composition of Rat Plasma and Erythrocytes. *J. Nutr.* **117**, 1514–1519
234. Kirsch, R., Sijtsema, H. P., Tlali, M., Marais, A. D., and Hall, P. de la M. (2006) Effects of iron overload in a rat nutritional model of non-alcoholic fatty liver disease. *Liver Int.* **26**, 1258–1267
235. Senates, E., Yilmaz, Y., Colak, Y., Ozturk, O., Altunoz, M. E., Kurt, R., Ozkara, S., Aksaray, S., Tuncer, I., and Ovunc, A. O. K. (2011) Serum levels of hepcidin in patients with biopsy-proven nonalcoholic fatty liver disease. *Metab. Syndr. Relat. Disord.* **9**, 287–290
236. Hamza, R. T., Hamed, A. I., and Kharshoum, R. R. (2013) Iron homeostasis and serum hepcidin-25 levels in obese children and adolescents: relation to body mass index. *Horm. Res. Pædiatrics*. **80**, 11–17
237. Sam, A. H., Busbridge, M., Amin, A., Webber, L., White, D., Franks, S., Martin, N. M., Sleeth, M., Ismail, N. A., Daud, N. M., Papamargaritis, D., Le Roux, C. W., Chapman, R. S., Frost, G., Bloom, S. R., and Murphy, K. G. (2013) Hepcidin levels in diabetes mellitus and polycystic ovary syndrome. *Diabet. Med.* **30**, 1495–1499
238. Tsuchiya, H., Ebata, Y., Sakabe, T., Hama, S., Kogure, K., and Shiota, G. (2013) High-fat, high-fructose diet induces hepatic iron overload via a hepcidin-independent mechanism prior to the onset of liver steatosis and insulin resistance in mice. *Metabolism*. **62**, 62–69
239. Nelson, J. E., Brunt, E. M., Kowdley, K. V., and for the Nonalcoholic Steatohepatitis Clinical Research Network (2012) Lower serum hepcidin and greater parenchymal iron in

nonalcoholic fatty liver disease patients with C282Y HFE mutations. *Hepatology*. **56**, 1730–1740

Figure 1.1. Illustration of fatty acid structure and metabolic pathways: (**A**) The structure of fatty acids. Saturated fatty acids, palmitic and stearic acid, and unsaturated fatty acid, oleic acid are shown as representative structures. Triacylglycerol is synthesized from glycerol and three molecules of fatty acids through esterification reactions. (**B**) Schematic diagram of metabolic pathways induced by fatty acids. Dietary fats, absorbed by the enterocytes, enter circulation in the form of chylomicrons, which are digested by lipoprotein lipases (LPL) present in the peripheral vascular beds to release fatty acids (FA). The remnants are readily taken up by the liver. In the adipose tissue, triacylglycerol (TAG) is hydrolyzed through a two-step reaction by adipose triglyceride lipase (ATGL) and hormone-sensitive lipase (HSL) to release FA. Hepatocytes take up circulating FA through passive diffusion or transporter-dependent mechanisms. Dietary glucose furthermore stimulates de novo lipogenesis in the liver for the production of FAs. The liver disposes of FAs by oxidation or secretion in the form of very low density lipoproteins (VLDL). Microsomal triglyceride transfer protein (MTP) plays a key role in the assembly and secretion of VLDL. Additionally, FAs serve as substrates for the synthesis of lipid intermediates, as represented by ceramide.

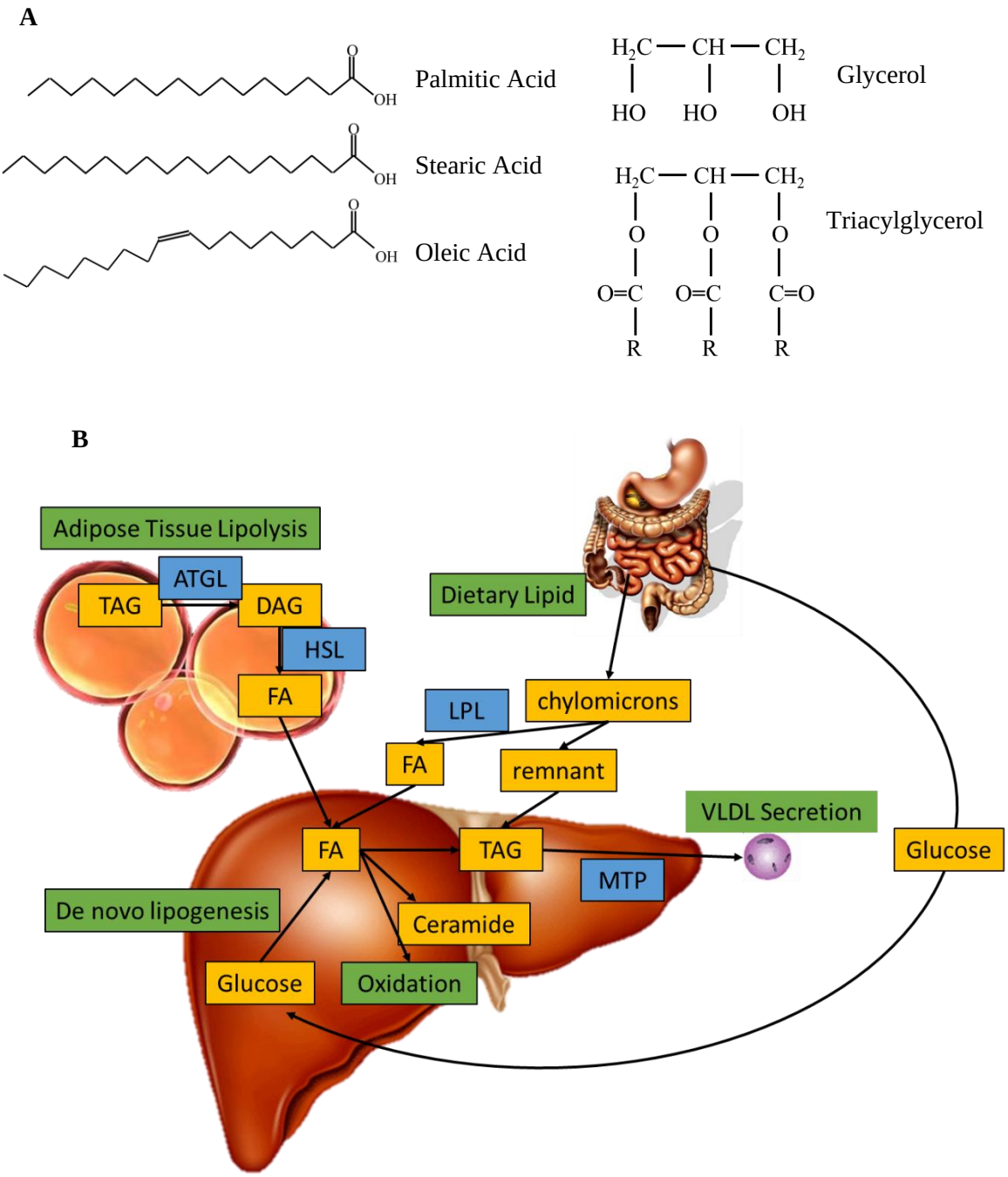
A
Palmitic Acid
Stearic Acid
Oleic Acid
Glycerol
Triacylglycerol
B
Adipose Tissue Lipolysis
ATGL
TAG
DAG
HSL
FA
Dietary Lipid
LPL
chylomicrons
FA
remnant
VLDL Secretion
FA
TAG
MTP
Glucose
De novo lipogenesis
Ceramide
Glucose
Oxidation

Figure 1.1

Figure 1.2. Ceramide synthesis pathways: The de novo synthesis pathway produces ceramide through a four-step sequential reaction cascade. Serine palmitoyltransferase (SPT) catalyzes the initial rate-limiting step. Alternatively, ceramide can be synthesized from the hydrolysis of sphingomyelin located in the cell membrane by sphingomyelinase (SMase) (SMase pathway) and from the recycling of spingosine into ceramide (Salvage pathway). Ceramide also serves as a substrate for the production of sphingomyelin, spingosine and ceramide-1-phosphate.

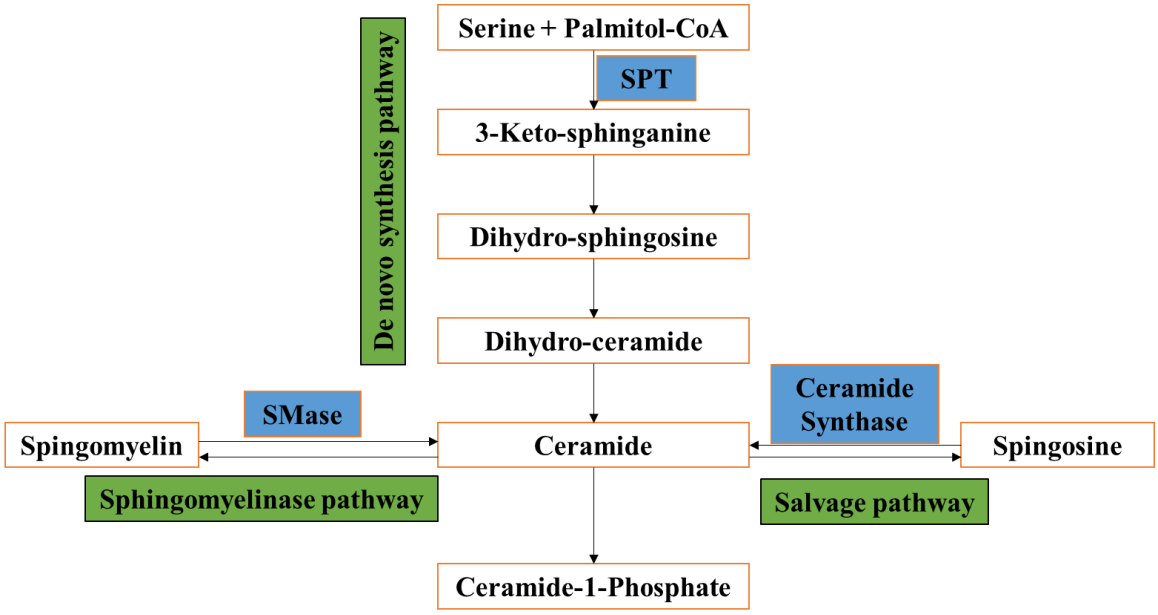
Serine + Palmitol-CoA
SPT
3-Keto-sphinganine
Dihydro-sphingosine
Dihydro-ceramide
De novo synthesis pathway
Ceramide Synthase
SMase
Spingomyelin
Ceramide
Spingosine
Sphingomyelinase pathway
Salvage pathway
Ceramide-1-Phosphate

Figure 1.2

Figure 1.3. Mechanisms of hepatic lipid accumulation: Peripheral insulin resistance (e.g. insulin resistance in myocytes) hinders the uptake and utilization of glucose by the tissues and elevates serum glucose, which in turn stimulates de novo fatty acid (FA) synthesis in the liver. Insulin resistance in adipocytes accelerates lipolysis by desensitizing lipases to insulin and results in elevated serum FA, which are then taken up by the hepatocytes. Additionally, dietary fats are a major source of hepatic FA. FA is esterified to form non-toxic triglycerides. FA oxidation in mitochondria and triglyceride secretion in the form of VLDL are the major FA disposal pathways. Steatosis develops when the capacity of FA disposal in the liver is overwhelmed by the increased levels of FA input and de novo lipogenesis.

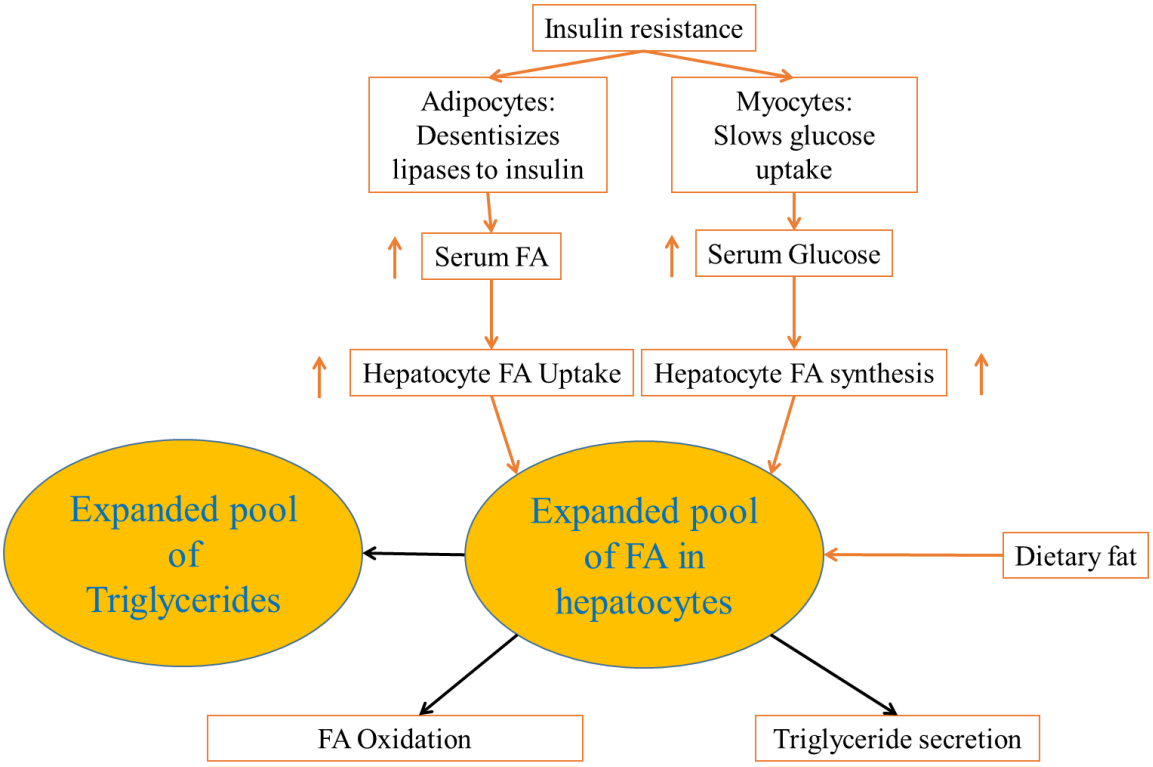
Insulin resistance
Adipocytes: Desentisizes lipases to insulin
Myocytes: Slows glucose uptake
Serum FA
Serum Glucose
Hepatocyte FA Uptake
Hepatocyte FA synthesis
Expanded pool of Triglycerides
Expanded pool of FA in hepatocytes
Dietary fat
FA Oxidation
Triglyceride secretion

Figure 1.3

Figure 1.4. The function and synthesis of hepcidin: (**A**) Hepatocytes are the major site of hepcidin synthesis. After initial processing of pre-prohepcidin, the 25-amino acid biologicaly active mature hepcidin peptide is secreted into the circulation. As the central iron-regulatory protein, hepcidin inhibits iron absorption from the enterocytes in the duodenum and iron release from the reticuloendothelial macrophages, and thereby decreases circulating iron levels. Hepcidin accomplishes this regulatory function by binding to and inducing the internalization and lysosomal degradation of the only known iron exporter, ferroportin. (*Image adopted from World J Gastroenterol. 2009 Mar 14; 15(10): 1186–1193 with permission*). (**B**) Schematic diagram of pre-prohepcidin. Hepcidin is synthesized as an 84 amino acid pre-proprotein. The N-terminal 24-amino acid signal sequence is cleaved to produce prohepcidin, which is further cleaved by furin-like prohormone convertases to yield the 25-amino acid mature hepcidin peptide.

A

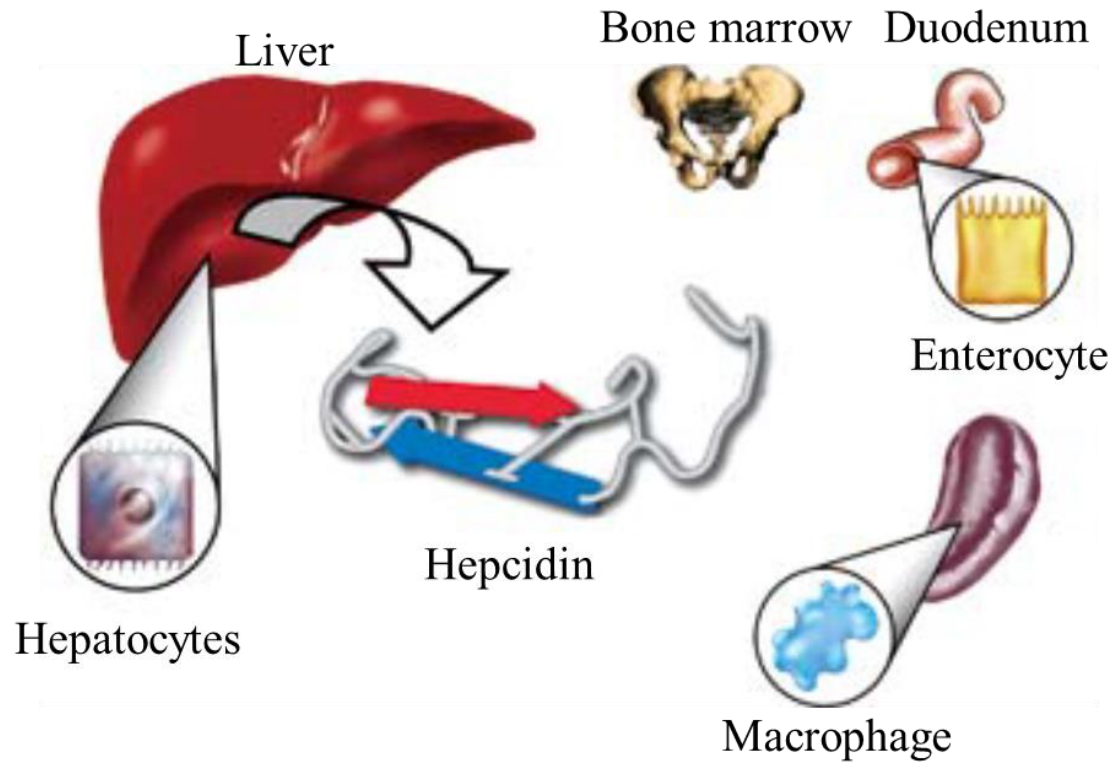
Liver
Bone marrow
Duodenum
Enterocyte
Hepcidin
Hepatocytes
Macrophage

B

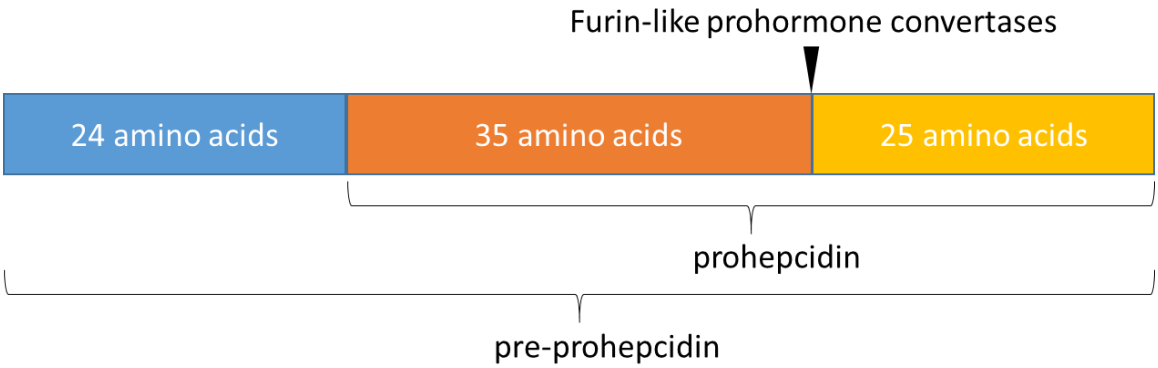
Furin-like prohormone convertases
24 amino acids
35 amino acids
25 amino acids
prohepcidin
pre-prohepcidin

Figure 1.4

Figure 1.5. Regulation of iron homeostasis by hepcidin: (**A**) Under normal physiological conditions, hepcidin is expressed at the basal level. Enterocytes absorb dietary iron at the apical site and export it into the circulation through ferroportin at the basolateral membrane. Iron in senescent red blood cells are phogocytosed by macrophages and recycled into circulation via ferroportin. The liver stores excess iron in hepatocytes and Kupffer cells. (**B**) In iron deficiency, hepcidin expression is reduced, which leads to elevated levels of ferroportin, duodenal iron transport and iron egress by macrophages. (**C**) In iron overload, hepcidin expression is induced, which reduces ferroportin levels and limits duodenal iron transport and iron release by macrophages to restore iron homeostasis. (*Figure adopted from Annu Rev Pathol. 2009;4:489-515. with permission*)

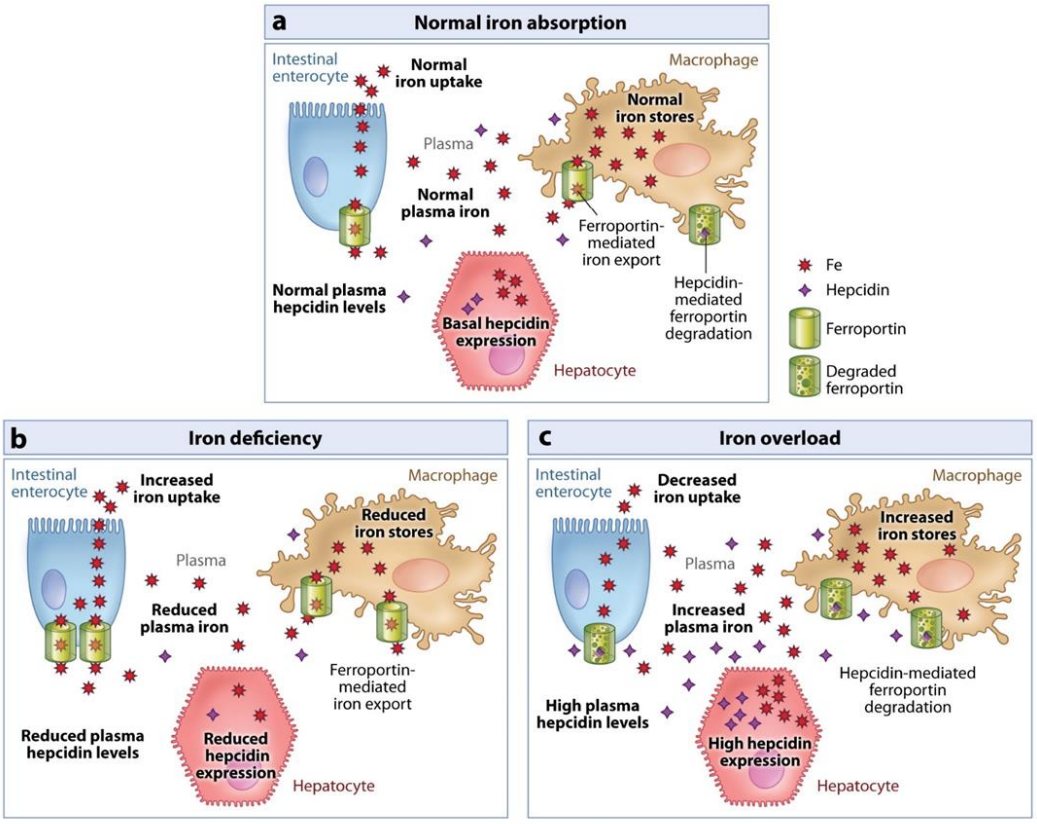

Lee PL, Beutler E. 2009.
Annu. Rev. Pathol. Mech. Dis. 4:489–515

Figure 1.5

Chapter II

Experimental Procedures

1 CELL CULTURE

The cells were grown in a MCO-17AIC CO2 incubator (Sanyo, Moriguchi, Osaka, Japan) with 5% CO_2 and humidified atmosphere at 37^{o}C. HepG2 cells, a human hepatoma cell line, were obtained from the Biochemistry Department of University of Adelaide in Australia. HepG2 cells were cultured in a high glucose (4.5 g/L glucose) Dulbecco's modified Eagle's medium supplemented with glutamine (2 mM) and 10% fetal calf serum (Atlantic Biologicals, GA., USA). Cell culture medium was replenished every 2-3 days. For sub-culturing, cells were detached by incubating with a 0.25% trypsin-1 mM EDTA (Life Technologies., CA., USA) solution for 2 min. at 37^{o}C. For the studies described in later sections, 1.3×10^{6} or 3.9×10^{6} cells were seeded in 25 cm^2 or 75 cm^2 flasks, respectively, 12-24 h. prior to the start of the experiment.

2 ANIMAL MODELS

Animal experiments were approved by the Institutional Animal Care and Use Committee at the University of Nebraska Medical Center. The wild-type mice strains used in this dissertation include C57BL/6J (the Jackson Laboratory, ME., USA), C57BL/6NCR (National Institute of Health, USA). *Hamp* Floxed and *Hamp* Knockout mice on C57BL/6J genetic background were generated in our laboratory in cooperation with a commercial company (Ozgene Pty. Ltd., Perth, Australia), as published previously (1). The mouse colonies were maintained in a controlled environment behind a sterile barrier at the Animal Care facility at the University of Nebraska with constant temperature, humidity and 12:12-h light-dark cycle. Free access to food and water was provided. Transgenic mice were genotyped, as described below (*see section 16 of this chapter)*. At the end of experiments, mice were anesthetized with a Ketamine (100 mg/kg b.w.) and Xylazine (10 mg/kg b.w.) solution and sacrificed to harvest organs and cardiac blood.

Serum was isolated from clotted blood by centrifuging at 1300 RPM for 15 min. at room temperature. The harvested livers were kept frozen at -80°C ultra-freezer for RNA extraction or protein lysate preparations. For histological analysis, fresh liver tissues were fixed in 10% Buffered

Formalin (Thermo Fisher Scientific, Waltham, MA, USA) and delivered to the Tissue Science Core Facility at the University of Nebraska Medical Center for paraffin-embedding, and subsequent sectioning and staining with Hematoxylin and Eosin (H & E).

3 RNA EXTRACTION

Procedures involving RNA studies were performed using RNase-free tubes (Ambion®, Life Technologies) and pipette tips with barriers (ART™, Thermo Fisher Scientific) to avoid RNA degradation. For RNA extractions, 50mg of liver tissue or 4–5x 10^6 HepG2 cells were re-suspended in 1 mL. TRIzol reagent (Invitrogen, CA., USA). Prior to re-suspension in Trizol, the liver tissues were cut into fine pieces in a sterile petri dish on ice using clean disposable razor blades. To re-suspend HepG2 cells, 1 mL of TRIzol reagent was directly pipetted onto the cells attached to the tissue culture flasks, which were rinsed twice with sterile 1X phosphate-buffered saline (PBS) solution (Invitrogen).The TRIzol suspensions of tissues or cells were then incubated at room temperature for 5 min. prior to the addition of 200 μL of chloroform. The tubes were vortexed vigorously for 15 seconds and incubated at room temperature for 3 min. The organic and aqueous phases were separated by centrifugation at 12000 x g for 15 min. at 4 ^oC. The aqueous phase, which contained RNA, was carefully removed into a clean RNAase-free tube, and mixed with 500 μL of isopropanol, and incubated at room temperature for 10min. To pellet RNA, the tubes were centrifuged at 12000 x g for 10 min. at 4 ^oC. To remove salt contamination, RNA pellets were re-suspended in 1 mL of 75% ethanol and centrifuged at 7500 x g for 5 min. To dry out residual ethanol, the tubes containing RNA pellets were kept at room temperature. Subsequently, RNA were dissolved in 30–50 μL of diethylpyrocarbonate (DEPC)-treated RNAase-free distilled water (Thermo Fisher Scientific) by incubating at 45 ^oC for 10 minutes. The quality and purity of extracted RNA were validated by agarose gel electrophoresis. RNA concentrations were determined by measuring the absorption at 260 nm with Biomate3 spectrometer (Thermo Fisher Scientific). RNA suspensions were aliquoted and kept at -80 ^oC ultrafreezer for further use.

4 cDNA SYNTHESIS AND QUANTITATIVE REAL-TIME PCR

cDNA was synthesized from 3 μg of isolated RNA (see above) using 6.25 μM random hexamers (Applied Biosystems, Life Technologies) and Superscript II reverse transcriptase enzyme (Invitrogen) according to the manufacturer's instructions. cDNA was diluted with 60 μL of autoclaved distilled water and separated into 3 aliquots for real time PCR experiments. Real-time PCR (qPCR) reactions were performed in triplicates using either Taqman universal PCR master mix (Life Technologies) or iTaq Universal SYBR Green Supermix (Bio-Rad, CA, USA) with StepOnePlus instrument (Life Technologies). Taqman fluorescent probe (5' 6-[FAM]; 3' [TAMRA-Q]) and primers, spanning through exon boundaries, were designed with Primer Express 1.0 Program (Applied Biosystems) and synthesized commercially (Sigma-Aldrich, PA., USA and Thermo Fisher Scientific). Pre-designed primers used for SYBR green qPCR were obtained from PrimerBank (2). Glyceraldehyde dehydogenase (GAPDH) gene was used as the endogenous control for qPCR experiments. The qPCR assays were performed with ABI PRISM 7700 Sequence Detection System (applied Biosystems) with the following cycling conditions: Taqman [50^{o}C 2min., 95 ^{o}C 10min., 40 cycles of (95 ^{o}C 15sec., 60 ^{o}C 1min)]; SYBR green [50 ^{o}C 2min., 95 ^{o}C 30sec., 40 cycles of (95 ^{o}C 15sec., 60 ^{o}C 1min)]. Melting curve analysis was performed for SYBR green qPCR assays to validate the specificity of the primers. Gene amplification was calculated using comparative CT method, as described (3). The sequences of Taqman probe and primers, and SYBR green primers, which were used for the experiments in this dissertation, are shown below (see Table 2.1 and Table 2.2).

5 RNA HALF-LIFE MEASUREMENT

HepG2 cells were treated with palmitic acid (PA) or solvent (isopropanol) in the presence of the transcription inhibitor, actinomycin D for indicated time points. The level of *HAMP* mRNA expression, as measured by qPCR (*see above*), was expressed as fold-change of that in control cells, which were treated with solvent in the presence of DMSO, at corresponding time points. Rate

constant for RNA decay (k_{decay}) was determined with linear regression (least-square) analysis. RNA half-life was calculated with the equation: $t_{1/2} = \ln 2 / k_{decay}$.

6 XBP1-SPLICING ASSAY

XBP1-splicing assay is based on the fact that spliced form of XBP1 mRNA lacks the recognition sequence for Pst1, which is present in the unspliced form. In brief, PCR was performed with cDNA using a specific primer set for XBP1: (forward: 5'-AAACAGAGTAGCAGCTCAGACTGC-3' reverse: 5'-TCCTTCTGGGTAGACCTCTGGGAG-3'). The amplicons 448 bp and 474 bp, which indicate spliced and unspliced forms of XBP-1, respectively were subsequently digested with Pst I at 37^{o}C for 2 hours. Following digestion, unspliced XBP1 amplicon (474 bp) yielded 290 bp and 183 bp fragments. The digested products were subjected to DNA agarose gel electrophoresis. GAPDH was amplified with the following primers as loading control: forward: 5'-TGGTATCGTGGAAGGACTC-3' reverse: 5'- AGTAGAGGCAGGGATGATG-3'.

7 WHOLE CELL LYSATE ISOLATION AND SUBCELLULAR FRACTIONATION OF CELLS

To prepare whole cell lysates, HepG2 cells or liver tissues were incubated for 15 min. in lysis buffer [10 mM Tris-HCl (pH 7.4), 100 mM NaCl, 5 mM EDTA and 10% glycerol] supplemented with 1 mM PMSF, 0.5% Triton X-100, protease inhibitor cocktail, pepstatin A (Sigma-Aldrich), and activated sodium orthovanadate (ACROS Organics, Thermo Fisher Scientific). The lysates were sonicated (50% amplitude, 3 x 5 sec. cycles) with ultrasonic dismembrator 150T (Thermo Fisher Scientific) to facilitate cell lysis. Following centrifugation at 3000 x g for 5 min. (4°C), supernatants were collected and used for western blotting.

To isolate cytosolic and nuclear fractions, HepG2 cells were trypsinized and washed twice with 1 X PBS. The cell pellets were subsequently re-suspended in a hypotonic buffer (10 mM Tris-HCl, 10 mM NaCl, 2.5 mM $MgCl_2$) and incubated on ice for 5 min. Following centrifugation at 1700 x

g for 10 min. (4°C), supernatants were collected and used as cytosolic fractions. The nuclei pellets were then washed twice with hypotonic buffer to eliminate residual cytosol contamination. Washed pellets were re-suspended in an extraction buffer (50 mM Tris-HCl, 420 mM NaCl, 2.5 mM $MgCl_2$, 1% Igepal, 0.5% deoxycholate) and sonicated (30% amplitude, 3 x 5 sec. cycles). Sonicated lysates were centrifuged at 2800 x g for 10 min. (4°C) to remove cell debris. The supernatants were utilized as nuclear fractions. The protein concentrations in whole cell lysates or cellular fractions were determined by a commercial protein assay dye reagent (BioRad) based on Bradford-dye-binding method.

8 WESTERN BLOTTING

The cell lysate proteins (10-50 μg) were resolved with SDS-polyacrylamide gel electrophoresis (SDS-PAGE) using Mini-PROTEAN gel electrophoresis system (Bio-Rad). The resolved proteins were subsequently transferred onto polyvinylidene fluoride (PVDF) membranes (Bio-Rad) via electrophoresis in a transfer buffer (Thermo Fisher Scientific) containing 10 % methanol overnight at 4°C with constant 20 volts, followed by 1 h. of 40 volts transfer the next day. PVDF membranes, which were washed briefly with 1 x Tris-buffered saline (TBS) solution (Sigma-Aldrich), were blocked with 2% nonfat milk (BioRad) dissolved in 1 x TBS buffer for 1 h. at room temperature. Blocked and TBST (1 x TBS supplemented with 0.1% TWEEN-20)-washed membranes were then incubated with respective primary antibodies (as listed in **Table 2.5**) overnight rotating at 4°C in heat-sealed plastic pouches (Thermo Fisher Scientific). The next day, membranes were washed twice with TBST and incubated with corresponding secondary (anti-mouse or anti-rabbit) antibodies (Cell Signaling, MA., USA) for 1 h. at room temperature. Immune-reactive bands were detected by the ImmunStar-AP Substrate (Bio-Rad Laboratories) using Genemate films (Thermo Fisher Scientific).

9 CASPASE-3/7 ACTIVITY ASSAY

The livers harvested from mice or cultured HepG2 cells were homogenized in a lysis buffer [20 mM KCl, 20 mmol/L MOPS, 2 mM MgCl2, 1 mM EDTA, 0.5% Triton X-100, (pH 7.2)] and incubated for 30 min. on ice. The lysates were centrifuged at 14500 x g for 30 min. at 4 °C, to collect supernatants, which were used for the assay. Caspase-3/7 enzyme activity was measured by using 5 μg Ac-DEVD-AMC caspase-3 fluorogenic substrate (BD Biosciences, NJ., USA). The amount of AMC released in the assay was quantified with a Perkin-Elmer Luminescence Spectrophotometer LS 55 (Perkin Elmer, MA., USA). A standard curve was generated by using commercially-obtained free AMC reagent (Sigma-Aldrich). Caspase-3 enzyme activity is expressed as nmoles of AMC released per mg of protein. The protein concentrations in liver lysates were determined, as described above (*see section 7 of this chapter*).

10 LIPID DROPLET STAINING

Following treatment with fatty acids, HepG2 cells were washed twice with 1 X PBS solution and fixed with 4% paraformaldehyde (Sigma-Aldrich) at room temperature for 15 min. The fixed cells were stained with 0.2 mg/mL Nile Red (ACROS Organics) for 5 min. at room temperature. The nuclei were counter-stained with Hoechst 33342 dye (Invitrogen). Fluorescent images were obtained with a Nikon Eclipse E400 fluorescence microscope with red and UV filter sets for Nile Red and Hoechst 33342 dye, respectively (Nikon, NY, USA) using a CC-12 digital camera (Olympus, NY, USA) and analySIS software (Olympus Soft Imaging System).

11 IMMUNOFLUORESCENT STAINING

HepG2 cells were seeded onto poly-L-lysine-coated coverslips in 24-well plates. After treatments, cells were washed twice with 1 X PBS solution and fixed with 4% paraformaldehyde (Sigma-Aldrich) for 15 min. at room temperature. Fixed cells were permeabilized with 0.5% Triton X-100 for 15 min. prior to blocking with 5% BSA (Sigma-Aldrich) for 1 h. After washes with 1x PBS, cells were incubated with an anti-HuR primary antibody (1:50 dilution, sc-5261, Santa Cruz, CA,

USA) by rotating overnight at 4°C. Control cells were incubated in parallel with normal mouse IgG (Santa Cruz). The next day, cells were washed three times with 1X TBS buffer supplemented with 0.1% TWEEN-20 (TBST) and incubated with a secondary Texas Red-conjugated horse anti-mouse IgG (1:300 dilution, Vector Laboratories) for 1 h. at room temperature. Subsequently, coverslips were washed with 1X TBST 3 times and mounted with VECTASHIELD® Hard-Set Mounting Medium with DAPI (Vector Laboratories, CA, USA).

Fluorescent images were obtained, as described above (*see section 10 of this chapter*). ImageJ software (National Institutes of Health, USA) was used to process microscopic images. The merging of HuR and DAPI images into a two-channel image was performed for co-localization analysis using ImageJ plug-in Squassh (4). The percentage of nuclei-localized HuR (C_{signal}) was calculated by computing the percentage of HuR pixels, which are co-localizing with DAPI pixels. The percentage of cytosolic HuR was subsequently calculated by using the formula, 100% -$_{Csignal}$.

12 CHROMATIN IMMUNOPRECIPITATION (ChIP)

50 x 10^6 HepG2 cells were fixed with 1% formaldehyde (Sigma-Aldrich) for 10 min. at room temperature. The cross-linking was stopped with 0.1375M glycine (Thermo Fisher Scientific) solution. The cells were subsequently washed twice with ice-cold 1 x PBS and lysed with ChIP lysis buffer [5 mM PIPES (pH 8.0), 85 mM KCl, 0.5% Nonidet P-40 (NP-40)] supplemented with protease inhibitors (*see section 7 of this chapter above*). Nuclear fractions, which were collected by centrifugation at 1000rpm for 10 min. at 4°C, were lysed on ice for 10 min. with lysis buffer [50 mM Tris-Cl (pH 8.0), 10 mM EDTA, 1% SDS] supplemented with protease inhibitors. The lysates were sonicated using ultrasonic Dismembrator 150T (Thermo Fisher Scientific) to shear chromatin using the following settings: 50% amplitude, 6 x 30 sec. cycles with 1 min. incubation on ice in between cycles. The shearing efficiency of chromatin was analyzed using standard techniques and DNA-Agarose Gel electrophoresis. For immunoprecipitation, 100 μg of sheared chromatin was first pre-cleared for 2 hours at 4°C with 50 μL protein A-Agarose beads (Santa Cruz), which were

blocked with Herring Sperm DNA (Promega, WI, USA). 5 µL of pre-cleared chromatin solution was saved as Input DNA control for further analysis (see below). The rest of pre-cleared chromatin was then incubated with anti-STAT3 (Cell Signaling, #9132), anti-NF-κB p65 (Cell Signaling, #4764) or anti-c-Jun (Santa Cruz, #sc-45) primary antibodies by rotating overnight at 4°C. Normal rabbit or mouse IgG (Santa Cruz) was used as negative controls. The next day, chromatin and IgG complexes were captured by incubating with 50 µL of blocked protein A-Agarose beads for 2 hours at 4^{o}C. Immunoprecipitates were subjected to several round of washes as follows: 1x with low salt buffer [20 mM Tris/HCl (pH 8.0), 2 mM EDTA, 150 mM NaCl, 0.1% SDS and 1% Tritonx-100], 1 X with high salt buffer [20 mM Tris/HCl (pH 8.0), 2 mM EDTA, 500 mM NaCl, 0.1% SDS and 1% Tritonx-100], 1X with lithium chloride wash buffer [10 mM Tris/HCl (pH 8.0), 1 mM EDTA, 250 mM LiCl, 1% Triton x-100, 1% Igepal and 1% deoxycholic acid] and 3x with 1x TE buffer. Chromatin was subsequently eluted using a freshly-prepared elution buffer (100 mM NaHCO3 and 1% SDS). Cross-linking of eluted chromatin and Input DNA controls (*see above*) was reversed by incubating overnight in 200 mM NaCl at 65°C. The reverse-cross-linked samples were treated with DNase-free RNase (0.1 mg/mL Thermo Fisher Scientific) and proteinase K (0.1 mg/mL, Thermo Fisher Scientific) solutions and subsequently purified by a commercial Qiaquick PCR purification kit (Qiagen, MD, USA). Purified chromatin solutions were used as a template in PCR reactions to amplify *HAMP* promoter using specific primers designed with Primer-BLAST (NCBI), as listed in Table 2.4 and Taq polymerase (Thermo Fisher Scientific). The ChIP method was validated by using IL-6-treated HepG2 cells as positive control.

13 RIBONUCLEOPROTEIN IMMUNOPRECIPITATION ASSAYS

Ribonucleoprotein immunoprecipitation (RNP-IP) assays were performed, as described (5). Briefly, 30 µg of HuR antibody (RN004P, MBL International, MA, USA) or normal rabbit IgG (Santa Cruz) was pre-conjugated to 100 µL of protein A-Agarose beads (Santa Cruz) overnight at 4°C. HepG2 cells were trypsinized and lysed to isolate cytosolic fractions with lysis buffer containing 0.5 mM

Tris-HCl (pH 7.4), 100 mM NaCl, 2.5 mM $MgCl_2$. Cytosolic proteins were first pre-cleared with 50 µL of plain protein A-Agarose for 30 min. at 4°C. For immunoprecipitation (IP), pre-cleared lysates were mixed with 100 µL of antibody-conjugated protein A-Agarose and incubated at 4°C for 3 h. Following centrifugation at 5,000 x g for 5 min. at 4°C, the supernatants were discarded and the beads were subsequently washed twice with wash buffer [50 mM Tris-HCl (pH 7.5), 150 mM NaCl, 1 mM MgCl2 and 0.05% NP-40]. 10 µl of IP aliquots were saved for further immunoblotting analysis. Immunoprecipitated RNA were then eluted using 0.1% SDS and proteinase K (0.1 mg/ mL, Thermo Fisher Scientific), and purified with TRIzol (Life Technologies). *HAMP* mRNA was quantified by qPCR, as described above (*see section 4 of this chapter*). 18s rRNA, which has been shown not to interact with HuR (6, 7), was used as a negative control for RNP-IP assays.

14 GENERATION OF PLASMID DNA CONSTRUCTS AND DUAL LUCIFERASE REPORTER ASSAYS

1.5 kbp or 0.6 kbp *HAMP* promoter regions were amplified by PCR using Phusion High-Fidelity DNA Polymerase (Thermo Scientific) and specific primers, as listed in Table 2.3. Following restriction enzyme digestions, PCR products were inserted into pGL3-Basic Luciferase Reporter Vector (Promega Corp.). The ligated plasmids were electroporated into competent DH5α bacterial cells with a MicroPulse electroporator system (BioRad) and plated on antibiotic-containing LB-agar plates using standard techniques. DNA, isolated from bacterial colonies, were subsequently sequenced to verify correct plasmid clones harboring *HAMP* promoter sequences in the forward direction. The 101 bp full length *HAMP* 3'UTR region was also amplified by PCR using specific primers harboring a 5'phosphate group (*see Table 2.3*). PCR amplicons were inserted into PmeI site of the pMIR-REPORT reporter vector (Life Technologies) by a standard blunt end cloning technique. The plasmid clone harboring 3'UTR in the "forward" direction was confirmed by DNA sequencing.

Mutagenesis of a specific cis-element in the *HAMP* promoter or 3'UTR regions was performed with a commercial mutagenesis kit (Quickchange II Site-Directed Mutagenesis. Agilent Technologies, CA., USA) using specific primers, as listed in Table 2.3 below.

Plasmid DNA were purified using a commercial kit (Plasmid Maxi Prep, Qiagen). HepG2 cells were transfected with either empty (as control) or recombinant reporter vectors using lipofectamine 3000 reagent (Life Technologies). pRL-SV40 plasmid encoding renila luciferase was co-transfected to standardize the transfection efficiency. Dual luciferase reporter assays were performed according to manufacturer's instructions (Promega). IL-6 treatment was employed as a positive control to validate the assay system.

15 TRANSFECTION OF miRNA MIMIC AND siRNA

30 pmol of negative control miRNA or miR-214 mimic (Life Technologies) were introduced into HepG2 cells with Nucleofector transfection apparatus (Lonza, IL, USA). Plasmids and siRNA were transfected by using Lipofectamine 3000 or Lipofectamine RNAiMax (Life Technologies), respectively, according to the instructions of the manufacturer. For siRNA experiments, two consecutive transfections were performed to increase transfection efficiency.

16 GENOTYPING of *Hamp* KNOCKOUT (KO) MICE

Genotyping was performed using genomic DNA, isolated from mice tails by a commercial kit (Promega Corp.), as a template in PCR reactions. PCR was performed using allele-specific primer sets. The diagnosis of wild-type (860 bp) *Hamp* allele was performed by using primers, 5'-ACTCTAATGAGGAAGGACCAGAGG-3' and 5'-CTGTCTCATCTGTGAAAGCAGAAG-3', which also amplified wild-type *Hamp2* allele (968 bp). Null *Hamp* allele (439 bp) was amplified by using primers, 5'-ACTCTAATGAGGAAGGACCAGAGG-3' and 5'-AGTACTGATATCATCGATGGCG-3'. PCR conditions were: 1 cycle of 95°C for 5 min., 35

cycles of [95°C for 30 sec., 58°C for 1.5 min., 72°C for 30 sec.], and 1 cycle of final extension at 72°C for 5 min.

17 INDUCTIVELY COUPLED MASS SPECTROMETRY (ICP-MS)

To quantify tissue iron, mice livers were analyzed by ICP-MS at the Redox Biology Center of the University of Nebraska in Lincoln. Tissues were weighed and digested with metal-grade nitric acid for 2–3 h at room temperature followed by overnight digestion at 80°C. The digestions were subsequently cooled and diluted 20-fold prior to ICP-MS analysis. Gallium (50 ppb) was added as internal standard. Iron was quantitated by measuring at m/z = 56 and 57Fe was used for confirmation. Helium (5 mL/min) was employed as collision gas for the elimination of polyatomic interferences. Each sample was analyzed in triplicate.

18 QUANTIFICATION OF HEPATIC TRIGLYCERIDES

Triglycerides were quantified in Dr. K. Kharbanda's laboratory at Omaha VA Medical Center, as published previously (8, 9). Briefly, 50 mg of mice liver tissues were homogenized using a tissuemizer (Tekmar Ultra-Turrax) in 2 mL $CHCl_3$:MeOH (2:1) solution. Residual tissue particles were filtered through Whatman #1 filter paper (Thermo Fisher Scientific). The total volume of filtered lysates were brought to 2.5 mL with $CHCl_3$:MeOH (2:1). After the addition of 0.5 mL of water containing 0.04% $CaCl_2$ (i.e. total volume of 3 mL), the samples were thoroughly mixed by vortexing and then centrifuged at 3,000 rpm for 5 min. at room temperature. The upper aqueous phase was removed and lower organic phase was washed thrice with 1mL of an organic solution/water mix (3.06 % chloroform, 48.98 % methanol, 47.94% water and 0.02% $CaCl_2$). After sequential separation of phases to eliminate non-lipid substances, the organic solution mix containing the lipids was evaporated using a centrivac apparatus overnight. The next day, dried samples were hydrolyzed in 0.25 mL of 95% ethanol and 25 µL of 8.0 M KOH solution by incubating for 20 min. at 65°C. The triglyceride content was determined by using a commercial kit (Thermo DMA kit 2750) according to manufacturer's instructions (Thermo Scientific), and

measuring absorbance at 510nm wavelength with a DU-640 Spectrophotometer (Beckman Coulter). The final hepatic triglyceride amount was calculated by standardizing the amount in the whole liver to the body weight, and expressed as μmol per liver per 100 gram body weight (μmol/L/100 g b.w.).

19 SIRIUS RED STAINING AND QUANTIFICATION

Paraffin-embedded liver tissues were prepared as described above (*see section 2 of this chapter*). Tissue sections were de-waxed with sequential incubations in organic solutions (3x in xylene for 3min., 2 X in 100% ethanol for 2 min., and 1X each in 95%, 80%, and 50% ethanol for 2 min). They were then stained with a Picrosirius Red solution (0.1% Sirius Red in saturated picric acid) for 60 min. The sections were subsequently washed twice with acetic acid for 2 min. and thrice with 100% ethanol followed with three cycles of xylene washes, each for 3 min. The washed sections were mounted using a ShandonMount mounting medium (Thermal Fisher Scientific).

Images of Sirius Red-stained mice livers were obtained using a Nikon Eclipse E400 light microscope with a CC-12 digital camera and analySIS software. The quantification of the images was performed with ImageJ software using 10 independent images (10 x magnification) obtained from each stained section. Briefly, the microscopic images were split into red, green, and blue channels with the RGB stack command. The green channel was selected and threshold was manually set for each image to correctly reflect the staining in the original image. 10 non-overlapping fields in each image were selected and the staining was quantified with the ROI manager of ImageJ**.**

20 STATISTICAL ANALYSIS

The significance of differences between groups was determined by Student’s t-test or one-way ANOVA with Tukey's HSD post-hoc test by using SPSS software (IBM, Armonk, NY). A value of $P < 0.05$ was accepted as statistically significant.

21 REFERENCES

1. Lu, S., Seravalli, J., and Harrison-Findik, D. (2015) Inductively coupled mass spectrometry analysis of biometals in conditional Hamp1 and Hamp1 and Hamp2 transgenic mouse models. *Transgenic Res.* 10.1007/s11248-015-9879-3
2. Wang, X., Spandidos, A., Wang, H., and Seed, B. (2012) PrimerBank: a PCR primer database for quantitative gene expression analysis, 2012 update. *Nucleic Acids Res.* **40**, D1144–D1149
3. Schmittgen, T. D., and Livak, K. J. (2008) Analyzing real-time PCR data by the comparative CT method. *Nat. Protoc.* **3**, 1101–1108
4. Rizk, A., Paul, G., Incardona, P., Bugarski, M., Mansouri, M., Niemann, A., Ziegler, U., Berger, P., and Sbalzarini, I. F. (2014) Segmentation and quantification of subcellular structures in fluorescence microscopy images using Squassh. *Nat. Protoc.* **9**, 586–596
5. Lal, S., Burkhart, R. A., Beeharry, N., Bhattacharjee, V., Londin, E. R., Cozzitorto, J. A., Romeo, C., Jimbo, M., Norris, Z. A., Yeo, C. J., Sawicki, J. A., Winter, J. M., Rigoutsos, I., Yen, T. J., and Brody, J. R. (2014) HuR Posttranscriptionally Regulates WEE1: Implications for the DNA Damage Response in Pancreatic Cancer Cells. *Cancer Res.* **74**, 1128–1140
6. Lal, A., Mazan-Mamczarz, K., Kawai, T., Yang, X., Martindale, J. L., and Gorospe, M. (2004) Concurrent versus individual binding of HuR and AUF1 to common labile target mRNAs. *EMBO J.* **23**, 3092–3102
7. García-Domínguez, D. J., Morello, D., Cisneros, E., Kontoyiannis, D. L., and Frade, J. M. (2011) Stabilization of Dll1 mRNA by Elavl1/HuR in neuroepithelial cells undergoing mitosis. *Mol. Biol. Cell.* **22**, 1227–1239
8. Folch, J., Lees, M., and Stanley, G. H. S. (1957) A Simple Method for the Isolation and Purification of Total Lipides from Animal Tissues. *J. Biol. Chem.* **226**, 497–509
9. Kharbanda, K. K., Mailliard, M. E., Baldwin, C. R., Beckenhauer, H. C., Sorrell, M. F., and Tuma, D. J. (2007) Betaine attenuates alcoholic steatosis by restoring phosphatidylcholine generation via the phosphatidylethanolamine methyltransferase pathway. *J. Hepatol.* **46**, 314–321

Table 2.1. Taqman qPCR Fluorescent Probe and Primer Sequences of human (Hu) and mouse (Mu) genes

Gene	Forward Primer (*5′-3′*)	Reverse Primer (*5′-3′*)	Taqman Probe (*5'-3'*)
Hu-*HAMP*	TGCCCATGTTCCAGAGGC	CCGCAGCAGAAAATGCAGAT	AAGGAGGCGAGACACCCACTTCCC
Hu-GAPDH	TGAAGGTCGGAGTCAACGG	AGAGTTAAAAGCAGCCCTGGTG	TTTGGTCGTATTGGGCGCCTGG
Mu-*Hamp*	TGCAGAAGAGAAGGAAGAGAGACA	CACACTGGGAATTGTTACAGCATT	CAACTTCCCCATCTGCATCTTCTGCTGT
Mu-*Hamp2*	GCGATCCCAATGCAGAAGAG	TGTTACAGCACTGACAGCAGAATC	AGGAAGAGAGACATCAACTTCCCCATCTGC
Mu-GAPDH	TCACTGGCATGGCCTTCC	GGCGGCACGTCAGATCC	TTCCTACCCCCAATGTGTCCGTCG

Table 2.2. SYBR qPCR primer sequences of mouse (Mu) genes

Gene	Forward Primer *(5'-3')*	Reverse Primer *(5'-3')*
Mu-MTP	CTCTTGGCAGTGCTTTTTCTCT	GAGCTTGTATAGCCGCTCATT
Mu-CPT1	CTCCGCCTGAGCCATGAAG	CACCAGTGATGATGCCATTCT
Mu-FSP27	ATGAAGTCTCTCAGCCTCCTG	AAGCTGTGAGCCATGATGC
Mu- G6PC	CGACTCGCTATCTCCAAGTGA	GTTGAACCAGTCTCCGACCA
Mu-PCK1	CTGCATAACGGTCTGGACTTC	CAGCAACTGCCCGTACTCC
Mu-PPARα	AGAGCCCCATCTGTCCTCTC	ACTGGTAGTCTGCAAAACCAAA
Mu-SREBP-1C	GCAGCCACCATCTAGCCTG	CAGCAGTGAGTCTGCCTTGAT
Mu-Col1a1	GCTCCTCTTAGGGGCCACT	CCACGTCTCACCATTGGGG
Mu-SAA3	GCCTGGGCTGCTAAAGTCAT	TGCTCCATGTCCCGTGAAC
Mu-IL-6	CTGCAAGAGACTTCCATCCAG	AGTGGTATAGACAGGTCTGTTGG
Mu-GAPDH	GTGGAGATTGTTGCCATCAACGA	CCCATTCTCGGCCTTGACTGT

Table 2.3. Sequences of primers used for cloning and site-directed mutagenesis experiments

Gene	Forward Primer *(5'-3')*	Reverse Primer *(5'-3')*
1.5 kbp *HAMP* promoter	GGACGCGTCTGGGCCTGGTAGTGGAAAG	GACTCGAGTGAGCTTGCTCTGGTGTCTG
0.6 kbp *HAMP* promoter	GGACGCGTTGTCATTTATGGCCAAAAGTTTGCT	GACTCGAGTGAGCTTGCTCTGGTGTCTG
0.6 kbp *HAMP* promoter ΔSTAT3	CTGTCTCATTTCCAGGTGGTGGCGCCGAAAA	TTTTCGGCGCCACCACCTGGAAATGAGACAG
***HAMP* 3'UTR**	AACCTACCTGCCCTGCCC	TTTGGAAAACAAAAGAACCAGCC
***HAMP* 3'UTR ΔARE**	CTGGGGCAGCAGGAATTAAGGAAGGGAGGG	CCCTCCCTTCCTTAATTCCTGCTGCCCCAG

Table 2.4. The sequence of primers employed in ChIP assays specific for human (Hu) and mouse (Mu) gene promoters

Gene	Forward Primer *(5'-3')*	Reverse Primer *(5'-3')*
Hu-STAT3	GAGGGTGACACAACCCTGTT	ACCGAGTGACAGTCGCTTTT
Hu-NF-κB	TCATTTATGGCCAAAAGTTTGCT	CAAGCATCAGCGTGTGCC
Hu-c-Jun/AP-1	TGAGGGTGACACAACCCTGT	CTGCTGGGTCTTGAGCTTGC
Mu-*Hamp*	GCCATACTGAAGGCACTGA	GTGTGGTGGCTGTCTAGG

Table 2.5. Primary antibodies used for western blotting

Antigen	Company	Catalog number	Dilution
P-SMAD 1/5	Cell Signaling	#9516	1:1000
HuR	Santa Cruz	sc-5261	1:2000
P-JNK	Cell Signaling	#9251	1:1000
P-STAT3 (Ser 727)	Cell Signaling	#9134	1:1000
P-STAT3 (Tyr 705)	Cell Signaling	#9131	1:1000
STAT3	Cell Signaling	#9132	1:1000
P-NF-κB p65	Cell Signaling	#3033	1:1000
NF-κB p65	Cell Signaling	#4764	1:1000
αSMA	Sigma	A2547	1:2000
Histone H3	Active Motif	#39163	1:4000
gapdh	Millipore	MAB374	1:4000

Chapter III

Apoptosis Induced by Fas Signaling Does Not Alter Hepatic Hepcidin Expression

This chapter has been adopted from

Lu, S., Zmijewski, E., Gollan, J., and Harrison-Findik, D. D. (2014) Apoptosis induced by Fas signaling does not alter hepatic hepcidin expression. *World J Biol Chem*. **5**, 387–397

1 ABSTRACT

A connection between hepcidin expression and lipid metabolism in non-alcoholic fatty liver disease (NAFLD) has been implicated. Our studies with hepatoma cells also indicated induction of hepcidin expression by saturated fatty acids. Fatty acids are well-recognized for promoting apoptosis, which contributes to the pathogenesis of NAFLD. However, the direct effect of apoptosis on hepcidin is unknown. We therefore investigated whether apoptosis induced via Fas ligand directly affects hepcidin expression in HepG2 cells and the livers of wild-type male C57BL/6J and C57BL/6NCR mice. HepG2 cells were treated with CH11, an activating antibody for human Fas receptor, for 12 hours to induce extrinsic apoptotic pathway. Mice were injected with sublethal doses (0.2 µg/g b.w.) of Jo2, an activating antibody for mouse Fas receptor. Although CH11 promoted apoptosis in HepG2 cells, as shown by significant activation of caspase-3/7, it did not alter the expression of human hepcidin gene, *HAMP*. Jo2 treatment of mice for 6 hours, but not 1 hour, induced significant apoptosis, acute phase reaction and IL-6 expression in the liver. Similar to HepG2 cells, Jo2 did not affect hepatic mRNA expression of mouse hepcidin gene, *Hamp*. IL-6 is a strong activator of JAK/STAT signaling pathway and STAT3 is known to induce hepcidin transcription. Accordingly, Jo2-induced phosphorylation (i.e. activation) of STAT3 in the liver. However, no interaction of STAT3 with *Hamp* promoter was observed, as confirmed by chromatin immunoprecipitation assays. The effect of Jo2 was stronger in the livers of C57BL/6J than C57BL/6NCR mice. C57BL/6J mice exhibited more prominent activation of apoptosis, liver injury and acute phase reaction. However, C57BL/6J mice did not display any changes in hepatic *Hamp* expression. Taken together, the results obtained with our *in vitro* and *in vivo* experimental models strongly suggest that neither human nor mouse hepcidin genes are regulated by apoptosis induced through Fas receptor activation in the liver.

2 INTRODUCTION

Apoptosis is involved in the pathogenesis of various liver diseases (1). Hepatocyte apoptosis can be activated via the extrinsic apoptotic pathway through the binding of ligands to death receptors such as Fas, TNF Receptor 1 (TNFR1), TRAIL receptor 2 (TRAIL-R2) and TRAIL receptor 1 (TRAIL-R1). Upon ligand binding, the receptor will trimerize and the C-terminal death domain will recruit Fas-associated protein with death domain (FADD) to form death-inducing signaling complex (DISC), which subsequently recruits procaspase-8 and induces its self-cleavage and activation. Activated caspase-8 can directly cleave and activate caspase-3/7, the executioner caspase, which is responsible for the cleavage of target proteins to execute apoptosis. Caspase-3/7 activation is frequently used as a marker for apoptosis. Flice-Inhibitory Protein Long form (FLIPL) blocks apoptosis by inhibiting the recruitment and auto-proteolytic cleavage of procaspase-8. In addition, in hepatocytes, the signal from death receptor can be amplified through the mitochondrial apoptotic pathway. Activated caspase-8 can cleave Bcl-2 family protein, Bid. The truncated form of Bid (tBid) then activates pro-apoptotic Bcl-2 family proteins, and induces permeabilization of the mitochondrial outer membrane and the leakage of mitochondrial content, including cytochrome *c*. Cytochrome *c* in turn forms a complex with apoptotic peptidase activating factor 1 (APAF-1), and recruits and activates caspase-9, which subsequently cleaves caspase-3/7 and executes apoptosis.

A role for apoptosis has been suggested in hepcidin regulation (2, 3). Hepcidin is the central iron-regulatory hormone. It is synthesized primarily by the liver, as an 84 amino acid precursor antimicrobial peptide. Pre-propeptide is subsequently cleaved to 25 amino acid biologically active circulatory form of hepcidin. Unlike humans with one copy of hepcidin gene, *HAMP*, mice express two hepcidin genes, *Hamp* and *Hamp2*. *Hamp* has been shown to be the equivalent of human gene. Our studies with different *Hamp* transgenic mouse lines have also confirmed the function of *Hamp* as the key iron regulator (4). The exact role of *Hamp2* is as yet unknown. Hepcidin exerts its regulatory function by blocking the transport of dietary iron in the intestine and the release of iron from macrophages. The suppression of hepcidin expression in the liver therefore leads to systemic

iron overload whereas its induction causes iron deficiency and anemia. Besides its role as an iron-regulatory hormone, hepcidin also serves as an acute phase protein and is connected to innate immunity (5–7). Inflammatory cytokines such as IL-6, endotoxin and infections trigger hepcidin transcription in the liver. The effect of IL-6 is mediated through the activation of JAK/STAT3 pathway and the binding of STAT3 to the hepcidin gene promoter (8, 9). Fas receptor signaling and apoptosis are involved in controlling inflammatory innate immune responses (10). Apoptosis also plays a major role in the pathogenesis of liver diseases including NAFLD (11, 12). It is therefore important to investigate the regulation of hepcidin by Fas signaling and apoptosis in the liver.

Weizer-Stern *et al.* have demonstrated that p53, a tumor suppressor and inducer of apoptosis, participates in the regulation of hepcidin (13). In their study, a putative p53 response element on the hepcidin gene promoter has been identified and validated by chromatin immunoprecipitation assays. Over-expression of p53 in hepatoma cells has been shown to induce hepcidin gene transcription and conversely, the silencing of p53 resulted in down-regulation of hepcidin expression (13). It is however unclear whether p53-mediated apoptosis is involved in the regulation of hepatic hepcidin expression (13). On the other hand, Li et al. have suggested a role for Fas signaling in the regulation of hepcidin expression in tissue culture cells and female mouse livers (14). A lethal dose of anti-Fas activating antibody, Jo2 has been reported to exert an immediate stimulatory and a late suppression effect on *Hamp* mRNA expression in the liver (14). Although a relationship between FLIPL, IL-6, STAT3 and hepcidin expression has been shown, they did not however establish a direct correlation between apoptosis and hepcidin. Besides causing cell death, Fas induced DISC formation also participates in the activation of cell signaling pathways, including IL-6 and NF- κB (15). As mentioned above, hepcidin transcription is induced by inflammatory cytokine signaling (5–7), which is mediated through the activation of JAK/STAT3 pathway (8, 9). As an iron regulatory protein, hepcidin is also regulated by the signals from iron sensors, such as bone morphogenetic protein 6 (BMP6) (16–18). The BMP receptor-specific Smad pathway (via

the phosphorylation of transcription factors, Smad1/5/8) has been shown to be involved in the up-regulation of hepcidin transcription. BMP6 knockout mice exhibit iron overload and reduced hepcidin expression (19–21). Similarly, mice lacking the expression of the common Smad protein, Smad4 exhibit iron overload and a dramatic decrease in the expression of hepcidin in the liver (22). In addition, growth factors such as epidermal growth factor and hepatocyte growth factor suppress the expression of hepcidin by inhibiting the signaling of the BMP-Smad pathway (23).

The main aim of the studies described in this chapter is to investigate the causal relationship between Fas-signaling-induced effector caspase activation and apoptosis, and the regulation of human and mouse hepcidin gene transcription. These studies will help us to further understand the regulation and the role of hepcidin in liver diseases including NAFLD.

3 RESULTS

3.1 Effect of fatty acids and apoptosis on *HAMP* expression in HepG2 cells.

We first validated whether saturated fatty acid, palmitic acid (PA) induced apoptosis in HepG2 cells under our experimental conditions. For these experiments, HepG2 cells were treated with 0.1-0.3 mM palmitic acid and 0.3 mM unsaturated fatty acid, oleic acid (OA, as control), for 8 hours. The effect of isopropanol (i.e. the solvent for fatty acids) was also examined. The levels of apoptosis in these cells were determined by caspase-3/7 activity assays (**Figure 3.1A**). In agreement with previous reports (24, 25), PA, but not OA, induced apoptosis in HepG2 cells, as shown by significantly elevated caspase-3/7 activity levels (**Figure 3.1A**). The effect of PA on apoptosis was concentration-dependent (**Figure 3.1A**). Due to the fact, that PA is capable of inducing other signaling pathways besides apoptosis (26), we selected a better defined system of apoptosis to study its direct effect on hepcidin regulation. For these studies, CH11 antibody, an activating antibody for human Fas receptor, was selected to induce apoptosis in HepG2 cells. CH11 antibody treatment for 12 hours induced apoptosis in HepG2 cells in a concentration-dependent manner, as confirmed by caspase-3/7 activity assays (**Figure 3.1B**). A significant induction of caspase-3/7 activity was

observed with all concentrations of CH11 (50-500 ng/mL) (**Figure 3.1B**). The level of apoptosis detected with 500 ng/mL CH11 treatment was similar to that observed with cells incubated with 0.3 mM palmitic acid (**Figure 3.1A and 3.1B**). To test the effect of PA or CH11-induced apoptosis on *HAMP* mRNA expression, we performed qPCR experiments (**Figure 3.1C**). *HAMP* expression in 0.3 mM PA-treated cells was significantly up-regulated compared to solvent-treated control cells. Unlike PA, CH11-induced apoptosis did not significantly alter the level of *HAMP* mRNA expression compared to control cells treated with PBS (**Figure 3.1C**). These findings exclude a role for Fas-mediated apoptotic pathway in the regulation of *HAMP* transcription in hepatoma cells. This also strongly suggests that the induction of *HAMP* expression observed in PA-treated cells is facilitated by mechanisms other than PA-mediated apoptosis signaling pathways.

3.2 The effect of short-term and long-term Jo2 treatment on apoptosis, acute phase response and mouse *Hamp* expression in the livers of C57BL/6NCR mice

Since activation of human Fas did not alter human hepcidin gene expression, we performed experiments with Jo2, which is an activating antibody specific to mouse Fas. In our animal studies, we used a sublethal (0.2 µg/g b.w.) dose of Jo2 antibody to eliminate complications such as massive liver injury and mortality. In agreement, this dose of Jo2 did not cause mortality in any of our time-points studied. Since previous studies (14) suggested a time-dependent effect of Jo2 on hepcidin expression, we injected male C57BL/6NCR strain wild-type mice with Jo2 or NaCl (control), and sacrificed after either 1 (short-term) or 6 (long-term) hrs. The macroscopic appearances of mouse livers after 6 h Jo2 treatment did not present any significant changes compared to NaCl-injected control mice livers (**Figure 3.2**).

Following 1 hr. of Jo2 treatment, no significant increase in caspase-3/7 activity in the liver was observed compared to control mice (**Figure 3.3A**). The activation of acute phase reaction in the livers of these mice was evaluated by determining the levels of IL-6 and SAA3 mRNA expression by qPCR. Similar to caspase-3/7 activity, no significant changes were observed with the expression of these acute phase reaction genes (**Figures 3.3B and C**). The mRNA expression of *Hamp* in mice

livers was unaltered by Jo2 exposure either, as confirmed by qPCR (**Figure 3.3D**). In contrast, 1 hour Jo2 treatment induced a small but significant increase in *Hamp2* mRNA expression (**Figure 3.3E**). By comparison, C57BL/6NCR mice sacrificed 6 hours after Jo2 injections displayed a significant increase in caspase-3/7 activity in the livers compared to NaCl-injected control mice (**Figure 3.3A**). Similarly, the expression of acute phase reaction markers, IL-6 and SAA3 were also elevated in mice exposed to Jo2 for 6 hours compared to control mice (**Figures 3.3B and C**). The levels of *Hamp* and *Hamp2* mRNA expression in mice treated with Jo2 for 6 hours were not significantly different from that in control mice (**Figures 3.3D and E**).

3.3 Jo2-mediated STAT3, SMAD1/5 activation and *Hamp* promoter occupancy

The cytokine, IL-6 is known to activate hepcidin transcription via the JAK/STAT3 signaling pathway (8, 9). We therefore investigated the activation of STAT3 in mice treated with Jo2 or NaCl (control) for 1 or 6 hours. Six hours, but not 1 hour of Jo2 exposure, was sufficient to induce the phosphorylation of STAT3 in the livers of mice, compared to respective control mice (**Figure 3.4**). Despite the activation of STAT3, we did not observe any significant changes in STAT3 binding to *Hamp* promoter in Jo2-treated mice compared to control mice, as determined by chromatin immunoprecipitation (ChIP) assays (**Figure 3.5**).

NF-κB is one of the prominent transcription factors activated by Fas ligand binding. NF-κB activates the transcription of inflammatory cytokines including IL-6 (1). We therefore investigated the phosphorylation of the p65 subunit of NF-κB in mice treated with Jo2 for 1 or 6 hrs. time periods. In contrast to STAT3, Jo2 induced a fast and transient activation of NF-κB. The phosphorylation of p65 in the liver was observed within 1 hour after Jo2 injection and was absent at 6 hours after Jo2 exposure (**Figure 3.4**).

Besides JAK/STAT3 pathway, hepcidin is also regulated by bone morphogenetic protein 6 (BMP6) and SMAD pathway. This pathway has also been suggested to play a negative role in growth factor-induced regulation of hepcidin expression in the liver (23). We therefore determined the activation of transcription factors, SMAD1 and SMAD5, which are activated downstream of BMP signaling

pathway. Similar to NF-κB, Jo2 treatment induced an early and transient activation of SMAD1/5 in the liver. The induction in SMAD1/5 phosphorylation observed by 1 hr. Jo2 exposure was significantly weakened by 6 hr. after Jo2 injection (**Figure 3.4**). The binding of SMAD4, the common mediator of SMAD signaling, to mouse *Hamp* promoter was also examined by ChIP assays. No significant increase in SMAD4 occupancy of *Hamp* promoter region harboring a SMAD4 binding site was observed at 6 hrs. after Jo2 injection, as compared to controls (**Figure 3.5**).

3.4 The effect of long-term Jo2 treatment on apoptosis, acute phase response and mouse hepcidin gene expression in the livers of C57BL/6J mice

In order to investigate the effect of Jo2 further, we employed a sub-strain of C57BL/6 mice. Of note, C57BL/6NCR and C57BL/6J strains exhibit substantial genetic differences (27). In contrast to C57BL/6NCR mice, the macroscopic appearances of C57BL/6J livers after 6 h Jo2 treatment were significantly different than control livers (**Figure 3.2**). Compared to that observed with C57BL/6NCR, C57BL/6J mice treated with a sublethal dose of Jo2 (0.2 µg/g b.w.) for 6 hours exhibited a significantly higher elevation of caspase-3/7 activity (**Figure 3.6A**). Similar robust activation was also observed with the expression of acute phase marker genes, IL-6 and SAA3 (**Figures 3.6B and 3.6C**). However, despite stronger apoptosis and acute phase reactions, Jo2 treatment did not induce any significant changes in the expression of both *Hamp* and *Hamp2* in the livers of C57BL/6J mice, as was the case with C57BL/6NCR mice (**compare Figures 3.6D, E and 3.3D, E**). Furthermore, we tested the effect of an even higher concentration of Jo2 (0.32 µg/g b.w.). Although this concentration of Jo2 caused mortality (40 %), it did not induce any changes in the mRNA level of *Hamp*. (**Figure 3.6D**). In contrast to the effect of sublethal Jo2 dose in C57BL/6NCR mice (**Figure 3.2E**), the treatment with 0.32 µg/g of Jo2 induced a significant suppression of *Hamp2* mRNA expression in C57BL/6J mice livers (**Figure 3.6E**).

3.5 The effect of Jo2 on liver enzymes in C57BL/6J and C57BL/6NCR mice

Since Jo2-induced apoptosis and acute phase reactions were stronger in the livers of C57BL/6J mice, compared to C57BL/6NCR mice, we measured the serum levels of ALT and AST. These liver enzymes are commonly used as diagnostic markers in the clinic to determine liver injury. The sublethal dose of Jo2 (0.2 µg/g) did not cause a significant elevation of serum ALT or AST levels in C57BL6/NCR mice (**Figures 3.7A and B**). However, the sera of C57BL/6J mice injected with this concentration of Jo2 exhibited a dramatic increase in both ALT and AST levels, compared to controls (**Figures 3.7A and B**). The injection of C57BL/6J mice with a higher dose of Jo2 (0.32 µg/g) induced further increase in serum ALT and AST levels (*data not shown*). These findings with ALT and AST further support our previous findings that Fas ligand activation and apoptosis do not alter hepatic hepcidin gene expression.

4 DISCUSSION

Apoptosis is one of the key factors which contribute to the pathogenesis of liver diseases including NAFLD (1, 11, 28). Apoptosis not only causes hepatocyte death directly but also induces inflammation and hepatic fibrosis (29, 30). The inhibition of caspase enzymes via known caspase inhibitors has been shown to effectively alleviate hepatocyte apoptosis and tissue damage in animal models of liver injury (31). Due to its highly reactive nature, and the liver serving as the major storage organ for it, iron is considered an important secondary risk factor in the progression of various liver diseases (32, 33). Therefore, it is of great importance to understand the interaction between apoptosis and iron metabolism. Since hepcidin is the central regulator of iron homeostasis and is primarily synthesized in the liver, this study investigated the effect of apoptosis on the regulation of hepcidin expression in the liver. Previously, Weizer-Stern *et al.* have elegantly demonstrated that p53, a tumor suppressor gene and an inducer of apoptosis, elevates human hepcidin gene transcription in HepG2 cells by binding to the corresponding response elements in hepcidin gene promoter (13). They have also reported that the overexpression of p53 blunts the

stimulatory effect of IL-6 on hepcidin gene expression. Although indirect, these findings, for the first time, suggested a relationship between apoptosis and hepcidin and thereby the regulation of iron metabolism. However, due to various reasons, the *in vivo* relevance of this potential interaction is unclear. First, apoptosis signaling in cancer cell lines is frequently distorted and secondly, forced overexpression of p53 might have caused artificial effects. However, in a recent study, Li *et al.* have investigated the relationship between Fas-activated apoptosis signaling and expression of hepcidin gene expression (14). Fas activation decreased both mouse and human hepcidin mRNA expression *in vitro*. They have also shown that Balb/C3 female mice injected with a lethal dose of Jo2 antibody (which killed mice within 4 hours) exhibit a biphasic regulation of mouse hepcidin mRNA expression in the liver. Namely, an immediate elevation (observed within 0.5-1 hour) was followed by a suppression (observed within 4 hours). They suggested that these changes in hepcidin expression correlate with the changes in FLIPL and IL-6 expression, as well as the activation of the transcription factors, NF-κB, and STAT3. The knock-down or over-expression of FLIPL exerted a negative and a positive effect, respectively, on hepcidin expression. Based on their data, Li *et al.* have proposed a model suggesting that the stimulatory effect of Fas on hepcidin expression is achieved via IL-6 and STAT3, which themselves are activated by FLIPL and NF-κB. However, Li *et al.* did not establish a direct association between Fas-induced apoptosis and hepcidin up-regulation. Thus, it is unclear whether Fas-mediated apoptosis is directly involved in the regulation of hepcidin gene expression in the liver.

We examined the effect of Fas signaling on hepatic hepcidin gene expression both *in vivo* and *in vitro*. In our *in vitro* studies, the effect of CH11 was evaluated on human hepcidin gene, *HAMP* expression in HepG2 hepatoma cells. Despite the induction of apoptosis by CH11 in a concentration dependent manner, as confirmed by the increased caspase-3/7 activity, *HAMP* expression was not significantly altered in HepG2 cells. Although we cannot exclude the possibility that Fas-mediated signaling in HepG2 cells might be different than primary human hepatocytes, our findings strongly suggest that hepatic *HAMP* expression does not correlate with the significant induction of caspase

activation. Of note, the liver is composed of various cell types and it is therefore feasible that not only hepatocytes, but other cells such as Kupffer cells, might be involved in the regulation of hepcidin gene by apoptosis. Hence, an *in vivo* experimental model whereby male C57BL/6NCR mice are injected with Jo2 antibody to specifically activate Fas-mediated apoptosis was employed to study hepcidin gene expression in the whole liver. Male mice were chosen for these studies because unlike humans, female mice express higher levels of hepcidin compared to male mice (34). As described in Results section above, a sublethal concentration of Jo2 antibody was chosen based on reports showing, that this dose is optimal to specifically study the activation of Fas-mediated apoptosis in liver diseases (35). This was also confirmed by the lack of lethality in our experiments. The absence of significant changes both in caspase activation and acute phase gene expression indicates that short-term (1h) Jo2 treatment is not sufficient to promote apoptosis or acute phase responses in mice livers. Accordingly, no macroscopic changes in the livers were observed, as compared to control mice. Further, mouse hepcidin gene, *Hamp* expression in the liver was also not altered. In contrast, longer (6 h) treatment significantly induced apoptosis and acute phase reactions. Concurrently, the livers of these mice displayed macroscopic differences, such as a darker color, suggesting the presence of hepatic hemorrhage and liver injury. Interestingly, these changes did not correlate with the level of *Hamp* mRNA expression in the liver. Similar to short-term, the longer treatment of mice with Jo2 did not alter the level of hepcidin gene expression.

It is well known that hepcidin gene transcription is strongly stimulated by IL-6 and JAK/STAT3 signaling pathway. Since, we have shown that long-term, but not short-term, Jo2 treatment can induce acute phase reactions in the liver, the phosphorylation status of STAT3 was investigated to confirm its activation. In accordance with our acute phase gene expression findings, we observed STAT3 phosphorylation following 6 hours, but not 1 hour, of Jo2 treatment. Taken together, our findings show that the activation of IL-6/ STAT3 axis by Fas is not sufficient to induce *Hamp* transcription and strongly suggest the presence of inhibitory mechanisms. This is also supported by our ChIP findings, which show that the occupancy of *Hamp* promoter by STAT3 is similar in

the livers of both Jo2-treated and control mice, despite the differences in the activation status of STAT3. In contrast to STAT3, the phosphorylation of NF-κB was observed with short-term, but not long-term, Jo2 treatment. NF-κB is involved in inflammatory cytokine production in the liver including IL-6 (28). It is therefore possible that Jo2-mediated early phase activation of NF-κB subsequently facilitates the induction of IL-6 transcription and consequent activation of STAT3, which was observed in the livers of mice with longer Jo2 treatment.

Hepcidin is also activated by BMP/Smad pathway and SMAD4 knockout mice display reduced hepcidin expression (22). However, 6 hour Jo2 administration did not significantly alter the phosphorylation of SMAD1/5 proteins, which are transcription factors known to be activated by BMP pathway. Growth factors have been shown to suppress the signaling of BMP/SMAD pathway and its stimulatory effect on hepcidin gene expression in the liver (23). Of note, liver injury is known to stimulate the expression of growth factors as part of the liver regeneration process. It is therefore feasible that Fas-induced liver injury might suppress Smad activation and thereby counteract the stimulation of *Hamp* transcription by STAT3. However, it should also be noted that despite significant differences in the level of liver injury, acute phase response and apoptosis, both C57BL/6J and C57BL/6NCR mice (under similar experimental conditions) did not display any significant changes in liver *Hamp* expression. This suggests that mechanisms other than growth factors and inhibitory SMADs might play a role in this process. Jo2-induced liver damage accompanied by DNA damage and the activation of p53 might be involved since p53 has been shown to suppress the stimulatory effect of IL-6 on hepcidin gene expression (13). Furthermore, we observed differential regulation of *Hamp2* expression by Jo2 in the liver. Since the function of *Hamp2* is yet unknown, the significance of this finding and its potential role in liver injury and disease require further future studies.

In our current study presented in this chapter, we validated that hepatic expression of hepcidin is not altered by apoptosis induced through Fas signaling. We therefore believe that, palmitic acid-mediated activation of hepcidin expression in hepatoma cells was mediated by mechanisms other

than apoptosis. Apoptosis is widely recognized as a secondary risk factor in NAFLD/NASH pathogenesis. However, the findings presented in this chapter exclude a role for apoptosis in the regulation of hepcidin and iron metabolism in NAFLD.

5 REFERENCES

1. Schattenberg, J. M., Galle, P. R., and Schuchmann, M. (2006) Apoptosis in liver disease. *Liver Int.* **26**, 904–911
2. Ganz, T. (2011) Hepcidin and iron regulation, 10 years later. *Blood*. **117**, 4425 –4433
3. Ganz, T., and Nemeth, E. (2011) Hepcidin and Disorders of Iron Metabolism. *Annu. Rev. Med.* **62**, 347–360
4. Lu, S., Seravalli, J., and Harrison-Findik, D. (2015) Inductively coupled mass spectrometry analysis of biometals in conditional Hamp1 and Hamp1 and Hamp2 transgenic mouse models. *Transgenic Res.* 10.1007/s11248-015-9879-3
5. Villarroel, P., Blanc, S. L., and Arredondo, M. (2012) Interleukin-6 and Lipopolysaccharide Modulate Hepcidin mRNA Expression by Hepg2 Cells. *Biol. Trace Elem. Res.* **150**, 496–501
6. Nemeth, E., Valore, E. V., Territo, M., Schiller, G., Lichtenstein, A., and Ganz, T. (2003) Hepcidin, a Putative Mediator of Anemia of Inflammation, Is a Type II Acute-Phase Protein. *Blood*. **101**, 2461–2463
7. Nemeth, E., Rivera, S., Gabayan, V., Keller, C., Taudorf, S., Pedersen, B. K., and Ganz, T. (2004) IL-6 mediates hypoferremia of inflammation by inducing the synthesis of the iron regulatory hormone hepcidin. *J. Clin. Invest.* **113**, 1271–1276
8. Falzacappa, V., Vittoria, M., Vujic Spasic, M., Kessler, R., Stolte, J., Hentze, M. W., and Muckenthaler, M. U. (2007) STAT3 Mediates Hepatic Hepcidin Expression and Its Inflammatory Stimulation. *Blood*. **109**, 353–358
9. Pietrangelo, A., Dierssen, U., Valli, L., Garuti, C., Rump, A., Corradini, E., Ernst, M., Klein, C., and Trautwein, C. (2007) STAT3 Is Required for IL-6-gp130–Dependent Activation of Hepcidin In Vivo. *Gastroenterology*. **132**, 294–300
10. Strasser, A., Jost, P. J., and Nagata, S. (2009) The Many Roles of FAS Receptor Signaling in the Immune System. *Immunity*. **30**, 180–192
11. Rust, C., and Gores, G. J. (2000) Apoptosis and liver disease. *Am. J. Med.* **108**, 567–574
12. Ibrahim, S. H., Kohli, R., and Gores, G. J. (2011) Mechanisms of Lipotoxicity in NAFLD and Clinical Implications. *J. Pediatr. Gastroenterol. Nutr.* **53**, 131–140
13. Weizer-Stern, O., Adamsky, K., Margalit, O., Ashur-Fabian, O., Givol, D., Amariglio, N., and Rechavi, G. (2007) Hepcidin, a key regulator of iron metabolism, is transcriptionally activated by p53. *Br. J. Haematol.* **138**, 253–262
14. Li, X., Xu, F., Karoopongse, E., Marcondes, A. M., Lee, K., Kowdley, K. V., Miao, C. H., Trobridge, G. D., Campbell, J. S., and Deeg, H. J. (2013) Allogeneic Transplantation, Fas Signaling, and Dysregulation of Hepcidin. *Biol. Blood Marrow Transplant.* **19**, 1210–1219
15. Guicciardi, M. E., and Gores, G. J. (2009) Life and death by death receptors. *FASEB J.* **23**, 1625–1637
16. Babitt, J. L., Huang, F. W., Wrighting, D. M., Xia, Y., Sidis, Y., Samad, T. A., Campagna, J. A., Chung, R. T., Schneyer, A. L., Woolf, C. J., Andrews, N. C., and Lin, H. Y. (2006) Bone morphogenetic protein signaling by hemojuvelin regulates hepcidin expression. *Nat. Genet.* **38**, 531–539
17. Truksa, J., Peng, H., Lee, P., and Beutler, E. (2006) Bone Morphogenetic Proteins 2, 4, and 9 Stimulate Murine Hepcidin 1 Expression Independently of Hfe, Transferrin Receptor 2 (Tfr2), and IL-6. *Proc. Natl. Acad. Sci.* **103**, 10289–10293
18. Lin, L., Valore, E. V., Nemeth, E., Goodnough, J. B., Gabayan, V., and Ganz, T. (2007) Iron transferrin regulates hepcidin synthesis in primary hepatocyte culture through hemojuvelin and BMP2/4. *Blood*. **110**, 2182 –2189

19. Shanmugam, N. K. N., and Cherayil, B. J. Serum-induced up-regulation of hepcidin expression involves the bone morphogenetic protein signaling pathway. *Biochem. Biophys. Res. Commun.* **441**, 383–386
20. Andriopoulos Jr, B., Corradini, E., Xia, Y., Faasse, S. A., Chen, S., Grgurevic, L., Knutson, M. D., Pietrangelo, A., Vukicevic, S., Lin, H. Y., and Babitt, J. L. (2009) BMP6 is a key endogenous regulator of hepcidin expression and iron metabolism. *Nat. Genet.* **41**, 482–487
21. Meynard, D., Kautz, L., Darnaud, V., Canonne-Hergaux, F., Coppin, H., and Roth, M.-P. (2009) Lack of the bone morphogenetic protein BMP6 induces massive iron overload. *Nat. Genet.* **41**, 478–481
22. Wang, R.-H., Li, C., Xu, X., Zheng, Y., Xiao, C., Zerfas, P., Cooperman, S., Eckhaus, M., Rouault, T., Mishra, L., and Deng, C.-X. (2005) A role of SMAD4 in iron metabolism through the positive regulation of hepcidin expression. *Cell Metab.* **2**, 399–409
23. Goodnough, J. B., Ramos, E., Nemeth, E., and Ganz, T. (2012) Inhibition of hepcidin transcription by growth factors. *Hepatology*. **56**, 291–299
24. Cazanave, S. C., Mott, J. L., Elmi, N. A., Bronk, S. F., Werneburg, N. W., Akazawa, Y., Kahraman, A., Garrison, S. P., Zambetti, G. P., Charlton, M. R., and Gores, G. J. (2009) JNK1-dependent PUMA Expression Contributes to Hepatocyte Lipoapoptosis. *J. Biol. Chem.* **284**, 26591–26602
25. Ricchi, M., Odoardi, M. R., Carulli, L., Anzivino, C., Ballestri, S., Pinetti, A., Fantoni, L. I., Marra, F., Bertolotti, M., Banni, S., Lonardo, A., Carulli, N., and Loria, P. (2009) Differential effect of oleic and palmitic acid on lipid accumulation and apoptosis in cultured hepatocytes. *J. Gastroenterol. Hepatol.* **24**, 830–840
26. Malhi, H., and Gores, G. J. (2008) Molecular Mechanisms of Lipotoxicity in Nonalcoholic Fatty Liver Disease. *Semin. Liver Dis.* **28**, 360–369
27. Mekada, K., Abe, K., Murakami, A., Nakamura, S., Nakata, H., Moriwaki, K., Obata, Y., and Yoshiki, A. (2009) Genetic Differences among C57BL/6 Substrains. *Exp. Anim.* **58**, 141–149
28. Chakraborty, J. B., Oakley, F., and Walsh, M. J. (2012) Mechanisms and Biomarkers of Apoptosis in Liver Disease and Fibrosis. *Int. J. Hepatol.* **2012**, 1–10
29. Canbay, A., Taimr, P., Torok, N., Higuchi, H., Friedman, S., and Gores, G. J. (2003) Apoptotic body engulfment by a human stellate cell line is profibrogenic. *Lab. Investig. J. Tech. Methods Pathol.* **83**, 655–663
30. Canbay, A., Feldstein, A., Baskin-Bey, E., Bronk, S. F., and Gores, G. J. (2004) The Caspase Inhibitor IDN-6556 Attenuates Hepatic Injury and Fibrosis in the Bile Duct Ligated Mouse. *J. Pharmacol. Exp. Ther.* **308**, 1191–1196
31. Natori, S., Higuchi, H., Contreras, P., and Gores, G. J. (2003) The caspase inhibitor IDN-6556 prevents caspase activation and apoptosis in sinusoidal endothelial cells during liver preservation injury. *Liver Transpl.* **9**, 278–284
32. Fargion, S., Valenti, L., and Fracanzani, A. L. (2011) Beyond hereditary hemochromatosis: New insights into the relationship between iron overload and chronic liver diseases. *Dig. Liver Dis.* **43**, 89–95
33. Datz, C., Felder, T. K., Niederseer, D., and Aigner, E. (2013) Iron homeostasis in the Metabolic Syndrome. *Eur. J. Clin. Invest.* 10.1111/eci.12032
34. Spasic, M. V., Kiss, J., Herrmann, T., Kessler, R., Stolte, J., Galy, B., Rathkolb, B., Wolf, E., Stremmel, W., Hentze, M. W., and Muckenthaler, M. U. (2007) Physiologic systemic iron metabolism in mice deficient for duodenal Hfe. *Blood*. **109**, 4511–4517
35. Haga, S., Terui, K., Zhang, H. Q., Enosawa, S., Ogawa, W., Inoue, H., Okuyama, T., Takeda, K., Akira, S., Ogino, T., Irani, K., and Ozaki, M. (2003) Stat3 protects against Fas-induced liver injury by redox-dependent and -independent mechanisms. *J. Clin. Invest.* **112**, 989–998

Figure 3.1. Caspase-3/7 activity and human hepcidin gene (*HAMP*) expression. (**A**) HepG2 cells were treated with 0.1- 0.3mM palmitic acid (PA) or 0.3mM oleic acid (OA) for 8 hours. Untreated (unt.) and solvent (isopropanol)-treated (solv.) cells were employed as control. Caspase-3/7 activity was determined, as described in the experimental procedures (*see Chapter II*) and was expressed as nanomole of flurogenic substrate cleaved per milligram of cell lysate (nmol/mg). (**B**) HepG2 cells were treated with 50,100,150 and 500 ng/mL of CH11 antibody for 12 hours. Induction of apoptosis was confirmed by measuring caspase-3/7 activity. (**C**) cDNA, synthesized from RNA isolated from CH11-treated, PA-treated and respective control cells, was employed as a template in Taqman qPCR assays to determine *HAMP* mRNA expression, as described in experimental procedures. *HAMP* expression in CH11-treated or 0.3mM PA-treated cells was expressed as fold expression of that in respective control cells.

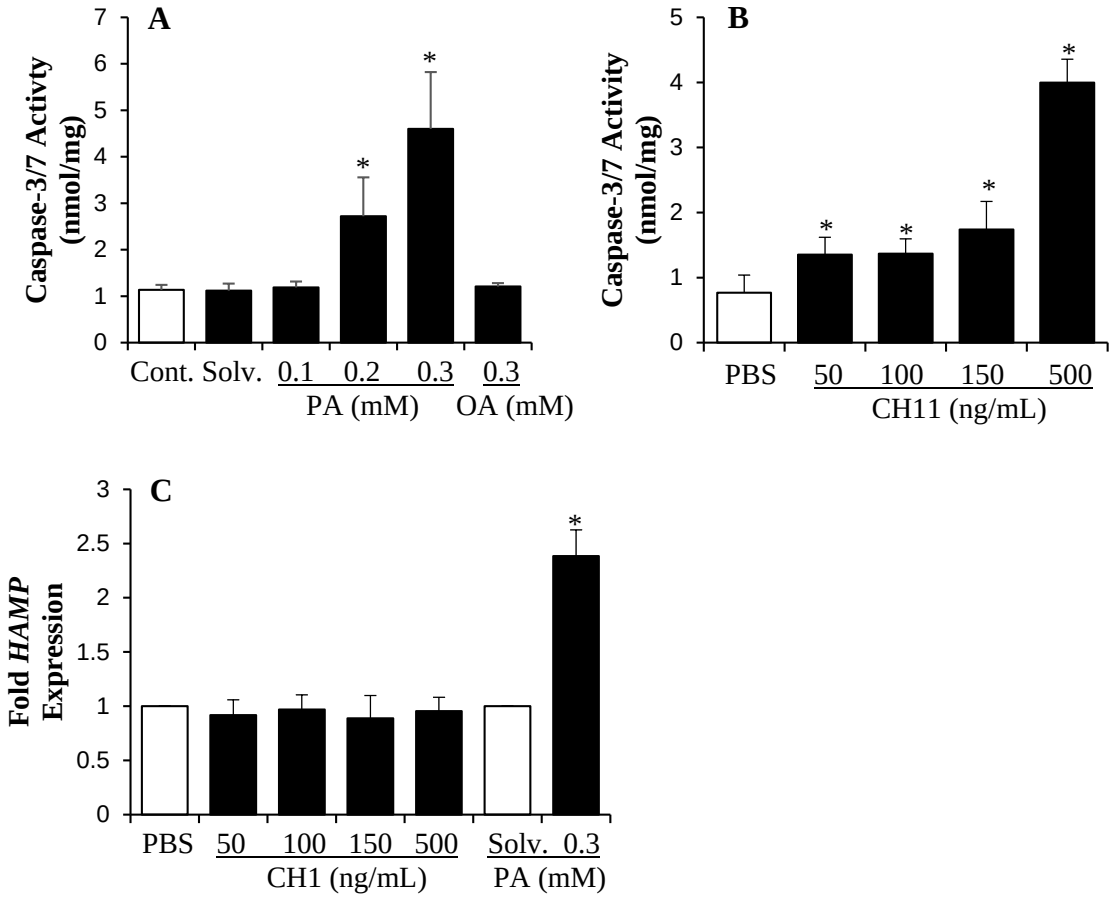
A
Caspase-3/7 Activty (nmol/mg)
0
1
2
3
4
5
6
7
*
*
Cont. Solv.
0.1
0.2
0.3
0.3
PA (mM)
OA (mM)
B
Caspase-3/7 Activity (nmol/mg)
0
1
2
3
4
5
*
*
*
*
PBS
50
100
150
500
CH11 (ng/mL)
C
Fold HAMP Expression
0
0.5
1
1.5
2
2.5
3
*
PBS
50
100
150
500
CH1 (ng/mL)
Solv.
0.3
PA (mM)

Figure 3.1

Figure 3.2. Macroscopic analysis of livers from Jo2-treated mice. C57BL/6J and C57BL/6NCR strain wild-type male mice, which were injected with Jo2 antibody (0.2 µg/g b.w.) or NaCl (as control), were sacrificed 6 hours later. Representative images are shown.

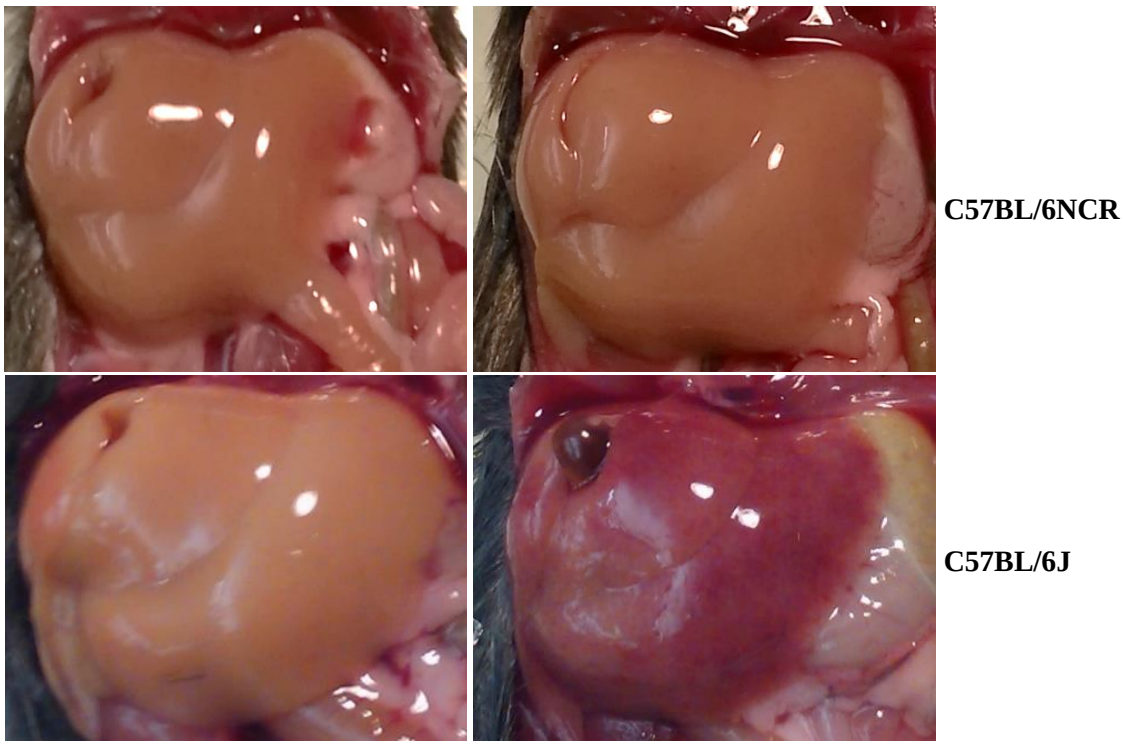

Figure 3.2

Figure 3.3. Caspase-3/7 activity, and the expression of acute phase response genes and mouse hepcidin genes, *Hamp* and *Hamp2* in the liver. C57BL/6NCR strain wild-type male mice, which were injected with Jo2 antibody (0.2 µg/g b.w.) or NaCl (as control), were sacrificed 1 hr. or 6 hrs. later. (**A**) Caspase-3/7 activity was measured, as described in experimental procedures. IL-6 (**B**), SAA3(**C**), *Hamp* (**D**) and *Hamp2* (**E**) gene expression was determined by qPCR and mRNA expression in Jo2-treated mice expressed as fold change of that in corresponding control mice.

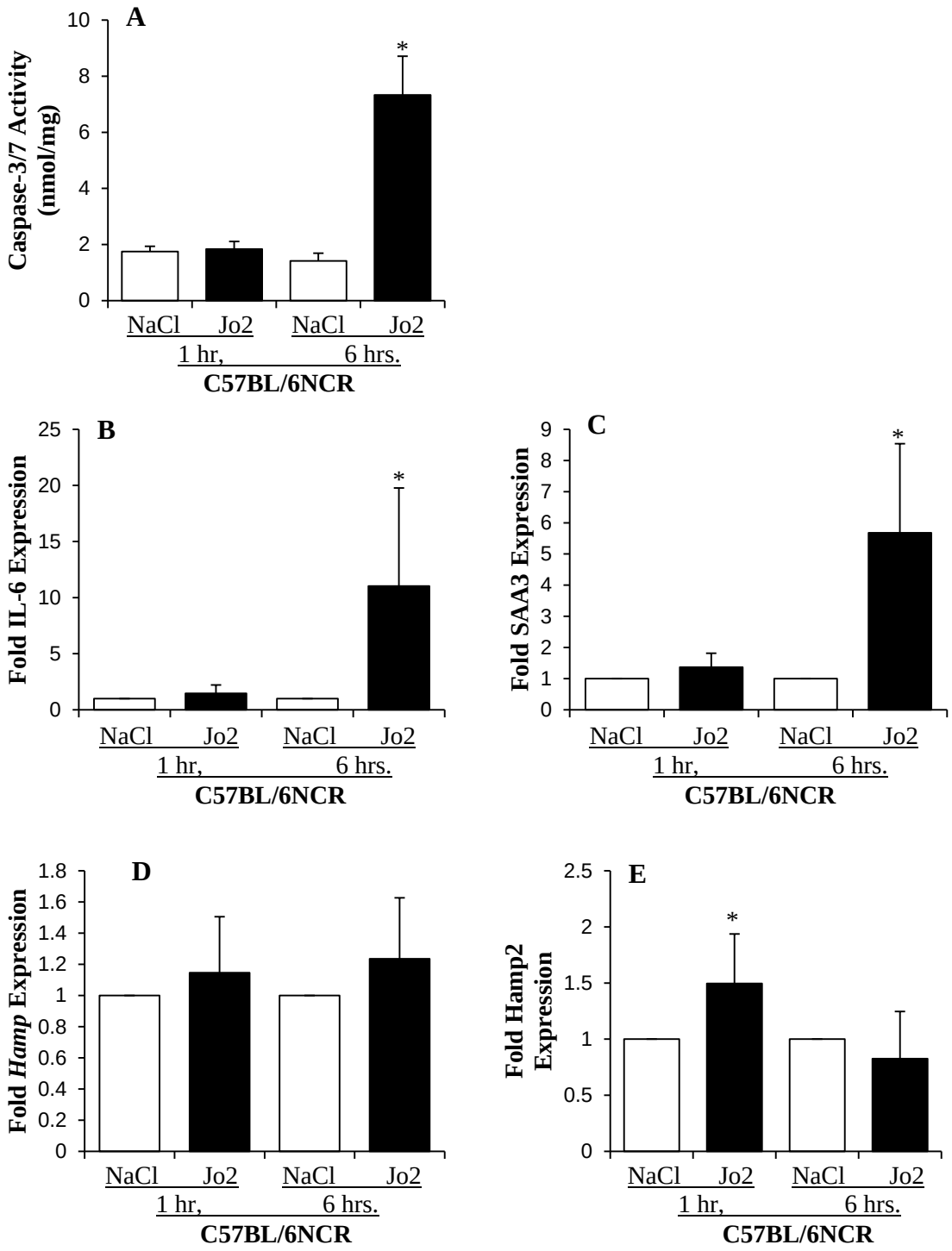
A
Caspase-3/7 Activity (nmol/mg)
10
8
6
4
2
0
*
NaCl Jo2 NaCl Jo2
1 hr, 6 hrs.
C57BL/6NCR
B
Fold IL-6 Expression
25
20
15
10
5
0
*
NaCl Jo2 NaCl Jo2
1 hr, 6 hrs.
C57BL/6NCR
C
Fold SAA3 Expression
9
8
7
6
5
4
3
2
1
0
*
NaCl Jo2 NaCl Jo2
1 hr, 6 hrs.
C57BL/6NCR
D
Fold Hamp Expression
1.8
1.6
1.4
1.2
1
0.8
0.6
0.4
0.2
0
NaCl Jo2 NaCl Jo2
1 hr, 6 hrs.
C57BL/6NCR
E
Fold Hamp2 Expression
2.5
2
1.5
1
0.5
0
*
NaCl Jo2 NaCl Jo2
1 hr, 6 hrs.
C57BL/6NCR

Figure 3.3

Figure 3.4. Phosphorylation of STAT3, NF-κB (P65) and SMAD 1/5 in the liver. Whole cell lysates prepared from the livers of C57BL/6NCR mice injected with Jo2 (0.2 μg/g b.w.) and sacrificed after 1 or 6 hours were employed for western blotting using anti-phospho-STAT3 (P-STAT3), anti-total STAT3, anti-phospho-P65 (P65) and anti-phospho-SMAD1/5 antibodies, as described in experimental procedures with specific antibodies (*see Chapter II* ***TABLE 2.5***). Anti-gapdh antibody was used as protein loading control.

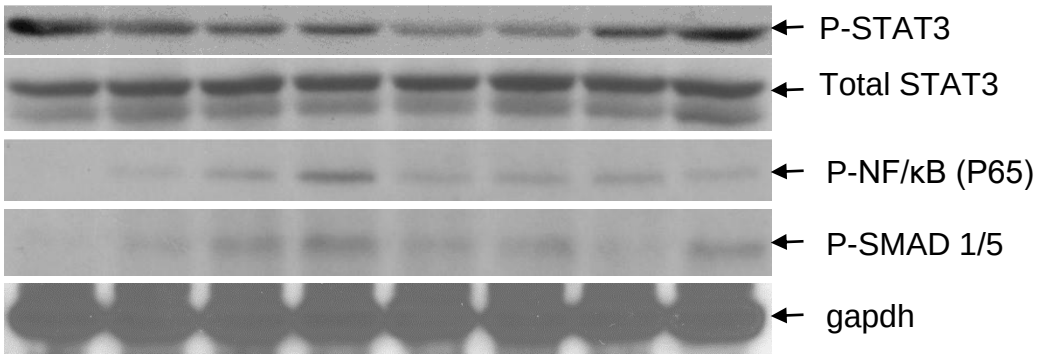
P-STAT3
Total STAT3
P-NF/κB (P65)
P-SMAD 1/5
gapdh
NaCl NaCl Jo2 Jo2 NaCl NaCl Jo2 Jo2
1hr
6hr
C57BL/6NCR

Figure 3.4

Figure 3.5. Chromatin Immunoprecipitation (ChIP) assays. The binding of STAT3 or SMAD4 to the *HAMP* promoter in the livers of C57BL/6NCR mice, which were injected with Jo2 (0.2 µg/g b.w.) or NaCl (control) and sacrificed 6 hours later, was determined by ChIP assays, as described in experimental procedures. Total input DNA was used as control to evaluate the amount of chromatin.

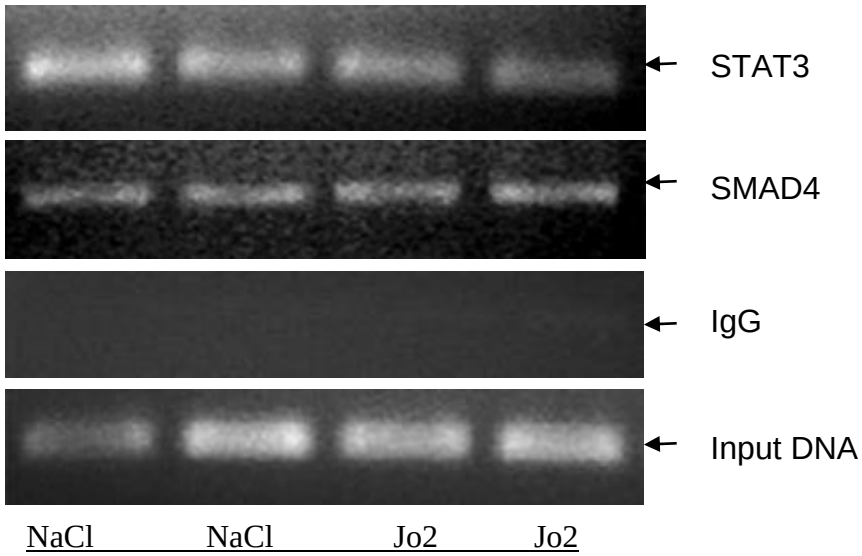

Figure 3.5

Figure 3.6. The effect of Jo2 on apoptosis, acute phase response, and *Hamp* and *Hamp2* gene expression in C57BL/6J mice. C57BL/6J male mice (n = 21) were injected with 0.2 µg/g b.w. and 0.32 µg/g b.w. Jo2 or saline and sacrificed 6 hours later. Cell lysates and RNA isolated from the livers were employed in caspase-3/7 assays (**A**) or to synthesize cDNA as a template for SYB green qPCR assays to determine IL-6 (**B**) or SAA3 (**C**) gene expression. *Hamp* (**D**) and *Hamp2* (**E**) mRNA expression was determined by Taqman qPCR. Gene expression in Jo2 injected mice was expressed as fold change of that in control mice.

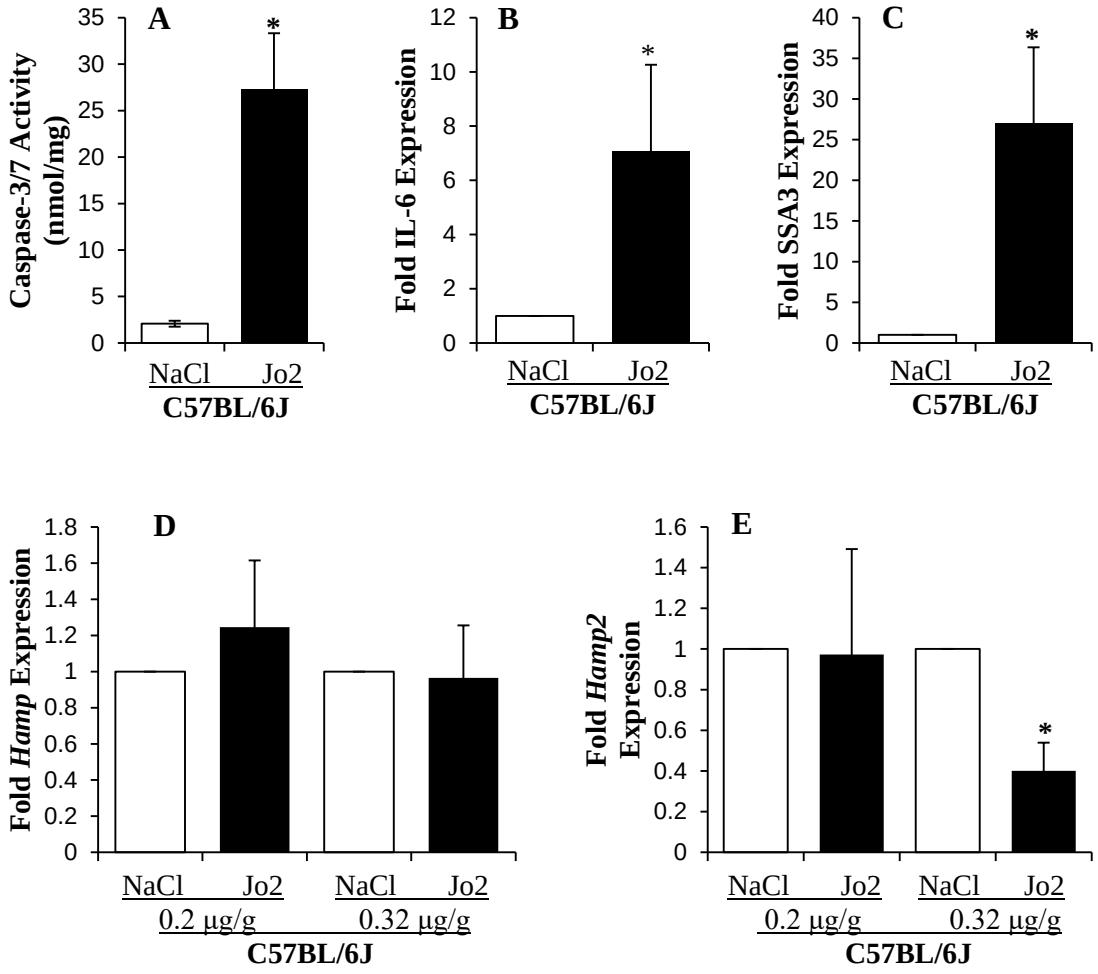
A
Caspase-3/7 Activity (nmol/mg)
35
30
25
20
15
10
5
0
*
NaCl
Jo2
C57BL/6J
B
Fold IL-6 Expression
12
10
8
6
4
2
0
*
NaCl
Jo2
C57BL/6J
C
Fold SSA3 Expression
40
35
30
25
20
15
10
5
0
*
NaCl
Jo2
C57BL/6J
D
Fold Hamp Expression
1.8
1.6
1.4
1.2
1
0.8
0.6
0.4
0.2
0
NaCl
Jo2
NaCl
Jo2
0.2 µg/g
0.32 µg/g
C57BL/6J
E
Fold Hamp2 Expression
1.6
1.4
1.2
1
0.8
0.6
0.4
0.2
0
*
NaCl
Jo2
NaCl
Jo2
0.2 µg/g
0.32 µg/g
C57BL/6J

Figure 3.6

Figure 3.7. Comparison of liver enzyme levels in sera of Jo2 injected C57BL/6J and C57BL/6NCR mice. Mice injected with Jo2 (0.2µg/g b.w.) were sacrificed 6 hours later. Serum ALT (**A**) and AST (**B**) enzymes were measured at Clinical Chemistry Laboratory of University of Nebraska Medical Center.

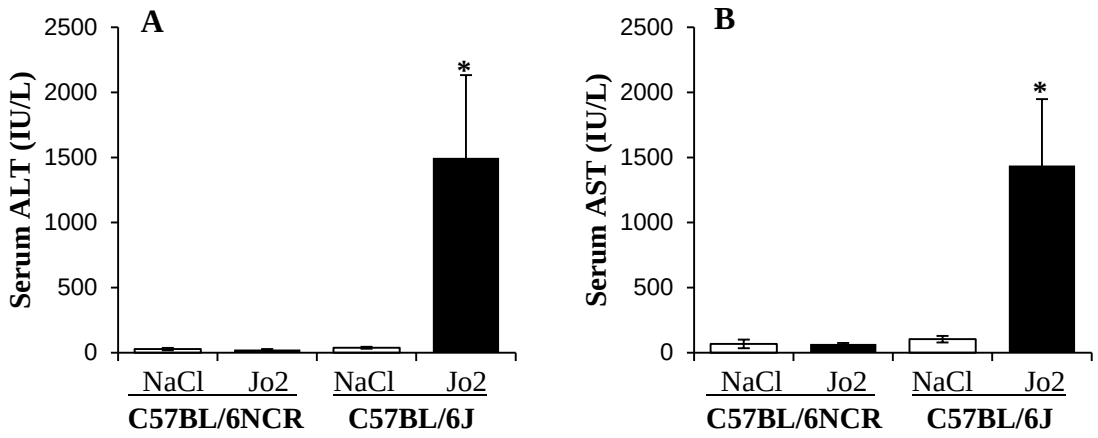
A
Serum ALT (IU/L)
2500
2000
1500
1000
500
0
*
NaCl
Jo2
NaCl
Jo2
C57BL/6NCR
C57BL/6J
B
Serum AST (IU/L)
2500
2000
1500
1000
500
0
*
NaCl
Jo2
NaCl
Jo2
C57BL/6NCR
C57BL/6J

Figure 3.7

Chapter IV

Saturated Fatty Acids Induce Post-transcriptional Regulation of *HAMP* mRNA via AU-rich Element Binding Protein, HuR in Human Hepatoma Cells

This chapter has been adopted from a publication re-submitted to Journal of Biological Chemistry (**S.L**. et. al, Manuscript ID.JBC/2015/648212).

1 ABSTRACT

Iron is implicated in the pathogenesis of nonalcoholic fatty liver disease (NAFLD). Hepcidin, synthesized primarily in the liver, is the master switch of iron metabolism. The aim of this study is to investigate the regulation of human hepcidin gene, *HAMP* expression by fatty acids in HepG2 human hepatoma cells. For these studies, both saturated fatty acids, palmitic or stearic acid, and unsaturated fatty acid, oleic acid were used. Palmitic acid and to a lesser extent stearic acid, but not oleic acid, up-regulated *HAMP* mRNA levels, as determined by qPCR. Published studies up-to-now have mainly described the transcriptional regulation of *HAMP*. To understand whether fatty acids regulate *HAMP* mRNA at the transcriptional or post-transcriptional level, we employed the transcription inhibitor, actinomycin D in our experiments. Palmitic acid-mediated induction of *HAMP* mRNA expression was not blocked by actinomycin D. Furthermore, palmitic acid activated *HAMP* 3'UTR, but not promoter, activity, as shown by reporter assays. *HAMP* 3'UTR harbors a single AU-rich element (ARE). Mutation of this ARE abolished the effect of palmitic acid suggesting the involvement of ARE-binding proteins (ARE-BP). The ARE-BP, HuR stabilizes mRNA through direct interaction with AREs on 3'UTR. HuR is regulated by phosphorylation-mediated nucleo-cytoplasmic shuttling. Palmitic acid activated this process. The binding of HuR to *HAMP* mRNA was also induced by palmitic acid in HepG2 cells. Silencing of HuR by siRNA abolished palmitic acid-mediated up-regulation of *HAMP* mRNA levels. Protein kinase C is known to phosphorylate HuR. Staurosporine, a broad-spectrum protein kinase C inhibitor inhibited both saturated fatty acid-mediated translocation of HuR and induction of *HAMP* expression. Similarly, rottlerin, a novel class protein kinase C inhibitor, abrogated palmitic acid-mediated up-regulation of *HAMP* expression. In conclusion, our findings clearly show that saturated, but not unsaturated, fatty acids control post-transcriptional regulation of *HAMP* through novel protein kinase C- and HuR-dependent mechanisms. The studies in this chapter are also demonstrating for the first time that *HAMP* is directly regulated at 3'UTR by a functional AU-rich element sequence and RNA-binding proteins.

2 INTRODUCTION

Due to the increasing prevalence of obesity worldwide, metabolic syndrome, characterized by visceral adiposity, dyslipidemia and insulin resistance is becoming a major public health problem. Nonalcoholic fatty liver disease (NAFLD) is the hepatic manifestation of metabolic syndrome. The accumulation of fat in the liver, which occurs in the absence of significant alcohol consumption, is a key feature of NAFLD (1). Increased lipolysis as a result of insulin resistance and lipid uptake from the diet contributes to the elevated levels of free fatty acids (FFA) in the circulation. The increase in both the uptake of FFA by hepatocytes and de novo FA synthesis leads to fat accumulation in the livers of NAFLD patients (*see Chapter I for detailed overview*) (2).

Although lipid accumulation alone may be benign, more aggressive forms of NAFLD can develop. Iron has been shown to be one of the risk factors in the pathogenesis of NAFLD (3). Clinical studies with NAFLD patients have shown a clear correlation between hepatic iron deposition and more advanced disease stages with liver fibrosis (4–6). Iron acts as a risk factor by inducing oxidative stress and mitochondrial dysfunction (3). Hepcidin is the key iron-regulatory protein, which is primarily synthesized in the liver (7). Humans express a single hepcidin gene, *HAMP*. It controls iron absorption from the duodenum and iron release from macrophages by inhibiting the iron exporter, ferroportin (8). Besides being an iron-regulatory protein, hepcidin also acts as an acute phase protein. In NAFLD patients, *HAMP* expression has been suggested to be regulated by both systemic iron levels (6, 9) and inflammation (10). A role for lipids in the regulation of *HAMP* expression has not been established. A microarray study however reported that the saturated fatty acid, palmitic acid (PA) modulates *HAMP* expression in HepG2 cells but the underlying mechanisms are unknown (11).

Previous studies on hepcidin expression have mainly focused on the transcriptional regulation of *HAMP*. Inflammatory cytokines, serum transferrin, erythropoiesis signaling and elevated hepatic iron stores have all been shown to stimulate the promoter activities of both human and mouse

hepcidin genes via the activation of specific transcription factors (12–15). It should however be noted that other iron-regulatory proteins, transferrin receptor 1 and ferritin are regulated at the post-transcriptional and translational level, respectively by iron-regulatory RNA-binding proteins (IRP), IRP1 and IRP2 (16). Although no IRP recognition sequences have been identified in *HAMP* mRNA, the involvement of post-transcriptional mechanisms warrant further investigation.

In addition to transcriptional regulation, post-transcriptional regulation serves the purpose of modulating gene expression by regulating the half-life of specific transcripts or changing the rate of translation (17). Both proteins and non-coding RNAs (ncRNAs) participate in post-transcriptional regulation by direct interaction with specific sequences in the target mRNA. MicroRNAs (miRNAs) are small (~22nt) RNAs that are processed from endogenous hairpin structured precursor transcripts by Dicer (18). Upon being fully processed, mature miRNAs are mounted onto RNA-induced silencing complex (RISC) and thereby guide the latter to target sequences by pairing of nucleotides 2 to 8 of the miRNA (seed sequence) with corresponding sequences in the 3'UTR of target mRNA, and degrade or sequester the latter (19). miRNA is a very versatile post-transcriptional regulator targeting transcripts of genes involved in different biological processes such as cancer development and metabolism (20, 21). In addition, AU-rich element (ARE) (i.e. AUUUA pentamer embedded in a U-rich context) in the 3'UTR of mRNA is also a well-recognized cis-element in the regulation of mRNA stability targeted by AU-rich element binding proteins (ARE-BPs) (17). ARE-BPs include human antigen R (HuR), tristetraprolin (TTP), butyrate response factor 1 (BRF1), ARE/poly(U)-binding/degradation factor 1 (AUF1), and KH-type splicing regulatory protein (KSRP) among others (17). Unlike other ARE-BPs, which mostly act as negative regulators and induce mRNA decay, HuR, has however been shown to exert a stabilization effect on the target mRNA (17). Phosphorylation is important for HuR function. HuR harbors several phosphorylation sites for various kinases including AMP-activated kinase (AMPK), p38-MAPK (mitogen-activated protein kinase), and protein kinase C (PKC) (22). Following phosphorylation, HuR translocates from the nucleus to the cytoplasm (17,

22). The phosphorylation-mediated nucleo-cytoplasmic shuttling of HuR is essential for its mRNA stabilization function (22).

The limited studies conducted up-to-now examined mainly the role of microRNAs in the regulation of hepcidin genes. An indirect role for miR-122 and miR-130a has been reported in the regulation of mouse and human hepcidin gene expression. Namely, miR-122 and miR-130a modulated *HAMP* expression by altering the mRNA stability of transcriptional activators, which are known to activate *HAMP* transcription (23, 24). Other post-transcriptional regulation mechanisms besides microRNAs directly targeting *HAMP* 3'UTR have not been identified. *HAMP* 3'UTR harbors a single AU-rich element (ARE) but its functional role in the post-transcriptional regulation of *HAMP* expression is unknown.

Saturated fatty acids have been shown to activate various signaling pathways in hepatoma cells including protein kinase C isoforms (25–29), which, as mentioned above, is a potent HuR activator. However, the role of HuR or PKC in *HAMP* regulation has not been investigated. The objective of the studies in this chapter is to understand the mechanisms by which hepatic *HAMP* mRNA expression is regulated by saturated fatty acids. As described below, we have identified a functional role for a single ARE in *HAMP* 3'UTR and the ARE-binding protein, HuR in post-transcriptional regulation of *HAMP* expression by lipids in human hepatoma cells. These findings will help us to further understand the role of hepcidin and iron in obesity and fatty liver disease pathogenesis.

3 RESULTS

3.1 Regulation of *HAMP* mRNA expression by fatty acids in HepG2 cells

For these studies, HepG2 cells were treated with saturated fatty acids, palmitic acid (PA) and stearic acid (SA) or unsaturated fatty acid, oleic acid (OA). Most of the studies reported in the literature use fatty acids which are conjugated to bovine serum albumin (BSA) to facilitate their uptake by hepatocytes. Our preliminary studies however have shown that BSA by itself

dramatically suppresses the basal hepcidin expression in HepG2 cells. We observed this effect with different commercial BSA preparations including high quality tissue culture-grade BSA (*data not shown*). We therefore performed all the experiments described in this chapter using un-conjugated fatty acids. We also chose 0.1 and 0.3 mM fatty acid concentrations for our studies based on the studies reported in the literature, which describe optimal lipid signaling in tissue culture cells (30, 31).

Hepatocytes take up free fatty acids through diffusion and specific transporters such as CD36 and fatty acid transport polypeptide (FATP) (32). In order to validate that un-conjugated fatty acids were taken up by HepG2 cells under our experimental conditions, the intracellular lipid content was examined by Nile Red staining, as described in experimental procedures (**Figure 4.1**). A significant increase in lipid content was observed in cells treated with 0.3 mM saturated fatty acids, PA and SA or unsaturated fatty acid, OA, as compared to control cells treated with solvent (isopropanol) (**Figure 4.1**). In contrast to PA or SA-treated cells, OA-treated cells exhibited punctate lipid droplet-like structures (**Figure 4.1**). This is consistent with previous reports showing that unsaturated fatty acids are more readily esterified to produce triglycerides (33, 34).

To investigate the role of fatty acids in the regulation of *HAMP* expression, HepG2 cells were treated with different concentrations of PA, SA or OA for 8 h. Control cells were treated with solvent, as described in experimental procedures. *HAMP* mRNA expression was determined by real-time PCR (qPCR), as described in experimental procedures (*see Chapter II*). Cells treated with PA displayed a concentration-dependent increase in *HAMP* mRNA expression compared to solvent-treated control cells (**Figure 4.2A**). Similar concentrations of SA exerted a less prominent induction than PA. In contrast to PA and SA, OA treatment did not significantly alter *HAMP* expression compared to control cells (**Figure 4.2A**). In accordance with *HAMP* mRNA expression, PA treatment also elevated the level of hepcidin protein expression compared to control cells treated with solvent, as determined by western blotting **(Figure 4.2B)**. These

findings strongly suggest a role for saturated fatty acids, in particular PA, but not saturated fatty acids in the regulation of hepatic hepcidin expression.

Earlier studies mainly concentrated on the regulation of *HAMP* expression at the transcriptional level (12–15). We therefore examined the effect of fatty acids on *HAMP* transcription by performing luciferase reporter assays. For these studies, HepG2 were cells transfected with pGL-3 Basic vector harboring 1.5 kbp *HAMP* promoter (*HAMP* Prom-Luc), which contains consensus DNA-binding sequences for various transcription factors implicated in the regulation of *HAMP* transcription (12–15). As control, HepG2 cells were also transfected with empty vector, as described in experimental procedures. HepG2 cells transfected with the recombinant vector displayed higher luciferase activity compared to cells transfected with the empty vector (**Figure 4.2C**). However, the levels of *HAMP* promoter activity were similar in HepG2 cells treated with PA or solvent control (**Figure 4.2C**). These reporter assay studies indicated that PA did not stimulate 1.5 kbp *HAMP* promoter activity and therefore suggested that transcriptional mechanisms might not be responsible for *HAMP* regulation by saturated fatty acids. In order to investigate this further, we treated HepG2 cells with the transcription inhibitor, actinomycin D. as expected, actinomycin D by itself significantly inhibited basal *HAMP* mRNA expression in HepG2 cells (**Figure 4.2D**). On the other hand, HepG2 cells treated with PA in the presence of actinomycin D exhibited a significant increase in *HAMP* mRNA expression compared to cells treated with actinomycin D and solvent control (**Figure 4.2E**). Actinomycin experiments yielded results, which were in agreement with reporter studies in that despite the inhibition transcriptional mechanisms, saturated fatty acids can activate *HAMP* expression. This prompted us to investigate post-transcriptional regulation mechanisms.

First we conducted experiments to investigate the effect of palmitic acid on *HAMP* mRNA stability. For these investigations, time course experiments (0-10 h.) were performed with HepG2 cells treated with PA or solvent in the presence of actinomycin D. From 4 h. onwards, PA-treated cells displayed significantly higher levels of *HAMP* mRNA compared to solvent treated control

cells (**Figure 4.2F**). The half-lives of *HAMP* mRNA, calculated as described in experimental procedures, were 2.70 ± 0.08 and 4.44 ± 0.01 h. in solvent and PA-treated cells, respectively (**Figure 4.2G**). Our findings strongly suggest that palmitic acid stabilized *HAMP* mRNA in HepG2 cells. We then conducted further studies to investigate the mechanisms by which saturated fatty acid, PA regulates *HAMP* expression at the post-transcriptional level, which are described below.

3.2 The role of palmitic acid in *HAMP* 3'UTR regulation

3'UTR regions of mRNA are important in the regulation of mRNA stability by various post-transcriptional pathways (17). The effect of PA on the 3'UTR region of *HAMP* was therefore investigated by reporter assays. For these studies, the entire (101bp) 3'UTR region of *HAMP* gene was inserted downstream of the luciferase gene in pMIR reporter vector, as described in experimental procedures (*see Chapter II*). To perform dual luciferase reporter assays, HepG2 cells, transfected with either the empty pMIR vector (control) or recombinant pMIR vector harboring *HAMP* 3'UTR (*HAMP* 3'UTR), were co-transfected with the reference plasmid, pRL-SV40. Treatment with PA significantly stimulated luciferase activity in cells transfected with the *HAMP* 3'UTR but not with empty vector (**Figure 4.3A**). Our reporter assay experiments strongly suggested the involvement of 3'UTR in the regulation of *HAMP* mRNA expression by PA.

3.3 Functional role of AU-rich element (ARE) in *HAMP* 3'UTR

AU-rich element binding proteins (ARE-BP) regulate mRNA stability through the recognition of AU-rich elements (ARE) in 3'UTR (17). The examination of *HAMP* 3'UTR revealed a single ARE (**Figure 4.3B)**. We performed mutagenesis with the ARE by deleting the "UUU" in the AUUUA sequence. Recombinant pMIR vector harboring mutant *HAMP* 3'UTR (3'UTR ΔAU) was employed in luciferase reporter assays. Unlike in cells transfected with wild-type 3'UTR, PA failed to up-regulate luciferase activity in cells transfected with mutant *HAMP* 3'UTR (3'UTR ΔAU) (**Figure 4.3C**). Mutagenesis experiments strongly suggest a functional role for *HAMP*

3'UTR ARE in PA-mediated up-regulation of *HAMP* RNA expression. Since we have established a clear functional role for this single ARE-sequence within *HAMP* 2'UTR, we explored the role of RNA-binding proteins that may bind to *HAMP* 3'UTR for post-transcriptional regulation of hepcidin expression, as described below.

3.4 AU-rich element RNA-binding proteins (ARE-BP) and *HAMP* 3'UTR activation

The ARE-BP, HuR is well-known for its role in enhancing mRNA stability (17). The activation of HuR is achieved via phosphorylation and subsequent nucleo-cytoplasmic shuttling (22). We therefore examined the sub-cellular distribution of HuR in HepG2 cells treated with either PA or solvent by immunofluorescent staining. Cells stained with normal mouse IgG as negative control did not display any specific signal (**Figure 4.4A**). In solvent-treated control cells, HuR protein was mainly located in the nucleus (**Figure 4.4A**). Upon PA treatment, HuR shuttled from nucleus to the cytosol and exhibited a more diffuse distribution (**Figure 4.4A**). In contrast, unsaturated fatty acid (OA) did not induce the translocation of HuR to the cytosol (**Figure 4.4A**). The percentage of HuR localized in the cytosol was quantified, as described in experimental procedures. In HepG2 cells treated with solvent, PA or OA, 8.01 ± 2.56%, 35.33 ± 3.89% and 10.07 ± 3.16% of HuR resided in the cytosol, respectively (**Figure 4.4B**).

The PA-induced nucleo-cytoplasmic shuttling of HuR was further supported by western blotting performed with whole cell lysates, and nuclear and cytosolic fractions isolated from control or PA-treated HepG2 cells. PA treatment did not affect the basal protein expression levels of HuR (**Figure 4.5**). PA-treated cells displayed a significant increase in the level of cytosolic HuR protein compared to that in control cells (**Figure 4.5**). Accordingly, the expression level of HuR protein in the nucleus was decreased following PA treatment (**Figure 4.5**). Both immunofluorescent staining and western blotting experiments indicate that nucleo-cytoplasmic shuttling of HuR protein is induced by saturated fatty acids in hepatoma cells.

Phosphorylation by protein kinases including protein kinase C (PKC) is important for the shuttling and activation of HuR (22). Independently, PA has also been shown to induce the activation of multiple isoforms of PKC (25–29). We therefore examined the role of PKC in post-transcriptional regulation of *HAMP* by PA. For these studies, HepG2 cells were first treated with staurosporine, a potent broad-spectrum protein kinase C inhibitor (35, 36). The level of HuR shuttling was determined in HepG2 cells treated with PA in the presence of 0.2 μM staurosporine or DMSO as control. PA-induced nucleo-cytoplasmic shuttling of HuR was abolished in cells treated with staurosporine, but not with DMSO, as confirmed by immunofluorescent staining and further quantification (**Figures 4.6A and 4.6B**). Cells treated with PA in the presence of DMSO as control displayed a significant increase (from 7.51 ± 2.67% to 38.55 ± 5.18%) in the level of cytosolic HuR (**Figure 4.6B**). In contrast, HepG2 cells treated with PA and staurosporine did not exhibit a significant change (from 9.30 ± 4.83% to 11.76 ± 6.48%) in HuR translocation compared to cells treated with solvent and staurosporine (**Figure 4.6B**). Contrary to DMSO, staurosporine treatment significantly blocked PA-mediated induction of *HAMP* mRNA expression in HepG2 cells. (**Figures 4.7A and 4.7B**).

Both classical and novel classes of PKC isoforms have been suggested to phosphorylate HuR (22). We therefore employed PKC inhibitors, Go6976 and rottlerin, which have been shown to block classical or novel class of PKC isoforms, respectively (28, 37). Rottlerin (10 μM), but not Go6976 (1 μM), treatment abolished PA-induced *HAMP* mRNA increase in HepG2 cells (**Figures 4.7C and 4.7D**).

3.5 The effect of HuR silencing on *HAMP* mRNA expression

To determine the direct role of ARE and HuR in *HAMP* mRNA regulation by PA, we employed a commercial human HuR siRNA pool, comprised of four different specific siRNAs, as described in experimental procedures, to suppress HuR expression. In parallel, HepG2 cells were transfected with control siRNA (**Figures 4.8A and 4.8B**). The expression levels of HuR mRNA

and protein in cells transfected with control or HuR siRNA was determined by qPCR and western blotting (**Figure 4.8A**). Significant inhibition of HuR was achieved in HuR siRNA-transfected cells compared to control cells under our experimental conditions. Subsequently, transfected HepG2 cells were treated with 0.3 mM PA or solvent and *HAMP* mRNA expression was determined by qPCR. In solvent-treated HepG2 cells, the basal expression level of *HAMP* mRNA was down-regulated by HuR siRNA compared to control siRNA (**Figure 4.8B**). PA-induced increase in *HAMP* mRNA levels was significantly abrogated in HuR siRNA-transfected cells compared to cells transfected with control siRNA (**Figure 4.8B**). Our siRNA experiments clearly show that HuR is required for PA-mediated up-regulation of *HAMP* mRNA expression.

3.6 The Physical Interaction of HuR with HAMP 3'UTR

To confirm the direct interaction of HuR with *HAMP* mRNA, ribonucleoprotein immunoprecipitation (RNP-IP) assays were performed, as described in experimental procedures (*see Chapter II*). For these assays, we used cytosolic fractions, which were isolated from HepG2 cells, as described in experimental procedures. Specific immunoprecipitation of HuR proteins by our anti-HuR antibody was confirmed by western blotting (**Figure 4.9A inset**). The amount of *HAMP* mRNA in HuR or control IgG co-precipitated total RNA was quantified by qPCR. The level of *HAMP* mRNA present in control IgG immunoprecipitates was not different between PA and solvent-treated HepG2 cells (**Figure 4.9A**). In contrast, 8.58 ± 0.51-fold more *HAMP* mRNA was detected in HuR-immunoprecipitates of PA-treated HepG2 cells compared to those from solvent-treated cells (**Figure 4.9A**). To confirm specificity, the presence of 18s rRNA in HuR immunoprecipitates was determined, as a negative control. PA treatment did not significantly alter the level of 18s rRNA validating our RNP-IP assays (**Figure 4.9B**).

3.7 The regulation of microRNAs by palmitic acid and its effect on *HAMP* mRNA

Micro RNAs (miRNAs) are negative regulators of mRNA stability and translation (38, 39). We therefore determined whether PA-mediated up-regulation of *HAMP* mRNA involves the

suppression of miRNAs, which might potentially target *HAMP* 3'UTR. Online algorithms (e.g. TargetScan, miRGen, RNA22) for in silico identification of miRNA targets were employed to scan *HAMP* 3'UTR sequence. The results obtained from different databases commonly identified miR-214. Previous studies have also shown that miR-122 indirectly regulates *HAMP* gene expression by targeting 3'UTR of other upstream iron-regulatory genes, such as Hfe and Hjv (23). We therefore included these two microRNAs in our investigations and determined the expression levels in PA or solvent-treated HepG2 cells by qPCR, as described in experimental procedures. PA elevated the expression of miR-214 but not miR-122 (**Figures 4.10A and 4.10B**). Contrary to our hypothesis, PA treatment did not suppress, but induced, the expression of miR-214. Nevertheless, we further investigated the potential role of miR-214 in *HAMP* regulation by transfecting HepG2 cells with miR-214 mimic or negative control miRNA. *HAMP* mRNA expression was determined 24 h. after transfections. In parallel, the mRNA expression level of mitogen-activated protein kinase kinase 3 (MEK3), which is a validated miR-214 target (40), was also determined by qPCR. Compared to negative control miRNA, miR-214 mimic significantly elevated *HAMP* mRNA expression (**Figure 4.10C)**. However, the expression of MEK3 mRNA was significantly suppressed by miR-214 mimic confirming its specificity under our experimental conditions (**Figure 4.10D**). These findings in concert with the defined role of miRNAs as mRNA destabilizers strongly suggest that miR-214, despite being regulated by PA, is not directly involved in the induction of *HAMP* mRNA expression in PA-treated HepG2 cells.

4 DISCUSSION

Hepatic iron overload in NAFLD patients has been shown to be associated with disease severity (3–5). Clinical studies have also reported changes in the expression levels of hepcidin, the key iron regulator, in the liver and sera of NAFLD patients (6, 9). However, the underlying mechanisms are unclear. Hepcidin expression has been suggested to respond to changes in iron levels or obesity-mediated inflammatory cytokines (6, 9, 10)**.** Obesity and NAFLD are associated

with dysregulated lipid metabolism. This study investigated the regulation of human hepcidin gene, *HAMP* by fatty acids in hepatoma cells. Our findings have not only clearly shown that saturated fatty acids, particularly palmitic acid, stimulate hepcidin expression in human liver cells but also revealed that *HAMP* expression can be regulated at the post-transcriptional level. This post-transcriptional pathway utilizes a single AU-rich element (ARE) in *HAMP* 3'UTR. Furthermore, we have identified an additional role for the ARE-binding protein, HuR in the regulation of iron homeostasis. Interestingly, our findings also suggested an association of novel class protein kinase C isoforms with *HAMP* and iron metabolism. Collectively, we have shown unique mechanisms, which connect iron homeostasis with lipid metabolism in hepatoma cells, and have implications for the pathogenesis of fatty liver disease and obesity.

Previous studies have particularly focused on the transcriptional regulation of *HAMP*. Unlike other iron-regulatory proteins such as ferritin and transferrin receptor 1, which are regulated by RNA-binding proteins, IRP1 and IRP2, our knowledge on the post-transcriptional regulation of *HAMP* is very limited. An indirect role for microRNAs has been suggested in the regulation of mouse and human hepcidin genes via the targeting of transcriptional activators (23, 24). In agreement, our findings in this study have also indicated that miR-214 participates in *HAMP* regulation by saturated fatty acids, which likely occur through similar indirect mechanisms. In fact, miR-214 mimic up-regulated *HAMP* expression, which is in contrast to the widely accepted miRNA function. Namely, as explained in Introduction section above, microRNAs have been shown to destabilize mRNA by binding to their 3'UTR (21, 39). It is possible that miR-214 may have inhibited an as yet unidentified suppressor of *HAMP*. Nevertheless, our and other studies do not support a direct role for miRNAs in the regulation of human or mouse hepcidin gene expression. Further studies are required to accurately characterize the role of miR-214 in *HAMP* regulation. In this study we have shown other post-transcriptional mechanisms, which directly target and regulate the 3'UTR of *HAMP*.

Our studies with actinomycin D confirmed the post-transcriptional regulation of *HAMP* by saturated fatty acids. Namely, despite blocking transcription with actinomycin D, palmitic acid treatment induced *HAMP* up-regulation, which was similar to that in cells incubated with palmitic acid in the absence of actinomycin D. Accordingly, palmitic acid treatment significantly extended the half-life of *HAMP* mRNA. Furthermore, palmitic acid did not stimulate *HAMP* promoter, as shown by reporter assays using a construct harboring a 1.5 kbp *HAMP* promoter region. Similar results were obtained with shorter (0.6 and 0.9kbp) versions of *HAMP* promoter (*data not shown*). In contrast, palmitic acid directly stimulated *HAMP* 3'UTR, as shown by dual luciferase assays. Taken together, these findings clearly indicated that post-transcriptional mechanisms are responsible for the induction of hepatic *HAMP* mRNA by saturated fatty acids.

Numerous studies using different experimental models have clearly shown that palmitic acid treatment activates both the classical and novel class isoforms of protein kinase C (PKC) (26–28, 41). Our experiments suggested a role for these kinases in the regulation of *HAMP* by saturated fatty acids. The fact that palmitic acid treatment activated *HAMP* 3'UTR and that PKC inhibition abrogated saturated fatty acid-mediated *HAMP* mRNA up-regulation, prompted us to investigate the role of ARE-binding proteins, which are regulated by PKC signaling. The ARE-BP, HuR has been shown to be involved in the post-transcriptional regulation of genes mediating inflammatory reactions and tumorigenesis by targeting AU-rich elements (17, 22). Nucleo-cytoplasmic shuttling of HuR, regulated by phosphorylation, is crucial for its function (22). Both classical (PKCα) and novel (PKCδ) PKC isoforms have been shown to phosphorylate HuR at serine residues within or adjacent to the HuR-nucleo-cytoplasmic shuttling sequence (HNS) and thereby activate its translocation to the cytoplasm (42, 43). Saturated, but not unsaturated, fatty acids clearly induced the nucleo-cytoplasmic shuttling of HuR, which was confirmed both by immunofluorescence studies and subcellular fractionation of HepG2 cells. Accordingly, PKC inhibitors blocked both HuR translocation and induction of *HAMP* expression by palmitic acid. Inhibitor studies have also suggested that palmitic acid induces *HAMP* mRNA expression through

the activation of novel class of PKC isoforms. Further studies are required to confirm that the direct phosphorylation of HuR by PKC is essential for saturated fatty acid-mediated up-regulation of *HAMP* mRNA levels.

To further understand whether *HAMP* is a potential target of HuR, we analyzed *HAMP* 3'UTR and identified one classical AU-rich element (ARE). Mutation of this ARE completely abolished palmitic acid-mediated activation of *HAMP* 3'UTR, as shown by reporter assays, and thereby confirmed the importance of this cis-element. The direct role of HuR was subsequently confirmed by various experiments. RNP-IP assays indicated the physical interaction of HuR with *HAMP* mRNA. Further proof was obtained by HuR siRNA studies, which successfully knocked down HuR in HepG2 cells. HuR inhibition by siRNA abolished PA-induced elevation of *HAMP* mRNA. These findings confirm that *HAMP* is a target of HuR, which mediates the regulation of *HAMP* by saturated fatty acids. Although HuR binding is sufficient for *HAMP* activation, the interaction of other post-transcriptional regulators with HuR on *HAMP* 3'UTR cannot be excluded. Interestingly, we detected the presence of miR-214 in immune complexes pulled down with our anti-HuR antibody in HepG2 cells. Further investigations are required to understand the importance of ARE-BP and microRNA interaction in the regulation of *HAMP* mRNA stability.

In summary, we have identified a novel regulatory mechanism for human hepcidin gene expression, which occurs at the post-transcriptional level through AU-rich element RNA-binding protein, HuR and protein kinase C signaling. These findings have implications for understanding the role of iron metabolism in the pathogenesis of fatty liver disease and obesity. Since this ARE sequence is also present in 3'UTR of mouse hepcidin genes, mouse models of NAFLD can be used for further studies. Targeting of AU-rich element RNA-binding proteins might also provide novel therapeutic approaches for the treatment of diseases associated with metabolic syndrome.

5 REFERENCES

1. Ratziu, V., Bellentani, S., Cortez-Pinto, H., Day, C., and Marchesini, G. (2010) A position statement on NAFLD/NASH based on the EASL 2009 special conference. *J. Hepatol.* **53**, 372–384
2. Donnelly, K. L., Smith, C. I., Schwarzenberg, S. J., Jessurun, J., Boldt, M. D., and Parks, E. J. (2005) Sources of fatty acids stored in liver and secreted via lipoproteins in patients with nonalcoholic fatty liver disease. *J. Clin. Invest.* **115**, 1343–1351
3. Nelson, J. E., Klintworth, H., and Kowdley, K. V. (2012) Iron Metabolism in Nonalcoholic Fatty Liver Disease. *Curr. Gastroenterol. Rep.* **14**, 8–16
4. Valenti, L., Fracanzani, A. L., Bugianesi, E., Dongiovanni, P., Galmozzi, E., Vanni, E., Canavesi, E., Lattuada, E., Roviaro, G., Marchesini, G., and Fargion, S. (2010) HFE Genotype, Parenchymal Iron Accumulation, and Liver Fibrosis in Patients With Nonalcoholic Fatty Liver Disease. *Gastroenterology*. **138**, 905–912
5. Nelson, J. E., Wilson, L., Brunt, E. M., Yeh, M. M., Kleiner, D. E., Unalp-Arida, A., and Kowdley, K. V. (2010) Relationship between the pattern of hepatic iron deposition and histological severity in nonalcoholic fatty liver disease. *Hepatology*. **53**, 448–457
6. Nelson, J. E., Brunt, E. M., Kowdley, K. V., and for the Nonalcoholic Steatohepatitis Clinical Research Network (2012) Lower serum hepcidin and greater parenchymal iron in nonalcoholic fatty liver disease patients with C282Y HFE mutations. *Hepatology*. **56**, 1730–1740
7. Courselaud, B., Pigeon, C., Inoue, Y., Inoue, J., Gonzalez, F. J., Leroyer, P., Gilot, D., Boudjema, K., Guguen-Guillouzo, C., Brissot, P., Loréal, O., and Ilyin, G. (2002) C/EBPα Regulates Hepatic Transcription of Hepcidin, an Antimicrobial Peptide and Regulator of Iron Metabolism CROSS-TALK BETWEEN C/EBP PATHWAY AND IRON METABOLISM. *J. Biol. Chem.* **277**, 41163–41170
8. Nemeth, E., Tuttle, M. S., Powelson, J., Vaughn, M. B., Donovan, A., Ward, D. M., Ganz, T., and Kaplan, J. (2004) Hepcidin Regulates Cellular Iron Efflux by Binding to Ferroportin and Inducing Its Internalization. *Science*. **306**, 2090–2093
9. Aigner, E., Theurl, I., Theurl, M., Lederer, D., Haufe, H., Dietze, O., Strasser, M., Datz, C., and Weiss, G. (2008) Pathways Underlying Iron Accumulation in Human Nonalcoholic Fatty Liver Disease. *Am. J. Clin. Nutr.* **87**, 1374–1383
10. Bekri, S., Gual, P., Anty, R., Luciani, N., Dahman, M., Ramesh, B., Iannelli, A., Staccini–Myx, A., Casanova, D., Ben Amor, I., Saint–Paul, M., Huet, P., Sadoul, J., Gugenheim, J., Srai, S. K. S., Tran, A., and Le Marchand–Brustel, Y. (2006) Increased Adipose Tissue Expression of Hepcidin in Severe Obesity Is Independent From Diabetes and NASH. *Gastroenterology*. **131**, 788–796
11. Vock, C., Gleissner, M., Klapper, M., and Döring, F. (2007) Identification of palmitate-regulated genes in HepG2 cells by applying microarray analysis. *Biochim. Biophys. Acta BBA - Gen. Subj.* **1770**, 1283–1288
12. Wrighting, D. M., and Andrews, N. C. (2006) Interleukin-6 induces hepcidin expression through STAT3. *Blood*. **108**, 3204–3209
13. Falzacappa, V., Vittoria, M., Vujic Spasic, M., Kessler, R., Stolte, J., Hentze, M. W., and Muckenthaler, M. U. (2007) STAT3 Mediates Hepatic Hepcidin Expression and Its Inflammatory Stimulation. *Blood*. **109**, 353–358
14. Wang, R.-H., Li, C., Xu, X., Zheng, Y., Xiao, C., Zerfas, P., Cooperman, S., Eckhaus, M., Rouault, T., Mishra, L., and Deng, C.-X. (2005) A role of SMAD4 in iron metabolism through the positive regulation of hepcidin expression. *Cell Metab.* **2**, 399–409
15. Kautz, L., Jung, G., Valore, E. V., Rivella, S., Nemeth, E., and Ganz, T. (2014) Identification of erythroferrone as an erythroid regulator of iron metabolism. *Nat. Genet.* 10.1038/ng.2996

16. Rouault, T. A. (2006) The role of iron regulatory proteins in mammalian iron homeostasis and disease. *Nat. Chem. Biol.* **2**, 406–414
17. Schoenberg, D. R., and Maquat, L. E. (2012) Regulation of cytoplasmic mRNA decay. *Nat. Rev. Genet.* **13**, 246–259
18. Kim, V. N. (2005) MicroRNA biogenesis: coordinated cropping and dicing. *Nat. Rev. Mol. Cell Biol.* **6**, 376–385
19. Fabian, M. R., Sonenberg, N., and Filipowicz, W. (2010) Regulation of mRNA Translation and Stability by microRNAs. *Annu. Rev. Biochem.* **79**, 351–379
20. Li, M., Li, J., Ding, X., He, M., and Cheng, S.-Y. (2010) microRNA and Cancer. *AAPS J.* **12**, 309–317
21. Rottiers, V., and Näär, A. M. (2012) MicroRNAs in metabolism and metabolic disorders. *Nat. Rev. Mol. Cell Biol.* **13**, 239–250
22. Doller, A., Pfeilschifter, J., and Eberhardt, W. (2008) Signalling pathways regulating nucleo-cytoplasmic shuttling of the mRNA-binding protein HuR. *Cell. Signal.* **20**, 2165–2173
23. Castoldi, M., Vujic Spasic, M., Altamura, S., Elmén, J., Lindow, M., Kiss, J., Stolte, J., Sparla, R., Alessandro, L. A. D', Klingmüller, U., Fleming, R. E., Longerich, T., Gröne, H. J., Benes, V., Kauppinen, S., Hentze, M. W., and Muckenthaler, M. U. (2011) The liver-specific microRNA miR-122 controls systemic iron homeostasis in mice. *J. Clin. Invest.* **121**, 1386–1396
24. Zumbrennen-Bullough, K. B., Wu, Q., Core, A. B., Canali, S., Chen, W., Theurl, I., Meynard, D., and Babitt, J. L. (2014) MicroRNA-130a Is Up-regulated in Mouse Liver by Iron Deficiency and Targets the Bone Morphogenetic Protein (BMP) Receptor ALK2 to Attenuate BMP Signaling and Hepcidin Transcription. *J. Biol. Chem.* **289**, 23796–23808
25. Lee, J., Cho, H.-K., and Kwon, Y. H. (2010) Palmitate induces insulin resistance without significant intracellular triglyceride accumulation in HepG2 cells. *Metabolism.* **59**, 927–934
26. Greene, M. W., Burrington, C. M., Ruhoff, M. S., Johnson, A. K., Chongkrairatanakul, T., and Kangwanpornsiri, A. (2010) PKCδ Is Activated in a Dietary Model of Steatohepatitis and Regulates Endoplasmic Reticulum Stress and Cell Death. *J. Biol. Chem.* **285**, 42115–42129
27. Dasgupta, S., Bhattacharya, S., Maitra, S., Pal, D., Majumdar, S. S., Datta, A., and Bhattacharya, S. (2011) Mechanism of lipid induced insulin resistance: Activated PKCε is a key regulator. *Biochim. Biophys. Acta BBA - Mol. Basis Dis.* **1812**, 495–506
28. Tan, S. H., Shui, G., Zhou, J., Li, J. J., Bay, B.-H., Wenk, M. R., and Shen, H.-M. (2012) Induction of Autophagy by Palmitic Acid via Protein Kinase C-mediated Signaling Pathway Independent of mTOR (Mammalian Target of Rapamycin). *J. Biol. Chem.* **287**, 14364–14376
29. Greene, M. W., Burrington, C. M., Lynch, D. T., Davenport, S. K., Johnson, A. K., Horsman, M. J., Chowdhry, S., Zhang, J., Sparks, J. D., and Tirrell, P. C. (2014) Lipid Metabolism, Oxidative Stress and Cell Death Are Regulated by PKC Delta in a Dietary Model of Nonalcoholic Steatohepatitis. *PLoS ONE*. **9**, e85848
30. Cazanave, S. C., Mott, J. L., Elmi, N. A., Bronk, S. F., Werneburg, N. W., Akazawa, Y., Kahraman, A., Garrison, S. P., Zambetti, G. P., Charlton, M. R., and Gores, G. J. (2009) JNK1-dependent PUMA Expression Contributes to Hepatocyte Lipoapoptosis. *J. Biol. Chem.* **284**, 26591–26602
31. Akazawa, Y., Guicciardi, M. E., Cazanave, S. C., Bronk, S. F., Werneburg, N. W., Kakisaka, K., Nakao, K., and Gores, G. J. (2013) Degradation of cIAPs contributes to hepatocyte lipoapoptosis. *Am. J. Physiol. - Gastrointest. Liver Physiol.* **305**, G611–G619
32. Bradbury, M. W. (2006) Lipid Metabolism and Liver Inflammation. I. Hepatic fatty acid uptake: possible role in steatosis. *Am. J. Physiol. - Gastrointest. Liver Physiol.* **290**, G194–G198

33. Listenberger, L. L., Han, X., Lewis, S. E., Cases, S., Farese, R. V., Ory, D. S., and Schaffer, J. E. (2003) Triglyceride Accumulation Protects Against Fatty Acid-Induced Lipotoxicity. *Proc. Natl. Acad. Sci.* **100**, 3077–3082
34. Ricchi, M., Odoardi, M. R., Carulli, L., Anzivino, C., Ballestri, S., Pinetti, A., Fantoni, L. I., Marra, F., Bertolotti, M., Banni, S., Lonardo, A., Carulli, N., and Loria, P. (2009) Differential effect of oleic and palmitic acid on lipid accumulation and apoptosis in cultured hepatocytes. *J. Gastroenterol. Hepatol.* **24**, 830–840
35. Tamaoki, T., Nomoto, H., Takahashi, I., Kato, Y., Morimoto, M., and Tomita, F. (1986) Staurosporine, a potent inhibitor of phospholipidCa++dependent protein kinase. *Biochem. Biophys. Res. Commun.* **135**, 397–402
36. Martiny-Baron, G., Kazanietz, M. G., Mischak, H., Blumberg, P. M., Kochs, G., Hug, H., Marmé, D., and Schächtele, C. (1993) Selective inhibition of protein kinase C isozymes by the indolocarbazole Gö 6976. *J. Biol. Chem.* **268**, 9194–9197
37. Kubitz, R., Saha, N., Kühlkamp, T., Dutta, S., Dahl, S. vom, Wettstein, M., and Häussinger, D. (2004) Ca2+-dependent Protein Kinase C Isoforms Induce Cholestasis in Rat Liver. *J. Biol. Chem.* **279**, 10323–10330
38. Valencia-Sanchez, M. A., Liu, J., Hannon, G. J., and Parker, R. (2006) Control of translation and mRNA degradation by miRNAs and siRNAs. *Genes Dev.* **20**, 515–524
39. Bartel, D. P. (2009) MicroRNAs: Target Recognition and Regulatory Functions. *Cell.* **136**, 215–233
40. Yang, Z., Chen, S., Luan, X., Li, Y., Liu, M., Li, X., Liu, T., and Tang, H. (2009) MicroRNA-214 is aberrantly expressed in cervical cancers and inhibits the growth of HeLa cells. *IUBMB Life*. **61**, 1075–1082
41. Eitel, K., Staiger, H., Rieger, J., Mischak, H., Brandhorst, H., Brendel, M. D., Bretzel, R. G., Häring, H.-U., and Kellerer, M. (2003) Protein Kinase C δ Activation and Translocation to the Nucleus Are Required for Fatty Acid-Induced Apoptosis of Insulin-Secreting Cells. *Diabetes*. **52**, 991–997
42. Doller, A., Huwiler, A., Muller, R., Radeke, H. H., Pfeilschifter, J., and Eberhardt, W. (2007) Protein Kinase Cα-dependent Phosphorylation of the mRNA-stabilizing Factor HuR: Implications for Posttranscriptional Regulation of Cyclooxygenase-2. *Mol. Biol. Cell*. **18**, 2137–2148
43. Doller, A., Akool, E.-S., Huwiler, A., Müller, R., Radeke, H. H., Pfeilschifter, J., and Eberhardt, W. (2008) Posttranslational Modification of the AU-Rich Element Binding Protein HuR by Protein Kinase Cδ Elicits Angiotensin II-Induced Stabilization and Nuclear Export of Cyclooxygenase 2 mRNA. *Mol. Cell. Biol.* **28**, 2608–2625

Figure 4.1. Fatty acid-induced lipid accumulation in HepG2 cells. HepG2 cells cultured on coverslips coated with poly-lysine were treated with 0.3 mM palmitic acid (PA), stearic acid (SA), oleic acid (OA) or solvent control (Solv.) for 8 h. Intracellular lipid content was stained with Nile Red and nuclei counterstained with Hoechst 33342, as described in experimental procedures (*see Chapter II*). The images obtained with Nikon Eclipse E400 fluorescence microscope were processed and overlaid with ImageJ. Representative fluorescent images are shown (X 40).

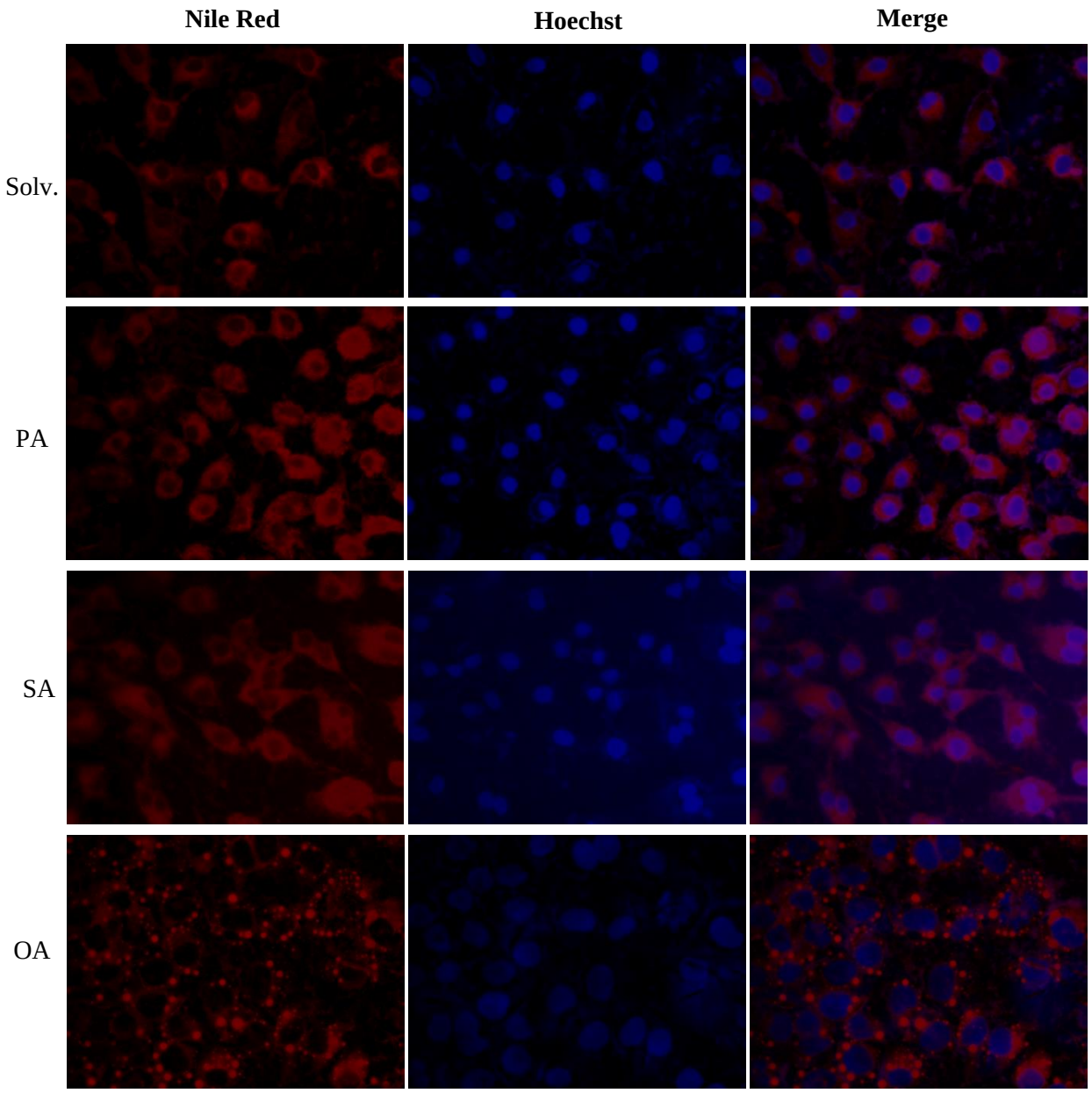

Figure 4.1

Figure 4.2. Post-transcriptional regulation of *HAMP* by saturated fatty acids. (**A**) HepG2 cells were treated with 0.1 mM or 0.3 mM PA, 0.3 mM SA and OA for 8 hours (h). cDNA synthesized from RNA was employed in Taqman qPCR to determine *HAMP* mRNA expression. Gene expression in fatty acid-treated cells was expressed as fold change of that in solvent-treated control cells. The inset shows hepcidin protein expression in solvent or PA-treated cells, as determined by western blotting. (**B**) Hepcidin protein expression levels in PA or solvent-treated cells were determined by western blotting. (**C**) pGL-3 Basic vector harboring a 1.5kb *HAMP* promoter region (*HAMP* Prom-Luc) or empty pGL-3 Basic vector was transfected into HepG2 cells together with pRL-SV40 plasmid as a reference for transfection efficiency. 24 h. after transfections, the cells were treated with 0.3 mM PA or solvent for 8 h. Dual luciferase reporter assays were performed, as described. The relative luciferase levels were expressed as fold change of that in solvent-treated cells transfected with empty vector. (**D**) HepG2 cells were treated with DMSO or 1µg/mL actinomycin D (ACTD) for 8 hours. *HAMP* mRNA expression, determined by qPCR, in ACTD-treated cells was expressed as fold change of that in DMSO-treated controls. (**E**) HepG2 cells were treated with 0.3 mM PA or solvent in the presence of ACTD for 8 h. *HAMP* mRNA expression, determined by qPCR, in PA and ACTD-treated cells was expressed as fold change of that in cells treated with solvent and ACTD (**F**) HepG2 cells were treated with solvent (solid line) or 0.3 mM PA (dashed line) in the presence of 1µg/mL actinomycin D (ACTD). Control cells were treated with solvent in the presence of DMSO. Cells were harvested every 2 h until 10 h. *HAMP* mRNA expression at different time points was expressed as fold change of that in respective control cells. (**G**) The half-life of *HAMP* mRNA in HepG2 cells treated with solvent or 0.3 mM PA was calculated, as described in experimental procedures and expressed in hours. Asterisks indicate statistical significance ($p<0.05$).

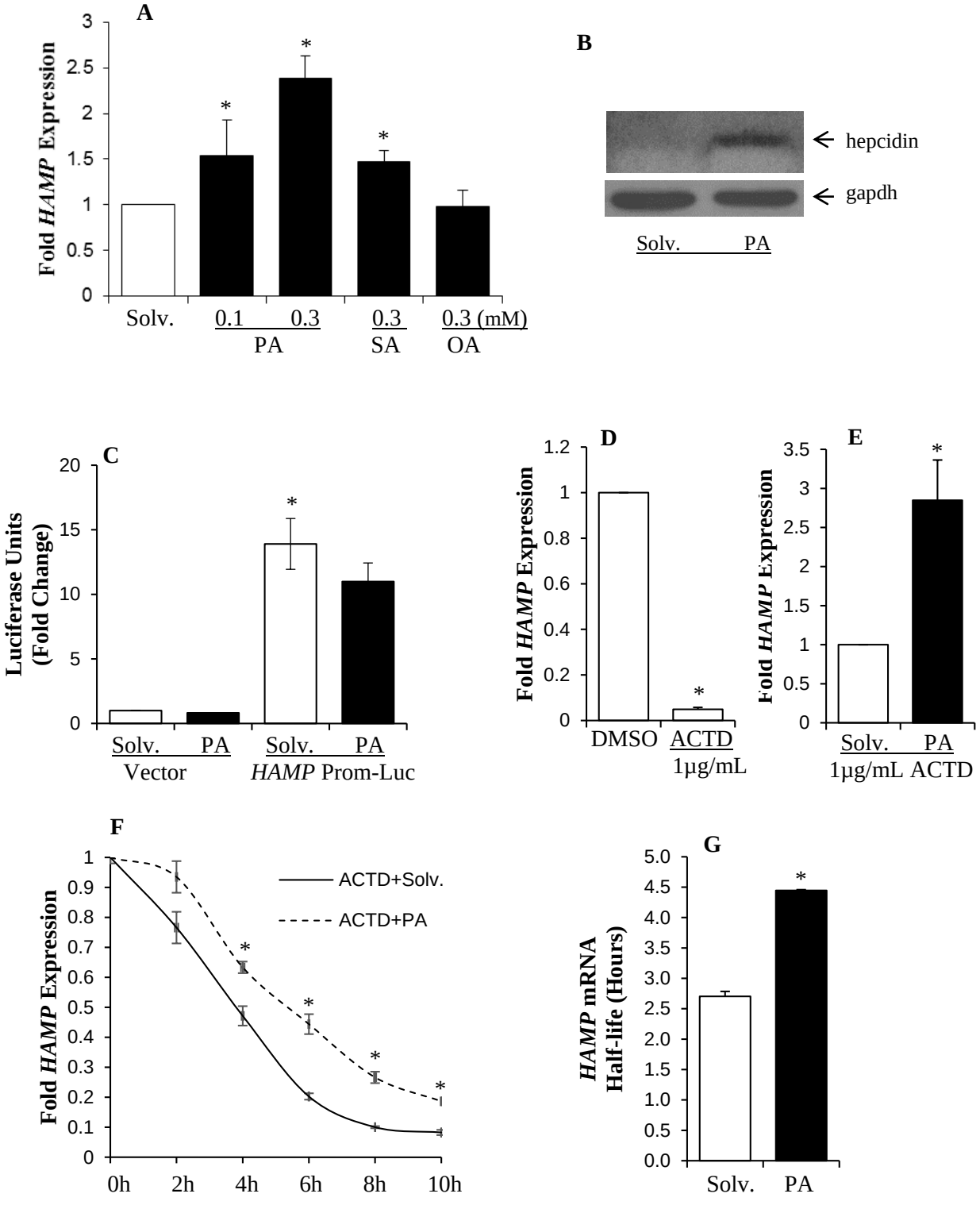
A
Fold HAMP Expression
Solv.
0.1
0.3
PA
0.3
SA
0.3 (mM)
OA
B
hepcidin
gapdh
Solv.
PA
C
Luciferase Units (Fold Change)
Solv.
PA
Vector
HAMP Prom-Luc
D
Fold HAMP Expression
DMSO
ACTD
1µg/mL
E
Fold HAMP Expression
Solv.
PA
1µg/mL ACTD
F
Fold HAMP Expression
ACTD+Solv.
ACTD+PA
0h
2h
4h
6h
8h
10h
G
HAMP mRNA Half-life (Hours)
Solv.
PA

Figure 4.2

Figure 4.3. The role of palmitic acid (PA) in the regulation of *HAMP* 3'UTR. (**A**) HepG2 cells, transfected with pMIR vector harboring 3'UTR of *HAMP* gene (3'UTR) or empty pMIR vector, were treated with PA or solvent. pRL-SV40 vector was co-transfected as a reference for transfection efficiency. Dual luciferase assays were performed, as described in experimental procedures. The relative luciferase levels were expressed as fold change of that in solvent-treated cells transfected with empty vector. (**B**) *HAMP* 3'UTR region harboring a single AU-rich element (ARE) is shown as a schematic diagram. The position of ARE sequence (AUUUA) is underlined. (**C**) Mutagenesis of AU-rich element in *HAMP* 3'UTR region was performed by deleting the UUU base pairs by site-directed mutagenesis, as described in the experimental procedures. HepG2 cells were transfected with pMIR vector harboring wild-type 3'UTR or 3'UTR with mutated AU-rich element (3'UTR ΔAU) to perform dual luciferase assays, as described above.

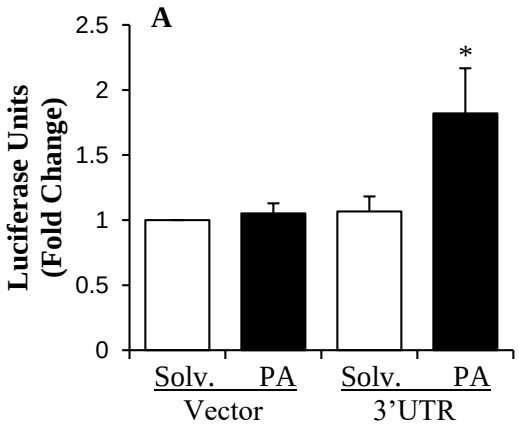
A
Luciferase Units (Fold Change)
2.5
2
1.5
1
0.5
0
*
Solv. PA
Vector
Solv. PA
3'UTR

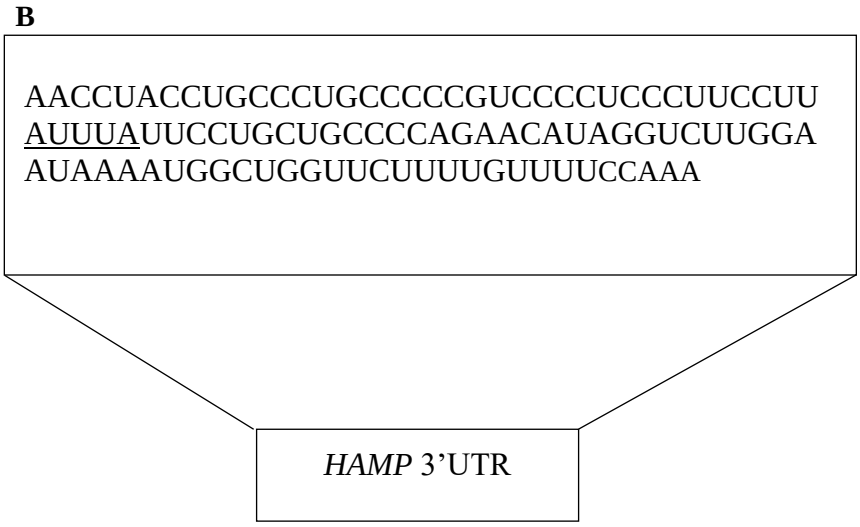
B
AACCUACCUGCCCUGCCCCCGUCCCCUCCCUUCCUU
AUUUAUUCCUGCUGCCCCAGAACAUAGGUCUUGGA
AUAAAAUGGCUGGUUCUUUUGUUUUCCAAA
HAMP 3'UTR

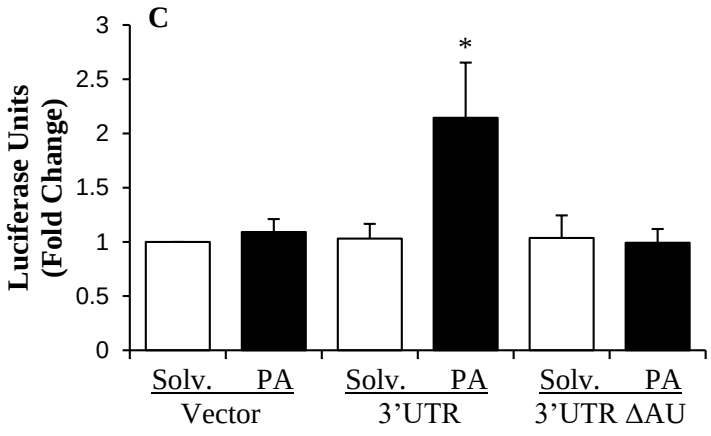
C
Luciferase Units (Fold Change)
3
2.5
2
1.5
1
0.5
0
*
Solv. PA
Vector
Solv. PA
3'UTR
Solv. PA
3'UTR ΔAU

Figure 4.3

Figure 4.4. PA-induced nucleo-cytoplasmic shuttling of HuR protein (immunofluorescent staining). (**A**) HepG2 cells cultured on coverslips were treated with 0.3 mM PA, OA or solvent (Solv.). HuR protein expression was detected with an anti-HuR primary antibody and secondary Texas Red-conjugated horse anti-mouse IgG. Normal mouse IgG was employed as negative control for the immunofluorescent staining. Nuclei were counterstained with DAPI. The images obtained with Nikon Eclipse E400 fluorescence microscope were processed and overlaid with ImageJ. Representative fluorescent images are shown (X 40). (**B**) Four independent 20X fluorescent images (120 ± 22 cells in each image) from each treatment group were analyzed with Squassh plugin of ImageJ. The percentage of cytosolic HuR signal intensity was calculated, as described in experimental procedures. Asterisks indicate statistical significance ($p<0.05$).

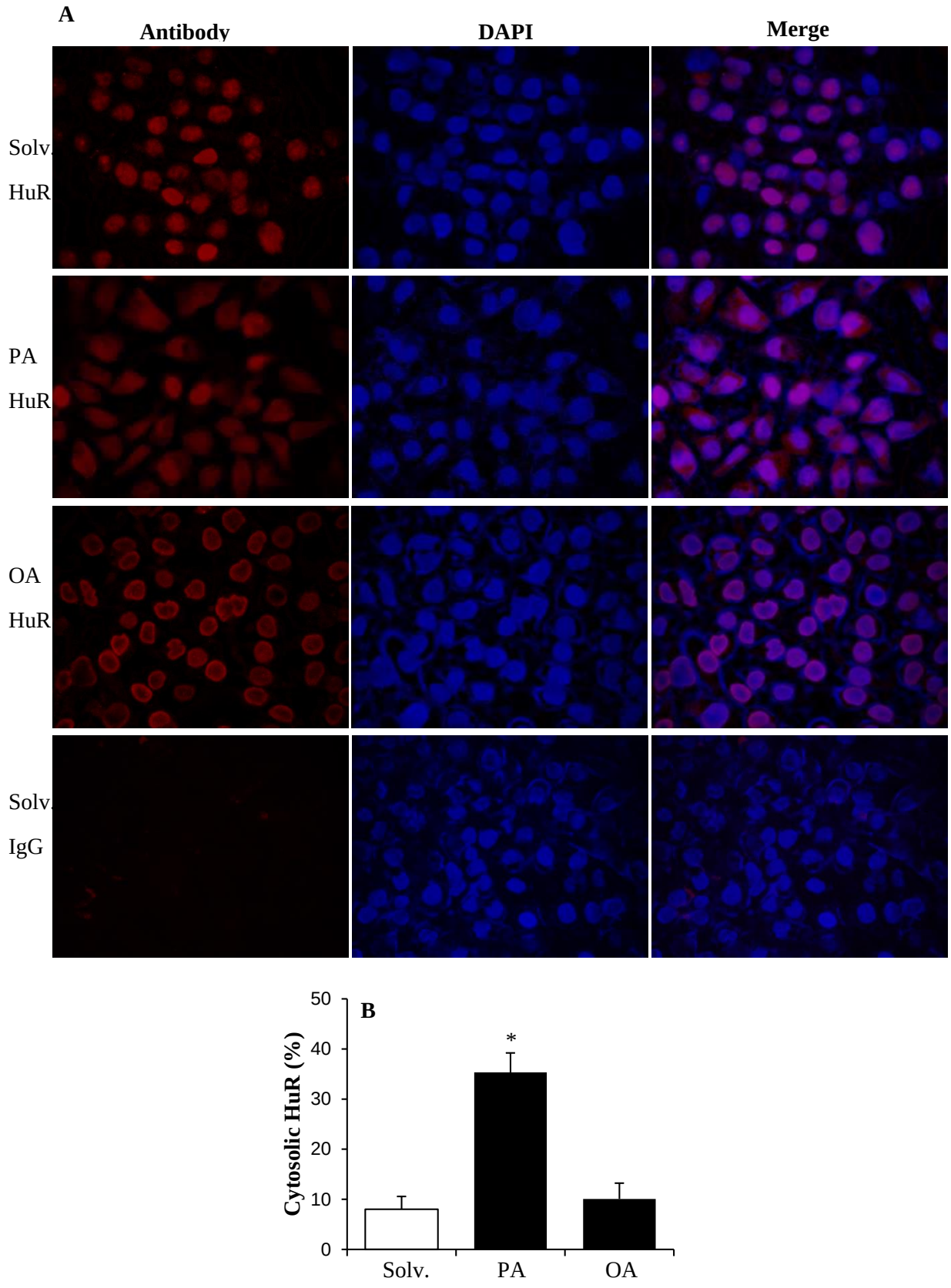
A
Antibody
DAPI
Merge
Solv.
HuR
PA
HuR
OA
HuR
Solv.
IgG
B
Cytosolic HuR (%)
50
40
30
20
10
0
*
Solv.
PA
OA

Figure 4.4

Figure 4.5. PA-induced nucleo-cytoplasmic shuttling of HuR protein (western blotting). Whole cell lysate, cytosolic and nuclear fractions were isolated from HepG2 cells treated with solvent (Solv.) or 0.3 mM PA for 8 h. The protein lysates were employed for western blotting to detect HuR protein expression with an anti-HuR primary and an anti-mouse secondary antibody in each fraction. An anti-gapdh or anti-histone H3 (H3) antibody was used as cytosol or nucleus marker, respectively.

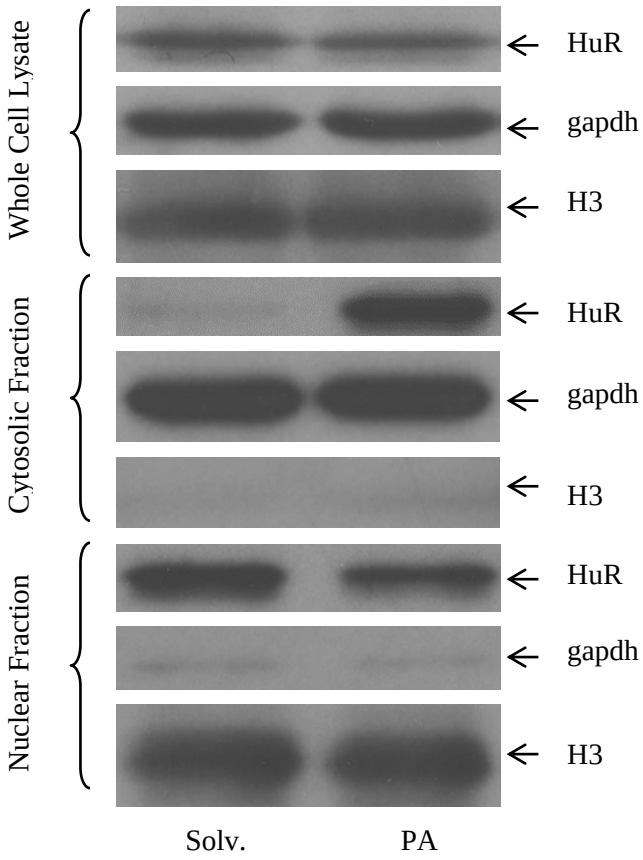
Whole Cell Lysate
HuR
gapdh
H3
Cytosolic Fraction
HuR
gapdh
H3
Nuclear Fraction
HuR
gapdh
H3
Solv.
PA

Figure 4.5

Figure 4.6. PA-mediated shuttling of HuR was abolished by staurosporine. (**A**) Immunofluorescent staining was performed with HepG2 cells treated with solvent or 0.3 mM PA in the presence of 0.2 µM staurosporine (STAU) or DMSO as control, as described. Representative fluorescent images are shown (X 40). (**B**) Quantification of HuR nuclear localization was performed, as described in experimental procedures.

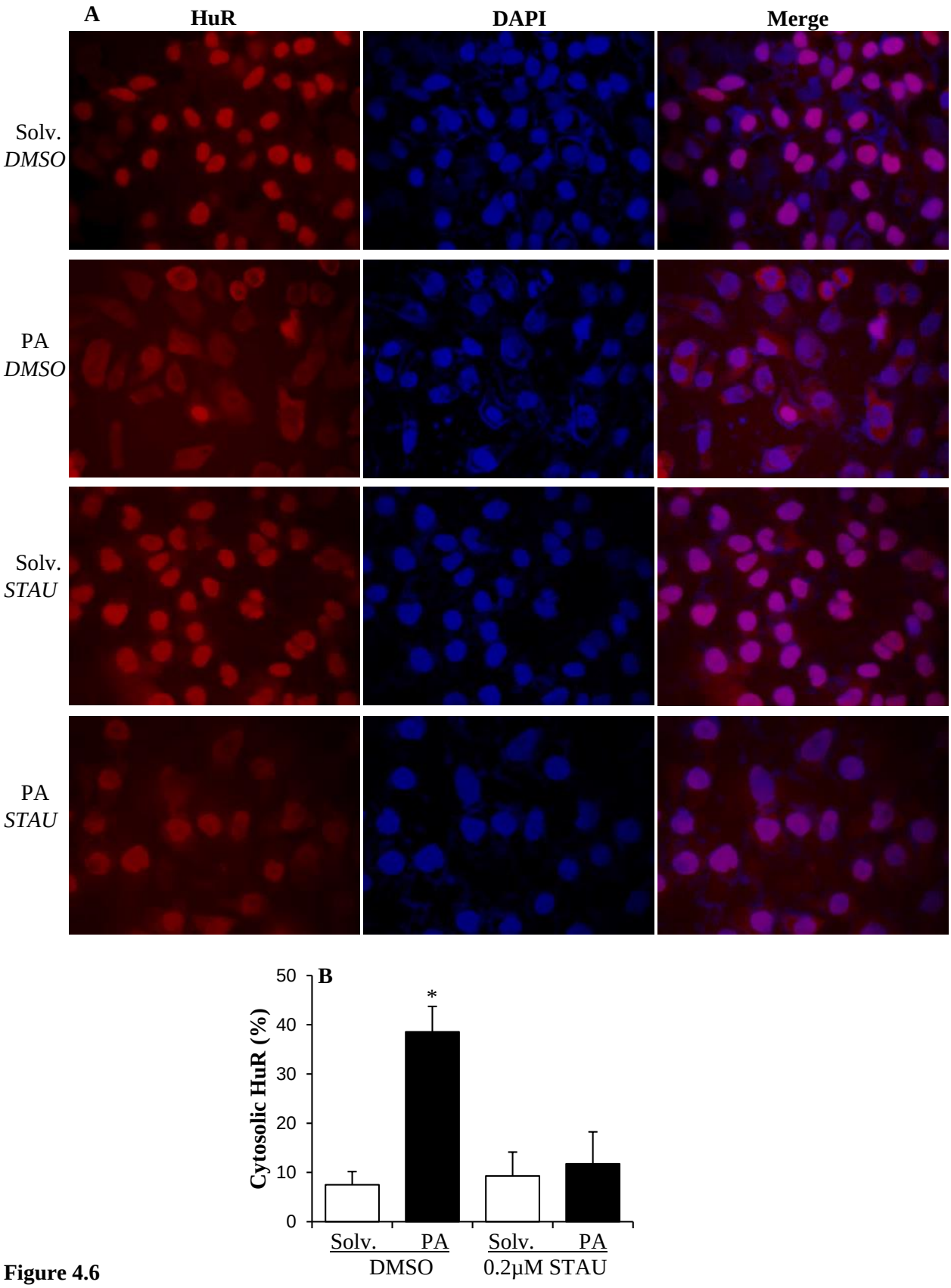
A
HuR
DAPI
Merge
Solv.
DMSO
PA
DMSO
Solv.
STAU
PA
STAU
B
Cytosolic HuR (%)
50
40
30
20
10
0
*
Solv.
PA
Solv.
PA
DMSO
0.2µM STAU

Figure 4.6

Figure 4.7. PA-mediated *HAMP* mRNA induction was abolished by PKC inhibitors. *HAMP* mRNA expression in HepG2 cells treated with solvent (Solv.) or 0.3 mM PA either in the presence of DMSO (**A**), 0.2µM staurosporine (STAU) (**B**), 1 µM Go6976 (**C**) or 10 µM rottlerin (**D**) was determined by qPCR. Gene expression in treated cells was expressed as fold expression of that in control cells incubated with solvent. Asterisks indicate statistical significance ($p<0.05$).

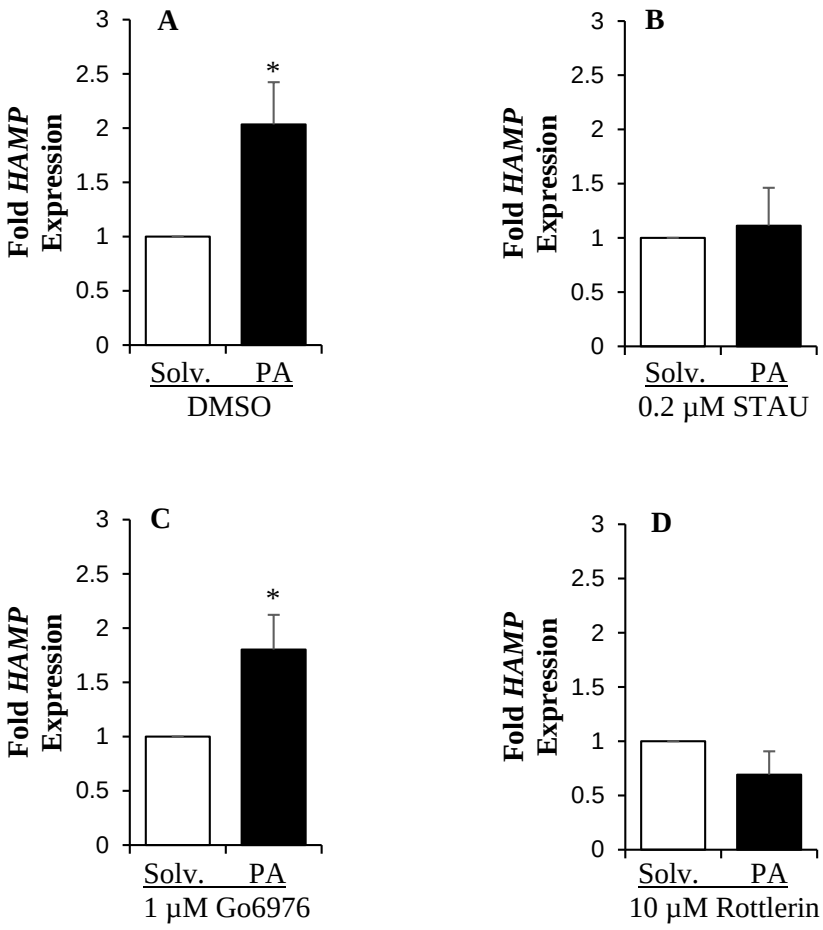
A
B
C
D
Fold HAMP Expression
3
2.5
2
1.5
1
0.5
0
*
Solv.
PA
DMSO
0.2 µM STAU
1 µM Go6976
10 µM Rottlerin

Figure 4.7

Figure 4.8. PA-induced up-regulation of *HAMP* expression was inhibited by HuR siRNA. HepG2 cells were transfected with 50 nM of HuR siRNA SMART pool or control siRNA, as described in experimental procedures. (**A**) The level of HuR mRNA expression in transfected cells was determined by qPCR. The inset shows HuR protein expression determined by western blotting. (**B**) The level of *HAMP* mRNA expression in siRNA-transfected cells treated with solvent or 0.3 mM PA for 8 h. was determined by qPCR. Asterisks indicate statistical significance ($p<0.05$).

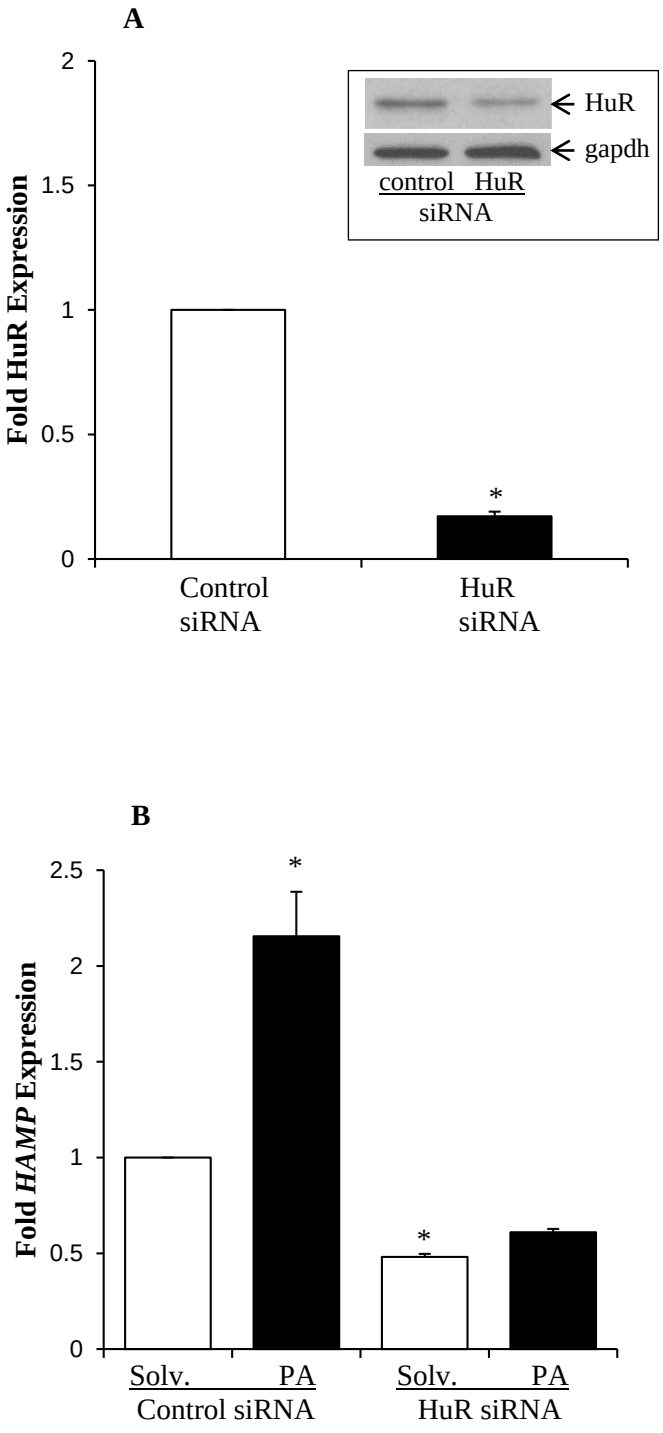
A
Fold HuR Expression
2
1.5
1
0.5
0
HuR
gapdh
control HuR
siRNA
*
Control siRNA
HuR siRNA
B
Fold HAMP Expression
2.5
2
1.5
1
0.5
0
*
*
Solv. PA
Control siRNA
Solv. PA
HuR siRNA

Figure 4.8

Figure 4.9. The physical interaction of HuR with *HAMP* mRNA. RNP-IP assays were performed to detect the binding of HuR to *HAMP* mRNA in HepG2 cells treated with solvent or 0.3 mM PA, as described in experimental procedures. (**A**) RNA isolated from control IgG or HuR immunoprecipitates was used to synthesize cDNA to determine *HAMP* expression by qPCR. *HAMP* expression in immunoprecipitates from PA-treated cells was expressed as fold change of that in corresponding solvent-treated cells. Asterisks indicate statistical significance ($p<0.05$). Inset: Detection of HuR protein in HuR or control IgG immunocomplexes by western blotting. (**B**) 18s rRNA expression in HuR immunoprecipitates was determined by qPCR as a negative control.

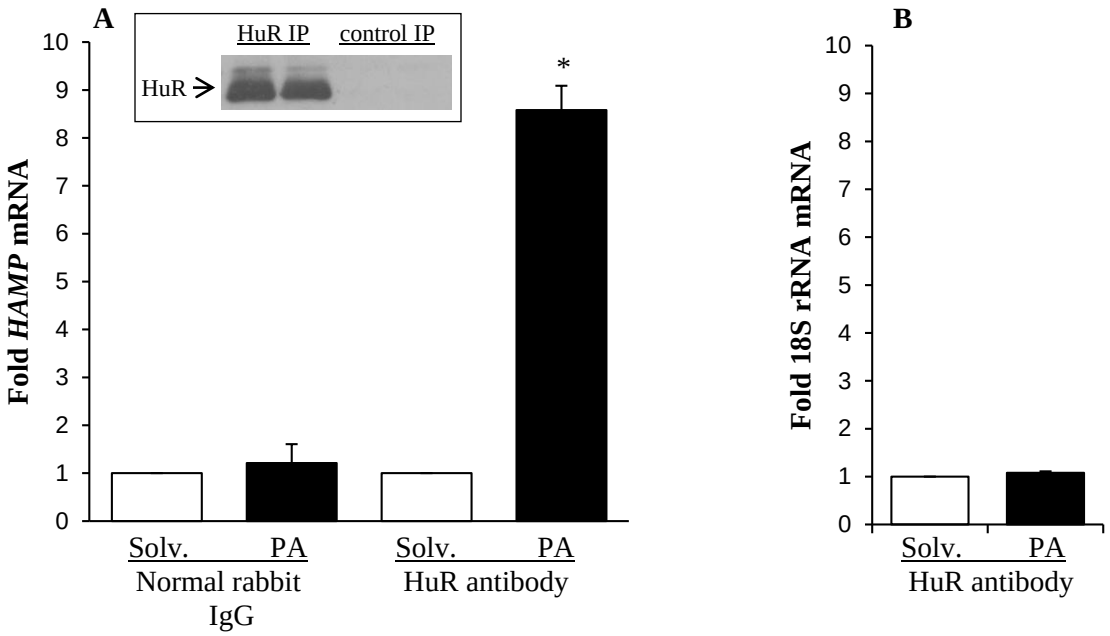
A
HuR IP
control IP
HuR
Fold HAMP mRNA
10
9
8
7
6
5
4
3
2
1
0
*
Solv.
PA
Solv.
PA
Normal rabbit IgG
HuR antibody
B
Fold 18S rRNA mRNA
Solv.
PA
HuR antibody

Figure 4.9

Figure 4.10. The regulation of microRNAs by PA and its effect on *HAMP* mRNA. The expression levels of miR-122 (**A**) and miR-214 (**B**) in PA or solvent-treated HepG2 cells were determined by qPCR. (**C**) miR-214 mimic and negative control (Neg.) was transfected into HepG2 cells and the expression levels of *HAMP* (**C**) and MEK3 (**D**) mRNA were determined by qPCR 24 h. after transfections. Asterisks indicate statistical significance ($p<0.05$).

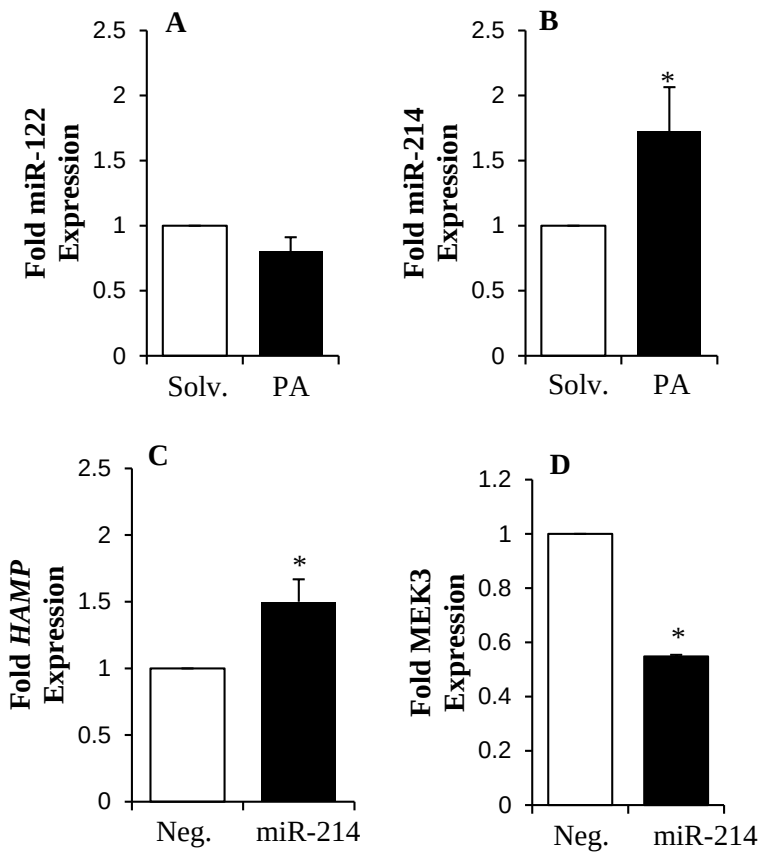
A
Fold miR-122 Expression
2.5
2
1.5
1
0.5
0
Solv.
PA
B
Fold miR-214 Expression
2.5
2
1.5
1
0.5
0
*
Solv.
PA
C
Fold HAMP Expression
2.5
2
1.5
1
0.5
0
*
Neg.
miR-214
D
Fold MEK3 Expression
1.2
1
0.8
0.6
0.4
0.2
0
*
Neg.
miR-214

Figure 4.10

Chapter V

Ceramide Regulates Human Hepcidin Gene Transcription through JAK/STAT3 Signaling Pathway

1 ABSTRACT

Hepcidin is both an acute phase and iron-regulatory protein, synthesized in the liver. As an acute phase protein, its expression is induced by inflammation and infection. Inflammatory processes in the liver play a major role in the pathogenesis of liver diseases including nonalcoholic fatty liver disease (NAFLD). Changes in iron metabolism and hepcidin expression in NAFLD patients have been observed but the causes and significance of these changes are unclear. It might be mediated by iron or inflammatory signaling in the liver. Transcription of the human hepcidin gene, *HAMP* is known to be activated by inflammatory cytokines, IL-1 and IL-6. The lipid intermediates such as ceramide, which are also generated in livers with lipid accumulation (i.e. NAFLD), have also been shown to induce inflammatory responses. Despite this knowledge, neither the role of ceramide and other and lipid intermediates in NAFLD nor their effect on *HAMP* transcription has been investigated. In the current study, we examined the regulation of *HAMP* expression by ceramide. For these studies, HepG2 human hepatoma cells were treated with two different cell-permeable ceramide analogs. They both significantly activated *HAMP* mRNA expression in a concentration-dependent manner. The effect of ceramide on *HAMP* expression was mediated at the transcriptional level because it was abolished with the transcription inhibitor, actinomycin D. Accordingly, ceramide significantly stimulated *HAMP* promoter activity, which occurred within the 0.6 kb *HAMP* promoter region proximal to the transcription start site. The transcription factors, STAT3, NF-κB and c-Jun/AP-1 play important roles in inflammation. Ceramide specifically induced the binding of STAT3, but not NF-κB or c-Jun/AP-1, to the *HAMP* promoter, as shown by chromatin immunoprecipitation assays. In fact, ceramide exerted a negative effect on c-Jun/AP-1 binding. Similarly, a chemical inhibitor of c-Jun N-terminal kinase (JNK) did not abolish the effect of ceramide on *HAMP* expression. Ceramide stimulated the phosphorylation of STAT3 on tyrosine 705 residue, NF-κB p65 subunit protein and JNK in HepG2 cells. These findings further confirm the specificity of ceramide-mediated STAT3 interaction with *HAMP*

promoter. To confirm the direct role of this interaction, we mutated the single STAT3 response element present within 0.6 kb *HAMP* promoter region. This deletion significantly abolished the activation of *HAMP* promoter by ceramide. Furthermore, siRNA-mediated silencing of STAT3 and the inhibition of JAK kinases with a specific chemical inhibitor significantly blunted the stimulatory effect of ceramide on *HAMP* mRNA expression. In conclusion, the studies in this chapter confirmed the direct and significant role of ceramide in the regulation of *HAMP* transcription through STAT3. These findings suggest that inflammatory signaling mediated by lipid intermediates in the liver may modulate iron metabolism and thereby disease severity in NAFLD patients.

2 INTRODUCTION

Non-alcoholic fatty liver disease (NAFLD) is the accumulation of fat in the liver of patients with no or little alcohol consumption (1). More than one third of the US adult population is estimated to have NAFLD and its prevalence is expanding to developing countries and to children (2). Benign fat accumulation in the liver (steatosis) can progress to nonalcoholic steatohepatitis (NASH) (3), characterized by inflammation (steatohepatitis) and fibrosis. Alternatively, patients can present with NASH without previous steatosis (4). If untreated, NASH can eventually lead to cirrhosis and hepatocellular carcinoma (5). The mechanisms of NAFLD/NASH progression are unclear. A role for secondary risk factors including iron (6, 7) and inflammation (8) has been proposed (*see Chapter I for detailed overview*).

NAFLD patients frequently display elevated levels of serum iron indices and hepatic iron content (9, 10). The deposition of iron in the liver correlates with disease severity and the development of fibrosis (11–13). The discovery of hepcidin has helped us to understand the connection between inflammation and iron homeostasis (14–17). Hepcidin, mainly synthesized in the hepatocytes of the liver, is both an acute phase protein and pivotal regulator of systemic iron homeostasis (14–17). As an acute phase protein, hepcidin responds to inflammation and its synthesis in the liver is

stimulated by inflammatory cytokines, such as IL-1 and IL-6. It has been shown that IL-6 induces hepcidin expression at the transcriptional level through the activation of JAK/STAT3 pathway (15, 16, 18). The binding of STAT3 to both human (*HAMP)* and mouse *(Hamp)* hepcidin gene promoters have been demonstrated in different experimental models (15, 16, 18).

Inflammation plays a major role in NAFLD pathogenesis. Several factors including increased gut permeability, adipose tissue derived cytokines and adipokines, Kupffer cell activation, and lipid accumulation have all been shown to induce inflammatory reactions in the livers of NAFLD patients (8, 19). In a study with overly obese patients undergoing bariatric surgery, a relationship between adipose tissue-derived-IL-6 and elevated hepcidin expression in the adipose tissue has been shown (20). However, elevated hepcidin expression could also be due to increase in the number of adipocytes in obese individuals compared to normal weight controls. Further studies investigating the direct effect of hepatic lipid accumulation and inflammation on hepcidin expression are therefore required. Although the *in vivo* relevance needs to be established, we have shown a direct effect of saturated fatty acids on hepcidin expression in human hepatoma cells (*see Chapter IV*). Namely, palmitic acid induced hepcidin expression at the post-transcriptional level through the activation of protein kinase C signaling and AU-rich element binding protein HuR (*see Chapter IV*).

Both inflammation and lipid accumulation are potent stimulators of ceramide synthesis in the liver through different well-defined pathways (i.e. de novo and sphingomyelinase pathways) (21, 22). Increased ceramide production and its association with hepatic fat content have been reported in obese and/or insulin resistant patients (23, 24). Similarly, animal studies with high fat diet feeding have also demonstrated an increase in hepatic ceramide content (25, 26). Despite all these observations, the involvement of ceramide in the pathogenesis of NAFLD has not been investigated. Nevertheless, weight loss studies have alluded to the importance of liver ceramide synthesis in NAFLD (27). Namely, the reversal of NASH pathogenesis correlated with weight loss-mediated decrease in pro-ceramide gene expression in the liver (27).

Although initially recognized only as a structural component of biomembranes, ceramide in recent years has gradually been appreciated as an important signaling molecule (28). Besides negatively modulating insulin signaling (29), ceramide also activates inflammatory signaling pathways. The tyrosine phosphorylation of the transcription factor, STAT3 and its DNA binding activity has been shown to be stimulated by ceramide in a JAK-dependent manner in cultured fibroblasts (30). Besides STAT3, ceramide has been reported to activate the transcription factor, NF-κB and its down-steam targets in HepG2 and other cells (31–33). The c-Jun N-terminal kinase (JNK) is also involved in inflammation. Deletion of JNK has been shown to reverse steatohepatitis in mice livers induced by methionine-choline deficient diets (34). JNK is activated by phosphorylation, which in turn phosphorylates c-Jun and transactivation of AP-1 enhancer-containing genes (35). Ceramide has been reported to stimulate JNK activation (36–38). Although ceramide has been shown to both modulate and be modulated by inflammation, the effect of these changes on hepatic *HAMP* expression is unknown. Understanding these mechanisms will further our knowledge of NAFLD/NASH pathogenesis. In this chapter we present studies, examining *HAMP* regulation by ceramide and the underlying mechanisms in human hepatoma cells.

3 RESULTS

3.1 Ceramide analogs-induced transcriptional regulation of *HAMP*

In order to study the role of ceramide in the regulation of human hepcidin gene, *HAMP* expression in human hepatoma cells, we treated HepG2 cells with synthetic cell-permeable ceramide analogs, C2 and C6 ceramide, which are extensively used for *in vitro* experiments (21, 37, 39). We chose 30 μM and 60 μM concentrations based on previous reports, which have shown that cells treated with these concentrations of ceramide analogs for 8 hours exhibit over 90 % cell viability (32, 40). Similar ceramide concentrations have been detected in the plasma of human NAFLD patients (41) and rats with acute lipid infusion (42). Control cells were treated with solvent (0.1 % DMSO). The effect of ceramide analogs on hepcidin expression was

determined by measuring the level of *HAMP* mRNA by qPCR, as described in the experimental procedures (*see Chapter II*). HepG2 cells treated with 30 μM or 60 μM of C2 ceramide displayed an 1.78 ± 0.35 and 3.43 ± 0.39-fold increase in *HAMP* expression, respectively, compared to control cells treated with solvent (**Figure 5.1A**). Compared to C2, similar concentrations of C6 ceramide analog induced a less potent but still significant elevation of *HAMP* mRNA expression (**Figure 5.1A**). We therefore employed C2 ceramide analog for further experiments.

Studies to this date have concentrated on transcriptional regulation of hepcidin gene expression (43–46). However, our recent studies also highlighted the importance of post-transcriptional mechanisms in the regulation of hepatic *HAMP* expression (see Chapter IV). We therefore determined whether the induction of *HAMP* expression by ceramide occurred at the transcriptional or post-transcriptional level. For these experiments, HepG2 cells were treated with ceramide or solvent in the presence of either actinomycin D (a transcription inhibitor) or DMSO control. DMSO by itself did not alter C2 ceramide-mediated induction of *HAMP* mRNA expression (**Figure 5.1B**). On the other hand. actinomycin D by itself significantly decreased the levels of *HAMP* mRNA in HepG2 cells (**Figure 5.1B**). Similarly, simultaneous treatment with actinomycin D and ceramide completely blocked ceramide-induced *HAMP* mRNA up-regulation (**Figure 5.1B and 5.1C**). To further confirm the role of transcriptional regulation, we performed luciferase reporter assays using a 0.6 kb region of *HAMP* promoter, which harbors binding sites for various transcription factors (46, 47) (**Figure 5.1D**). HepG2 cells were transfected with either empty pGL-3 basic vector or vector containing 0.6kb *HAMP* promoter (*HAMP* Prom-Luc). pRL-SV40 plasmid encoding renila luciferase was co-transfected as a reference for transfection efficiency, as described in experimental procedures (*see Chapter II*). Cells transfected with the vector harboring the *HAMP* promoter exhibited a significantly higher level of luciferase activity (**Figure 5.1D**). Ceramide treatment of HepG2 cells transfected with *HAMP* Prom-Luc, but not with empty vector, resulted in a significant increase of luciferase activity. In conjunction with actinomycin D experiments, our reporter assay studies with HepG2 cells indicated that ceramide

regulates *HAMP* expression at the transcriptional level and that this regulation is conveyed through *cis*-elements contained within the 0.6 kb *HAMP* promoter.

3.2 Physical interactions between transcription factors and *HAMP* promoter.

Various transcription factors such as STAT3, NF-κB and c-Jun/AP-1 are involved in the regulation of inflammatory processes (48–50). Recognition sequences for these transcription factors have been identified in the 0.6 kb promoter of *HAMP* (**Figure 5.2A**). In order to confirm the identity of transcription factors physically interacting with *HAMP* promoter in ceramide-treated HepG2 cells, chromatin immunoprecipitation (ChIP) assays were performed, as described in experimental procedures (**Figures 5.2B and 5.2C**). For these experiments, specific antibodies for transcription factors, STAT3, NF-κB and c-Jun/AP-1, which have been validated for ChIP experiments, were employed. Normal rabbit/mouse IgG was used as negative control. The primers used for ChIP analysis (**Chapter II Table 2.4**) amplified promoter sequences spanning consensus sites for respective transcription factors (STAT3: -135bp to -143bp, c-Jun/AP-1: -126bp to -134bp, NF-κB P65: -583bp to -592bp proximal to the start codon, ATG). Ceramide treatment significantly increased the binding of STAT3 to *HAMP* promoter (**Figure 5.2B**). HepG2 cells treated with the cytokine, IL-6 were employed as a positive control (16). The binding of STAT3 to *HAMP* promoter was also induced by IL-6 treatment, which validated our anti-STAT3 antibody and ChIP protocol (**Figure 5.2C**). Unlike STAT3, the binding of NF-κB p65 subunit to *HAMP* promoter was not activated by ceramide treatment (**Figure 5.2B**). On the other hand, the binding of c-Jun/AP-1 to *HAMP* promoter was weakened in ceramide-treated HepG2 cells compared solvent-treated cells (**Figure 5.2C**). The findings of our ChIP experiments were specific because no significant promoter enrichment was observed when similar chromatin preparations were incubated with the control IgG (representative images are shown in **Figures 5.2B and 5.2C**). Furthermore, the total amount of chromatin input was equal across all samples in our ChIP assays (**Figure 5.2B and 5.2C**).

3.3 Phosphorylation and activation of STAT3 and NF-κB in ceramide-treated cells

Western blots were performed with specific phospho-antibodies, which recognize the phosphorylated (i.e. activated) forms of STAT3 and NF-κB proteins to determine the effect of ceramide on their activation status (**Figure 5.3A and 5.3B**). STAT3 is regulated by phosphorylation both on serine (Ser 727) and tyrosine (Tyr 705) residues (51). Following ceramide treatment, HepG2 cells displayed a significant increase in tyrosine (Tyr 705), but not serine (Ser 727), phosphorylation of STAT3 (**Figure 5.3A**). As a positive control, HepG2 cells were also treated with recombinant IL-6. Unlike ceramide, IL-6 treatment stimulated phosphorylation of STAT3 both at Tyr 705 and Ser 727 compared to that in PBS-treated control cells (**Figure 5.3A**). Neither ceramide nor recombinant IL-6 altered the expression level of total STAT3 protein in HepG2 cells (**Figure 5.3A**). Similar to STAT3, ceramide also stimulated the phosphorylation of NF-κB subunit, p65 (**Figure 5.3B**). Our findings collectively suggested, that despite ceramide inducing the phosphorylation of both transcription factors, only STAT3 (and not NF-KB) is capable of binding to and stimulating *HAMP* promoter activity.

3.4 The relationship between ceramide-induced JNK phosphorylation and *HAMP* up-regulation.

MAP kinases such as c-Jun N-terminal kinase (JNK) and extracellular signal-regulated protein kinases 1 and 2 (ERK1/2) have been suggested to target serine 727 of STAT3 for phosphorylation (51). We therefore examined the phosphorylation of JNK and ERK1/2 by western blotting. Ceramide suppresses extracellular signal-regulated protein kinases 1 and 2 (ERK1/2) in some (52, 53) but not all (32) experimental systems. Under our experimental conditions, C2 ceramide significantly suppressed the phosphorylation of ERK1/2. IL-6 treatment exerted only a minor effect (**Figure 5.3A**). In contrast, C2 ceramide significantly induced the phosphorylation of JNK compared to DMSO (control) (**Figure 5.3B**).

To further study the effect of ceramide and JNK on *HAMP* expression, we employed the chemical inhibitor, SP600125, which has been documented to specifically inhibit JNK activation (54).

HepG2 cells were treated in the presence of both ceramide and SP600125. In parallel, co-incubation with DMSO was also performed, as control. Western blotting was performed to examine the effect of SP600125 on ceramide-induced JNK phosphorylation (**Figure 5.4A**). DMSO did not have any specific effect on ceramide-induced JNK activation (**Figure 5.4A**). In contrast, SP600125 co-incubation significantly blocked ceramide-induced activation of JNK (**Figure 5.4A**). We then examined the effect of SP600125 co-incubation on ceramide-induced *HAMP* expression by qPCR. The inhibitor by itself did not exert any significant effect on basal *HAMP* mRNA expression (**Figure 5.4B**). Similarly, SP600125 was not capable of blocking the positive effect of ceramide on *HAMP* mRNA expression (**Figure 5.4B**). These results indicated that although activated by ceramide, JNK is not directly involved in transcriptional regulation of *HAMP* by ceramide in hepatoma cells.

3.5 The role of STAT3 activation in ceramide-induced *HAMP* transcriptional regulation.

To validate the specific role of STAT3 in ceramide-mediated transcriptional regulation of *HAMP*, the STAT3 response element in the 0.6kbp *HAMP* promoter was mutated, as described in the experimental procedures (*see Chapter II*). Luciferase reporter assays were then performed with pGL-3 basic vectors harboring the wild-type or mutated *HAMP* promoter (**Figure 5.5A**). Mutation of the STAT3 response element (ΔSTAT3) significantly diminished the stimulatory effect of ceramide on *HAMP* promoter, confirming the direct involvement of the STAT3 binding site (**Figure 5.5A**). We validated the mutated promoter construct by IL-6 treatment based on the rationale that this STAT3 response element is essential for IL-6-responsiveness of *HAMP* promoter (16, 45). Accordingly, the mutation of STAT3 response element (ΔSTAT3) abolished IL-6-induced *HAMP* promoter activation (**Figure 5.5B**).

In order to study the involvement of JAK/STAT3 signaling pathway in ceramide-mediated transcriptional regulation of *HAMP* expression, we employed STAT3 siRNA and a chemical pan-JAK kinase inhibitor, JAK inhibitor I (55) (**Figure 5.6A and 5.6B**). The efficacy of STAT3 siRNA was confirmed by qPCR and western blotting experiments. The level of STAT3 mRNA

(**Figure 5.6A**) and protein (**Figure 5.6A inset**) expression were significantly inhibited by STAT3 siRNA, but not control siRNA, in HepG2 cells. The potency of JAK inhibitor I was also validated by western blotting. Namely, JAK inhibitor I significantly blocked the ceramide-induced phosphorylation of STAT3 at residue Tyr 705 (**Figure 5.6B**). The effect of JAK inhibitor I on the regulation of *HAMP* mRNA expression by ceramide was determined by qPCR (**Figure 5.7A**). The addition of DMSO, which is the vehicle for JAK inhibitor I, did not affect ceramide-induced *HAMP* up-regulation (3.44 ± 0.41 fold). In comparison, ceramide-mediated induction of *HAMP* expression was significantly attenuated by JAK inhibitor I (2.28 ± 0.23 fold) (**Figure 5.7A**). The inhibition was however incomplete. HepG2 cells were therefore pre-treated with both STAT3 siRNA and JAK inhibitor I. In parallel, control cells were administered control siRNA and DMSO. Both groups of pre-treated cells were then subjected to either ceramide or DMSO (control) treatment, and *HAMP* mRNA expression was determined **(Figure 5.7B)**. Control siRNA and DMSO pre-treatment did not alter the effect of ceramide on *HAMP* mRNA expression levels (3.15 ± 0.05 fold increase) (**Figure 5.7B**). By contrast, the combined pre-treatment with STAT3 siRNA and JAK inhibitor I decreased the induction of *HAMP* mRNA expression by ceramide (1.57 ± 0.09 fold increase) (**Figure 5.7B**). The effect of JAK inhibitor I and STAT3 siRNA on ceramide-induced *HAMP* promoter activation was further examined with luciferase reporter assays (**Figure 5.7C and 5.7D**). HepG2 cells, transfected with pGL-3 basic vector harboring 0.6 kbp *HAMP* promoter, were treated with ceramide or solvent in the presence of either JAK inhibitor I or DMSO as control. Ceramide treatment induced a 2.16 ± 0.32 fold increase in *HAMP* promoter activity, as compared to control cells treated with solvent in the presence of DMSO. In contrast to DMSO, the addition of JAK inhibitor I significantly diminished ceramide-induced *HAMP* promoter activation (1.69 ± 0.21 fold) (**Figure 5.7C**). The level of inhibition was stronger with the combined pre-treatment of STAT3 siRNA and JAK inhibitor I (1.39 ± 0.10 fold) (**Figure 5.7D**). HepG2 cells pre-treated with control siRNA and DMSO displayed 2.22 ± 0.36 fold increase in *HAMP* promoter activity following ceramide treatment (**Figure 5.7D**).

3.6 The involvement of ER stress in ceramide-induced signaling and *HAMP* up-regulation.

ER stress has also been reported to induce *HAMP* transcription (56) and ceramide is a known inducer of ER stress (57–59). We therefore determined the presence of ER stress in ceramide-treated HepG2 cells by XBP1 assays, as described in the experimental procedures (*see Chapter II*). Briefly, ER stress activates the inositol-requiring enzyme 1 (IRE1) which splices X-box binding protein 1 (XBP1) mRNA (60). Spliced form of XBP1, which was detected, as described in the experimental procedures, has been employed as ER stress marker. Besides ceramide, cells were treated with tunicamycin, a well-known experimental ER stress inducer (61), as a positive control. HepG2 cells treated with ceramide did not exhibit any significant changes in the spliced and unspliced forms of XBP1, as compared to the solvent-treated control cells (**Figure 5.8A**). In contrast, cells treated with tunicamycin exhibited a significant increase in the spliced form, and a decrease in the unspliced form, of XBP1, which confirmed the validity of our assay (**Figure 5.8A**). These findings clearly demonstrated that, unlike tunicamycin, ceramide is not capable of inducing ER stress in HepG2 cells. Accordingly, the treatment of HepG2 cells with a chemical inhibitor of ER stress, salubrinal (57), did not abolish ceramide-mediated up-regulation of *HAMP* expression (**Figure 5.8B**).

4 DISCUSSION

Iron accumulation accompanies NAFLD pathology and contributes to disease severity (6, 7). Since hepcidin is the key iron regulatory hormone, a clear understanding of the mechanisms which regulate its expression in NAFLD is important. This may enable the development of novel treatment strategies to prevent the harmful effects of iron in NAFLD/NASH progression. Although we have identified novel molecular mechanisms by which lipids regulate hepcidin expression at the post-transcriptional level, the role of lipid-mediated inflammatory processes is still unclear. Of note, hepcidin as an acute phase protein is strongly regulated by inflammation. Furthermore, excess lipid accumulation in the livers of NAFLD patients elevate the production of

lipid metabolites, such as ceramide, which take part in inflammatory and insulin signaling cascades (21, 62, 63). However, the role of these biologically active lipid intermediates either in NAFLD pathology or in the hepcidin regulation have so far not been addressed.

The studies presented in this chapter have collectively shown that the transcription of human hepcidin gene, *HAMP* is significantly activated by ceramide in hepatoma cells. Furthermore, our findings clearly confirmed the role of ceramide-activated JAK/STAT3 signaling in this process. Interestingly, we have also established a new and unique function for ceramide (i.e. sphingolipids), namely the regulation of iron metabolism. This novel role of ceramide was mediated through a specific region in *HAMP* promoter, which was 0.6kb proximal to transcription start site, as confirmed by our reporter assays and mutagenesis studies.

We have further dissected the mechanisms involved in ceramide-mediated activation of STAT3. Ceramide has previously been shown to activate the tyrosine-phosphorylation of STAT3 in cultured fibroblast cells (30). However, its effect on JAK/STAT3 signaling in hepatoma cells is unknown. Under our experimental conditions, ceramide exerted differential effects on STAT3 phosphorylation. Namely, it stimulated the phosphorylation at tyrosine 705, but not serine 727, residue of STAT3. In contrast, IL-6, a classical activator of JAK/STAT3 pathway (and hepcidin transcription) (16) induced both serine and tyrosine phosphorylation of STAT3. The published studies up-to-now have established a prominent role for tyrosine, but not serine, phosphorylation as the key requirement for activation of STAT3 as a transcription factor (51). We therefore believe that the induction of tyrosine 705 phosphorylation should be sufficient for STAT3 activation in ceramide-treated hepatoma cells. The precise role of serine 727 phosphorylation is still unclear (64, 65). It has been predicted to support the trans-activation capability of STAT3, as a DNA-binding protein (66, 67). Other studies have suggested a role for serine phosphorylation to limit the duration of tyrosine phosphorylation by recruiting a phosphatase (65). Although we did not observe strong inhibition of serine 727 phosphorylation, a prominent inhibition of ERK phosphorylation was detected by ceramide. ERK has been shown to phosphorylate STAT3 on

serine 727 (51, 67). However, whether ERK inhibition and STAT3 stimulation by ceramide are connected (and the consequences for *HAMP* transcription) remains to be investigated in future studies. The findings of our ChIP assays, which validated ceramide-mediated physical interaction between STAT3 and the corresponding cis-element in *HAMP* promoter, are also in agreement with the tyrosine-phosphorylation status of STAT3. Collectively, our data strongly suggest that ceramide-mediated binding of STAT3 to *HAMP* promoter is facilitated by the activation of STAT3 via tyrosine phosphorylation.

The conclusive evidence for the direct involvement of STAT3 in ceramide-induced *HAMP* transcription was provided by the following findings: 1- Mutation of the STAT3 response element in *HAMP* promoter significantly blunted ceramide-induced promoter activation. 2- Experiments using a commercial siRNA pool for STAT3 and a pan-JAK inhibitor have demonstrated successful inhibition of STAT3 activation in conjunction with the abrogation of ceramide-induced *HAMP* mRNA induction and promoter activation. Taken together, these results confirmed the dependence of ceramide-induced *HAMP* transcription on JAK/STAT3 signaling pathway. The reasons, as to why we could not completely block the effect of ceramide on *HAMP* mRNA up-regulation and promoter activation following either siRNA silencing of STAT3 in combination with JAK inhibition or mutation of STAT3 response element in *HAMP* promoter, is unclear. It is however feasible that additional signaling pathways may be involved.

The specificity of JAK/STAT3 signaling was also confirmed by our results with NF-κB and JNK activation, which are known to be involved in inflammation. Namely, we confirmed the activation (i.e. phosphorylation) of NF-κB and JNK in ceramide treated HepG2 cells, as has been previously reported in other cell types (31, 32, 36–38). Despite the activation, NF-κB failed to physically interact with the putative response element in the *HAMP* promoter as shown by our ChIP assays. JNK is involved in activation of c-Jun/AP-1 but ceramide decreased the binding of c-Jun/AP-1 to *HAMP* promoter. This might be due to a competition by STAT3 because their DNA-binding sites are in close proximity on *HAMP* promoter (*see Results section above*).

Furthermore, JNK inhibitor studies also confirmed that JNK activation is not required for *HAMP* regulation by ceramide.

Experimental ER stress models indicated a role for it in the activation of hepcidin gene transcription (56). A direct link between dysregulated lipid metabolism in the liver and ER stress has been demonstrated in mouse models of obesity (68). Moreover, as shown by *in vitro* studies using various cell lines, a role for ceramide in lipid-mediated ER stress has also been suggested (57, 69, 70). We therefore examined whether ceramide-induced *HAMP* transcription involved ER stress. Ceramide did not trigger ER stress in HepG2 cells under experimental conditions. Furthermore, ER stress inhibition by salubrinal (57, 58) did not abolish the stimulatory effect of ceramide on hepcidin mRNA expression. Taken together, these results excluded the contribution of ER stress to the activation of *HAMP* transcription by ceramide.

In summary, we have demonstrated a novel role for the lipid intermediate, ceramide in the regulation of *HAMP* expression. Similarly, our findings also demonstrate a unique regulatory mechanism for *HAMP* transcription in liver cells mediated by ceramide. The fact, that ceramide could directly achieve this through the activation of JAK/STAT3 signaling in hepatoma cells, has clinical implications. Namely, it suggests that the involvement of other inflammatory cells, such as Kupffer cells, is not required for this regulation. These findings will therefore help us to understand the connection between lipid intermediates and inflammatory processes in the regulation of iron metabolism including its relevance to NAFLD/NASH disease progression.

5 REFERENCES

1. Dowman, J. K., Tomlinson, J. W., and Newsome, P. N. (2010) Pathogenesis of non-alcoholic fatty liver disease. *QJM*. **103**, 71–83
2. Loomba, R., and Sanyal, A. J. (2013) The global NAFLD epidemic. *Nat. Rev. Gastroenterol. Hepatol.* 10.1038/nrgastro.2013.171
3. Singh, S., Allen, A. M., Wang, Z., Prokop, L. J., Murad, M. H., and Loomba, R. (2015) Fibrosis Progression in Nonalcoholic Fatty Liver vs Nonalcoholic Steatohepatitis: A Systematic Review and Meta-analysis of Paired-Biopsy Studies. *Clin. Gastroenterol. Hepatol.* **13**, 643–654.e9
4. McPherson, S., Hardy, T., Henderson, E., Burt, A. D., Day, C. P., and Anstee, Q. M. (2015) Evidence of NAFLD progression from steatosis to fibrosing-steatohepatitis using paired biopsies: Implications for prognosis and clinical management. *J. Hepatol.* **62**, 1148–1155
5. Marchesini, G., Bugianesi, E., Forlani, G., Cerrelli, F., Lenzi, M., Manini, R., Natale, S., Vanni, E., Villanova, N., Melchionda, N., and Rizzetto, M. (2003) Nonalcoholic fatty liver, steatohepatitis, and the metabolic syndrome. *Hepatology*. **37**, 917–923
6. Nelson, J. E., Klintworth, H., and Kowdley, K. V. (2012) Iron Metabolism in Nonalcoholic Fatty Liver Disease. *Curr. Gastroenterol. Rep.* **14**, 8–16
7. Aigner, E. (2014) Dysregulation of iron and copper homeostasis in nonalcoholic fatty liver. *World J. Hepatol.* **7**, 177
8. Tilg, H., and Moschen, A. R. (2010) Evolution of inflammation in nonalcoholic fatty liver disease: The multiple parallel hits hypothesis. *Hepatology*. **52**, 1836–1846
9. Mendler, M.-H., Turlin, B., Moirand, R., Jouanolle, A.-M., Sapey, T., Guyader, D., le Gall, J.-Y., Brissot, P., David, V., and Deugnier, Y. (1999) Insulin resistance–associated hepatic iron overload. *Gastroenterology*. **117**, 1155–1163
10. Martinelli, N., Traglia, M., Campostrini, N., Biino, G., Corbella, M., Sala, C., Busti, F., Masciullo, C., Manna, D., Previtali, S., Castagna, A., Pistis, G., Olivieri, O., Toniolo, D., Camaschella, C., and Girelli, D. (2012) Increased Serum Hepcidin Levels in Subjects with the Metabolic Syndrome: A Population Study. *PLoS ONE*. **7**, e48250
11. Valenti, L., Fracanzani, A. L., Bugianesi, E., Dongiovanni, P., Galmozzi, E., Vanni, E., Canavesi, E., Lattuada, E., Roviaro, G., Marchesini, G., and Fargion, S. (2010) HFE Genotype, Parenchymal Iron Accumulation, and Liver Fibrosis in Patients With Nonalcoholic Fatty Liver Disease. *Gastroenterology*. **138**, 905–912
12. Nelson, J. E., Wilson, L., Brunt, E. M., Yeh, M. M., Kleiner, D. E., Unalp-Arida, A., and Kowdley, K. V. (2010) Relationship between the pattern of hepatic iron deposition and histological severity in nonalcoholic fatty liver disease. *Hepatology*. **53**, 448–457
13. Nelson, J. E., Brunt, E. M., Kowdley, K. V., and for the Nonalcoholic Steatohepatitis Clinical Research Network (2012) Lower serum hepcidin and greater parenchymal iron in nonalcoholic fatty liver disease patients with C282Y HFE mutations. *Hepatology*. **56**, 1730–1740
14. Pigeon, C., Ilyin, G., Courselaud, B., Leroyer, P., Turlin, B., Brissot, P., and Loréal, O. (2001) A New Mouse Liver-specific Gene, Encoding a Protein Homologous to Human Antimicrobial Peptide Hepcidin, Is Overexpressed during Iron Overload. *J. Biol. Chem.* **276**, 7811–7819
15. Nemeth, E., Rivera, S., Gabayan, V., Keller, C., Taudorf, S., Pedersen, B. K., and Ganz, T. (2004) IL-6 mediates hypoferremia of inflammation by inducing the synthesis of the iron regulatory hormone hepcidin. *J. Clin. Invest.* **113**, 1271–1276
16. Wrighting, D. M., and Andrews, N. C. (2006) Interleukin-6 induces hepcidin expression through STAT3. *Blood*. **108**, 3204–3209

17. Hunter, H. N., Fulton, D. B., Ganz, T., and Vogel, H. J. (2002) The Solution Structure of Human Hepcidin, a Peptide Hormone with Antimicrobial Activity That Is Involved in Iron Uptake and Hereditary Hemochromatosis ,. *J. Biol. Chem.* **277**, 37597–37603
18. Lee, P., Peng, H., Gelbart, T., Wang, L., and Beutler, E. (2005) Regulation of hepcidin transcription by interleukin-1 and interleukin-6. *Proc. Natl. Acad. Sci. U. S. A.* **102**, 1906–1910
19. György, B. (2009) Kupffer cells in non-alcoholic fatty liver disease: The emerging view. *J. Hepatol.* **51**, 212–223
20. Bekri, S., Gual, P., Anty, R., Luciani, N., Dahman, M., Ramesh, B., Iannelli, A., Staccini–Myx, A., Casanova, D., Ben Amor, I., Saint–Paul, M., Huet, P., Sadoul, J., Gugenheim, J., Srai, S. K. S., Tran, A., and Le Marchand–Brustel, Y. (2006) Increased Adipose Tissue Expression of Hepcidin in Severe Obesity Is Independent From Diabetes and NASH. *Gastroenterology*. **131**, 788–796
21. Pagadala, M., Kasumov, T., McCullough, A. J., Zein, N. N., and Kirwan, J. P. (2012) Role of ceramides in nonalcoholic fatty liver disease. *Trends Endocrinol. Metab.* **23**, 365–371
22. Donnelly, K. L., Smith, C. I., Schwarzenberg, S. J., Jessurun, J., Boldt, M. D., and Parks, E. J. (2005) Sources of fatty acids stored in liver and secreted via lipoproteins in patients with nonalcoholic fatty liver disease. *J. Clin. Invest.* **115**, 1343–1351
23. Adams, J. M., Pratipanawatr, T., Berria, R., Wang, E., DeFronzo, R. A., Sullards, M. C., and Mandarino, L. J. (2004) Ceramide Content Is Increased in Skeletal Muscle From Obese Insulin-Resistant Humans. *Diabetes*. **53**, 25–31
24. Kolak, M., Westerbacka, J., Velagapudi, V. R., Wågsäter, D., Yetukuri, L., Makkonen, J., Rissanen, A., Häkkinen, A.-M., Lindell, M., Bergholm, R., Hamsten, A., Eriksson, P., Fisher, R. M., Orešič, M., and Yki-Järvinen, H. (2007) Adipose Tissue Inflammation and Increased Ceramide Content Characterize Subjects With High Liver Fat Content Independent of Obesity. *Diabetes*. **56**, 1960–1968
25. Holland, W. L., Brozinick, J. T., Wang, L.-P., Hawkins, E. D., Sargent, K. M., Liu, Y., Narra, K., Hoehn, K. L., Knotts, T. A., Siesky, A., Nelson, D. H., Karathanasis, S. K., Fontenot, G. K., Birnbaum, M. J., and Summers, S. A. (2007) Inhibition of Ceramide Synthesis Ameliorates Glucocorticoid-, Saturated-Fat-, and Obesity-Induced Insulin Resistance. *Cell Metab.* **5**, 167–179
26. Kurek, K., Piotrowska, D. M., Wiesiołek-Kurek, P., Łukaszuk, B., Chabowski, A., Górski, J., and Żendzian-Piotrowska, M. (2014) Inhibition of ceramide de novo synthesis reduces liver lipid accumulation in rats with nonalcoholic fatty liver disease. *Liver Int.* **34**, 1074–1083
27. Promrat, K., Longato, L., Wands, J. R., and la Monte, S. M. de (2011) Weight loss amelioration of non-alcoholic steatohepatitis linked to shifts in hepatic ceramide expression and serum ceramide levels. *Hepatol. Res.* **41**, 754–762
28. Bikman, B. T., and Summers, S. A. (2011) Ceramides as modulators of cellular and whole-body metabolism. *J. Clin. Invest.* **121**, 4222–4230
29. Gill, J. M. R., and Sattar, N. (2009) Ceramides: A new player in the inflammation–insulin resistance paradigm? *Diabetologia*. **52**, 2475–2477
30. Mazière, C., Conte, M.-A., and Mazière, J.-C. (2001) Activation of the JAK/STAT pathway by ceramide in cultured human fibroblasts. *FEBS Lett.* **507**, 163–168
31. Fillet, M., Bentires-Alj, M., Deregowski, V., Greimers, R., Gielen, J., Piette, J., Bours, V., and Merville, M.-P. (2003) Mechanisms involved in exogenous C2- and C6-ceramide-induced cancer cell toxicity. *Biochem. Pharmacol.* **65**, 1633–1642
32. Demarchi, F., Bertoli, C., Greer, P. A., and Schneider, C. (2005) Ceramide triggers an NF-κB-dependent survival pathway through calpain. *Cell Death Differ.* **12**, 512–522

33. Kreydiyyeh, S. I., and Dakroub, Z. (2014) Ceramide and its metabolites modulate time-dependently the activity of the Na+/K+ ATPase in HepG2 cells. *Int. J. Biochem. Cell Biol.* **53**, 102–107
34. Schattenberg, J. M., Singh, R., Wang, Y., Lefkowitch, J. H., Rigoli, R. M., Scherer, P. E., and Czaja, M. J. (2006) Jnk1 but not jnk2 promotes the development of steatohepatitis in mice. *Hepatology*. **43**, 163–172
35. Davis, R. J. (2000) Signal Transduction by the JNK Group of MAP Kinases. *Cell*. **103**, 239–252
36. Kurinna, S. M., Tsao, C. C., Nica, A. F., Jiffar, T., and Ruvolo, P. P. (2004) Ceramide Promotes Apoptosis in Lung Cancer-Derived A549 Cells by a Mechanism Involving c-Jun NH2-Terminal Kinase. *Cancer Res.* **64**, 7852–7856
37. Chen, C.-L., Lin, C.-F., Chang, W.-T., Huang, W.-C., Teng, C.-F., and Lin, Y.-S. (2008) Ceramide induces p38 MAPK and JNK activation through a mechanism involving a thioredoxin-interacting protein-mediated pathway. *Blood*. **111**, 4365–4374
38. Saslowsky, D. E., Tanaka, N., Reddy, K. P., and Lencer, W. I. (2009) Ceramide activates JNK to inhibit a cAMP-gated K+ conductance and Cl– secretion in intestinal epithelia. *FASEB J.* **23**, 259–270
39. Gentil, B., Grimot, F., and Riva, C. (2003) Commitment to apoptosis by ceramides depends on mitochondrial respiratory function, cytochrome C release and caspase-3 activation in HEP-G2 cells. *Mol. Cell. Biochem.* **254**, 203–210
40. Adiseshaiah, P. P., Clogston, J. D., McLeland, C. B., Rodriguez, J., Potter, T. M., Neun, B. W., Skoczen, S. L., Shanmugavelandy, S. S., Kester, M., Stern, S. T., and McNeil, S. E. (2013) Synergistic Combination Therapy with Nanoliposomal C6-Ceramide and Vinblastine is Associated with Autophagy Dysfunction in Hepatocarcinoma and Colorectal Cancer Models. *Cancer Lett.* **337**, 254–265
41. Kasumov, T., Li, L., Li, M., Gulshan, K., Kirwan, J. P., Liu, X., Previs, S., Willard, B., Smith, J. D., and McCullough, A. (2015) Ceramide as a Mediator of Non-Alcoholic Fatty Liver Disease and Associated Atherosclerosis. *PLoS ONE*. **10**, e0126910
42. Watt, M. J., Barnett, A. C., Bruce, C. R., Schenk, S., Horowitz, J. F., and Hoy, A. J. (2012) Regulation of plasma ceramide levels with fatty acid oversupply: evidence that the liver detects and secretes de novo synthesised ceramide. *Diabetologia*. **55**, 2741–2746
43. Ganz, T. (2013) Systemic Iron Homeostasis. *Physiol. Rev.* **93**, 1721–1741
44. Wang, R.-H., Li, C., Xu, X., Zheng, Y., Xiao, C., Zerfas, P., Cooperman, S., Eckhaus, M., Rouault, T., Mishra, L., and Deng, C.-X. (2005) A role of SMAD4 in iron metabolism through the positive regulation of hepcidin expression. *Cell Metab.* **2**, 399–409
45. Falzacappa, V., Vittoria, M., Vujic Spasic, M., Kessler, R., Stolte, J., Hentze, M. W., and Muckenthaler, M. U. (2007) STAT3 Mediates Hepatic Hepcidin Expression and Its Inflammatory Stimulation. *Blood*. **109**, 353–358
46. Courselaud, B., Pigeon, C., Inoue, Y., Inoue, J., Gonzalez, F. J., Leroyer, P., Gilot, D., Boudjema, K., Guguen-Guillouzo, C., Brissot, P., Loréal, O., and Ilyin, G. (2002) C/EBPα Regulates Hepatic Transcription of Hepcidin, an Antimicrobial Peptide and Regulator of Iron Metabolism CROSS-TALK BETWEEN C/EBP PATHWAY AND IRON METABOLISM. *J. Biol. Chem.* **277**, 41163–41170
47. Truksa, J., Lee, P., and Beutler, E. (2007) The role of STAT, AP-1, E-box and TIEG motifs in the regulation of hepcidin by IL-6 and BMP-9: lessons from human HAMP and murine Hamp1 and Hamp2 gene promoters. *Blood Cells. Mol. Dis.* **39**, 255–262
48. Stark, G. R., and Darnell Jr., J. E. (2012) The JAK-STAT Pathway at Twenty. *Immunity*. **36**, 503–514
49. Ip, Y. T., and Davis, R. J. (1998) Signal transduction by the c-Jun N-terminal kinase (JNK) — from inflammation to development. *Curr. Opin. Cell Biol.* **10**, 205–219

50. Hoesel, B., and Schmid, J. A. (2013) The complexity of NF-κB signaling in inflammation and cancer. *Mol. Cancer*. **12**, 86
51. Schindler, C., Levy, D. E., and Decker, T. (2007) JAK-STAT Signaling: From Interferons to Cytokines. *J. Biol. Chem.* **282**, 20059–20063
52. Bourbon, N. A., Yun, J., Berkey, D., Wang, Y., and Kester, M. (2001) Inhibitory actions of ceramide upon PKC-ε/ERK interactions. *Am. J. Physiol. - Cell Physiol.* **280**, C1403–C1411
53. Kitatani, K., Akiba, S., Hayama, M., and Sato, T. (2001) Ceramide Accelerates Dephosphorylation of Extracellular Signal-Regulated Kinase 1/2 to Decrease Prostaglandin D2 Production in RBL-2H3 Cells. *Arch. Biochem. Biophys.* **395**, 208–214
54. Bennett, B. L., Sasaki, D. T., Murray, B. W., O'Leary, E. C., Sakata, S. T., Xu, W., Leisten, J. C., Motiwala, A., Pierce, S., Satoh, Y., Bhagwat, S. S., Manning, A. M., and Anderson, D. W. (2001) SP600125, an anthrapyrazolone inhibitor of Jun N-terminal kinase. *Proc. Natl. Acad. Sci.* **98**, 13681–13686
55. Lepiller, Q., Abbas, W., Kumar, A., Tripathy, M. K., and Herbein, G. (2013) HCMV Activates the IL-6-JAK-STAT3 Axis in HepG2 Cells and Primary Human Hepatocytes. *PLoS ONE*. **8**, e59591
56. Vecchi, C., Montosi, G., Zhang, K., Lamberti, I., Duncan, S. A., Kaufman, R. J., and Pietrangelo, A. (2009) ER Stress Controls Iron Metabolism Through Induction of Hepcidin. *Science*. **325**, 877–880
57. Gong, T., Wang, Q., Lin, Z., Chen, M., and Sun, G. (2012) Endoplasmic reticulum (ER) stress inhibitor salubrinal protects against ceramide-induced SH-SY5Y cell death. *Biochem. Biophys. Res. Commun.* **427**, 461–465
58. Contreras, C., González-García, I., Martínez-Sánchez, N., Seoane-Collazo, P., Jacas, J., Morgan, D. A., Serra, D., Gallego, R., Gonzalez, F., Casals, N., Nogueiras, R., Rahmouni, K., Diéguez, C., and López, M. (2014) Central Ceramide-Induced Hypothalamic Lipotoxicity and ER Stress Regulate Energy Balance. *Cell Rep.* **9**, 366–377
59. Pehar, M., Jonas, M. C., Hare, T. M., and Puglielli, L. (2012) SLC33A1/AT-1 Protein Regulates the Induction of Autophagy Downstream of IRE1/XBP1 Pathway. *J. Biol. Chem.* **287**, 29921–29930
60. Yoshida, H., Matsui, T., Yamamoto, A., Okada, T., and Mori, K. (2001) XBP1 mRNA Is Induced by ATF6 and Spliced by IRE1 in Response to ER Stress to Produce a Highly Active Transcription Factor. *Cell*. **107**, 881–891
61. Kaufman, R. J. (1999) Stress signaling from the lumen of the endoplasmic reticulum: coordination of gene transcriptional and translational controls. *Genes Dev.* **13**, 1211–1233
62. Nagle, C. A., Klett, E. L., and Coleman, R. A. (2008) Hepatic triacylglycerol accumulation and insulin resistance. *J. Lipid Res.* **50**, S74–S79
63. Chavez, J. A., and Summers, S. A. (2012) A Ceramide-Centric View of Insulin Resistance. *Cell Metab.* **15**, 585–594
64. Serine phosphorylation of STATs (2000) *Publ. Online 22 May 2000 Doi101038sjonc1203481*. 10.1038/sj.onc.1203481
65. Wakahara, R., Kunimoto, H., Tanino, K., Kojima, H., Inoue, A., Shintaku, H., and Nakajima, K. (2012) Phospho-Ser727 of STAT3 regulates STAT3 activity by enhancing dephosphorylation of phospho-Tyr705 largely through TC45. *Genes Cells.* **17**, 132–145
66. Shen, Y., Schlessinger, K., Zhu, X., Meffre, E., Quimby, F., Levy, D. E., and Darnell, J. E. (2004) Essential Role of STAT3 in Postnatal Survival and Growth Revealed by Mice Lacking STAT3 Serine 727 Phosphorylation. *Mol. Cell. Biol.* **24**, 407–419
67. Lee, H., Herrmann, A., Deng, J., Kujawski, M., Niu, G., Li, Z., Forman, S., Jove, R., Pardoll, D., and Yu, H. (2009) Persistently-activated Stat3 maintains constitutive NF-κB activity in tumors. *Cancer Cell*. **15**, 283–293

68. Fu, S., Yang, L., Li, P., Hofmann, O., Dicker, L., Hide, W., Lin, X., Watkins, S. M., Ivanov, A. R., and Hotamisligil, G. S. (2011) Aberrant lipid metabolism disrupts calcium homeostasis causing liver endoplasmic reticulum stress in obesity. *Nature*. **473**, 528–531
69. Boslem, E., MacIntosh, G., Preston, A. M., Bartley, C., Busch, A. K., Fuller, M., Laybutt, D. R., Meikle, P. J., and Biden, T. J. (2011) A lipidomic screen of palmitate-treated MIN6 β-cells links sphingolipid metabolites with endoplasmic reticulum (ER) stress and impaired protein trafficking. *Biochem. J.* **435**, 267–276
70. Senkal, C. E., Ponnusamy, S., Manevich, Y., Meyers-Needham, M., Saddoughi, S. A., Mukhopadyay, A., Dent, P., Bielawski, J., and Ogretmen, B. (2011) Alteration of Ceramide Synthase 6/C16-Ceramide Induces Activating Transcription Factor 6-mediated Endoplasmic Reticulum (ER) Stress and Apoptosis via Perturbation of Cellular Ca2+ and ER/Golgi Membrane Network. *J. Biol. Chem.* **286**, 42446–42458

Figure 5.1. Ceramide analogs induce *HAMP* expression at the transcriptional level. (**A**) HepG2 cells were treated with 30 μM or 60 μM of C2 or C6 ceramide for 8 hours. cDNA, synthesized from RNA isolated from these cells, were employed as templates in Taqman qPCR to determine *HAMP* mRNA expression, as described in experimental procedures (*see Chapter II*). *HAMP* mRNA expression in ceramide-treated cells was calculated as fold change of that in solvent (solv.)-treated control cells. (**B**) HepG2 cells were treated with 60 μM C2 ceramide or solvent (solv.) in the presence of 1μg/ mL actinomycin D (ACTD) or DMSO, as control. *HAMP* mRNA expression, determined by qPCR, in ceramide and/or ACTD-treated cells was calculated as fold change of that in cells treated with solvent and DMSO. (**C**) *HAMP* expression in cells treated with ACTD and ceramide was expressed as fold change of that in cells treated with ACTD and solvent. (**D**) HepG2 cells were transfected with pGL-3 basic vector harboring 0.6kbp *HAMP* promoter (*HAMP*-Prom-Luc) or empty pGL-3 basic vector (vector), as described in the experimental procedures. pRL-SV40 plasmid was co-transfected as reference for transfection efficiency. The transfected cells were treated with solvent (solv.) or 60 μM C2 ceramide for 8 hours. The cells were lysed and dual luciferase report assays were performed, as described. Relative luciferase unit was expressed as fold change of that in the empty vector-transfected and solvent-treated cells.

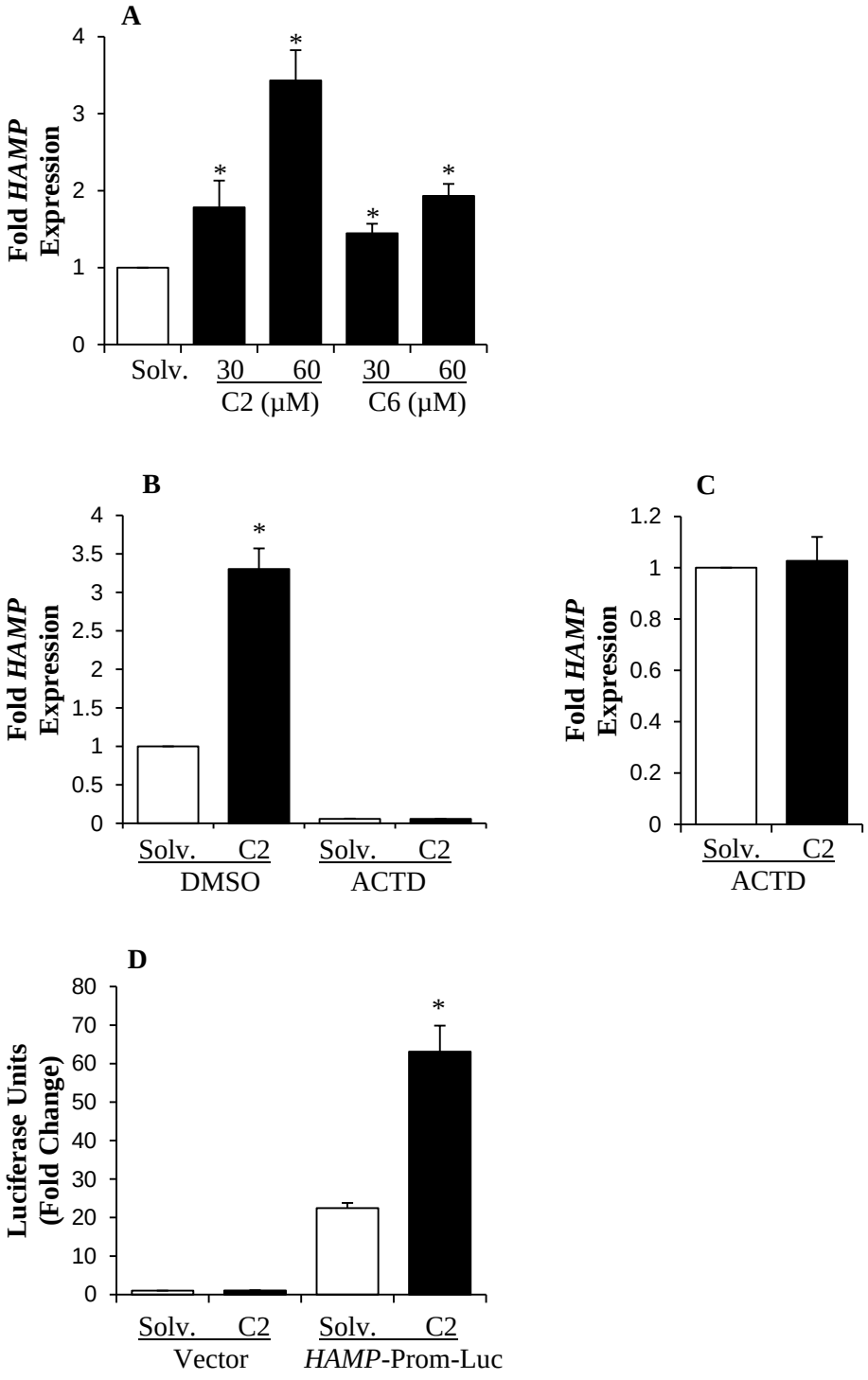
A
Fold HAMP Expression
Solv.
30
60
30
60
C2 (µM)
C6 (µM)
B
Fold HAMP Expression
Solv.
C2
Solv.
C2
DMSO
ACTD
C
Fold HAMP Expression
Solv.
C2
ACTD
D
Luciferase Units (Fold Change)
Solv.
C2
Solv.
C2
Vector
HAMP-Prom-Luc

Figure 5.1

Figure 5.2. Ceramide treatment stimulated the binding of STAT3, but not NF-κB subunit p65 or c-Jun/AP-1, to *HAMP* promoter. (**A**) Schematic diagram of 0.6kb *HAMP* promoter showing recognition sequence for NF-κB P65 (P65), STAT3, and c-Jun/AP-1 (AP-1). (**B**) Chromatin, isolated from ceramide or solvent (solv.)-treated HepG2 cells fixed with 1% formaldehyde, was immunoprecipitated with anti-STAT3, -NF-κB subunit p65 or -c-Jun antibodies or normal IgG , as control, as described in experimental procedures. Eluted and purified chromatin fractions, and total input chromatin (equal loading controls) were used as templates in PCR to amplify a 0.6 kbb *HAMP* promoter region using specific primers. PCR products were resolved with DNA agarose gel electrophoresis and images captured with Gel Doc XR+ system (Bio-Rad). Representative gel images have been shown. (**C**) HepG2 cells, treated with recombinant IL-6 or PBS (control), were employed for ChIP assays using an anti- STAT3 antibody, as described above. PCR products were visualized with ethidium bromide staining of DNA agarose gels.

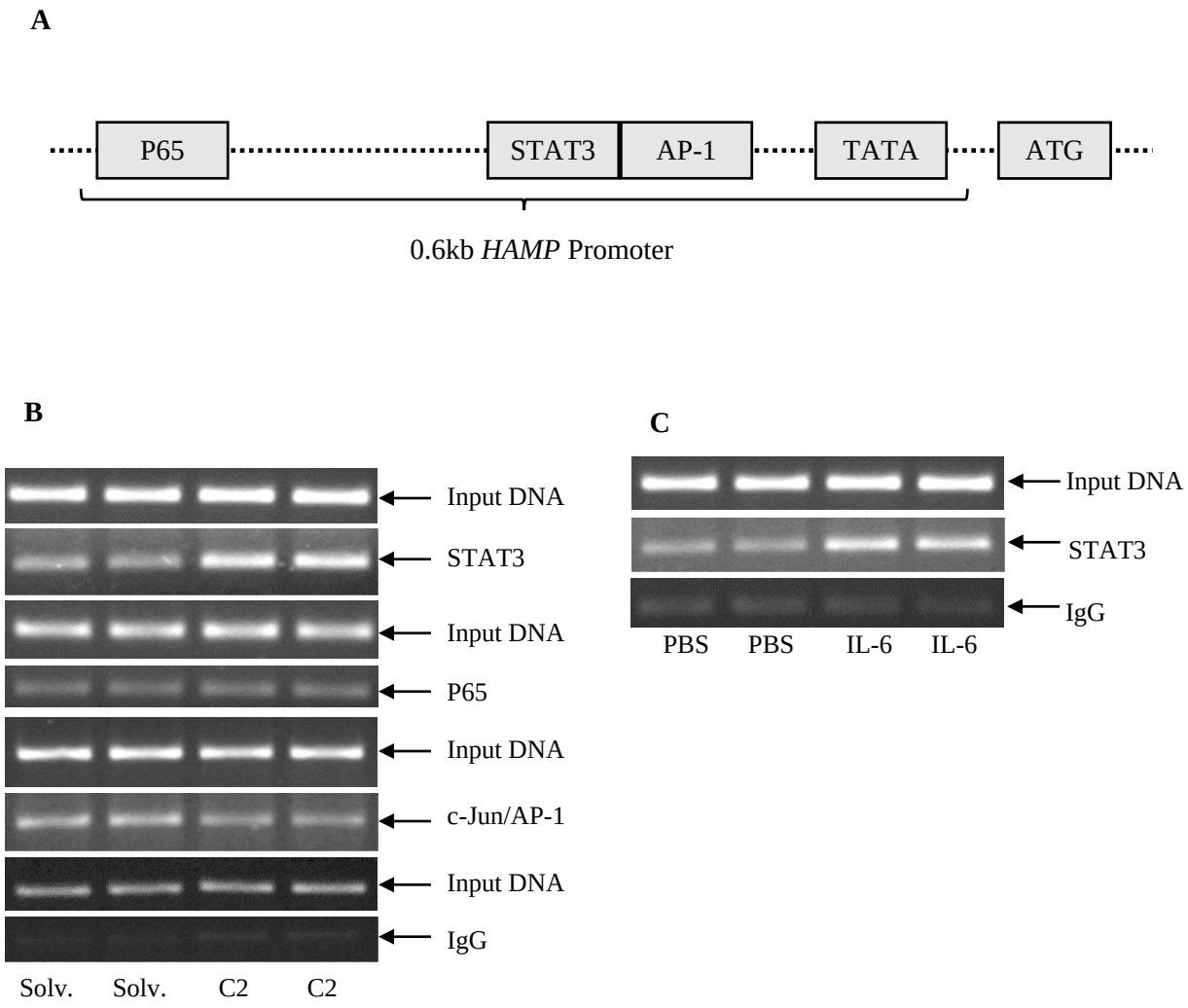
A
P65
STAT3
AP-1
TATA
ATG
0.6kb *HAMP* Promoter
B
Input DNA
STAT3
Input DNA
P65
Input DNA
c-Jun/AP-1
Input DNA
IgG
Solv.
Solv.
C2
C2
C
Input DNA
STAT3
IgG
PBS
PBS
IL-6
IL-6

Figure 5.2

Figure 5.3. The effect of ceramide on STAT3, JNK, NF-κB, and ERK1/2 phosphorylation in HepG2 cells. Whole cell lysates, purified from HepG2 cells treated with solvent (solv.), 60 μM C2 ceramide, 40 ng/mL recombinant IL-6 or PBS for 8 hours, were employed for western blotting. PVDF membranes were incubated with anti-phospho-STAT3 (P-STAT3 Tyr 705), anti-phospho-STAT3 (P-STAT3 Ser 727), anti-phospho-ERK1/2 (P-ERK1/2) (**A**), anti-phospho-P65 (P-P65), -total NF-κB P65 (P-65), and anti-phospho-JNK (P-JNK) antibodies (**B**). Immune reactive bands were detected by chemiluminescence, as described in experimental procedures. An anti- gapdh antibody was employed as a control for equal protein loading.

A

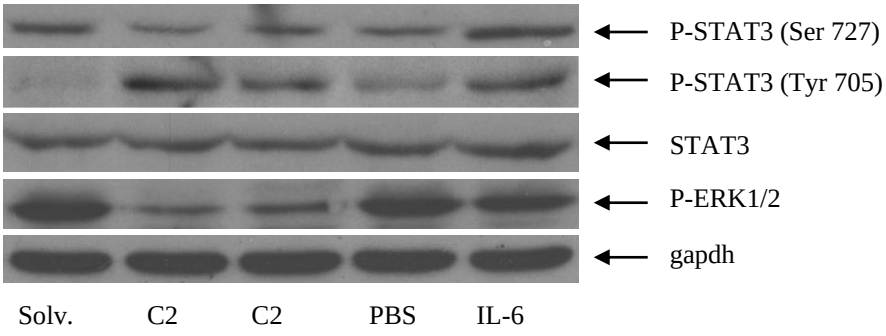
P-STAT3 (Ser 727)
P-STAT3 (Tyr 705)
STAT3
P-ERK1/2
gapdh
Solv.
C2
C2
PBS
IL-6

B

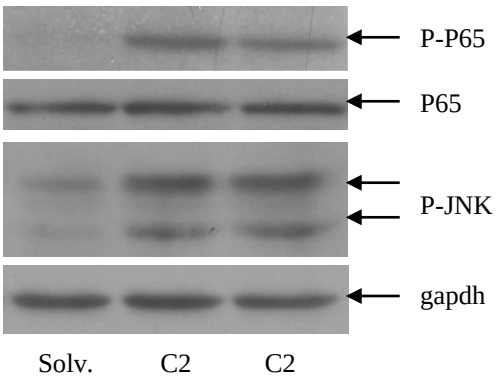
P-P65
P65
P-JNK
gapdh
Solv.
C2
C2

Figure 5.3

Figure 5.4. Ceramide-induced *HAMP* mRNA expression is not dependent on JNK activation. HepG2 cells were treated with ceramide or solvent (solv.) in the presence of 50 μM SP600125 inhibitor or DMSO, as control. (**A**) Whole cell lysates isolated from these cells were used for western blots performed with an anti-phospho-JNK (P-JNK) antibody, as described in experimental procedures. (**B**) cDNA, synthesized from RNA isolated from these cells, were used as templates for Taqman qPCR assays to determine *HAMP* mRNA expression. Gene expression in treated cells were expressed as fold change of that in control cells treated with solvent and DMSO.

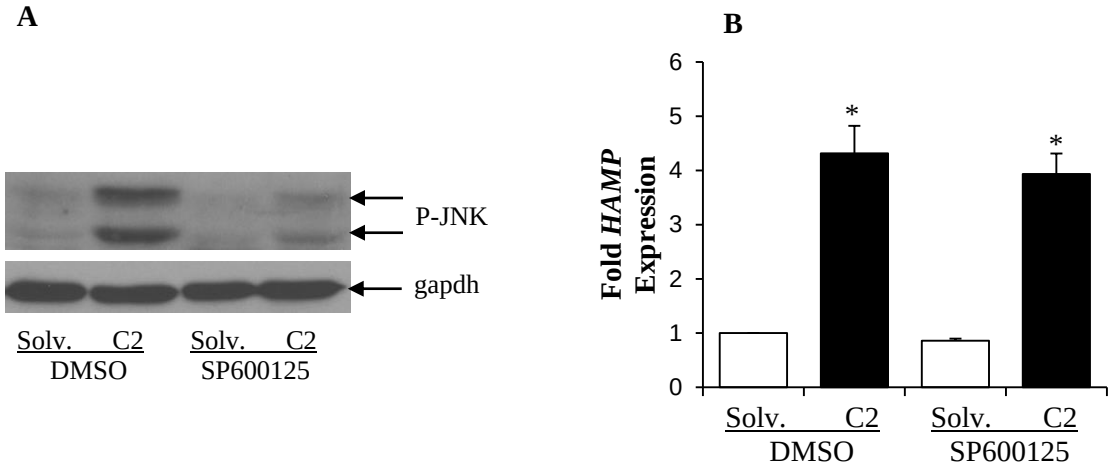
A
P-JNK
gapdh
Solv. C2
DMSO
Solv. C2
SP600125
B
Fold HAMP Expression
0
1
2
3
4
5
6
*
*
Solv. C2
DMSO
Solv. C2
SP600125

Figure 5.4

Figure 5.5. The effect of STAT3 response element mutation on *HAMP* promoter activation by ceramide. The single STAT3 response element within 0.6kbp *HAMP* promoter region cloned in pGL3 basic vector was mutated, as described in the experimental procedures. HepG2 cells, transfected with pGL3-basic vector harboring wild-type (WT) or mutated (ΔSTAT3) 0.6 kb *HAMP* promoter, or empty vector (vector) as negative control, and pRL-SV40 plasmid, as control for transfection efficiency, were treated with (**A**) 60 μM C2 ceramide (C2) and solvent control (solv.) or (**B**) 40 ng/mL IL-6 and PBS control for 8 hours. Dual luciferase reporter assays were performed, as described in the experimental procedures. *HAMP* promoter activity, expressed in relative luciferase units, in treated cells was calculated as fold change of that in control cells transfected with empty vector-and treated with solvent. Asterisks indicate statistical significance ($P<0.05$).

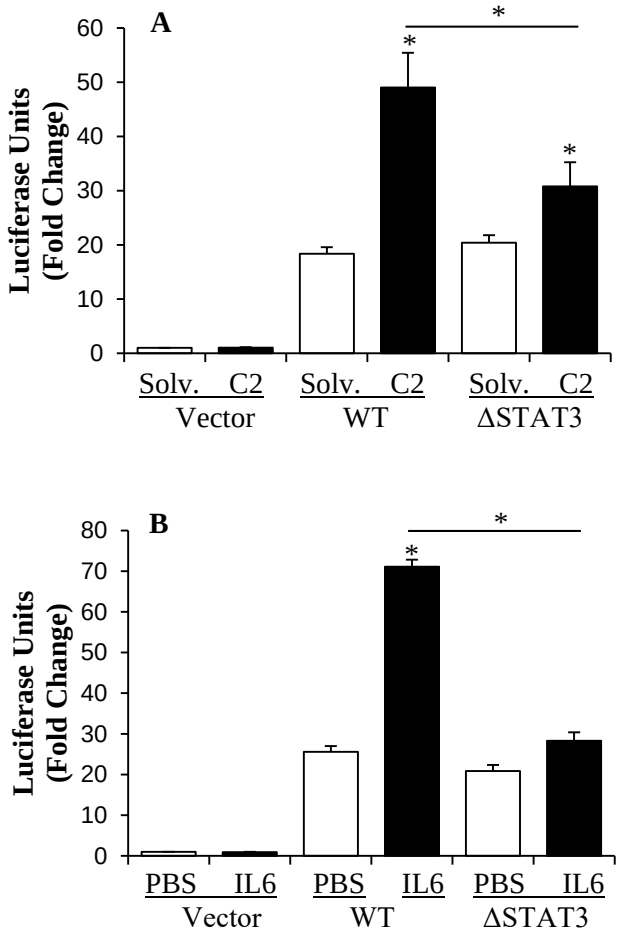
A
Luciferase Units
(Fold Change)
60
50
40
30
20
10
0
*
*
*
Solv. C2
Vector
Solv. C2
WT
Solv. C2
ΔSTAT3
B
Luciferase Units
(Fold Change)
80
70
60
50
40
30
20
10
0
*
*
PBS IL6
Vector
PBS IL6
WT
PBS IL6
ΔSTAT3

Figure 5.5

Figure 5.6 STAT3 expression and ceramide-induced activation of STAT3 were inhibited by STAT3 siRNA and JAK inhibitor I, respectively. (**A**) STAT3 mRNA and protein (inset) levels in HepG2 cells transfected with STAT3 siRNA or control siRNA were determined by qPCR or western blotting, respectively. Asterisks indicate statistical significance ($P<0.05$). (**B**) Cell lysates prepared from HepG2 cells, treated with 60 μM C2 ceramide or solvent (solv.) in the presence of 5 μM JAK inhibitor I or DMSO as control, were used for western blotting to detect total or tyrosine-phosphorylated (P-STAT3) STAT3 protein levels using specific antibodies. An antibody for gapdh was used as control for protein loading.

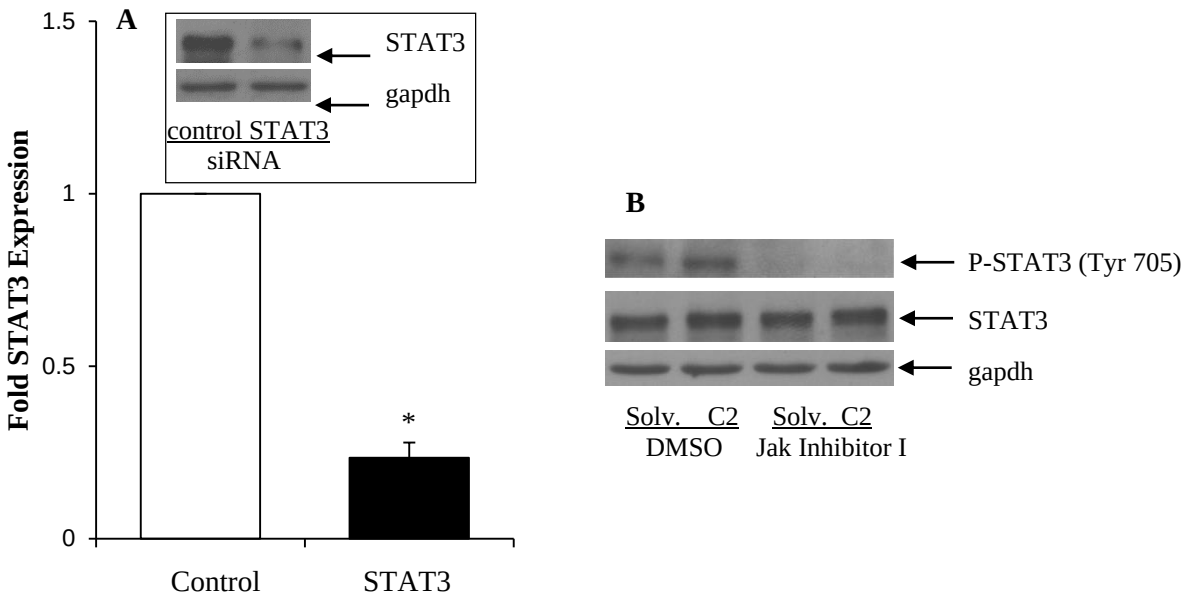
A
STAT3
gapdh
control STAT3
siRNA
Fold STAT3 Expression
1.5
1
0.5
0
*
Control
STAT3
B
P-STAT3 (Tyr 705)
STAT3
gapdh
Solv. C2
DMSO
Solv. C2
Jak Inhibitor I

Figure 5.6

Figure 5.7 Activation of STAT3 signaling was required for the induction of *HAMP* transcription by ceramide. (**A**) *HAMP* mRNA expression in HepG2 cells, treated with solvent (solv.) or C2 ceramide for 8 hours in the presence of either 5 μM JAK inhibitor I or DMSO (control), was determined by Taqman qPCR. *HAMP* expression in treated cells was calculated as fold change of that in respective control cells treated with solvent. (**B**) HepG2 cells, pre-transfected with STAT3 or control siRNA, were treated with C2 ceramide or solvent (solv.) in the presence of 5 μM JAK inhibitor I or DMSO. *HAMP* mRNA levels, determined by qPCR, were expressed as fold expression of that in respective controls treated with solvent. (**C**) HepG2 cells, transfected with pGL3-basic vector harboring 0.6 kb *HAMP* promoter, were treated with C2 ceramide or solvent (solv.) for 8 hours in the presence or absence of 5 μM JAK inhibitor I. Dual luciferase assays were performed and *HAMP* promoter activity, calculated as fold change of that in corresponding control cells treated with solvent, was expressed in relative luciferase units. (**D**) HepG2 cells, pre-transfected with STAT3 or control siRNA, were subsequently transfected with pGL3-basic vector harboring 0.6 kb wild-type *HAMP* promoter. After treatment with solvent (solv.) and C2 ceramide in the presence of either JAK inhibitor I or DMSO, dual luciferase reporter assays were performed. *HAMP* promoter activity, expressed as relative luciferase units, was expressed as fold change of that in respective control cells treated with solvent. Asterisks indicate statistical significance ($P<0.05$).

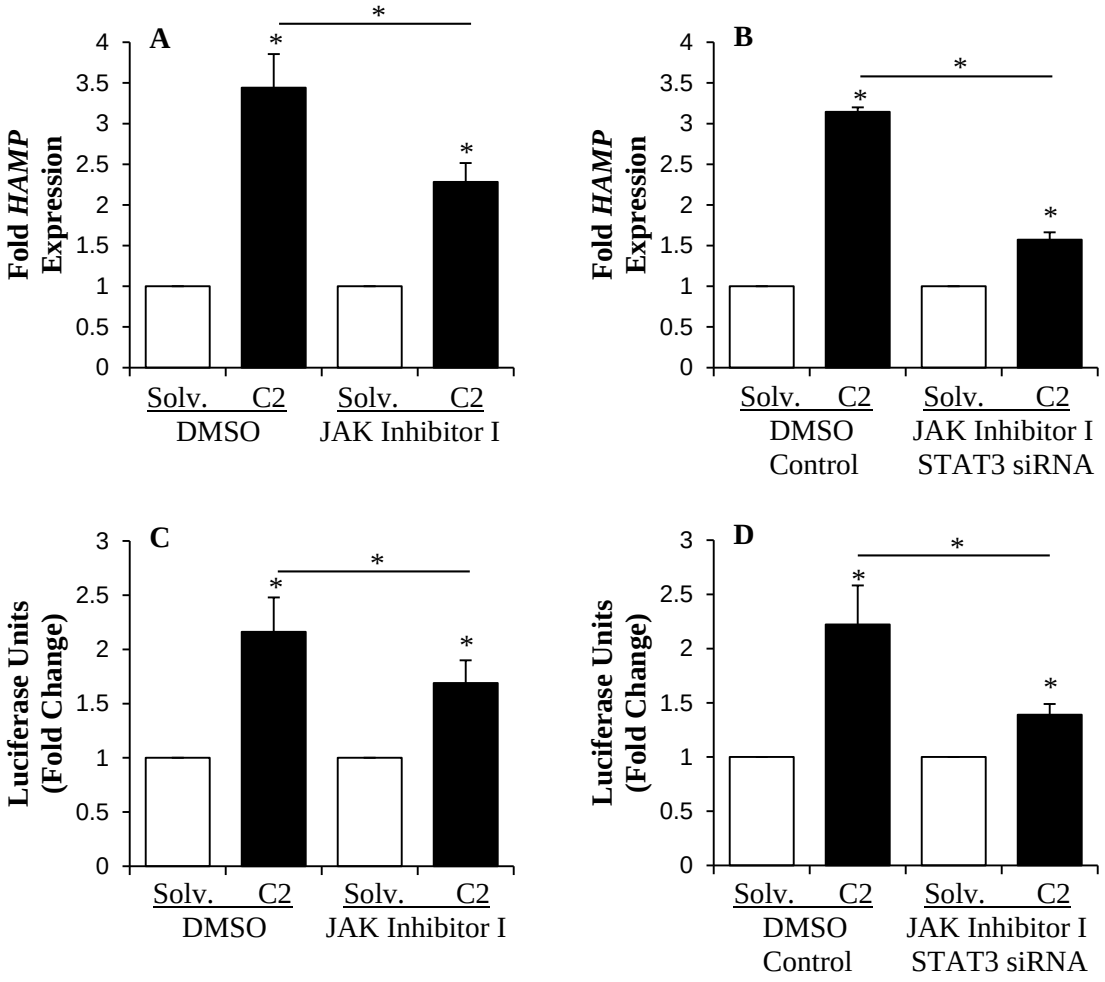
A
B
C
D
Fold HAMP Expression
Luciferase Units (Fold Change)
Solv.
C2
DMSO
JAK Inhibitor I
Control
STAT3 siRNA
*

Figure 5.7

Figure 5.8. ER stress is not involved in ceramide-induced *HAMP* expression. (**A**) HepG2 cells treated with solvent (solv.), 60 μM C2 ceramide or 10 μg/mL tunicamycin (TUNI) for 8 hours were employed for XBP-1 splicing assays, as described in experimental procedures. (**B**) HepG2 cells treated with solvent (solv.), 60 μM C2 ceramide in the presence of 20 μM salubrinal inhibitor or DMSO (control) were used to determine *HAMP* mRNA expression by qPCR, as described in experimental procedures. Gene expression in treated cells was expressed as fold change of that in cells treated with DMSO and solvent.

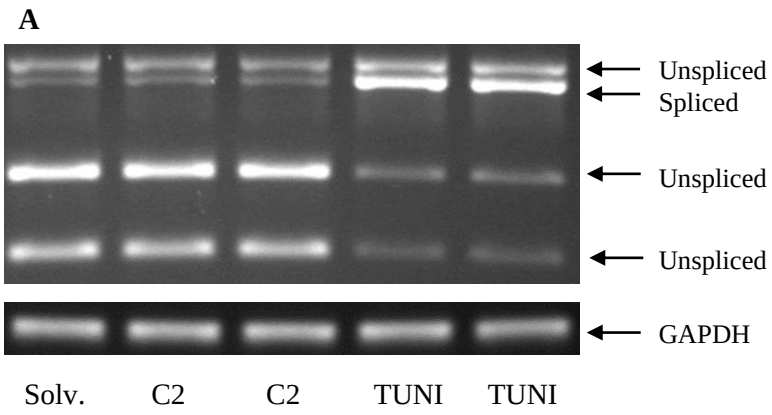
A
Unspliced
Spliced
Unspliced
Unspliced
GAPDH
Solv.
C2
C2
TUNI
TUNI

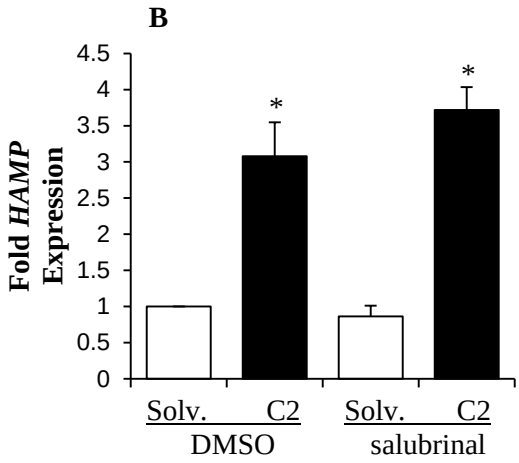
B
Fold HAMP Expression
4.5
4
3.5
3
2.5
2
1.5
1
0.5
0
*
*
Solv.
C2
Solv.
C2
DMSO
salubrinal

Figure 5.8

Chapter VI

Molecular Analysis of the Livers from hepcidin Knockout Mice with High-Fat and High-Sucrose Intake in Relationship to Nonalcoholic Steatohepatitis Pathology

1 ABSTRACT

The pathogenesis of nonalcoholic fatty liver disease (NAFLD) remains under ongoing investigation. Although current theories consider simple steatosis as benign, it can progress to nonalcoholic steatohepatitis (NASH). NASH is an advanced stage of disease characterized by inflammation (steatohepatitis), hepatocyte ballooning, fibrosis, which can ultimately lead to cirrhosis, hepatocellular carcinoma and mortality. The mechanisms of NAFLD/NASH progression are unclear but iron is considered as a risk factor for fibrosis development. The current chapter presents investigations on the potential role of iron in NASH pathology using hepcidin (*Hamp*) knockout (KO) mice with high-fat and high-sucrose (HFS) intake, as an experimental model. *Hamp* KO mice displaying primary iron overload were administered a high-fat high-sucrose (HFS) diet for different time periods (3 and 7 months) to mimic different stages of NAFLD/NASH pathology. Although HFS feeding induced similar increases in body weight in KO and control (Floxed) mice, the liver weights were significantly different. HFS intake resulted in pronounced hepatomegaly in control, but not in KO, mice. This was also confirmed with histological and biochemical analysis. Namely, control, but not KO, mice livers displayed pronounced steatosis and hepatic triglyceride content. Furthermore, the activation (i.e phosphorylation) of c-Jun N-terminal Kinase (JNK), which plays a role in steatosis, was higher in the livers of control than KO mice. In contrast, the livers from KO, but not control, mice exhibited significant level of fibrosis. As shown by Sirius Red staining, liver fibrosis in KO mice was detected at 3 months of HFS intake, which exacerbated over time, as observed with NASH patients. In agreement, the expression of α-smooth muscle actin protein, a marker for fibrogenesis, was more prominent in HFS-fed KO mice compared to controls. To understand the reasons behind blunted fat accumulation in the livers of KO mice with HFS intake, the expression of genes involved in lipid metabolism were examined by qPCR. Our results strongly suggested that lipogenesis and lipid storage capacity of the liver was diminished in *Hamp* KO mice with HFS intake. Namely, the expression levels of sterol regulatory element-binding protein 1c (SREBP-1c), a transcription factor controlling de novo lipogenesis, and fat-specific protein 27

(FSP27), which facilitates the development of lipid droplets, were significantly attenuated in KO mice livers. Furthermore, iron overload per se in *Hamp* KO mice affected hepatic expression of genes related to mitochondrial energy metabolism. In summary, *Hamp* KO mice with HFS intake exhibit a liver pathology similar to NASH and can therefore serve as a novel experimental model to study NASH development. Furthermore, our findings highlight a role for hepcidin and iron in the regulation of hepatic lipid metabolism, which has implications for NAFLD/NASH pathogenesis.

2 INTRODUCTION

NAFLD is a wide spectrum of disease, which ranges from simple steatosis to steatohepatitis and fibrosis. Although the large majority of NAFLD patients display simple steatosis, which in itself is benign, a small portion of patients present with aggressive nonalcoholic steatohepatitis (NASH). NASH pathology is characterized by the presence of lobular inflammation, fibrosis, hepatocellular ballooning and Mallory-Denk bodies (1, 2). The frequency of NASH with progressive fibrosis (i.e. stage 2 and higher based on Brunt criteria) is low among NAFLD patients but it is strongly associated with liver-related morbidity. Advanced fibrosis in NASH patients progresses to cirrhosis with severe clinical conditions, such as ascites, portal hypertension and hepatic encephalopathy ultimately causing hepatocellular carcinoma and liver failure (1, 3, 4).

Fibrosis, as observed in the livers of NASH patients, is the excessive accumulation of extracellular matrix (ECM) proteins in response to chronic liver injury (5, 6). Activated hepatic stellate cells, portal fibroblasts, and myofibroblasts of bone marrow origin play key roles in hepatic fibrosis (6). Upon activation by inflammatory cytokines and mitogens, these fibrogenic cells produce ECM proteins. The accumulation of ECM proteins changes the structure of hepatic parenchyma by forming fibrous scars, which ultimately lead to cirrhosis and end-stage liver disease (**Figure 6.1**). Histological examination and specific staining of ECM proteins are useful tools to determine the degree of fibrosis in the liver. Collagen (I, III, IV), fibronectin, elastin, laminin and proteoglycans are among the prominent ECM proteins produced by fibrogenic cells (7). In the injured liver,

activated hepatic stellate cells (HSC) secrete the major amount of ECM and stimulate ECM degradation. Following activation, HSC trans-differentiate into myofibroblast-like cells and migrate from the space of Disse into sites of tissue injury and repair (4, 6). Quiescent and activated HSC express different sets of cell surface markers. Alpha smooth muscle action (αSMA) is a myogenic marker expressed by activated stellate cells. The increased expression of αSMA is frequently selected as a marker for liver fibrosis (8, 9).

The precise mechanisms of NASH development are not well understood. Oxidative stress, inflammation and changes in mitochondrial function has been proposed as risk factors (10–13). Of note, due to the elevated triglyceride content, the hepatic β-oxidation capacity is challenged in NAFLD patients, and they display structural and functional abnormalities in liver mitochondria (14).

Recently, a role for iron has been proposed in NASH pathogenesis (15). Patients with NAFLD/NASH frequently display elevated serum iron indices and hepatic iron content (16, 17). Most importantly these studies have shown a strong correlation between hepatic iron content and the level of liver fibrosis, which determines disease severity in NAFLD/NASH patients (18–20). Interestingly, these studies have also suggested that the location of iron deposition in the liver is also a strong prognostic factor for disease severity in NASH patients. Independent studies have also shown that phlebotomy (iron letting) alleviates insulin resistance in NAFLD patients, which further support a role for iron in NAFLD pathogenesis (21).

The mechanisms by which iron contributes to NAFLD/NASH pathogenesis have mainly been attributed to the redox potential of iron, as a transition metal. Iron takes part in Fenton reaction promoting the production of highly toxic hydroxyl radicals (*see Chapter I for overview*) (22). Reactive oxygen species and oxidative stress are the most intensely studied secondary risk factors in NAFLD/NASH (23). The redox imbalance subsequently induces the peroxidation of intracellular lipids and the accumulation of toxic lipid radicals (23). All these changes ultimately cause the

activation of stellate cells and fibrotic signaling (24). Accordingly, the level of αSMA expression has been shown to be elevated in the livers of patients with genetic haemochromatosis (GH), a hereditary iron overload disorder. Following phlebotomy, the livers of GH patients displayed significantly decreased levels of αSMA expression further indicating the connection of iron with fibrosis (25). Other studies, using dietary experimental models, have suggested that iron modulates lipid metabolism. In rats, diet-induced iron overload correlated with a decrease in the level of hepatic triacylglycerols (26). In another study where hepatic triglyceride accumulation was induced by methionine-choline-deficient (MCD) diet intake, addition of iron into the diet significantly inhibited the MCD-induced triglyceride accumulation in rat livers (27). In contrast, a study using a mouse dietary model of iron and HFS failed to show any effect of iron on hepatic steatosis (28). Furthermore, it should also be noted, that in the MCD diet study where iron ameliorated steatosis, it also triggered necroinflammation and fibrosis (27). Taken together, these studies suggest a reverse connection between iron and steatosis but the consequences of these changes in liver lipid metabolism are unclear. This chapter uses mouse hepcidin-1 gene (*Hamp*) knockout mice, with documented iron overload phenotype, as an animal model to address some of these questions. In parallel, these studies will also establish whether *Hamp* knockout mice may serve as experimental NAFLD/NASH models.

Hepcidin is the central regulator of iron homeostasis. It is primarily synthesized by the hepatocytes in the liver and secreted into the circulation. Hepcidin controls iron homeostasis by decreasing iron absorption from the absorptive enterocytes in the duodenum and the release of iron from macrophages (*see Chapter I for overview*). The lack of hepcidin expression in hepcidin knockout mice, and in human iron disorders, will therefore result in iron accumulation both in the liver and other organs (29–31). Unlike humans, which express only one hepcidin gene, *HAMP*, mice express two hepcidin genes, *Hamp* and *Hamp2*, which arose from gene duplication (32). Overexpression

and structure analysis studies strongly suggested that *Hamp* is the mouse equivalent of *HAMP*, which by itself is sufficient to regulate iron metabolism (33).

NAFLD patients have been reported to show changes in hepcidin levels both in the serum and the liver. However, these studies are inconclusive and whether hepcidin and hepcidin-mediated changes in iron metabolism contribute to the disease progression in NAFLD is unclear.

As stated above, we used hepcidin knockout mice to further understand the role of hepcidin in NAFLD/NASH. For these studies, we administered a custom-made high-fat high-sucrose (HFS) to ubiquitous *Hamp* knockout mice with global hepcidin deficiency, which were created in our laboratory. Since severe forms of NAFLD develop over a long period of time in patients, mice were administered these diets for different time points (3 or 7 months). There are a number of animal models for NAFLD but the histological changes such as fibrosis, as observed in NASH patients, are not reproduced in many of these models. Methionine-choline-deficient diet-fed mice develop fibrosis but not the metabolic changes that lead to NAFLD (34). Recently prolonged exposure of mice to a western diet has been shown to induce fibrosis (35). Besides investigating the role of iron as a secondary risk factor, *Hamp* knockout mice might also serve as a novel animal model for NASH.

3 RESULTS

3.1 Generation and characterization of *Hamp* knockout (KO) mice

Hamp Floxed (Flx) mice were generated, as published previously (36). The generation of transgenic constructs are illustrated in **Figure 6.2A**. The targeting vector was designed by flanking exons 2 and exon 3 of *Hamp* gene with standard loxP sites, and by inserting a neomycin selection cassette (PGK-neo), flanked by FRT recognition sequences, downstream of exon 3. The 5’ and 3’ homology and loxP arms were generated by PCR from C57BL/6 genomic DNA. The *Hamp* targeting construct was electroporated into a C57BL/6 embryonic stem (ES) cell line, and ES cells with

positive homologous recombination were screened by Southern hybridization to be injected into Balb/CJ blastocysts. Male chimeric mice were obtained and crossed to C57BL/6J females to establish heterozygous germline offspring on C57BL/6 background. The germline mice were crossed to a FLP mouse line to remove the FRT-flanked selectable marker cassette. Heterozygous targeted mice were bred to generate homozygous *Hamp* Flx mice. These mice were further crossed with PGK-Cre transgenic mice, which ubiquitously express Cre recombinase protein (37), to excise the Flox genes. (**Figure 6.2A**). The F1 heterozygous pups generated from this breeding were backcrossed to generate homozygous ubiquitous knockout mice lacking *Hamp* expression in all the organs. The genotyping of these mice was performed by PCR (**Figure 6.2B**), as described in experimental procedures (*see Chapter II*). For PCR reactions, specific primers recognizing either the wild-type (WT) or knockout (KO) *Hamp* alleles (*see Chapter II section 15*) were used to identify homozygous ubiquitous knockout offspring (**Figure 6.2B**). Mice harboring both WT and KO alleles, or only KO allele were identified as heterozygous or homozygous knockout (KO) mice, respectively. The homozygous *Hamp* knockout mice were used for inbreeding to maintain the strain for the studies presented in this Chapter.

To further validate our experimental model and to confirm the effect of *Hamp* deletion on iron content in the liver, we performed inductively coupled mass spectrometry (ICP-MS) with stable 56Fe and 57Fe isotopes (**Figure 6.3A and 6.3B**). Our studies clearly indicated significant level of iron accumulation in the livers of *Hamp* KO, but not *Hamp* Flx control, mice (**Figure 6.3A and 6.3B)**, and validated the iron overload phenotype of our *Hamp* KO mice. Furthermore, Magnetic Resonance Imaging (MRI) analysis also confirmed the accumulation of iron in the livers of *Hamp* KO mice (**Figures 6.3C and 6.3D**). Namely, a characteristic T2* signal loss was observed in KO mice livers compared to Flx controls (**Figures 6.3C and 6.3D**).

3.2 Analysis of body and liver weights in *Hamp* KO and Floxed (Flx) control mice fed with high-fat high-sucrose (HFS) or regular diets

To study the interaction of hepcidin-mediated iron overload and lipid metabolism, 4-6 weeks old homozygous *Hamp* Flx (control) and KO mice were administered custom-made pelleted regular (control) diet (17.2% kcal. from fat, 100 g/ kg sucrose) or high-fat and high-sucrose (HFS) diet [42% kcal. from fat (54% saturated, 9.7% trans-fat), 0.4% cholesterol, 340 g/kg sucrose]. Similar rodent diets, which resemble human fast food, have been shown to induce liver pathology similar to NASH after extended periods of administration (35). To differentiate between the short and long-term effects of iron and/or HFS intake, mice were fed for 3 or 7 months. Water was given ad libitum, and contained sucrose (40 g/L) in HFS-fed groups to imitate the western diet with high-fat and soda consumption. The body weights of mice, which were monitored prior to the start of the diet and weekly throughout the feeding period, are shown in **Figure 6.4A and 6.4B**. The increase in body weights induced by HFS diet intake were similar in Flx (**Figure 6.4A**) and KO (**Figure 6.4B**) mice after either 3 or 7 months periods, as compared to respective controls, which were fed with the regular control diet. Interestingly, the liver weights of *Hamp* KO mice fed with regular diet was slightly but significantly higher than those of Flx mice at 3, but not 7, months (**Figure 6.4C and 6.4D**). This may suggest an initial effect of *Hamp* deletion (*i.e. iron deposition*) on basal metabolic activity, which is later compensated by the liver. 3 month-long HFS intake resulted in slightly lower liver weight increase in KO mice as compared to Flx mice but the difference was not statistically significant (**Figure 6.4D**). However, at 7 months, the liver weight of Flx mice were significantly higher (i.e. 3.5 ± 0.46 g) than those of KO mice (i.e. 2.42 ± 0.54 g) (**Figure 6.4D**). This discrepancy suggests that the gradual increase in iron deposition in *Hamp* KO mice may interfere with steatotic processes in the liver.

3.3 HFS diet-induced steatosis in *Hamp* KO and Flx mice.

To understand the reasons behind the differences observed regarding the body and liver weights of HFS-fed *Hamp* Flx and KO mice, further macroscopic and microscopic analysis of livers from mice fed for 3 months (**Figure 6.5)** and 7 months **(Figure 6.6**) were performed. The absence of *Hamp* gene altered the appearance of the liver in both mice fed on regular diet for 3 and 7 months. Namely, KO mice livers appeared bigger in size and exhibited a darker color compared to Flx mice (**Figure 6.5A and 6.6A**), which is probably mediated by iron deposition in the liver. HFS intake resulted in enlarged livers with lighter color, which indicates steatosis, and visceral fat depots in both Flx and KO mice, compared to control counterparts fed with regular diet (**Figure 6.5A and 6.6A**). However, 3 or 7 month-long HFS-induced hepatomegaly was more pronounced in the livers of Flx mice compared to KO mice (**Figure 6.5A and 6.6A**). This discrepancy was also confirmed with hematoxylin and eosin (H&E)-staining of liver sections (**Figure 6.5B and 6.6B**). Namely, both short and long-term HFS intake caused significantly higher levels of steatosis in the livers of Flx mice than in those of KO mice.

In addition to H&E staining, hepatic triglycerides were also quantified by a biochemical assay, as described (*see experimental procedures in Chapter II*). For these studies, lipids were extracted from the livers of mice fed with HFS or regular diets for 3 months (**Figure 6.7A**) or 7 months (**Figure 6.7B**). The quantification of liver triglycerides confirmed our histological analysis that HFS intake significantly increases hepatic triglyceride content but to different extents in *Hamp* Flx and KO mice (**Figures 6.7Aand 6.7B**). At the end of 3 month-long HFS intake, the level of hepatic triglyceride accumulation (expressed as μmol/L/100 gram b.w.) was 1876.64 ± 370.84 in Flx and 657.98 ± 186.89 in KO mice (**Figures 6.7A)**. Similar measurements at the end of 7 month-long feeding period yielded 1837.71 ± 118.12 in Flx and 886.91 ± 89.51 in KO mice livers. (**Figure 6.7B**). The inhibition of HFS-induced lipid accumulation in KO mice livers was higher at 3 months than at 7 months (**Figures 6.7 A and 6.7B**). In summary, the findings of our biochemical analysis

are in alignment with microscopic and macroscopic observations, as presented above. Taken together, these findings strongly indicated that the absence of hepcidin expression interferes with and suppresses liver triglyceride accumulation in response to HFS exposure.

3.4 HFS diet-induced fibrosis in *Hamp* KO and Flx Mice

Advanced stages of NAFLD pathology involve fibrosis. Animal experiments with MCD-diet administration and DGAT2 deletion (38, 39) have suggested a link between the inhibition of hepatic fat accumulation and fibrosis. Based on our observations of attenuated steatosis in *Hamp* KO mice (*see* ***Figures 6.3-6.6***), we examined the presence of fibrosis. The liver sections from *Hamp* Flx and knockout mice fed with HFS or regular diets for 3 (**Figure 6.8A**) and 7 (**Figure 6.9A**) months were stained with Sirius Red, as described in experimental procedures (*see Chapter II*). This staining technique detects the accumulation of ECM protein, collagen in the liver, as an indication for fibrogenesis. The level of fibrosis was also quantified by using ImageJ analysis, as described in experimental procedures (*see Chapter II*) (**Figures 6.8B and 6.9B**).

Sirius Red-stained livers from *Hamp* Flx mice fed with HFS or regular diets for 3 months did not display any significant changes (**Figures 6.8**). After 7 months of HFS intake, Flx mice livers exhibited increased levels of basal fibrosis (**Figures 6.9**). In contrast to Flx mice, *Hamp* KO mice exhibited significant levels of fibrosis both after 3 and 7 month-long HFS intake (**Figures 6.8 and 6.9**). However, the highest level of fibrosis was observed in the livers of *Hamp KO* mice with 7 months of HFS exposure (**Figures 6.9**). Although to a lesser extent, elevated level of basal fibrosis activity was also observed in *Hamp* KO mice fed with the regular control diet for 3 and 7 months (**Figures 6.8 and 6.9**). In summary, the quantification of our Sirius Red staining indicated that HFS feeding of *Hamp* KO mice for 3 months is sufficient to initiate fibrogenesis in the liver, which is exacerbated at 7 months. Interestingly, elevated hepatic iron content in the livers of *Hamp* knockout mice per se can induce fibrotic reactions. Taken together, our findings indicate that the synergistic

action of iron overload, originating from the absence *Hamp* gene expression, and HFS intake results in fibrosis, which gradually increases in severity.

3.5 JNK activation and αSMA expression in *Hamp* KO and Flx mice fed with HFS diet.

The presence of liver fibrosis was further confirmed by examining the expression levels of α smooth muscle actin (αSMA), a marker for hepatic stellate cell activation, by western blotting (**Figure 6.10A and 6.10B**). The livers of *Hamp* Flx mice fed with HFS diet for 3 months did not display any significant changes in αSMA expression compared to controls fed with regular diet. In contrast, *Hamp* KO mice displayed a significant increase in liver αSMA protein expression following 3 months HFS feeding. Furthermore, the basal αSMA expression level was also elevated *Hamp* KO mice compared *Hamp* Flx mice. With 7 month-long HFS intake, the levels of liver αSMA expression was elevated in both *Hamp* Flx and KO mice (**Figure 6.10A and 6.10B**).

c-Jun N-terminal kinase (JNK) signaling pathway has been reported to mediate steatosis in mice fed with MCD diets (40). JNK is activated by phosphorylation on serine residues (41). The expression levels of phosphorylated JNK (P-JNK) protein in the livers of *Hamp* mice were therefore determined by western blotting using specific anti-phospho JNK antibodies, as described in the experimental section (*see Chapter II*) (**Figure 6.10C and 6.10D**). The livers of *Hamp* Flx mice fed with HFS diet for 3 months displayed an increase in the level of P-JNK protein compared to controls fed with regular diet. In contrast, the livers of *Hamp* KO mice fed under similar conditions did not display any significant changes in JNK phosphorylation (**Figure 6.10C and 6.10D**). Namely, the level of P-JNK expression was similar in HFS or control diet-fed *Hamp* KO mice. It should however be noted, that after 7 months, the effect of HFS feeding on JNK activation was not as prominent as 3 months in Flx mice (**Figure 6.10C and 6.10D**). Compared to 3 months feeding, 7 months of HFS diet feeding slightly elevated P-JNK level in *Hamp* KO mice (**Figure 6.10C and 6.10D**). This suggests the involvement of JNK in the initial stages of the processes that underlie the attenuation of steatosis connected to *Hamp* deletion.

3.6 Expression of metabolic genes in HFS or regular diet-administered *Hamp* KO and Flx mice.

To further investigate the underlying mechanisms of attenuated fat accumulation in the livers of *Hamp* KO mice with HFS intake, mRNA expression levels of genes, which are known to be involved in lipid metabolism, were examined by real-time PCR (*see Chapter I for detailed review of these genes*). The results of these studies are presented below (**Figures 6.11 and 6.12**)

The transcription factor, sterol regulatory element-binding protein 1c (SREBP-1c) is well known for its role in mediating the stimulatory effect of insulin on genes connected to de novo lipogenesis pathway. The expression of SREBP-1c itself is also regulated at the transcriptional level (42, 43). The liver mRNA expression of SREBP-1c was significantly up-regulated in *Hamp* Flx mice with 3 month-long HFS intake compared to mice fed on control diet (**Figure 6.11A**). The deletion of *Hamp* alleles did not alter basal hepatic SREBP-1c expression (**Figure 6.11A**). Although to a significantly lesser extent than in Flx mice, 3 month-long HFS exposure also elevated liver SREBP-1c expression in *Hamp* KO mice compared KO controls (**Figure 6.11A**). Upon longer (i.e. 7 months) HFS exposure, the induction of liver SREBP-1c expression was attenuated but still significant in Flx mice (**Figure 6.11B**). In contrast, KO mice did not display any significant increase in SREBP-1c expression when fed with HFS diet compared to regular diet-fed controls (**Figure 6.11B**). Taken together, these findings with short and long-term HFS exposure suggested that diet-mediated changes in liver SREBP-1c expression are significantly attenuated in *Hamp* KO mice, which becomes more prominent with longer HFS exposure.

Fat-specific protein 27 (FSP27) plays an important role in lipid droplet formation (44). Similar to SREBP-1c, mRNA expression of FSP27 was significantly up-regulated in *Hamp* Flx mice exposed to HFS for 3 months compared to Flx mice fed with the regular diet (**Figure 6.11C**). In contrast to Flx mice, HFS-fed *Hamp* KO mice displayed a blunted increase in hepatic FSP27 mRNA expression (**Figure 6.11C**). The increase observed in liver FSP27 mRNA expression levels in

Hamp Flx mice was not significantly different between 3 and 7 month-long HFS intake. In contrast, HFS-induced FSP27 up-regulation is blunted in *Hamp* KO mice after 7 months of feeding as compared to that in Flx mice (**Figure 6.11D**). Similar to SREBP1-c data, the absence of *Hamp* in KO mice inhibited the induction of FSP27 in the liver.

Microsomal triglyceride transfer protein (MTP) is responsible for the production and secretion of VLDL particles (45). The liver mRNA expression level of MTP was not significantly altered in *Hamp* Flx and KO mice fed on regular or HFS diets for 3months (**Figure 6.11E**). The deletion of *Hamp* gene did not also affect the basal liver expression level of MTP gene (**Figure 6.11F**). Following 7 month-long HFS exposure, liver MTP expression was significantly suppressed in both *Hamp* Flx and KO mice to the same extent, as compared to Flx controls fed with the regular diet (**Figure 6.11F**).

Peroxisome Proliferator-Activated Receptor α (PPARα) activates the transcription of genes involved in fatty acid β-oxidation regulation (46). After 3 month-long HFS exposure, liver PPARα mRNA expression levels were stimulated in both *Hamp* Flx and KO mice compared to Flx controls fed with a regular diet (**Figure 6.12A**). In contrast, long term HFS exposure significantly inhibited PPARα mRNA expression in both *Hamp* Flx and KO mice compared to corresponding Flx controls (**Figure 6.12B**).

Carnitine palmitoyltransferase 1 (CPT1) is the rate-limiting enzyme in mitochondrial β-oxidation pathway (47). The expression of CPT1 did not significantly change in the livers of either *Hamp* Flx or KO mice after 3 months of HFS intake (**Figure 6.12C**). Interestingly, the livers of *Hamp* KO mice fed on the regular diet for 7 months expressed higher CPT1 levels compared to Flx mice fed under similar conditions (**Figure 6.12D**). On the other hand, 7 month-long HFS exposure significantly suppressed CPT1 expression in KO mice. This decrease was more prominent in *Hamp* KO mice considering the fact that CPT1 basal expression levels were elevated in KO mice (**Figure 6.12D**).

Phosphoenolpyruvate carboxykinase 1 (PCK1) and glucose-6-phosphatase (G6PC) both play an important role in the regulation of gluconeogenesis. The livers of *Hamp* Flx and KO mice with short or long-term HFS exposure displayed a significant inhibition of PCK1 and G6PC mRNA expression (**Figure 6.12E-H**). These findings suggest that HFS feeding exerts a consistent inhibitory of effect on gluconeogenesis in the liver under our experimental conditions. However, the basal mRNA expression levels of PCK1 and G6PC were different in the livers of *Hamp* KO and Flx mice (**Figure 6.12E-H**). Namely, KO mice expressed higher PCK1 and lower G6PC expression.

4 DISCUSSION

Liver, as an endocrine organ, plays an important role in both lipid and carbohydrate metabolism. By synthesizing hepcidin and serving as a major depot for excess iron, liver is also a key organ for iron metabolism. It is therefore important to understand the interaction of these pathways in the liver. NAFLD/NASH patients have been reported to frequently display changes in serum iron parameters and elevated hepatic iron content. The deposition of iron in the liver correlates with disease severity in NAFLD/NASH patients (17). The mechanisms by which excess iron contribute to NAFLD/NASH pathogenesis is unclear. Independent human and animal model studies have identified iron as an important risk factor for fibrogenesis in the liver (25, 48). A role for iron in lipid metabolism has also been suggested but the findings in published studies are inconclusive (26–28), where some reported stimulatory (28) but others indicated inhibitory (26, 27) effects of iron in this process. Although hepcidin is the key regulator of iron metabolism, the role of hepcidin in NAFLD/NASH pathogenesis has not been investigated in detail. We therefore examined the effect of hepcidin (i.e. iron homeostasis) on fatty liver disease by feeding hepcidin *(Hamp)* knockout (KO) mice with HFS diets. *Hamp* KO mice, generated in our laboratory, displayed significant iron accumulation in the liver, as shown by our MRI an ICP-MS analysis. Short and long-term exposure of *Hamp* KO and Flx controls to HFS diets led to differential changes in the

liver, both at macroscopic and microscopic levels, which is similar to the wide spectrum of NAFLD/NASH pathology observed in human patients (2).

The blunted effect of HFS in stimulating liver weight increase in KO mice compared to Flx mice indicated the presence of metabolic variations mediated by the absence of *Hamp* expression. This prompted us to conduct further histological and biochemical analysis of livers. Collectively, the findings of these studies strongly suggested, that hepatic iron deposition in KO mice, might exert an inhibitory effect on liver lipid accumulation. This is in agreement with previous studies showing a negative effect of iron on lipid metabolism (25, 26). Interestingly, the apparent amelioration of steatosis in *Hamp* KO mice exacerbated liver pathology. This was based on our observations that *Hamp* KO mice, compared to control counterparts, displayed an earlier and more pronounced development of fibrosis in the liver. Histological identification of fibrosis was also confirmed by western blotting showing elevated expression of αSMA protein as an indication of hepatic stellate cell activation. Our findings are consistent with previous studies using methionine-choline-deficient diet (MCD)-induced hepatic steatosis as an experimental model (27, 38). It has been reported that dietary iron supplementation is associated with decreased hepatic steatosis but increased necroinflammation and fibrosis (27). However, as stated above (*see Introduction*), although MCD diet model induces steatohepatitis, it fails to reproduce the metabolic changes observed in NAFLD patients, such as peripheral insulin resistance, obesity and dyslipidemia (49, 50). In fact MCD-diet induces weight loss and not weight gain (41). High-fat-diet experimental models are therefore advantageous because they present pathophysiology that is more representative of what is observed in NAFLD/NASH patients (50, 51). Furthermore, the dietary supplementation of iron as an experimental model has the disadvantage of creating secondary effects by indirectly altering hepcidin synthesis in the liver. It is well-recognized that iron is a potent stimulator of hepcidin transcription through the activation of bone morphogenic (BMP) and SMAD signaling pathway (52–54). Elevated hepcidin will then inhibit the expression of iron exporter,

ferroportin and thereby block iron release from macrophages (*see Chapter I for detailed review*). It is therefore feasible that experimental model of dietary iron overload will cause iron deposition in Kupffer cells and thereby exert an effect on liver inflammation. Accordingly, the study using rats administered an iron-rich diet reported significant iron accumulation in Kupffer cells (27). We therefore used a genetic model of iron overload caused by the deletion of key iron-regulatory gene, *Hamp* for the following reasons: 1: *Hamp* deletion is the direct cause of iron accumulation. 2: Artifacts associated with iron signaling (BMP/SMAD) and Kupffer cell iron deposition will be avoided due to the lack of hepcidin expression. Furthermore, the prevalence of HFE mutations, which are responsible for genetic hemochromatosis and inhibition of hepcidin expression, is high in some NAFLD/NASH patients (55). Accordingly this group of patients display lower levels of hepcidin, which is associated with increased disease severity (20). We therefore believe that our *Hamp* KO mouse model recapitulates the conditions observed in NAFLD patients with HFE mutations (i.e. inhibition of hepcidin expression) and serves as a good experimental model to study iron as a secondary risk factor in NAFLD/NASH pathogenesis.

The lipid accumulation in NAFLD (i.e. simple steatosis) is considered to be a benign condition. Studies with animal models of NAFLD have shown that inhibition of triglyceride production alleviates steatosis but exacerbates fibrogenesis and liver injury (38). The synthesis of triglycerides in the liver therefore serves the purpose of protecting the liver from potential lipotoxicity induced by the accumulation of free fatty acids. This has also been confirmed by *in vitro* studies (56). It is therefore possible that the decreased level of steatosis contributes to fibrosis in our HFS-fed *Hamp* KO mice. Nevertheless, the synergistic role of hepatic iron in this process cannot be excluded. Future studies, which involve feeding *Hamp* KO mice with HFS diets containing iron chelators, should address these questions directly.

To further understand the mechanisms leading to attenuated hepatic lipid accumulation in *Hamp* KO mice, we investigated JNK activation. In studies using JNK knockout mice fed with MCD or

high-fat diets, the deletion of JNK1, but not JNK2, has been shown to reverse hepatic steatosis (57, 58). JNK is well-known to be activated following phosphorylation on serine residues (41). Our western blotting studies examining the phosphorylation status of JNK indicated highest JNK activation in the livers of HFS-fed *Hamp* Flx mice, which also exhibited high levels of steatosis. In contrast, the livers of *Hamp* KO mice with alleviated steatosis did not display any significant JNK phosphorylation (i.e. activation). Interestingly, these findings were only observed with mice with short-term (3 months), but not long-term (7 months), HFS intake. Taken together, these findings are consistent with a potential role for JNK in inhibition on steatosis observed in *Hamp* KO mice livers with iron overload. This effect however is an early phenomenon because it was not observed in later stages of HFS feeding where more injury was developed. Accordingly, the deletion of JNK has been shown to reverse steatosis, but not fibrogenesis, in NASH animal models (57, 58). The direct effect of JNK and its regulation by hepcidin and iron need to be validated in future studies.

Lipid and carbohydrate metabolism in the liver is mediated by an intricate web of genes (*see Chapter I for detailed review*). The expression levels of most of these metabolic genes are regulated at the mRNA level. We therefore determined liver mRNA expression of important candidate genes in HFS-fed *Hamp* knockout mice. The analysis of genes involved in lipid metabolism (e.g. SREBP-1c) indicated that iron blunts the induction of genes involved in HFS intake-induced de novo lipogenesis in the liver. Furthermore, the expression of FSP27, the gene responsible for lipid droplet formation and lipid storage, was less responsive to HFS diet administration in livers with elevated hepatic iron content. These findings clearly establish a relationship between iron overload and lipogenic gene expression. Studies with rodent models of dietary iron deficiency have shown an up-regulation of lipogenic gene expression, which indirectly support our findings with *Hamp* KO mice (59–61). Lipid homeostasis in the liver is also regulated by lipid export, which is mediated by VLDL secretion. However, we did not determine any significant changes in the expression of genes regulating VLDL secretion (i.e. MTP). This suggests that hepcidin and iron do not have an effect

on HFS-mediated lipid vesicle secretion. Thus, the alleviated steatosis observed in high-fat-fed *Hamp* KO mice livers is probably not due to an elevated level of lipid export from the liver. In fact MTP expression was attenuated in the livers of both *Hamp* Flx and KO mice following long-term HFS exposure. Future studies should establish whether the inhibition of VLDL by prolonged fat intake directly contributes to fibrosis observed in the livers of these mice. Taken together, our data suggests that iron decreases steatosis by inhibiting lipid storage but not export.

Mitochondrial β-oxidation is also an important pathway to maintain hepatic lipid homeostasis. The transcription factor, PPARα induces the transcription of genes involved in β-oxidation (62). PPARα expression itself is also regulated at the transcriptional level (63). In our studies, we detected a time-dependent response of PPARα mRNA expression in the liver in response to HFS intake. Namely, short-term (3 months) intake up-regulated but long-term (7 months) intake suppressed PPARα expression regardless of *Hamp* genotype. Increased β-oxidation is essential to alleviate extra-hepatic fat burden in NAFLD by disposing of excess lipids in the liver (64). As a by-product of the mitochondrial respiratory chain activity, the levels of reactive oxygen species (ROS) in the liver are increased due to electron leakage. Of note, ROS is accepted to be a prominent secondary hit factor in the development of NASH pathology (65). It is therefore feasible, that the initial up-regulation of PPARα serves the purpose of disposing excess lipids in the liver via mitochondrial β-oxidation. The suppression of PPARα observed in later stages might either be a hepatic defense mechanism to limit mitochondrial ROS production or an indication of mitochondrial dysfunction in fibrotic livers. Similarly, the expression of CPT1, which is also involved in β-oxidation, was significantly suppressed in the livers of *Hamp* KO mice with long-term HFS intake. It is therefore possible that iron in conjunction with lipid accumulation exert a burden on mitochondria, which ultimately leads to profound mitochondrial dysfunction in the liver. Of note, changes in mitochondrial structure and function are regarded as secondary risk factors in NAFLD/NASH progression (13).

Besides lipid metabolism, changes in the expression of genes involved in gluconeogenesis were also observed in the livers of HFS-fed *Hamp* KO mice. HFS intake induced suppression of gluconeogenic gene expression (i.e. PCK1 and G6PC) independent of *Hamp* genotype and feeding period. However the deletion of *Hamp* by itself (*i.e. KO mice fed with the regular diet*) exhibited opposite effect on the expression of PCK1 and G6PC. Namely, the absence *Hamp* up-regulated PCK1 but suppressed G6PC mRNA levels. Overexpression of the Forkhead Transcription Factor, FKHR (a.k.a., FOXO1a) has been shown to stimulate the expression of G6PC, but not PCK1, in hepatocytes (66). ROS is known to suppress FOXO1a activity post-translationally (67). It is therefore feasible that increased ROS levels in *Hamp* KO mice may impose differential effects on PCK1 and G6PC through the inactivation of FOXO1a. Further studies are however required to determine the precise mechanisms of this differential regulation.

Despite being a useful NAFLD model, there are only limited number of studies with long-term HFS feeding of rodents, which have reported only mild levels of liver fibrosis (50). With our current model of *Hamp* KO, fibrosis developed at an early time point (i.e. 3 months) and increased in severity at 7 months. Our experimental data strongly suggests that the deletion of *Hamp*, and resultant hepatic iron overload, exacerbate liver fibrosis while decreasing steatosis. Therefore, *Hamp* KO mice might serve as a distinctive experimental model recapitulating NAFLD/NASH pathogenesis within a relatively short period of HFS diet administration.

In summary, our studies with *Hamp* KO mice established a correlation of increased hepatic iron content with both decreased steatosis and increased fibrosis in the liver. Our findings also suggested a role for hepcidin in HFS-induced mitochondrial dysfunction. Detailed future studies investigating metabolic signaling pathways in HFS-treated *Hamp* KO mice will enable us to understand the role of iron and hepcidin in the regulation of metabolic processes in the liver. We therefore believe that *Hamp* transgenic mice are a good new experimental model to study NAFLD/NASH pathogenesis.

5 REFERENCES

1. Anstee, Q. M., Targher, G., and Day, C. P. (2013) Progression of NAFLD to diabetes mellitus, cardiovascular disease or cirrhosis. *Nat. Rev. Gastroenterol. Hepatol.* **10**, 330–344
2. Brunt, E. M., Janney, C. G., Di Bisceglie, A. M., Neuschwander-Tetri, B. A., and Bacon, B. R. (1999) Nonalcoholic steatohepatitis: a proposal for grading and staging the histological lesions. *Am. J. Gastroenterol.* **94**, 2467–2474
3. Ekstedt, M., Franzén, L. E., Mathiesen, U. L., Thorelius, L., Holmqvist, M., Bodemar, G., and Kechagias, S. (2006) Long-term follow-up of patients with NAFLD and elevated liver enzymes. *Hepatology*. **44**, 865–873
4. Hernandez-Gea, V., and Friedman, S. L. (2011) Pathogenesis of Liver Fibrosis. *Annu. Rev. Pathol. Mech. Dis.* **6**, 425–456
5. Monga, S. P. S., and Cagle, P. T. (2010) *Molecular Pathology of Liver Diseases*, Springer Science & Business Media
6. Bataller, R., and Brenner, D. A. (2005) Liver fibrosis. *J. Clin. Invest.* **115**, 209–218
7. Friedman, S. L. (2008) Mechanisms of Hepatic Fibrogenesis. *Gastroenterology*. **134**, 1655–1669
8. Guy, C. D., Suzuki, A., Zdanowicz, M., Abdelmalek, M. F., Burchette, J., Unalp, A., Diehl, A. M., and for the NASH CRN (2012) Hedgehog pathway activation parallels histologic severity of injury and fibrosis in human nonalcoholic fatty liver disease. *Hepatology*. **55**, 1711–1721
9. Patel, K., and Shackel, N. A. (2014) Current status of fibrosis markers: *Curr. Opin. Gastroenterol.* **30**, 253–259
10. Basaranoglu, M. (2013) From fatty liver to fibrosis: A tale of "second hit." *World J. Gastroenterol.* **19**, 1158
11. Malaguarnera, M., Rosa, M. D., Nicoletti, F., and Malaguarnera, L. (2009) Molecular mechanisms involved in NAFLD progression. *J. Mol. Med.* **87**, 679–695
12. Takaki, A., Kawai, D., and Yamamoto, K. (2013) Multiple Hits, Including Oxidative Stress, as Pathogenesis and Treatment Target in Non-Alcoholic Steatohepatitis (NASH). *Int. J. Mol. Sci.* **14**, 20704–20728
13. Dowman, J. K., Tomlinson, J. W., and Newsome, P. N. (2010) Pathogenesis of non-alcoholic fatty liver disease. *QJM*. **103**, 71–83
14. Fabbrini, E., Sullivan, S., and Klein, S. (2010) Obesity and nonalcoholic fatty liver disease: Biochemical, metabolic, and clinical implications. *Hepatology*. **51**, 679–689
15. O'Brien, J., and Powell, L. W. (2011) Non-alcoholic fatty liver disease: is iron relevant? *Hepatol. Int.* **6**, 332–341
16. Martinelli, N., Traglia, M., Campostrini, N., Biino, G., Corbella, M., Sala, C., Busti, F., Masciullo, C., Manna, D., Previtali, S., Castagna, A., Pistis, G., Olivieri, O., Toniolo, D., Camaschella, C., and Girelli, D. (2012) Increased Serum Hepcidin Levels in Subjects with the Metabolic Syndrome: A Population Study. *PLoS ONE*. **7**, e48250
17. Aigner, E. (2014) Dysregulation of iron and copper homeostasis in nonalcoholic fatty liver. *World J. Hepatol.* **7**, 177
18. Valenti, L., Fracanzani, A. L., Bugianesi, E., Dongiovanni, P., Galmozzi, E., Vanni, E., Canavesi, E., Lattuada, E., Roviaro, G., Marchesini, G., and Fargion, S. (2010)

HFE Genotype, Parenchymal Iron Accumulation, and Liver Fibrosis in Patients With Nonalcoholic Fatty Liver Disease. *Gastroenterology*. **138**, 905–912
19. Nelson, J. E., Wilson, L., Brunt, E. M., Yeh, M. M., Kleiner, D. E., Unalp-Arida, A., and Kowdley, K. V. (2010) Relationship between the pattern of hepatic iron deposition and histological severity in nonalcoholic fatty liver disease. *Hepatology*. **53**, 448–457
20. Nelson, J. E., Brunt, E. M., Kowdley, K. V., and for the Nonalcoholic Steatohepatitis Clinical Research Network (2012) Lower serum hepcidin and greater parenchymal iron in nonalcoholic fatty liver disease patients with C282Y HFE mutations. *Hepatology*. **56**, 1730–1740
21. Valenti, L., Fracanzani, A. L., Dongiovanni, P., Bugianesi, E., Marchesini, G., Manzini, P., Vanni, E., and Fargion, S. (2007) Iron Depletion by Phlebotomy Improves Insulin Resistance in Patients With Nonalcoholic Fatty Liver Disease and Hyperferritinemia: Evidence from a Case-Control Study. *Am. J. Gastroenterol.* **102**, 1251–1258
22. Sutton, H. C., and Winterbourn, C. C. (1989) On the participation of higher oxidation states of iron and copper in fenton reactions. *Free Radic. Biol. Med.* **6**, 53–60
23. Browning, J. D., and Horton, J. D. (2004) Molecular mediators of hepatic steatosis and liver injury. *J. Clin. Invest.* **114**, 147–152
24. Ahmed, U. (2012) Interactions between hepatic iron and lipid metabolism with possible relevance to steatohepatitis. *World J. Gastroenterol.* **18**, 4651
25. Ramm, G. A., Crawford, D. H. G., Powell, L. W., Walker, N. I., Fletcher, L. M., and Halliday, J. W. (1997) Hepatic stellate cell activation in genetic haemochromatosis: Lobular distribution, effect of increasing hepatic iron and response to phlebotomy. *J. Hepatol.* **26**, 584–592
26. Cunnane, S. C., and McAdoo, K. R. (1987) Iron Intake Influences Essential Fatty Acid and Lipid Composition of Rat Plasma and Erythrocytes. *J. Nutr.* **117**, 1514–1519
27. Kirsch, R., Sijtsema, H. P., Tlali, M., Marais, A. D., and Hall, P. de la M. (2006) Effects of iron overload in a rat nutritional model of non-alcoholic fatty liver disease. *Liver Int.* **26**, 1258–1267
28. Choi, J. S., Koh, I.-U., Lee, H. J., Kim, W. H., and Song, J. (2013) Effects of excess dietary iron and fat on glucose and lipid metabolism. *J. Nutr. Biochem.* **24**, 1634–1644
29. Lesbordes-Brion, J.-C., Viatte, L., Bennoun, M., Lou, D.-Q., Ramey, G., Houbron, C., Hamard, G., Kahn, A., and Vaulont, S. (2006) Targeted disruption of the hepcidin 1 gene results in severe hemochromatosis. *Blood*. **108**, 1402–1405
30. Nemeth, E., Tuttle, M. S., Powelson, J., Vaughn, M. B., Donovan, A., Ward, D. M., Ganz, T., and Kaplan, J. (2004) Hepcidin Regulates Cellular Iron Efflux by Binding to Ferroportin and Inducing Its Internalization. *Science*. **306**, 2090–2093
31. Ganz, T. (2013) Systemic Iron Homeostasis. *Physiol. Rev.* **93**, 1721–1741
32. Pigeon, C., Ilyin, G., Courselaud, B., Leroyer, P., Turlin, B., Brissot, P., and Loréal, O. (2001) A New Mouse Liver-specific Gene, Encoding a Protein Homologous to Human Antimicrobial Peptide Hepcidin, Is Overexpressed during Iron Overload. *J. Biol. Chem.* **276**, 7811–7819

33. Lou, D.-Q., Nicolas, G., Lesbordes, J.-C., Viatte, L., Grimber, G., Szajnert, M.-F., Kahn, A., and Vaulont, S. (2004) Functional differences between hepcidin 1 and 2 in transgenic mice. *Blood*. **103**, 2816–2821
34. Larter, C. Z. (2007) Not all models of fatty liver are created equal: Understanding mechanisms of steatosis development is important. *J. Gastroenterol. Hepatol.* **22**, 1353–1354
35. Charlton, M., Krishnan, A., Viker, K., Sanderson, S., Cazanave, S., McConico, A., Masuoko, H., and Gores, G. (2011) Fast food diet mouse: novel small animal model of NASH with ballooning, progressive fibrosis, and high physiological fidelity to the human condition. *Am. J. Physiol. - Gastrointest. Liver Physiol.* **301**, G825–G834
36. Lu, S., Seravalli, J., and Harrison-Findik, D. (2015) Inductively coupled mass spectrometry analysis of biometals in conditional Hamp1 and Hamp1 and Hamp2 transgenic mouse models. *Transgenic Res.* 10.1007/s11248-015-9879-3
37. Lallemand, Y., Luria, V., Haffner-Krausz, R., and Lonai, P. (1998) Maternally expressed PGK-Cre transgene as a tool for early and uniform activation of the Cre site-specific recombinase. *Transgenic Res.* **7**, 105–112
38. Yamaguchi, K., Yang, L., McCall, S., Huang, J., Yu, X. X., Pandey, S. K., Bhanot, S., Monia, B. P., Li, Y.-X., and Diehl, A. M. (2007) Inhibiting triglyceride synthesis improves hepatic steatosis but exacerbates liver damage and fibrosis in obese mice with nonalcoholic steatohepatitis. *Hepatology*. **45**, 1366–1374
39. McClain, C. J., Barve, S., and Deaciuc, I. (2007) Good fat/bad fat. *Hepatology*. **45**, 1343–1346
40. Czaja, M. J. (2010) JNK REGULATION OF HEPATIC MANIFESTATIONS OF THE METABOLIC SYNDROME. *Trends Endocrinol. Metab. TEM*. **21**, 707–713
41. Ip, Y. T., and Davis, R. J. (1998) Signal transduction by the c-Jun N-terminal kinase (JNK) — from inflammation to development. *Curr. Opin. Cell Biol.* **10**, 205–219
42. Chen, G., Liang, G., Ou, J., Goldstein, J. L., and Brown, M. S. (2004) Central role for liver X receptor in insulin-mediated activation of Srebp-1c transcription and stimulation of fatty acid synthesis in liver. *Proc. Natl. Acad. Sci. U. S. A.* **101**, 11245–11250
43. Amemiya-Kudo, M., Shimano, H., Yoshikawa, T., Yahagi, N., Hasty, A. H., Okazaki, H., Tamura, Y., Shionoiri, F., Iizuka, Y., Ohashi, K., Osuga, J., Harada, K., Gotoda, T., Sato, R., Kimura, S., Ishibashi, S., and Yamada, N. (2000) Promoter Analysis of the Mouse Sterol Regulatory Element-binding Protein-1c Gene. *J. Biol. Chem.* **275**, 31078–31085
44. Gong, J., Sun, Z., and Li, P. (2009) CIDE proteins and metabolic disorders. *Curr. Opin. Lipidol.* **20**, 121–126
45. Hussain, M. M., Nijstad, N., and Franceschini, L. (2011) Regulation of microsomal triglyceride transfer protein. *Clin. Lipidol.* **6**, 293–303
46. Berger, J., and Moller, D. E. (2002) The Mechanisms of Action of PPARs. *Annu. Rev. Med.* **53**, 409–435
47. Bartlett, K., and Eaton, S. (2004) Mitochondrial β-oxidation. *Eur. J. Biochem.* **271**, 462–469
48. Lunova, M., Goehring, C., Kuscuoglu, D., Mueller, K., Chen, Y., Walther, P., Deschemin, J.-C., Vaulont, S., Haybaeck, J., Lackner, C., Trautwein, C., and Strnad,

P. (2014) Hepcidin knockout mice fed with iron-rich diet develop chronic liver injury and liver fibrosis due to lysosomal iron overload. *J. Hepatol.* **61**, 633–641
49. Larter, C. Z., and Yeh, M. M. (2008) Animal models of NASH: Getting both pathology and metabolic context right. *J. Gastroenterol. Hepatol.* **23**, 1635–1648
50. Schattenberg, J. M., and Galle, P. R. (2010) Animal models of non-alcoholic steatohepatitis: of mice and man. *Dig. Dis. Basel Switz.* **28**, 247–254
51. Imajo, K., Yoneda, M., Kessoku, T., Ogawa, Y., Maeda, S., Sumida, Y., Hyogo, H., Eguchi, Y., Wada, K., and Nakajima, A. (2013) Rodent Models of Nonalcoholic Fatty Liver Disease/Nonalcoholic Steatohepatitis. *Int. J. Mol. Sci.* **14**, 21833–21857
52. Ramos, E., Kautz, L., Rodriguez, R., Hansen, M., Gabayan, V., Ginzburg, Y., Roth, M., Nemeth, E., and Ganz, T. (2011) Evidence for distinct pathways of hepcidin regulation by acute and chronic iron loading in mice. *Hepatology*. **53**, 1333–1341
53. Feng, Q., Migas, M. C., Waheed, A., Britton, R. S., and Fleming, R. E. (2012) Ferritin upregulates hepatic expression of bone morphogenetic protein 6 and hepcidin in mice. *Am. J. Physiol. - Gastrointest. Liver Physiol.* **302**, G1397–G1404
54. Corradini, E., Meynard, D., Wu, Q., Chen, S., Ventura, P., Pietrangelo, A., and Babitt, J. L. (2011) Serum and liver iron differently regulate the bone morphogenetic protein 6 (BMP6)-SMAD signaling pathway in mice. *Hepatology*. **54**, 273–284
55. Lee, S. H., Jeong, S.-H., Lee, D., Lee, J. H., Hwang, S. H., Cho, Y. A., Park, Y. S., Hwang, J.-H., Kim, J.-W., Kim, N., Lee, D. H., and Kang, W. (2010) An epidemiologic study on the incidence and significance of HFE mutations in a Korean cohort with nonalcoholic fatty liver disease. *J. Clin. Gastroenterol.* **44**, e154–161
56. Listenberger, L. L., Han, X., Lewis, S. E., Cases, S., Farese, R. V., Ory, D. S., and Schaffer, J. E. (2003) Triglyceride Accumulation Protects Against Fatty Acid-Induced Lipotoxicity. *Proc. Natl. Acad. Sci.* **100**, 3077–3082
57. Schattenberg, J. M., Singh, R., Wang, Y., Lefkowitch, J. H., Rigoli, R. M., Scherer, P. E., and Czaja, M. J. (2006) Jnk1 but not jnk2 promotes the development of steatohepatitis in mice. *Hepatology*. **43**, 163–172
58. Singh, R., Wang, Y., Xiang, Y., Tanaka, K. E., Gaarde, W. A., and Czaja, M. J. (2009) Differential effects of JNK1 and JNK2 inhibition on murine steatohepatitis and insulin resistance. *Hepatology*. **49**, 87–96
59. Sherman, A. R. (1978) Lipogenesis in iron-deficient adult rats. *Lipids*. **13**, 473–478
60. Sherman, A. R., Guthrie, H. A., Wolinsky, I., and Zulak, I. M. (1978) Iron Deficiency Hyperlipidemia in 18-Day-Old Rat Pups: Effects of Milk Lipids, Lipoprotein Lipase, and Triglyceride Synthesis. *J. Nutr.* **108**, 152–162
61. Davis, M. R., Rendina, E., Peterson, S. K., Lucas, E. A., Smith, B. J., and Clarke, S. L. (2012) Enhanced expression of lipogenic genes may contribute to hyperglycemia and alterations in plasma lipids in response to dietary iron deficiency. *Genes Nutr.* **7**, 415–425
62. Pawlak, M., Lefebvre, P., and Staels, B. (2015) Molecular mechanism of PPARα action and its impact on lipid metabolism, inflammation and fibrosis in non-alcoholic fatty liver disease. *J. Hepatol.* **62**, 720–733

63. Pineda Torra, I., Jamshidi, Y., Flavell, D. M., Fruchart, J.-C., and Staels, B. (2002) Characterization of the Human PPARα Promoter: Identification of a Functional Nuclear Receptor Response Element. *Mol. Endocrinol.* **16**, 1013–1028
64. Begriche, K., Igoudjil, A., Pessayre, D., and Fromenty, B. (2006) Mitochondrial dysfunction in NASH: Causes, consequences and possible means to prevent it. *Mitochondrion*. **6**, 1–28
65. Begriche, K., Massart, J., Robin, M.-A., Bonnet, F., and Fromenty, B. (2013) Mitochondrial adaptations and dysfunctions in nonalcoholic fatty liver disease. *Hepatology*. **58**, 1497–1507
66. Barthel, A., Schmoll, D., Krüger, K.-D., Bahrenberg, G., Walther, R., Roth, R. A., and Joost, H.-G. (2001) Differential Regulation of Endogenous Glucose-6-Phosphatase and Phosphoenolpyruvate Carboxykinase Gene Expression by the Forkhead Transcription Factor FKHR in H4IIE-Hepatoma Cells. *Biochem. Biophys. Res. Commun.* **285**, 897–902
67. Klotz, L.-O., Sánchez-Ramos, C., Prieto-Arroyo, I., Urbánek, P., Steinbrenner, H., and Monsalve, M. (2015) Redox regulation of FoxO transcription factors. *Redox Biol.* **6**, 51–72

Figure 6.1. Pathology of hepatic fibrosis. Chronic liver injury induces inflammatory cell infiltration into the liver parenchyma. Hepatocyte apoptosis stimulates the activation of Kupffer cells, which releases fibrogenic mediators. Hepatic stellate cells (HSC) proliferate and differentiate into myofibroblasts for the production of extracellular matrix (ECM). Excessive ECM deposition further hampers liver function by inhibiting the blood flow in the hepatic sinusoid and nutrient exchanges. (*Image adopted from Bataller, R., and Brenner, D. A. (2005) Liver fibrosis. J Clin Invest. 115, 209–218 with permission*)

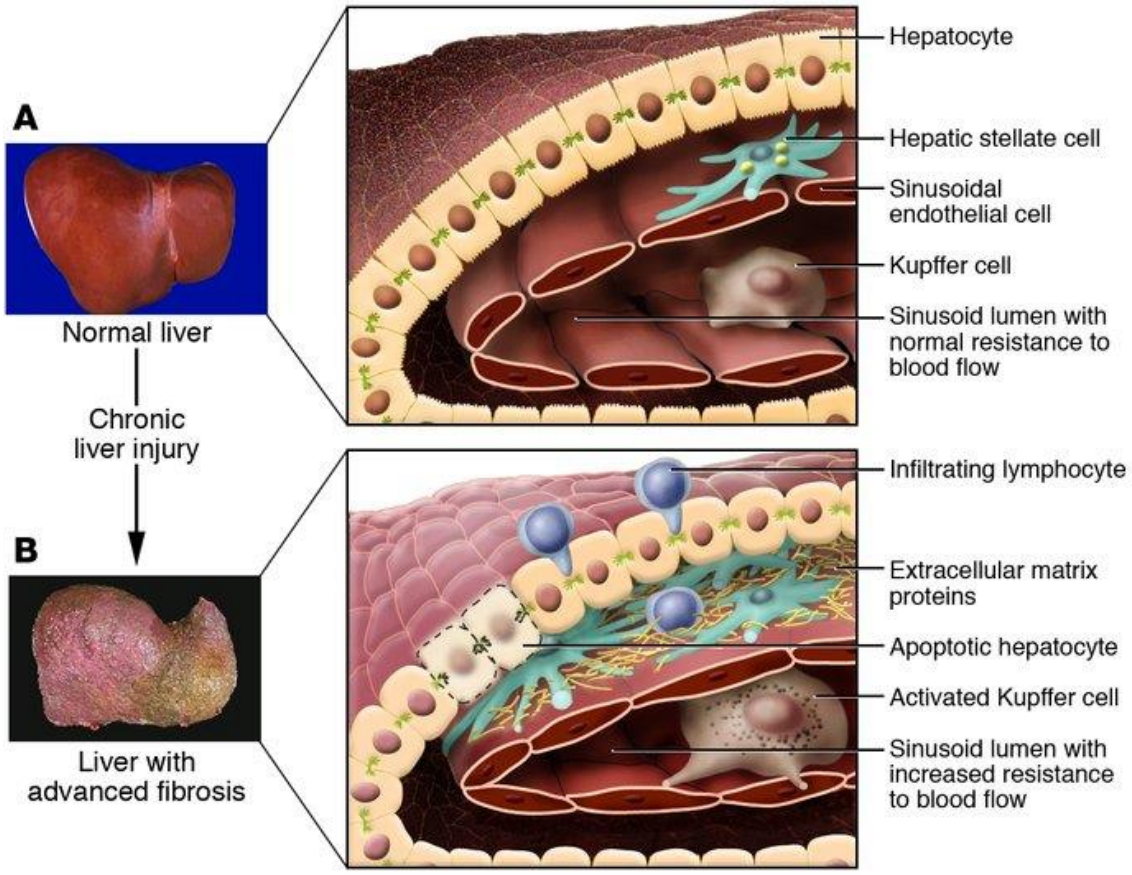
A
Normal liver
Chronic
liver injury
B
Liver with
advanced fibrosis
Hepatocyte
Hepatic stellate cell
Sinusoidal
endothelial cell
Kupffer cell
Sinusoid lumen with
normal resistance to
blood flow
Infiltrating lymphocyte
Extracellular matrix
proteins
Apoptotic hepatocyte
Activated Kupffer cell
Sinusoid lumen with
increased resistance
to blood flow

Figure 6.1

Figure 6.2. *Hamp* Floxed (Flx) and knockout (KO) mice generation and genotyping. (**A**) The schematic illustration of *Hamp* construct design has been adopted from a previous publication by Lu. S. et al (36). (**i**) The genomic structure of wild-type *Hamp* loci with exon1, 2, and 3 represented by gray boxes (E1, E2 and E3, respectively). (**ii**) *Hamp* targeting vector flanking E2 and E3 with loxP and neomycin (PGK-NEO) selection cassette with FRT recognition sequence was generated and electroporated into a C57BL/6 embryonic stem (ES) cell line to induce homologous recombination. (**iii**) Null alleles after Cre-mediated recombination excising E2 and E3 leaving a single lox P site, which encodes primarily signaling sequence of hepcidin-1. (**B**) Genotyping of wild-type (wt.), heterozygous (het.) and homozygous (hom.) *Hamp* KO mice were performed by PCR, as described in experimental procedures (*see Chapter II*) using primers specific for the corresponding alleles. PCR products were analyzed by DNA agarose gel electrophoresis and visualized by ethidium bromide staining. Representative images of DNA amplicons corresponding to *Hamp* wt. or KO alleles are shown. The selected primer pairs also amplify mouse wild-type *Hamp2* allele, which remained intact in *Hamp* KO mice.

A

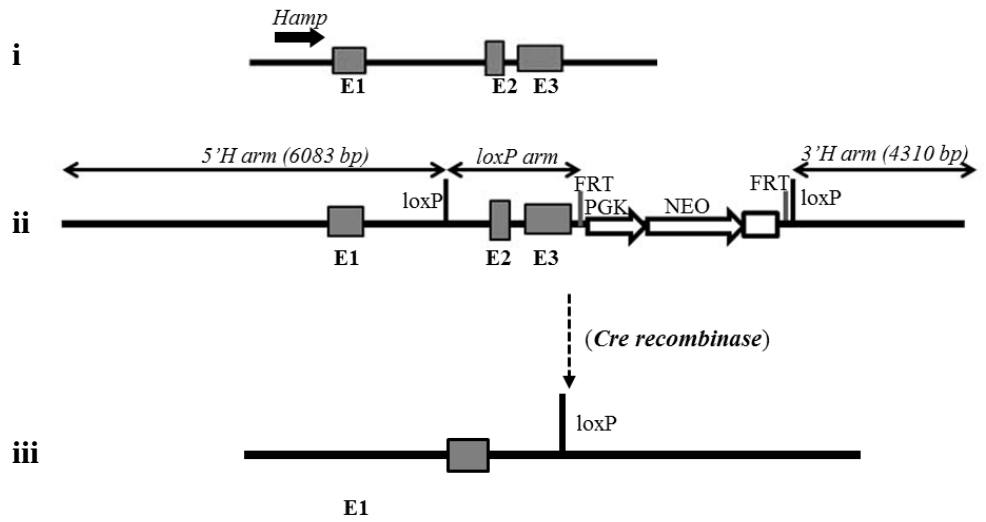
i
Hamp
E1
E2
E3
ii
5'H arm (6083 bp)
loxP arm
3'H arm (4310 bp)
loxP
FRT
PGK
NEO
FRT
loxP
E1
E2
E3
(Cre recombinase)
iii
loxP
E1

B

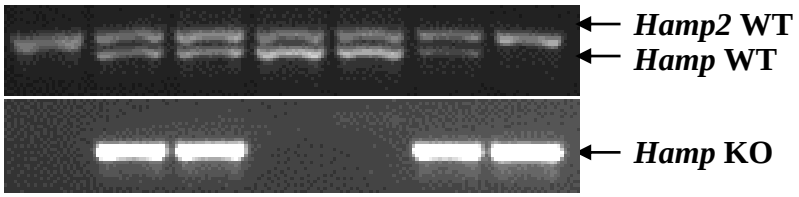
Hamp2 WT
Hamp WT
Hamp KO
WT. Het. Het. WT. WT. Het. Hom.

Figure 6.2

Figure 6.3. Quantification of hepatic iron content in *Hamp* Flx and KO mice. Inductively coupled mass spectrometry (ICP-MS) was performed (**A, B**) with the liver tissues from *Hamp* Flx and KO mice, as described in experimental procedures. The level of 56Fe (**A**) and 57Fe (**B**) isotopes, as detected by ICP-MS, are shown. Magnetic resonance imaging (MRI) was performed in Bioimaging Core Facility at University of Nebraska Medical Center to examine the iron content in the liver in situ (**C, D**). Single slice examples from 3D ultra-short echo time images through the liver of Flx (**C**) and homozygous KO (**D**) mice obtained at echo times of 0.02 ms (upper panel) and 3.0 ms (lower panel). The T2* of liver is much shorter in KO mice than in Flx mice, causing significant signal loss selectively in the liver by 3.0 ms.

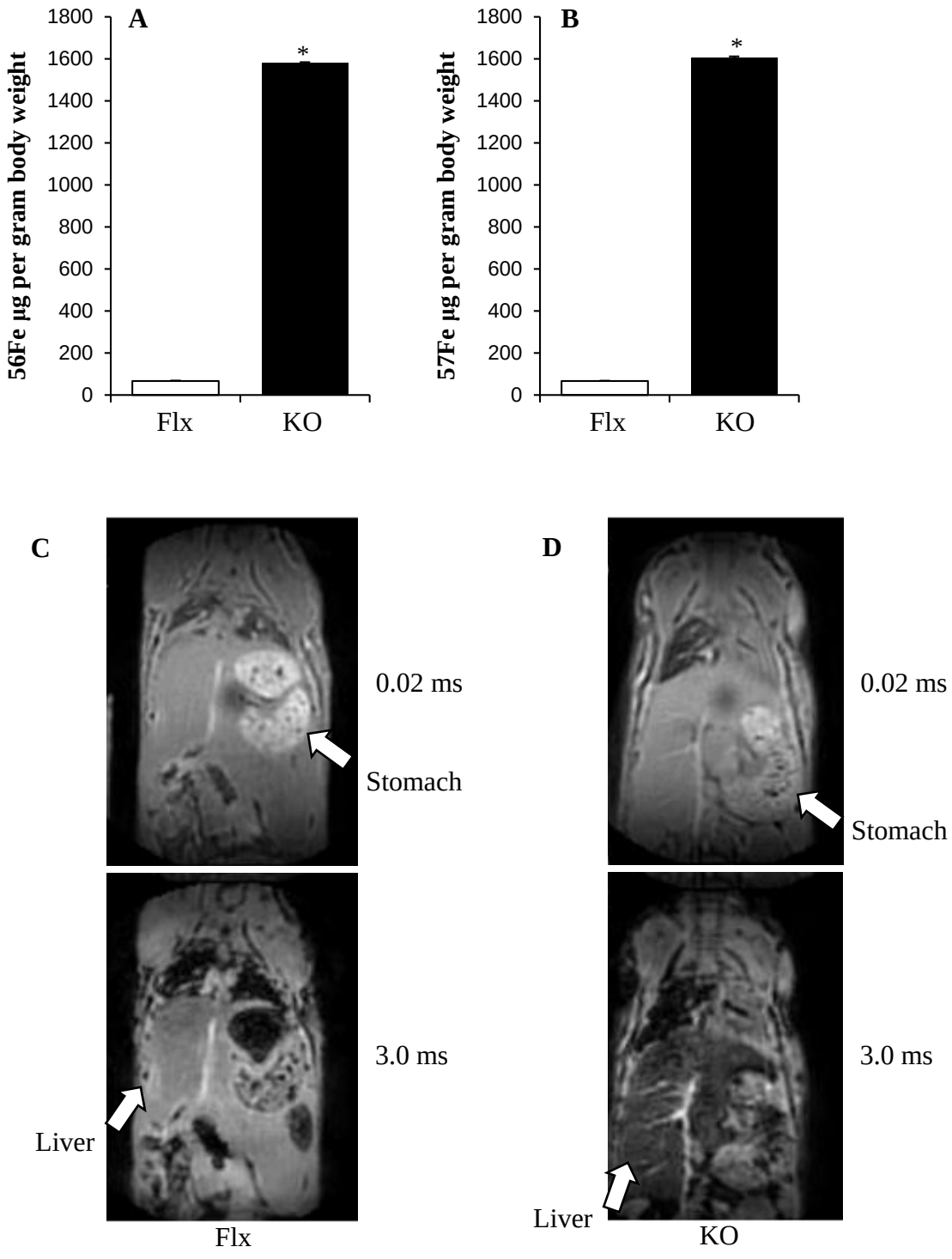
A
56Fe µg per gram body weight
1800
1600
1400
1200
1000
800
600
400
200
0
*
Flx
KO
B
57Fe µg per gram body weight
1800
1600
1400
1200
1000
800
600
400
200
0
*
Flx
KO
C
0.02 ms
Stomach
3.0 ms
Liver
Flx
D
0.02 ms
Stomach
3.0 ms
Liver
KO

Figure 6.3

Figure 6.4. The initial and end liver weights of *Hamp* Flx and KO mice fed high-fat and high-sucrose (HFS) or regular diets. Average body (**A, B**) and liver (**C, D**) weights of *Hamp* Floxed (Flx) (**A, C**) and knockout (KO) (**B, D**) mice fed with high-fat and high-sucrose (HFS) or regular control (Reg.) diets for 3 or 7 months are shown as gram weight. The average of initial (Ini.) body weights of mice in each group at the start of the experiments are also shown.

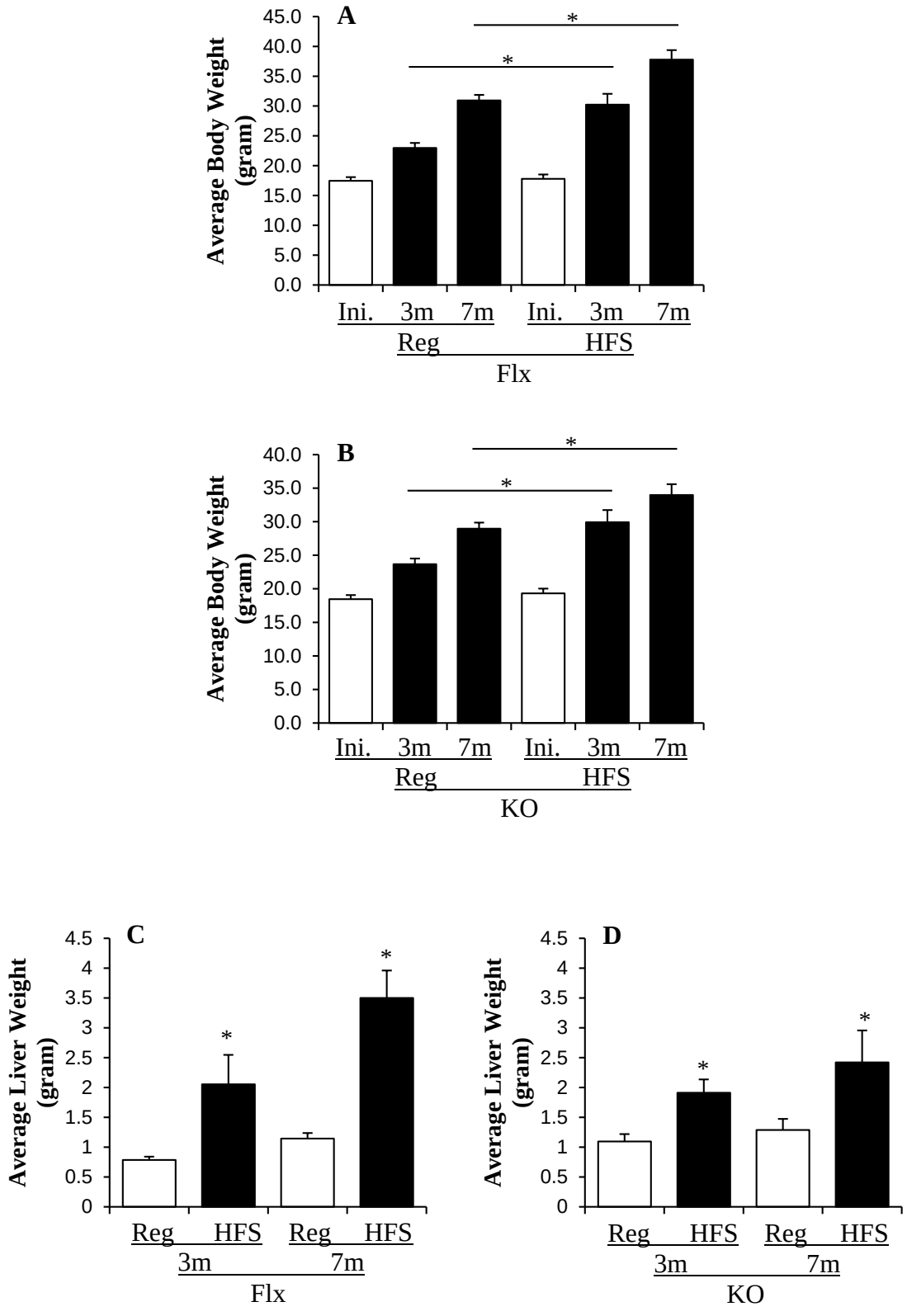
A
Average Body Weight (gram)
45.0
40.0
35.0
30.0
25.0
20.0
15.0
10.0
5.0
0.0
*
*
Ini. 3m 7m Ini. 3m 7m
Reg HFS
Flx
B
Average Body Weight (gram)
40.0
35.0
30.0
25.0
20.0
15.0
10.0
5.0
0.0
*
*
Ini. 3m 7m Ini. 3m 7m
Reg HFS
KO
C
Average Liver Weight (gram)
4.5
4
3.5
3
2.5
2
1.5
1
0.5
0
*
*
Reg HFS Reg HFS
3m 7m
Flx
D
Average Liver Weight (gram)
4.5
4
3.5
3
2.5
2
1.5
1
0.5
0
*
*
Reg HFS Reg HFS
3m 7m
KO

Figure 6.4

Figure 6.5. Macroscopic and microscopic changes in *Hamp* Flx and KO mice fed high-fat and high-sucrose (HFS) or regular diets for 3 months. Representative images showing the abdominal cavity of mice (**A**) and H&E staining of formalin-fixed and paraffin-embedded liver sections (**B**) of *Hamp* Flx and KO mice fed with high-fat and high-sucrose (HFS) or regular diets were obtained at the end of 3 month-long feeding period. Microscopic images were obtained with a Nikon Eclipse E400 light microscope using a CC-12 digital camera and analySIS software (Soft Imaging System), as described in experimental procedures (*see Chapter II*). Arrows indicate steatosis.

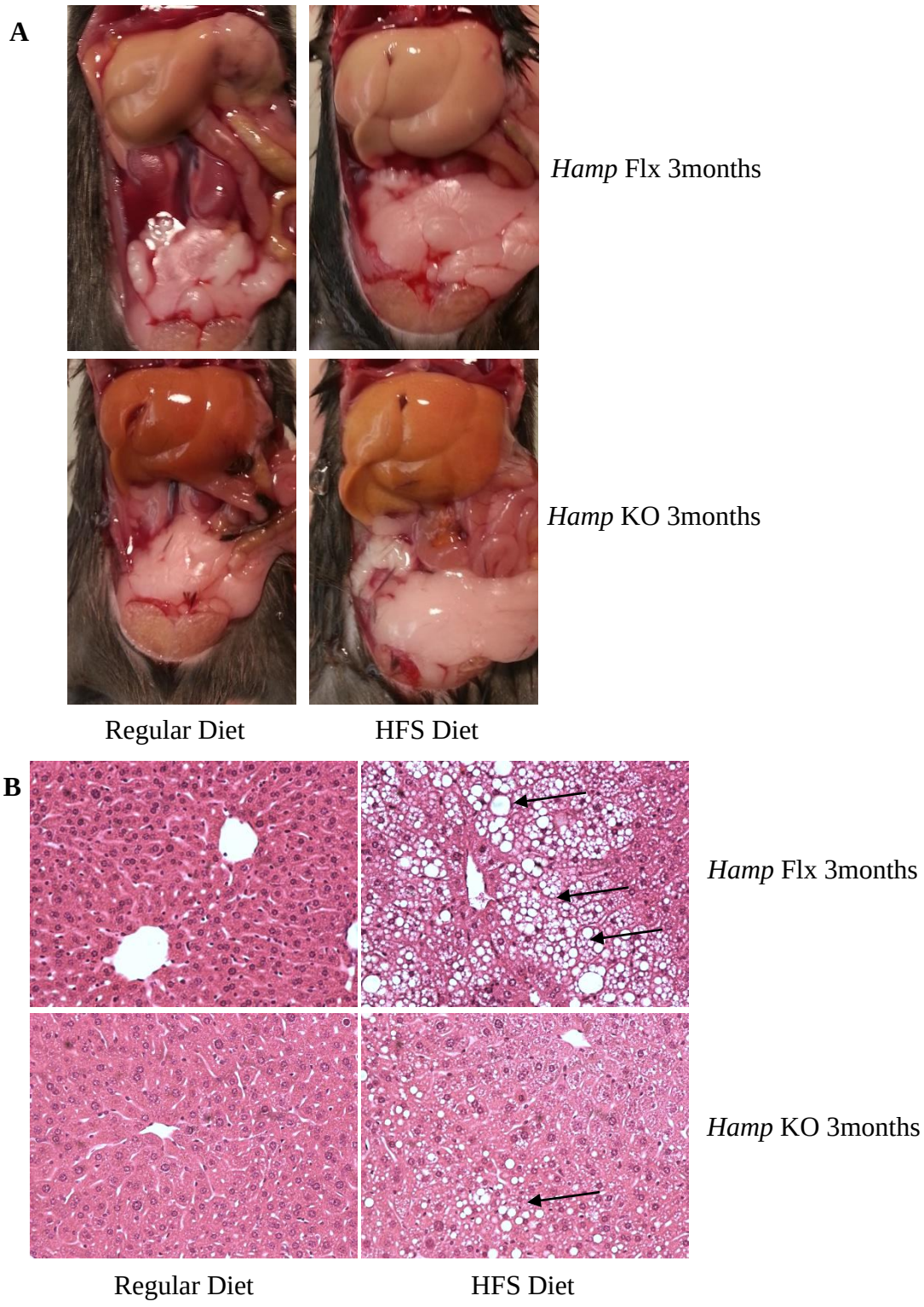
A
Hamp Flx 3months
Hamp KO 3months
Regular Diet
HFS Diet
B
Hamp Flx 3months
Hamp KO 3months
Regular Diet
HFS Diet

Figure 6.5

Figure 6.6. Macroscopic and microscopic changes in *Hamp* Flx and KO mice high-fat and high-sucrose (HFS) or regular diets for 7 months. Representative images showing the abdominal cavity of mice (**A**) and H&E staining of formalin-fixed and paraffin-embedded liver sections (**B**) of *Hamp* Flx and KO mice fed with high-fat and high-sucrose (HFS) or regular diets were obtained at the end of 7 month-long feeding period. Microscopic images were obtained with a Nikon Eclipse E400 light microscope using a CC-12 digital camera and analySIS software (Soft Imaging System), as described in experimental procedures (*see Chapter II*). Arrows indicate steatosis.

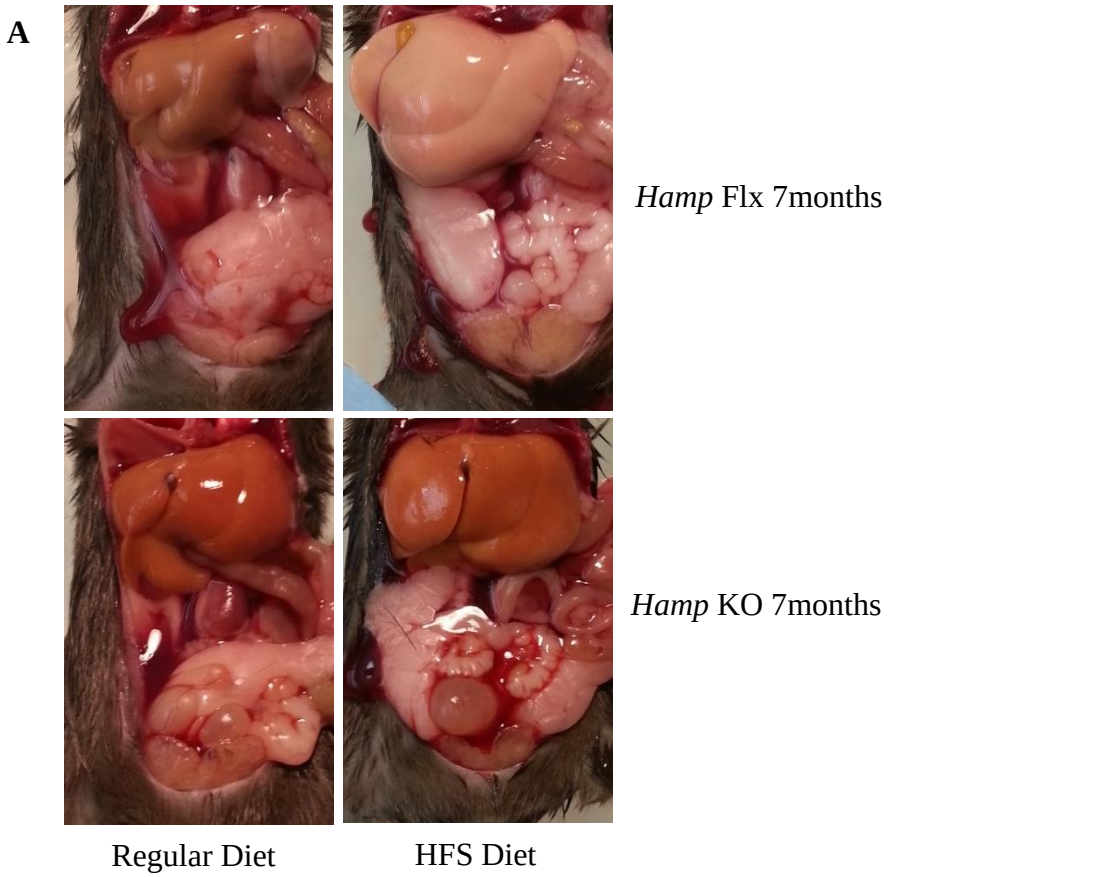
A
Hamp Flx 7months
Hamp KO 7months
Regular Diet
HFS Diet
B
Hamp Flx 7months
Hamp KO 7months
Regular Diet
HFS Diet

Figure 6.6

Figure 6.7. Liver triglyceride content in *Hamp* Flx and KO mice fed high-fat and high-sucrose (HFS) or regular diets. Hepatic triglyceride content in *Hamp* Floxed (Flx) and knockout (KO) mice fed with regular (Reg.) or high-fat and high-sucrose (HFS) diets for 3 (**A**) or 7 (**B**) months was quantified using 50 mg of wet liver tissue, as described in the experimental procedures (*see Chapter II*). Liver triglyceride amount was expressed as μmol per liver per 100 g body weight (μmol/L/ 100 g b.w.).

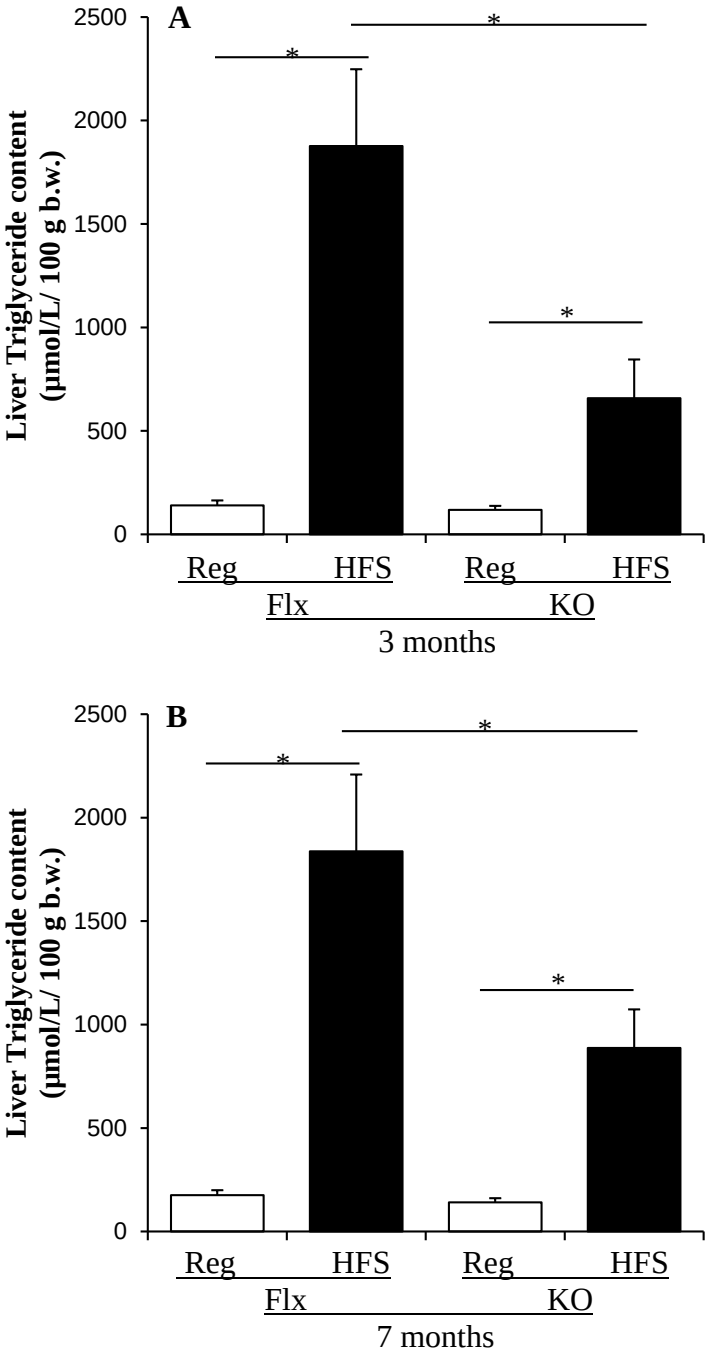
A
Liver Triglyceride content (µmol/L/ 100 g b.w.)
2500
2000
1500
1000
500
0
*
*
*
Reg
HFS
Reg
HFS
Flx
KO
3 months
B
Liver Triglyceride content (µmol/L/ 100 g b.w.)
2500
2000
1500
1000
500
0
*
*
*
Reg
HFS
Reg
HFS
Flx
KO
7 months

Figure 6.7

Figure 6.8. Fibrosis in *Hamp* Flx or KO mice fed high-fat and high-sucrose (HFS) or regular diets for 3 months. (**A)** Liver fibrosis in *Hamp* Floxed (Flx) and knockout (KO) mice fed on regular (Reg.) or high-fat and high-sucrose (HFS) diets for 3 months was detected by staining liver sections with Sirius Red, as described in experimental procedures. Representative microscopic images obtained with Nikon Eclipse E400 light microscope using a CC-12 digital camera and analySIS software (Soft Imaging System) are shown. (**B)** 10 images taken from each group were quantified using ImageJ software. The collagen proportional area (CPA) was determined by calculating the percentage of collagen-occupied pixels against the total pixel values.

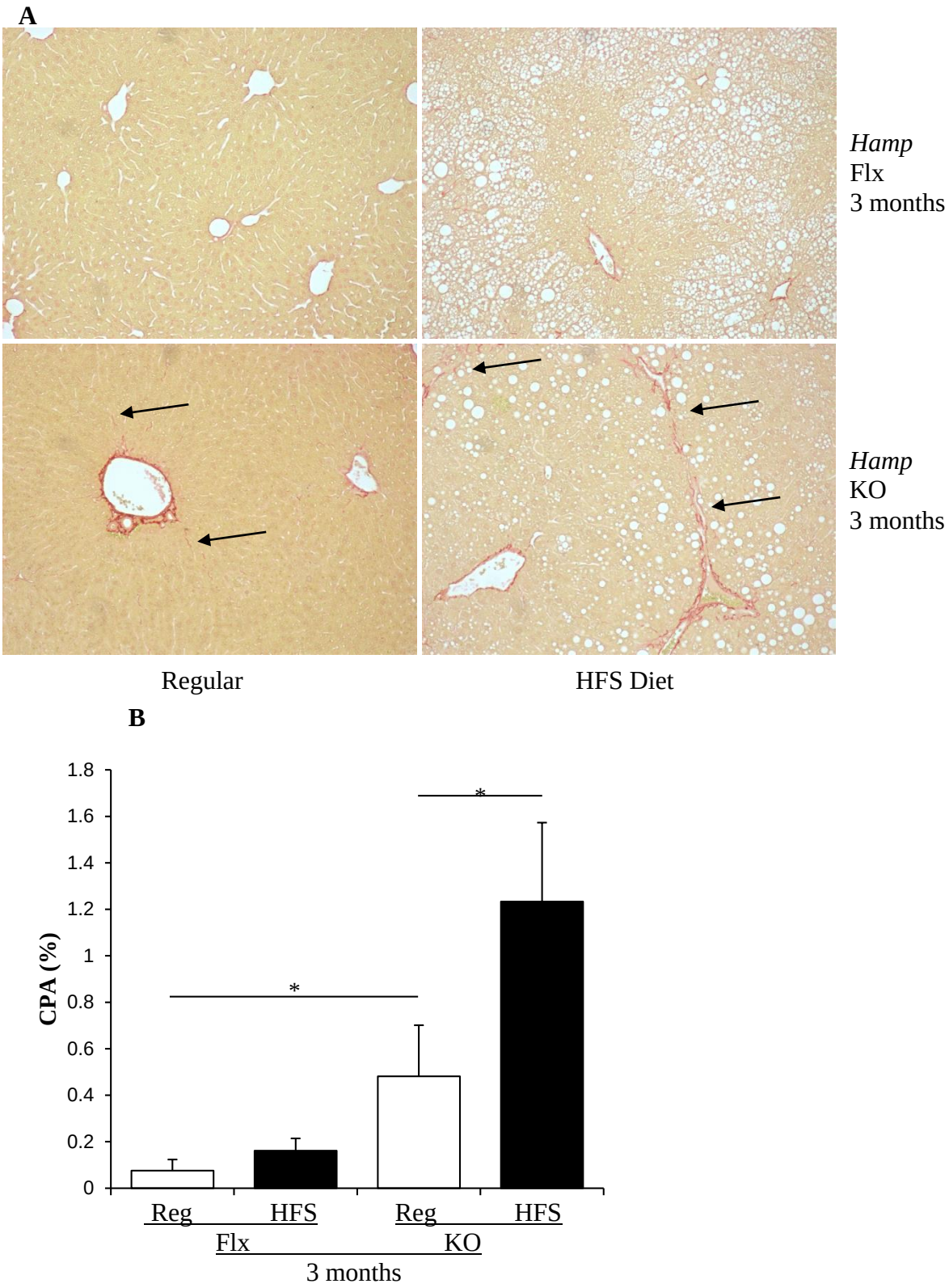
A
Hamp
Flx
3 months
Hamp
KO
3 months
Regular
HFS Diet
B
CPA (%)
1.8
1.6
1.4
1.2
1
0.8
0.6
0.4
0.2
0
*
*
Reg
HFS
Reg
HFS
Flx
KO
3 months

Figure 6.8

Figure 6.9. Fibrosis in *Hamp* Flx or KO mice fed high-fat and high-sucrose (HFS) or regular diets for 7 months. (**A**) Liver fibrosis in *Hamp* Floxed (Flx) and knockout (KO) mice fed on regular (Reg.) or high-fat and high-sucrose (HFS) diets for 7 months was detected by staining liver sections with Sirius Red, as described in experimental procedures. Representative microscopic images obtained with Nikon Eclipse E400 light microscope using a CC-12 digital camera and analySIS software (Soft Imaging System) are shown. (**B**) 10 images taken from each group were quantified using ImageJ software. The collagen proportional area (CPA) was determined by calculating the percentage of collagen-occupied pixels against the total pixel values.

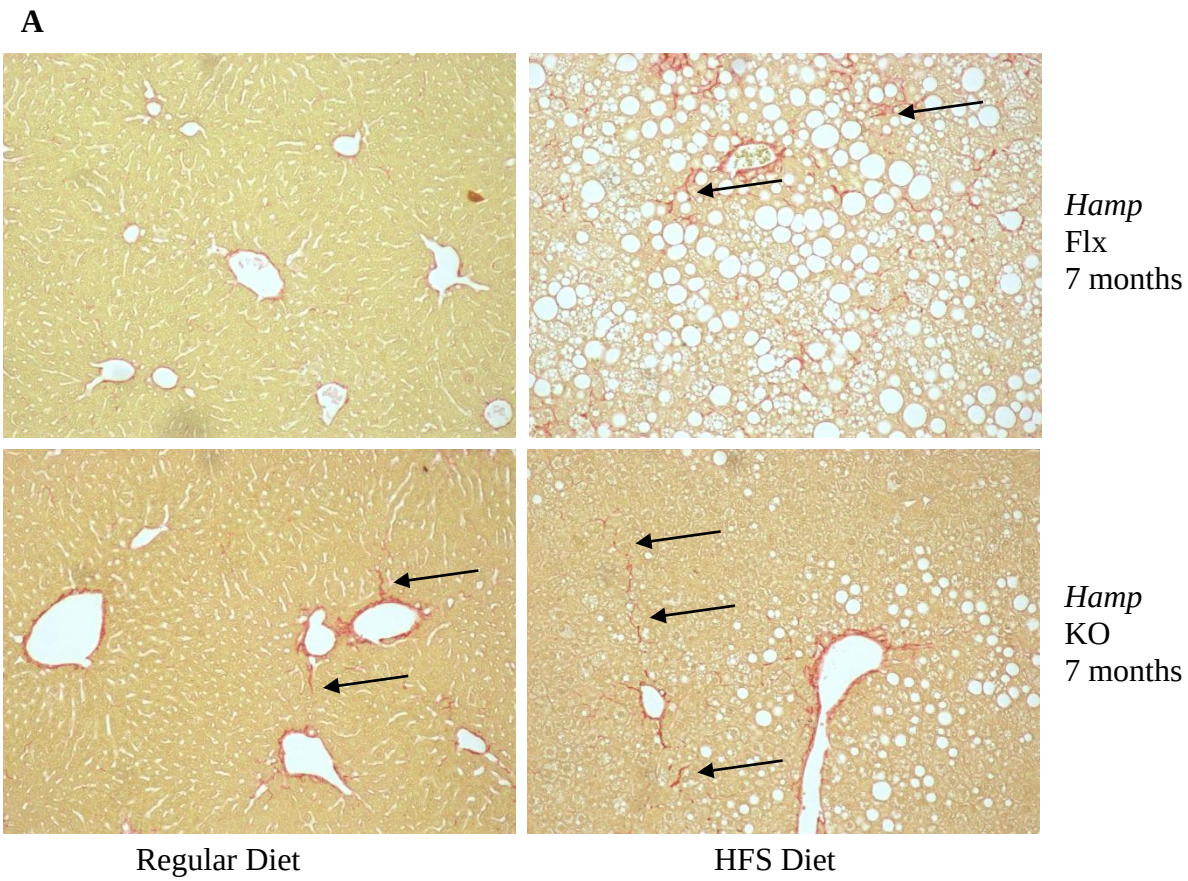
A
Hamp
Flx
7 months
Hamp
KO
7 months
Regular Diet
HFS Diet
B
CPA(%)
2.5
2
1.5
1
0.5
0
*
*
*
Reg
HFS
Reg
HFS
Flx
KO
7 months

Figure 6.9

Figure 6.10. **Protein expression levels of P-JNK and αSMA in *Hamp* Flx and KO mice fed HFS diet or regular diet for 3 or 7 months.** The expression levels of alpha smooth muscle action (αSMA) (**A**) and phosphorylated of JNK (P-JNK) (**C**) proteins in the livers of *Hamp* Floxed (Flx) and knockout (KO) mice fed with regular (Reg.) or high-fat and high-sucrose (HFS) diets for 3 or 7 months was determined by western blotting using whole liver cell lysates and commercial antibodies, as described in experimental procedures. An anti-gapdh antibody was used as control to determine equal protein loading. The western blots were quantified with densitometric analysis and normalized to gapdh expression. Normalized αSMA (**B**) and P-JNK (**D**) levels were expressed as fold-change of that in Flx mice fed with regular diet for 3 months.

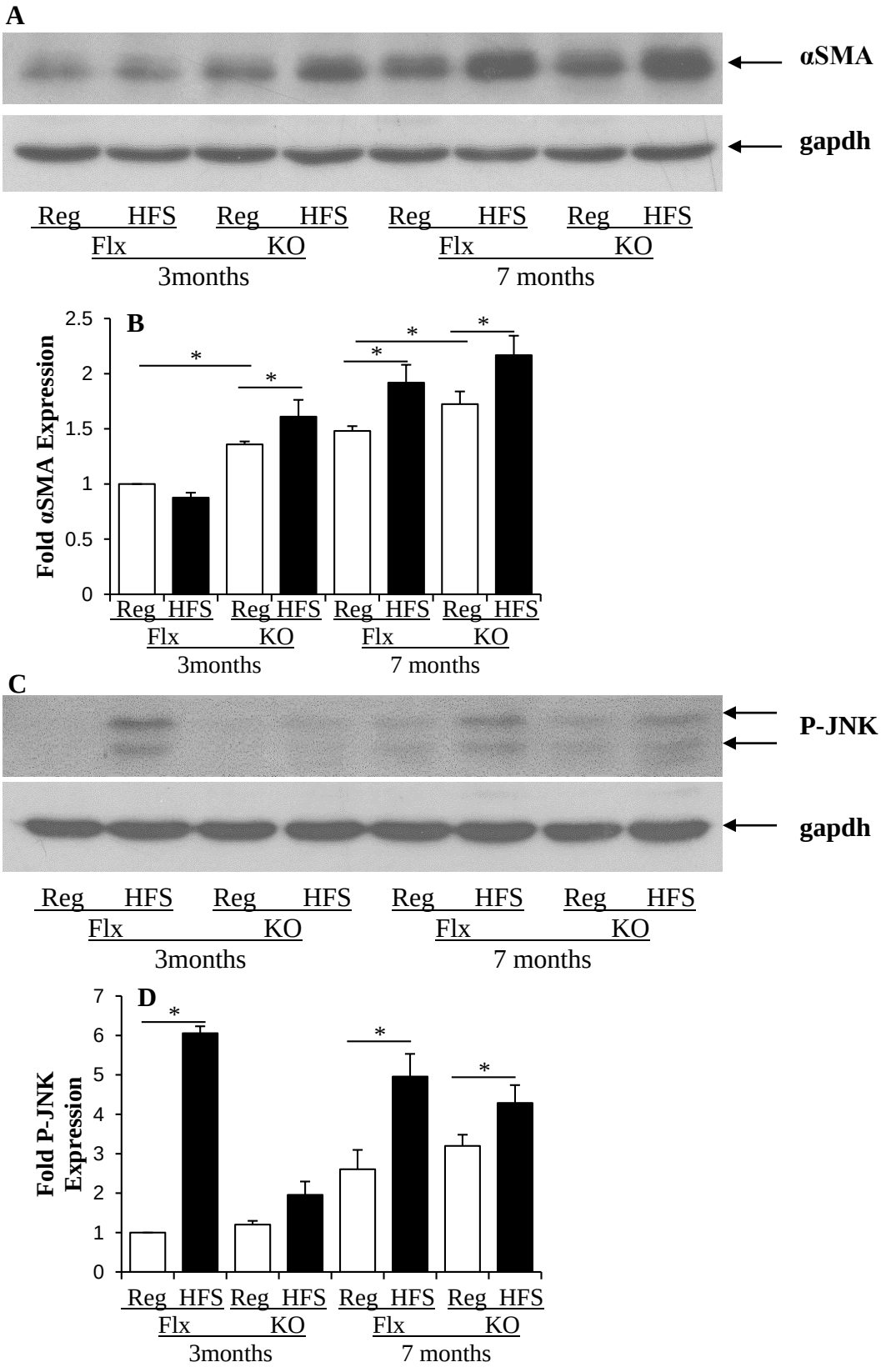
A
αSMA
gapdh
Reg HFS Reg HFS Reg HFS Reg HFS
Flx KO Flx KO
3months 7 months
B
Fold αSMA Expression
2.5
2
1.5
1
0.5
0
Reg HFS Reg HFS Reg HFS Reg HFS
Flx KO Flx KO
3months 7 months
C
P-JNK
gapdh
Reg HFS Reg HFS Reg HFS Reg HFS
Flx KO Flx KO
3months 7 months
D
Fold P-JNK Expression
7
6
5
4
3
2
1
0
Reg HFS Reg HFS Reg HFS Reg HFS
Flx KO Flx KO
3months 7 months

Figure 6.10

Figure 6.11. Expression of genes involved in lipogenesis, lipid storage and secretion. The mRNA expression levels of sterol regulatory element-binding protein-1c (SREBP-1c) (**A,B**), FSP27 (**C,D**), and microsomal triglyceride transfer protein (MTP) (**E,F**) in the livers of *Hamp* Floxed (Flx) and knockout (KO) mice fed with regular (Reg.) and high-fat and high-sucrose (HFS) diets, was determined by SYBR green qPCR using cDNA synthesized from total liver RNA and specific primers. Liver gene expression in HFS-fed *Hamp* Flx or KO and regular diet-fed KO mice for 3 (**A, C, E**) or 7 months (**B, D, F**) was expressed as fold change of that in *Hamp* Flx mice fed with a regular diet for the same time period.

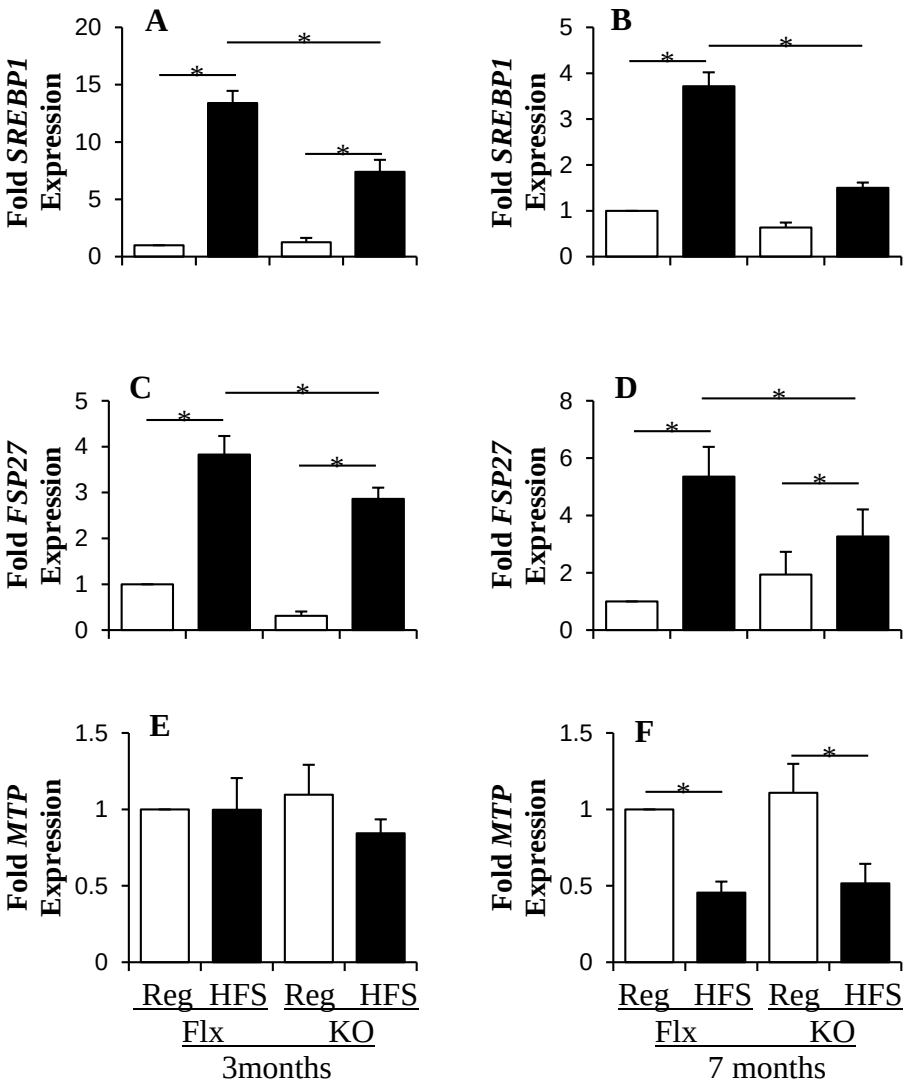
A
B
C
D
E
F
Fold SREBP1 Expression
Fold FSP27 Expression
Fold MTP Expression
Reg HFS Reg HFS
Flx KO
3months
7 months

Figure 6.11

Figure 6.12. Expression of genes involved in β-oxidation and gluconeogenesis. The mRNA expression levels of peroxisome proliferator-activated receptor alpha (PPARα) (**A, B**), carnitine palmitoyltransferase 1a (CPT1a) (**C, D**), phosphoenolpyruvate carboxykinase 1 (Pck1) (**E, F**) and glucose-6-phosphatase (G6PC) (**G, H**), in the livers of *Hamp* Floxed (Flx) and knockout (KO) mice fed with regular (Reg.) and high-fat and high-sucrose (HFS) diets, was determined by SYBR green cDNA synthesized from total liver RNA and qPCR using specific primers. Liver gene expression in HFS-fed *Hamp* Flx or KO and regular diet-fed KO mice for 3 (**A, C, E, G**) or 7 months (**B, D, F, H**) was expressed as fold change of that in *Hamp* Flx mice fed with a regular diet for the same time period.

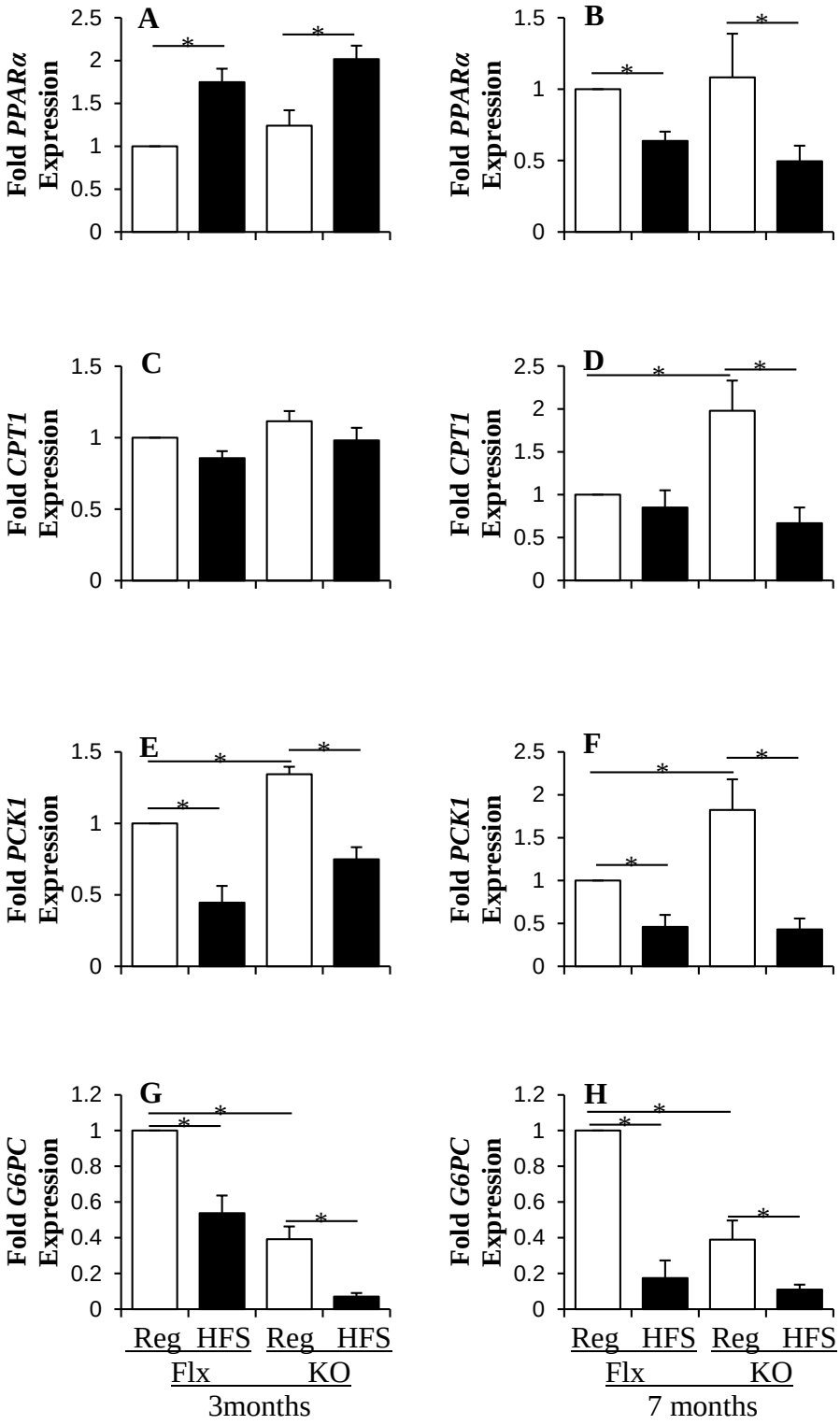
A
B
C
D
E
F
G
H
Fold PPARα Expression
Fold CPT1 Expression
Fold PCK1 Expression
Fold G6PC Expression
Reg HFS Reg HFS
Flx KO
3months
7 months

Figure 6.12

Chapter VII

Summary and Future Directions

1 SUMMARY AND FUTURE DIRECTIONS

Hepcidin is the central iron regulatory hormone. Hepcidin expression is frequently elevated in patients with obesity and nonalcoholic fatty liver disease (NAFLD). The underlying mechanisms are however unknown. Inflammatory cytokines or iron loading in NAFLD patients have been suggested to contribute to increased levels of hepcidin (1–3). Furthermore, an association between elevated serum hepcidin and lipid content in NAFLD patients has also been reported (4). Despite the importance of steatosis in NAFLD pathogenesis, the effect of hepatic lipid accumulation on hepcidin expression or iron homeostasis has not been investigated. In this dissertation, I have demonstrated novel and distinct regulatory mechanisms by which hepatic hepcidin expression is regulated by lipid-induced signaling. Saturated fatty acids, specifically palmitic acid, induced hepcidin mRNA stabilization via the activation and specific binding of AU-rich element binding protein, HuR to the 3'UTR of hepcidin mRNA (**Figure 7.1**). On the other hand, the sphingolipid, ceramide regulated hepcidin at the transcriptional level by activating STAT3 and its binding to *HAMP* promoter (**Figure 7.1**). My novel findings therefore confirmed the significant role of different lipid species in the regulation of hepcidin expression and iron metabolism. They have also elucidated the underlying mechanisms of these unique regulatory pathways. Most importantly, my results have for the first time demonstrated a direct role for post-transcriptional mechanisms, particularly an AU-rich element-binding protein and protein kinase C signaling, in hepcidin regulation. Moreover, I have confirmed the ceramide-specific activation of the JAK/STAT3 signaling pathway in hepatoma cells in the absence of inflammatory immune cells, which transcriptionally up-regulated hepcidin expression.

The elevation of hepcidin expression will subsequently lead to the sequestration of iron in Kupffer cells and hepatocytes via the inhibition of iron exporter, ferroportin (**Figure 7.2**). Iron accumulation in the hepatocytes (5) and reticuloendothelial cells (6) have both been shown to be associated with severe inflammation, injury and fibrosis in the liver. By using *Hamp* knockout mice, a genetic model of iron overload, I have directly examined the effect of iron, and high-fat and high-sucrose (HFS) intake on NAFLD pathogenesis. Compared to controls, *Hamp* knockout mice exhibited significantly attenuated steatosis but more prominent fibrosis following HFS administration. My *Hamp* knockout mice studies further supported the conclusion that iron overload correlates with NAFLD disease progression.

Since hepcidin is the central iron regulator, lipid-mediated changes in hepatic hepcidin expression may alter systemic iron homeostasis. The long term effect of hepcidin up-regulation should not be neglected. Furthermore, my studies with *Hamp* knockout mice have also strongly suggested a role for hepcidin and iron in the regulation of metabolic gene expression in the liver. Future studies are therefore required to determine the long-term *in vivo* consequences of increased hepcidin expression on iron homeostasis and metabolic processes with regard to NAFLD pathogenesis.

In summary, experiments in this dissertation have demonstrated novel mechanisms by which hepatic hepcidin expression is stimulated by lipid signaling. The *in vivo* relevance of these findings needs to be validated with other experimental models and human patients of NAFLD. My findings confirming that HFS-fed *Hamp* knockout mice develop fibrosis within 3 months have also underlined the advantages of this novel experimental model in the study of NAFLD disease progression. Taken together, the studies in this dissertation will improve our understanding of hepcidin regulation by lipid metabolism in the liver, and

its significance in NAFLD pathogenesis. Since there are currently no FDA-approved drug treatments for NAFLD, the elucidation of these pathways may be beneficial for the development of treatment strategies for patients with NAFLD and metabolic syndrome.

2 REFERENCES

1. Bekri, S., Gual, P., Anty, R., Luciani, N., Dahman, M., Ramesh, B., Iannelli, A., Staccini–Myx, A., Casanova, D., Ben Amor, I., Saint–Paul, M., Huet, P., Sadoul, J., Gugenheim, J., Srai, S. K. S., Tran, A., and Le Marchand–Brustel, Y. (2006) Increased Adipose Tissue Expression of Hepcidin in Severe Obesity Is Independent From Diabetes and NASH. *Gastroenterology*. **131**, 788–796
2. Aigner, E., Theurl, I., Theurl, M., Lederer, D., Haufe, H., Dietze, O., Strasser, M., Datz, C., and Weiss, G. (2008) Pathways Underlying Iron Accumulation in Human Nonalcoholic Fatty Liver Disease. *Am. J. Clin. Nutr.* **87**, 1374–1383
3. Nelson, J. E., Brunt, E. M., Kowdley, K. V., and for the Nonalcoholic Steatohepatitis Clinical Research Network (2012) Lower serum hepcidin and greater parenchymal iron in nonalcoholic fatty liver disease patients with C282Y HFE mutations. *Hepatology*. **56**, 1730–1740
4. Senates, E., Yilmaz, Y., Colak, Y., Ozturk, O., Altunoz, M. E., Kurt, R., Ozkara, S., Aksaray, S., Tuncer, I., and Ovunc, A. O. K. (2011) Serum levels of hepcidin in patients with biopsy-proven nonalcoholic fatty liver disease. *Metab. Syndr. Relat. Disord.* **9**, 287–290
5. Valenti, L., Fracanzani, A. L., Bugianesi, E., Dongiovanni, P., Galmozzi, E., Vanni, E., Canavesi, E., Lattuada, E., Roviaro, G., Marchesini, G., and Fargion, S. (2010) HFE Genotype, Parenchymal Iron Accumulation, and Liver Fibrosis in Patients With Nonalcoholic Fatty Liver Disease. *Gastroenterology*. **138**, 905–912
6. Nelson, J. E., Wilson, L., Brunt, E. M., Yeh, M. M., Kleiner, D. E., Unalp-Arida, A., and Kowdley, K. V. (2010) Relationship between the pattern of hepatic iron deposition and histological severity in nonalcoholic fatty liver disease. *Hepatology*. **53**, 448–457

Figure 7.1. Molecular mechanism of lipid-induced up-regulation of hepcidin. Different lipid species induce hepcidin up-regulation through distinct mechanisms. Saturated fatty acids activate HuR through PKC signaling. The subsequent binding of HuR to the 3'UTR of hepcidin mRNA stabilizes the mRNA of hepcidin and therefore up-regulates steady-state mRNA level through a post-transcriptional mechanism. Ceramide activates the JAK/STAT3 signaling pathway. The binding of STAT3 to the hepcidin promoter activates transcription of hepcidin mRNA.

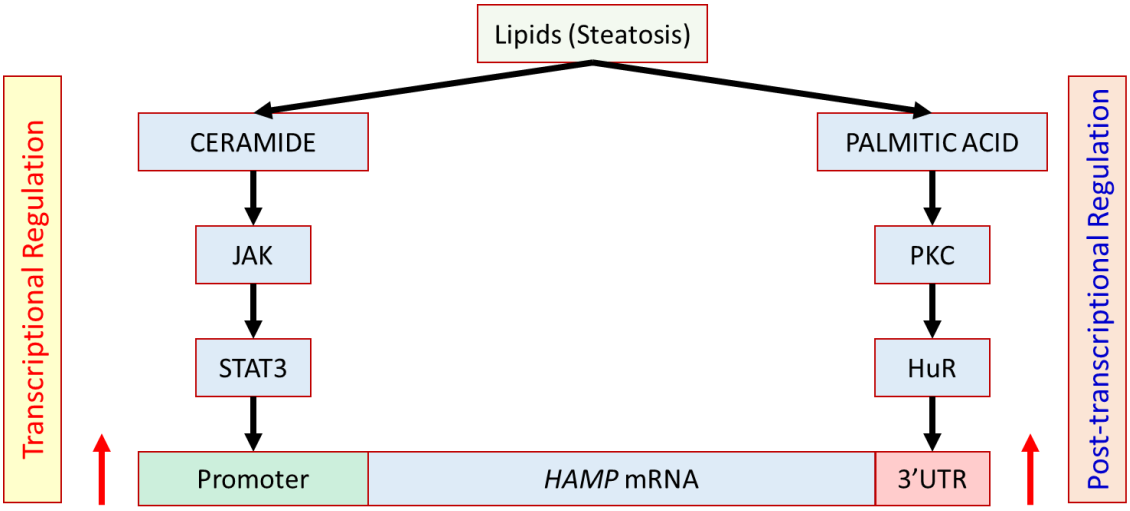
Lipids (Steatosis)
CERAMIDE
PALMITIC ACID
JAK
PKC
STAT3
HuR
Promoter
HAMP mRNA
3'UTR
Transcriptional Regulation
Post-transcriptional Regulation

FIGURE 7.1

Figure 7.2. Biological consequences of elevated hepcidin in the liver. Elevated hepcidin level results in the post-translational down-regulation of ferroportin, the iron exporter expressed on the plasma membrane of Kupffer cells and hepatocytes. Decreased ferroportin subsequently leads to decreased iron export and iron sequestration in the hepatocytes and macrophages, which exacerbates NAFLD/NASH pathogenesis.

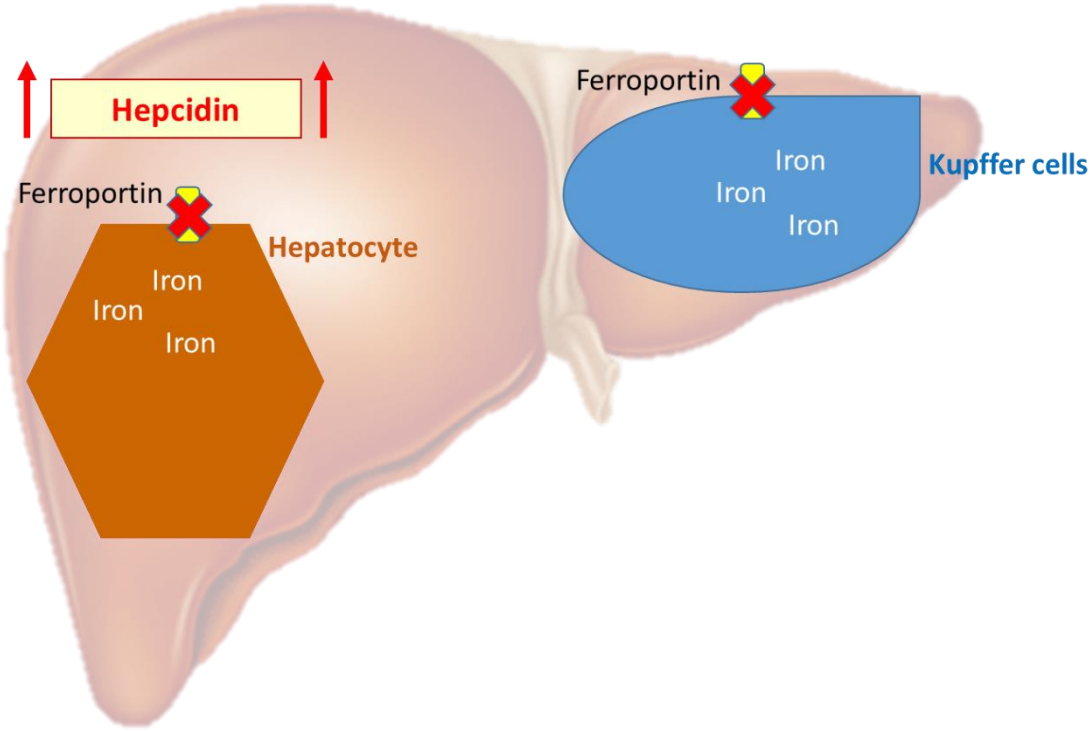
Hepcidin
Ferroportin
Hepatocyte
Iron
Iron
Iron
Ferroportin
Iron
Iron
Iron
Kupffer cells

Figure 7.2